2019

Phaeovirus Infections in Kelp

McKeown, Dean Andrew

UNIVERSITY OF
PLYMOUTH

PHAEOVIRUS INFECTIONS IN KELP

by

DEAN ANDREW MCKEOWN

A thesis submitted to the University of Plymouth
in partial fulfilment for the degree of

DOCTOR OF PHILOSOPHY

School of Biological and Marine Sciences

In collaboration with
the Marine Biological Association of the United Kingdom

June 2019

Acknowledgements

This research was funded by the University of Plymouth. The laboratory work was carried out at the Marine Biological Association of the UK (MBA), which also provided me with an office space and technical support. My attendance to the GlobalSeaweed Workshop 2017 and Microbiology Society Annual Conference 2016 were both supported by student grants from the Microbiology Society. My attendance to the Aquatic Virus Workshop 9 was supported by a PLYMSEF student grant.
Firstly, thanks to all of my PhD supervisors. Thanks to Murray Brown for his quick and thorough feedback on my work and keeping me on track. Thanks to Declan Schroeder, for introducing me to marine virology, all his support and advice, supporting the publication of our papers, and hosting me at the University of Minnesota. Thank you to Willie Wilson for taking on a supervisory role on short notice, and for his feedback on my work and presentations. I would like to thank Roy Moate for his input on my project proposal and progress reports.

Thank you to all those who provided kelp samples and cultures, including John Bolton, Mark Rothman, Jihae Park, Murray Brown, Claudio Sáez, and especially Akira Peters, who provided most of the kelp gametophyte cultures and taught me laboratory skills. Thanks also to those who provided help and advice regarding laboratory and field work including Dan Smale, Angela Ward, Glen Wheeler, and Andrea Highfield from the MBA. Thanks to Glenn Harper and Pete Bond for their help with the electron microscopy and for making the process enjoyable. Big thanks to all of my paper co-authors, without whom none of this work have been possible.

Thank you to my family and Poppy for their love and support, and everyone who joined me for a drink(s), various games, a swim, a bad movie, a rant, a trip, a climb, or a day in the sun. Finally, to Ganal'Rog, Heinrich, Balasor, Gert, a cat, Figwit, Galen, Atnas, Toma, Cuahautemoc, Axyss, Levei, Thalai, and the mysterious dice-wielding gods hidden behind screens, thank you for helping me escape from those strange delusions in which I am a junior scholar living in a safe, machine-based world, and reminding me that I am actually Inmua Sargaddaf, Wizard of the 1st Rank of Sargaland, Master of Illusion and Fashion, Lover of the 11 Gorgeous Terrors, Devourer of Insects, Champion of Sharing and Democracy, Known to the Orcs as Beloved Grandfather, Known to the Dwarves as Mishmosh Hoshuffle, and Known to the Humming Birds as Old Syrup Ears.

Author's Declaration

At no time during the registration for the degree of Doctor of Philosophy has the author been registered for any other University award without prior agreement of the Doctoral College Quality Sub-Committee.

Work submitted for this research degree at the University of Plymouth has not formed part of any other degree either at the University of Plymouth or at another establishment.

This study was financed with the aid of a studentship from the University of Plymouth and carried out in collaboration with the Marine Biological Association of the United Kingdom.

Publications (or public presentation of creative research outputs):

McKeown, D.A., Stevens, K., Peters, A.F., Bond, P., Harper, G.M., Brownlee, C., Brown, M.T. and Schroeder, D.C. (2017). Phaeoviruses discovered in kelp (Laminariales). The ISME journal. Vol. 11(12), pp.2869.
DOI: http://dx.doi.org/10.1038/ismej.2017.130
PEARL (OA): https://pearl.plymouth.ac.uk/handle/10026.1/9794

McKeown, D.A., Schroeder J.L., Peters. A.F., Saez, C.A., Park, J., Rothman, M.D., Bolton, J.J., Brown, M.T., and Schroeder, D.C. (2018). Phaeoviral infections are present in *Macrocystis*, *Ecklonia* and *Undaria* (Laminariales) and are influenced by wave exposure in Ectocarpales. Viruses. Vol. 10(8): pp.410.
DOI: http://dx.doi.org/10.3390/v10080410
PEARL (OA): https://pearl.plymouth.ac.uk/handle/10026.1/12498

McKeown, D.A., Schroeder, D.C. (2019). Virus replication in multicellular photosynthetic life forms. eLS, John Wiley & Sons (Ed.).
DOI: https://doi.org/10.1002/9780470015902.a0026418

Presentations at conferences:

McKeown, D.A., (2018), “Expanding the phaeovirus host range: the prevalence of kelp phaeoviruses” (Oral), Aquatic Virus Workshop 9, Lincoln, United States of America.

McKeown, D.A., (2016), “Imaging the elusive phaeoviruses of kelp” (Poster), Aquatic Virus Workshop 8, Plymouth, United Kingdom.

McKeown, D.A., (2016), “Giant host, giant virus: the viruses of kelp” (Poster), Microbiology Society Annual Conference 2016, Liverpool, United Kingdom.

McKeown, D.A., (2016 & 2019), “The phaeoviruses of kelp” (Oral), PLYMSEF Annual Student Conference, Plymouth, United Kingdom.

Word count of main body of thesis: 38, 512.

Signed …….. Date…….

Dean Andrew McKeown

PHAEOVIRUS INFECTIONS IN KELP

Abstract

The latent dsDNA viruses of the genus Phaeovirus (family *Phycodnaviridae*, clade Nucleo-cytoplasmic Large DNA Viruses; NCLDVs) employ genome integration in their brown algae hosts (class Phaeophyceae). The only phaeoviruses described in detail infected the order Ectocarpales, though Phaeovirus major capsid protein (MCP) occurs in 4 kelp (order Laminariales) species. Phaeoviruses are a major knowledge gap because brown algae are ecologically and economically important and have independently evolved complex multicellularity. This study aimed to investigate kelp Phaeovirus morphology, evolution, host range, distribution, host impacts, and genomics.

Microscopy of *Laminaria digitata* gametophytes revealed particles and cell morphology typical of Phaeovirus infections. This putative Laminaria digitata virus 1 (LdV-1) infection, unlike the Ectocarpales phaeoviruses, often occurred in vegetative cells. *L. digitata* Phaeovirus symptoms were ~3 times more common in 18 versus 15 ^{o}C culture, but overall were uncommon and highly variable. No impact on gametophyte reproduction was observed.

Broad-scale MCP PCRs and subsequent phylogeny identified 4 novel kelp phaeoviruses, placing the phaeoviruses of *Ecklonia maxima*, *Ecklonia radiata*, and *Undaria pinnatifida* in subgroup A, a *Macrocystis pyrifera* Phaeovirus in subgroup C, and a *Saccharina japonica* Phaeovirus in the novel subgroup D. Kelp phaeoviruses may follow the Ectocarpales Phaeovirus evolutionary trend of genome reduction (in subgroups B, C, and D versus A). Combined with all available data, 26 % of kelp were Phaeovirus MCP-positive.

Genomic data from LdV-1 and 3 available kelp genomes contained Phaeovirus orthologs from the following putative, integrated phaeoviruses: LdV-1, Ecklonia radicosa virus (ErcV), *S*accharina japonica virus (SjV), and Undaria pinnatifida virus (UpV). Subsequent phylogeny of 9 Phaeovirus core genes showed similar subgroups as before and non-core orthologs had implications for Phaeovirus evolution.

For kelp phaeoviruses, this study has revealed a partial infection cycle, preliminary observations of viral symptoms, a broader distribution and host range, and evolutionary insights for both viruses and hosts.

Table of Contents

List of Figures

List of Tables

List of Symbols and Abbreviations

%	Percentage
°C	Degrees Celsius
A	Adenosine
AMEV	Amsacta moorei entomopoxvirus
APMV	Acanthamoeba polyphaga mimivirus
ASFV	African swine fever virus
ATPase	Adenosine triphosphatase
BLAST	Basic local alignment search tool
BLASTn	Blast search of nucleotide sequence against nucleotide database
BLASTp	Blast search of protein sequence against protein database
BLASTx	Blast search of translated nucleotide against protein database
bp	Base pairs (nucleotide)
BSA	Bovine serum albumen
bya	Billion years before present time
C	Carbon
C	Cytosine
CDS	Coding sequence
Cl	Chlorine
CTAB	Cetyl trimethylammonium bromide
DAPI	4’,6-diamidino-2-phenylindole
DNA	Deoxyribonucleic acid
Dnase	Deoxyribonuclease
dsDNA	Double-stranded DNA
EA	Assembled to EsV-1 with method A
EB	Assembled to EsV-1 with method B
EDTA	Ethylenediaminetetraacetic acid
Efas	*Ectocarpus fasciculatus*
EfasV-1	Ectocarpus fasciculatus virus 1
EhV-86	Emiliania huxleyi virus 86
Emax	*Ecklonia maxima*
Erad	*Ecklonia radiata*
ErcV	Ecklonia radicosa virus
Esil	*Ectocarpus siliculosus*
EsV-1	Ectocarpus siliculosus virus 1
EVE	Endogenous viral element
FA	Assembled to FsV-158 with method A
FB	Assembled to FsV-158 with method B
Firr	*Feldmannia irregularis*
FirrV-1	Feldmannia irregularis virus 1
Flex	*Feldmannia simplex*
FsV-158	Feldmannia sp. Virus 158
g	Grams
G	Guanine
Gp1	Glycoprotein 1 of EsV-1
HaV01	Heterosigna akashiwo virus 1

HGT	Horizontal gene transfer
Hinc	*Hincksia hincksiae*
HincV-1	Hincksia hincksiae virus 1
hr	Hour
IIV-6	Invertebrate iridescent virus 6
IMM	Immediate upright protein
K	Carrying capacity of the environment in evolutionary model
K+	Potassium ion
kb	Kilobase (1000 base pairs)
kDa	Kilodalton
kV	Kilovolts
L	Litre
LCDV-1	Lymphocystis disease virus 1
Ldig	*Laminaria digitata*
LdV-1	Laminaria digitata virus 1
Lhyp	*Laminaria hyperborea*
m	Metre
Ma	Million years before present time
Mb	Megabase (1,000,000 base pairs)
Mcla	*Myriotrichia clavaeformis*
MclaV-1	Myriotrichia clavaeformis virus 1
MCP	Major capsid protein
mcp	Major capsid protein gene
Mg	Magnesium
mg	Milligram
min	Minute
mL	Millilitre
mm	Millimetre
mM	Millimolar
MOCV	Molluscum contagiosum virus
Mpyr	*Macrocystis pyrifera*
MSEV	Melanoplus sanguipes entomopoxvirus
NCBI	National Centre for Biotechnology Information
NCLDV	Nucleo-cytoplasmic large DNA virus
ng	Nanogram
nm	Nanometre
NPP	Net primary production
ORF	Open reading frame
OtV5	Ostreococcus tauri virus 5
PBCV-1	Paramecium bursaria chlorella virus 1
PCNA	Proliferating cell nuclear antigen
PCR	Polymerase chain reaction
PES	Provasoli's enriched seawater
Pg	Petagram
PgV-16T	Phaeocystis globosa virus 16T
PH	Perharidy
Plit	*Pylaiella littoralis*
PlitV-1	Pylaiella littoralis virus 1

PM	Plymouth
pmol	Picomolar
r	Growth rate in evolutionary model
RNA	Ribonucleic acid
rpm	Rotations per minute
RRLS	Ribonucleotide reductase, large subunit
RRSS	Ribonucleotide reductase, small subunit
SAR	Stramenopila Alveolata Rhizaria
SDS	Sodium dodecyl sulfate
sec	Second
Sjap	*Saccharina japonica*
SjV	Saccharina japonica virus
Slat	*Saccharina latissima*
sp.	Species
spp.	Multiple species
T	Thymine
TEM	Transmission electron microscopy
TM0-2	Transmembrane regions 0-2
Upin	*Undaria pinnatifida*
UpV	Undaria pinnatifida virus
V	Volts
VACV	Vaccinia virus
VLP	Virus-like particle
VLTF2	Very late transcription factor 2
VV A18-type helicase	Vaccina virus helicase gene
VV A32-type ATPase	Vaccina virus ATPase gene
VV D5-type ATPase	Vaccina virus ATPase gene
VV D6R-type helicase	Vaccina virus helicase gene
x g	Times gravity
yr	Year
µg	Microgram
µL	Microlitre
µm	Micrometre
µM	Micromolar
µmol m-2 s-1	Micromoles per square metre per second

INTRODUCTION

0.1 The Nucleo-cytoplasmic Large DNA Viruses

Viruses are intracellular obligate parasites which depend on a ribosome-encoding host cell for protein synthesis, most nucleic acid synthesis reactions, and, to a variable extent, transcription and replication. One nearly universal feature of viruses is the transmission between hosts as virus particles (virions) formed by packaging the genomic nucleic acid (RNA or DNA) into a protein capsid [1]. Beyond this, viruses have highly variable capsid and genome structures, evolutionary origins, replication mechanisms, and host cell interactions [2].

Virus lifestyles are generally lytic or lysogenic. Lytic viruses begin replication soon after cell entry, leading to cell lysis and the release of virions. In contrast, lysogenic viruses enter a cell and become latent, which is a dormant state that lasts until viral replication is induced by some cellular or environmental factor. Latent viruses persist as a viral genome integrated into the host genome (a provirus) or as a genetic element independent of the chromosomes (an episome). During latency, viral nucleic acids may be vertically transmitted via the host germline to the next generation. Pseudolysogeny is an intermediate strategy, often in response to host starvation, in which the lytic cycle is paused or slowed, such as the continual production of chloroviruses [3] or coccolithoviruses [4] with delayed cell lysis.

Evolutionarily, lytic viruses are 'acute' or *r*-selected, meaning they produce many progeny within a short time. In contrast, latent viruses usually have more 'persistent' or K-selected evolutionary strategies, producing few progeny which are more

competitive (successful at achieving infections). Compared to acute viruses, persistent viruses are usually less virulent and form stable relationships with their hosts, which are mostly organisms with complex multicellularity [5, 6].

Most of the known viral diversity is in dsDNA viruses. Most dsDNA viruses infect bacteria, but there are 18 dsDNA virus families which infect diverse eukaryotes ([7] and references within). Within eukaryotic dsDNA viruses is a clade called the Nucleo-cytoplasmic Large DNA Viruses (NCLDVs), or proposed order "Megavirales" [8]. 'Nucleo-cytoplasmic' refers to NCLDV replication, which either begins in the nucleus before finishing in the cytoplasm or occurs exclusively in organelle-like 'virus factories' in the cytoplasm [9–11]. There are currently seven NCLDV families (*Ascoviridae*, *Asfarviridae*, *Iridoviridae*, *Marseilleviridae*, *Mimiviridae*, *Phycodnaviridae*, and *Poxviridae*;[8, 12]) and various NCLDVs which have not yet been assigned to families (Figure 0.1; such as pandoraviruses, pithoviruses, and molliviruses, [13]). The common origin of NCLDVs is supported by phylogenetic analysis based on 28 to 50 conserved core genes involved in replication, DNA metabolism, or structural functions [14–16]. The NCLDVs are estimated to have evolved 2-2.7 billion year ago, close to the origin of eukaryotes [15].

The diverse virions of NCLDVs are mostly icosahedral, range in diameter from 100 to 1500 nm, and are constructed from conserved Major Capsid Proteins (MCPs) [11, 17]. NCLDV genomes range in size from around 150 kb to 2.5 Mb and have large GC content differences from their hosts compared to other viruses [17]. The large size of many NCLDV virions (>200 nm) and genomes (>200 kb) classifies them as 'giant viruses' [17].

0.1.1 The Evolution of NCLDVs

The complexity and size of certain NCLDV genomes and virions rivals bacteria and even some eukaryotes. Most NCLDV genes have no known homologues in databases (ORFans), but they also encode universal cellular genes such as those involved in translation and DNA metabolism. These unusual features have prompted the suggestion that NCLDVs have evolved via the reduction of a cellular ancestor, specifically from an extinct cellular domain in the case of the 'fourth domain' hypothesis [11].

However, the universal cellular genes of NCLDVs have likely originated from multiple and independent horizontal gene transfers (HGTs) from eukaryotes [12, 16, 18, 19] and none of the 50 conserved core genes of NCLDVs have cellular homologues [16]. Genome gigantism has evolved multiple times, leading to multiple NCLDV lineages which include members with genomes four to ten times larger than closely related NCLDVs, for example; ~1.2 Mb *Mimiviridae* versus ~300 kb *Phycodnaviridae* [20], ~600 kb *Pithovirus* versus ~150 kb *Iridoviridae* [20], and ~ 2.5 Mb *Pandoravirus* versus ~300 kb coccolithoviruses, [21]. In addition, as proposed by the 'genomic accordion' hypothesis, NCLDV genomes have undergone complex and lineage-specific patterns of gene loss and acquisition [16, 22]. These findings effectively falsify the hypothesis that NCLDVs originated from a cellular ancestor via reduction, as they show that the large and complex genomes of NCLDVs have originated via multiple genome expansions from a simpler viral ancestor [12].

ORFans are highly common in NCLDVs, comprising up to 80 % of NCLDV genes; in contrast, up to 33 % of cellular and bacteriophage genes are ORFans [23, 24]. The occurrence of these ORFans is hard to explain because they probably do not originate from common descent [12, 22] or horizontal gene transfer [25]. An emerging

hypothesis to explain these abundant ORFans is that NCLDVs create genes *de novo* [25], but the mechanisms of this are poorly understood, even in cellular organisms [26, 27].

The best supported origin of NCLDVs is that they evolved from Polintons, which are large (15-20 kb), vertically transmitted, transposon-like elements which encode type B DNA polymerase (pPolB) and RVE family integrase. Polintons are integrated into the genomes of a wide range of eukaryotes, and probably evolved from *Tectiviridae* bacteriophages which entered the eukaryotic lineage with the endosymbiotic α-proteobacteria which gave rise to mitochondria. Most Polintons are considered 'polintoviruses' because they encode the proteins required to form capsids [12, 28]. These and other key viral genes are shared by diverse DNA viruses (*Adenoviridae*, *Bidnaviridae*, virophages, and NCLDVs) and plasmids, which suggests they have evolved from polintoviruses [12, 29]. The NCLDVs emerged from polintoviruses with the acquisition of RNA polymerase, which allowed NCLDVs to replicate in the cytoplasm and therefore escape from the nucleus. The massive expansion of NCLDV genomes was made possible by replacement of Polinton pPolB with a more efficient RNA/DNA primed PolB acquired from the eukaryotic host [12], whilst retaining the Polinton capsid formation proteins and D5-like helicase-primase. The Polinton origin of NCLDVs is congruent with the many unrelated viral lineages which originated from selfish genetic elements that evolved capsid proteins [7, 30].

The known host range of NCLDVs includes multiple eukaryotic kingdoms, which is the broadest of any dsDNA virus group, which usually infect a single kingdom [12, 16]. However, an even broader host range was revealed by screening eukaryotic genomes in databases for integrated NCLDV core genes [31]. At least 1 NCLDV core gene was present in 48 out of 1282 eukaryotic genomes and 18 out of 1679 eukaryotic

transcriptomes, and only 4 of these 66 positive organisms were previously known to be infected by NCLDVs. Many of these NCLDV core genes were within viral inserts up to 300 kb long, indicating that NCLDV genome integration is common. Eukaryotic groups with the highest occurrence of NCLDV core genes were the brown algae (Phaeophyceae; 3/3 contained NCLDV homologs), Amoebozoa (11/32), green algae (Chlorophyta and Streptophyta; 9/28), and Oomycetes (10/40) [31]. It remains unknown how many NCLDV groups exist, but the NCLDVs are evidently far more widespread and diverse than is currently known [32].

Figure 0.1: Maximum likelihood tree of DNA polymerase B protein sequences encoded by NCLDV members. Node values are maximum likelihood bootstrap proportions (values <50 not shown). Scale units are the number of amino acid substitutions per site. * DNA polymerase phylogeny shows the putative polyphyly of the *Phycodnaviridae* [32, 33]. GenBank accession numbers for viruses are as follows: African swine fever virus, P0C974.1; Faustovirus, AIB52014.1; Heterocapsa circularisquama DNA virus 01, BAJ12120.1; Heliothis virescens ascovirus 3a, BBB16471.1; Trichoplusia ni ascovirus 2, AAY43139.1; Diadromus pulchellus ascovirus 4, CAC19127.1; Invertebrate iridescent virus 6, NP_149500.1; Anopheles minimus iridovirus, YP_009021128.1; Invertebrate iridescent virus 3, YP_654692.1; Infectious spleen and kidney necrosis virus, NP_612241.1; Lymphocystis disease virus 1, NP_078724.1; Frog virus 3, ASH99238.1; Lausannevirus, YP_004347308.1; Port-Miou virus, ALH07009.1; Tunisvirus fontaine2, YP_009507014.1; Insectomime virus, AHA45970.1; Cannes 8 virus, AGV01694.1; Marseillevirus, QBK86590.1; Pithovirus sibericum, YP_009000951.1; Emiliania huxleyi virus 86, YP_293784.1; Acanthocystis turfacea chlorella virus 1, YP_001427279.1; Paramecium bursaria Chlorella virus 1,

P30321.2; Ostreococcus tauri virus 5, YP_001648316.1; Heterosigma akashiwo virus 01, YP_009507574.1; Feldmannia species virus 158, YP_002154715.1; Feldmannia irregularis virus 1, AAR26842.1; Ectocarpus siliculosus virus 1, NP_077578.1; Pandoravirus dulcis, YP_008318996.2; Pandovravirus salinus, YP_009429988.1; Pandoravirus inopinatum, YP_009120445.1; Acanthamoeba polyphaga moumouvirus, YP_007354477.1 & YP_007354476.1; Moumouvirus goulette, AGF85231.1; Courdo11 virus, AFM52349.1; Megavirus courdo7, AFM52358.1; Megavirus lba, AGD92513.1; Megavirus chiliensis, AEQ33130.1; Megavirus terra1, AFM52356.1; Acanthamoeba polyphaga lentillevirus, EJN40770.1; Acanthamoeba polyphaga mimivirus, AKI79091.1; Hirudovirus, AHA45542.1; Mimivirus lactour, AFM52359.1; Terra virus 2, ADC39049.1; Mimivirus Cher, AFM52352.1; Mimivirus pointerouge1, AFM52353.1; Cafeteria roenbergensis virus BV-PW1, YP_003970130.1; Aureococcus anophagefferens virus, YP_009052217.1; Pyramimonas orientalis virus, ABU23717.1; Phaeocystis globosa virus, 12T AET73097.1; Phaeocystis globosa virus, YP_008052566.1; Phaeocystis pouchetii virus, A7U6F3.1; Prymnesium parvum DNA virus BW1, AQV04381.1; Organic Lake phycodnavirus 2, ADX06483.1; Organic Lake phycodnavirus 1, ADX06143.1; Chrysochromulina ericina virus, YP_009173620.1; Mollivirus sibericum, YP_009165284.1; Molluscum contagiosum virus, AAL40129.1; Vaccinia virus, YP_232947.1; Melanoplus sanguipes entomopoxvirus, NP_048107.1; Fowlpox virus, NP_039057.1; Canarypox virus, NP_955144.1.

0.2 The *Phycodnaviridae*

Algae are oxygen-evolving photosynthetic unicellular or multicellular autotrophs, including members of domain Bacteria (phylum Cyanobacteria) and various distinct eukaryotic lineages: Plantae (Charophyta, Chlorophyta, Glaucophyta, and Rhodophyta), the SAR clade (Stramenopila, Alveolata, and Rhizaria), Haptophyta, Cryptophyta, and Euglenozoa [34]. There are around 44,000 described algal species and there may be over 100,000 species in existence [34]. Most marine algae are unicellular phytoplankton which form the foundation of marine ecosystems and are responsible for around 50 % of global carbon fixation [35]. Recently it has been recognised that viral lysis of phytoplankton plays a vital role biogeochemical cycles, such as atmospheric sulfur cycles and the export of carbon to microbial food webs and marine sediments [3, 36].

The family *Phycodnaviridae* ("phyco"=algae, "dna"=DNA, "viridae"=virus family) are NCLDVs that infect algae. There are around 150 formally identified phycodnaviruses, with around another 100 mentioned in the literature [37], all of which have icosahedral capsids. Genomes from all major algae groups contain NCLDV core genes [31] and phycodnaviruses are the second most diverse marine viruses after bacteriophages (order Caudovirales) [38]. Three genomes from Chlorovirus, Phaeovirus, and Coccolithovirus share only 1.4-7.3 % of their genes (out of 1000 genes, [15, 39]). Furthermore, the intra-genera diversity of *Phycodnaviridae* is large, for example, 20 % of Chlorovirus and 17 % of Coccolithovirus genes are highly variable or absent between strains [37]. The orthologous genes of *Phycodnaviridae* show 4 distinct lineages: 1) Phaeovirus and Coccolithovirus, 2) Raphidovirus, 3) Chlorovirus and Prasinovirus, and 4) *Mimiviridae* and Prymnesiovirus. These lineages and genera are not necessarily monophyletic, and in future may become families or orders as

more phycodnaviruses are discovered [32, 33]. The best studied phycodnaviruses are Chlorovirus, Prasinovirus, and Coccolithovirus. Despite their diverse genomes and hosts, phycodnaviruses have been described in less than 0.1 % of algal species. Table 0.1 summarises the virions, genomes, infection strategies, host ranges, and species of *Phycodnaviridae* and Table 0.2 summarises the infection cycles of *Phycodnaviridae*.

Table 0.1: Properties of *Phycodnaviridae* virions, genomes, infection strategies, host range, and species numbers. References: Chlorovirus: [39–42]. Coccolithovirus: [4, 39, 40, 43–46]. Phaeovirus: [39, 40, 47–52]. Prasinovirus: [39, 40, 53–55]. Prymnesiovirus: [39, 40, 56]. Raphidovirus: [33, 39, 40, 57, 58].

Genus	Virion diameter (nm) and structure	Genome size (kb) number of ORFs G+C content (%) & structure	Host range	Sequenced genomes	Type species and no. of species
Chlorovirus	~190, icosahedral, internal membrane, cylindrical spike on one vertex, numerous capsid fibres	287-348 kb 600-800 ORFs 40-52 % 1 segment, linear, cross-linked hairpin ends, inverted 1-2.2 kb repeat termini, most of genome is single copy	Genus *Chlorella*, phyla Chlorophyta: unicellular symbiotic green freshwater algae	43	Paramecium bursaria Chlorella virus 1 (PBCV-1) 19
Coccolithovirus	150-200, icosahedral, internal membrane, putative tail, external membrane	377-422 kb 444-548 ORFs ~40 % 1 segment, circular, may have linear stage	Phyla Haptophyta, order Isochrysidales: unicellular coccolithophorid marine algae	13	Emiliania huxleyi virus 86 (EhV-86) 1
Prasinovirus	100-120, icosahedral, internal membrane	184-205 kb 203-268 ORFs 37-45 % 1 segment, probably linear	Class Prasinophyceae, phyla Chlorophyta: unicellular marine green prasinophyte algae, genera *Ostreococcus*, *Bathycoccus*, and *Micromonas*)	20	Micromonas pusilla virus SP1 (MpV-SP1) 2
Prymnesiovirus	100-170, icosahedral, internal membrane	120-485 kb ND ORFs 40 % 1 segment, probably linear	Unicellular marine prymnesiophyte algae Phyla Haptophyta, order Prymnesiales	0	Chrysochromulina brevifilum virus PW1 (CbV-PW1) 1
Raphidovirus	~200, icosahedral, internal membrane	275-294 kb 247 ORFs ~30 % 1 segment, probably linear	Unicellular marine raphidophyte algae (class Raphidophyceae)	1	Heterosigma akashiwo virus 01 (HaV01) 1
Phaeovirus	120-180, icosahedral, internal membrane	120-350 kb 156-231 ORFs 52 % 1 segment, circular, inverted terminal repeats, dispersed repetitive elements, and ssDNA regions of 10-60 kb	Class Phaeophyceae: multicellular marine brown algae	3	Ectocarpus siliculosus virus 1 (EsV-1) 9

Table 0.2: Infection cycles and strategies of the *Phycodnaviridae*. References: Chlorovirus: [40, 42, 59]. Coccolithovirus: [4, 40, 46]. Phaeovirus: [40, 49, 60, 61]. Prasinovirus: [40, 55]. Prymnesiovirus: [40, 56]. Raphidovirus: [40, 58]. Horizontal transmission is via virions and vertical transmission is via genetic inheritance of viral nucleic acids. P.i.= post infection.

Genus	Infection strategy and transmission	Cell entry	Latent period (hr p.i.) and transcription	Genome replication	Virion assembly	Cell exit and burst size
Chlorovirus	Lytic Horizontal	Vertex spike binds cell wall, viral enzymes degrade cell wall, and internal membrane fuses with cell membrane. Internal membrane K+ channel depolarises host membrane. Viral nucleo-protein core enters cytoplasm and moves to nucleus.	6-8 hr p.i. Nuclear with host RNA polymerase	Nuclear 60-90 min p.i. with viral DNA polymerase	Cytoplasmic 2-3 hr p.i.	Cell lysis 200-350
Coccolithovirus	Lytic Horizontal	Outer membrane binds with host membrane, intact capsid enters cytoplasm, nucleo-protein core enters nucleus	4-6 hr p.i. Early: nuclear with host RNA polymerase. Late: cytoplasmic with viral RNA polymerase	Cytoplasmic with viral DNA polymerase	Cytoplasmic 4.5 hr p.i.	Cell lysis or budding and gain of envelope from cell membrane 400-1000
Prasinovirus	Lytic Horizontal	Internal membrane fuses with cell membrane. Nucleo-protein core enters cytoplasm and moves to nucleus	7-70 hr p.i. Unknown	Unknown, with viral DNA polymerase	Cytoplasmic 6-20 hr p.i.	Cell lysis. Organelles remain intact throughout infection <100, as low as 6-15
Prymnesiovirus	Lytic Horizontal	Unknown	12-19 hr p.i. Unknown	Unknown, with viral DNA polymerase	Cytoplasmic	Cell lysis 400-4100
Raphidovirus	Lytic Horizontal	Unknown	30-33 hr p.i. Unknown	Unknown, with viral DNA polymerase	Cytoplasmic	Cell lysis 770

Table 0.2 (continued)

Genus	Infection strategy and transmission	Cell entry	Latent period (hr p.i.) and transcription	Genome replication	Virion assembly	Cell exit and burst size
Phaeovirus	Horizontal Vertical	Entry restricted to unwalled reproductive cells. Internal membrane fuses with cell membrane, K+ channel may depolarise cell membrane; nucleo-protein core enters cytoplasm and moves to nucleus. 5 min p.i., genome integration of viral DNA occurs using integrase Viral genome is transmitted via mitosis to every cell of the macroalga. The viral genome is inherited vertically between host generations in a Mendelian manner	ND; highly variable or indefinite Replication restricted mostly to reproductive organs (sporangia or gametangia). Nuclear with host RNA polymerase	Nuclear with viral DNA polymerase	Cytoplasmic	Cell lysis, induced by environmental triggers which also induce spore release $>1.10^6$ per host organ

0.2.1 Genus Chlorovirus

All described chloroviruses infect *Chlorella* (phylum Chlorophyta), a genus of unicellular freshwater green algae with simple life histories, a global distribution, and symbiotic relationships with the alveolate protozoan *Paramecium bursaria*, the heliozoan protozoan *Acanthocystis turfacea*, and the cnidarian animal *Hydrozoa viridis*. Chloroviruses are excellent models for algal viruses, as free-living *Chlorella* can be easily cultured. Paramecium bursaria Chlorella virus 1 (PBCV-1) is the Chlorovirus type species has been studied in great detail, which include unusual features such as many carbohydrate metabolism genes (most viruses rely on host carbohydrate metabolism [62]. More than 50% of predicted proteins in Chlorovirus genomes have been acquired

by horizontal gene transfer (HGT), but most are ORFans, possibly acquired from the vast unexplored reservoir of aquatic virus diversity [41].

0.2.2 Genus Coccolithovirus

The coccolithoviruses infect *Emiliania huxleyi*, a common coccolithophore (class Coccolithophyceae, phylum Haptophyta). Coccolithophores are unicellular marine algae with a global distribution, calcified scales, and important roles in primary production and carbon cycling. The termination of *E. huxleyi* blooms can be driven by Coccolithovirus infections [37], leading to increased zooplankton grazing and carbon export [63]. The Coccolithovirus type species is Emiliania huxleyi virus 86 (EhV-86, [64]). Notable findings include a selfish genetic element (intein), manipulation of host lipid metabolism [65], a persistent RNA stage [66], viral transmission via grazer faecal pellets and seawater aerosols, and the seasonal ecological dynamics of EhVs [44, 67]. Most acquired genes in EhVs have eukaryotic and bacterial origins, which suggests coccolithoviruses are major transporters of genes between life domains and kingdoms [44]. Coccolithoviruses are the only phycodnaviruses to encode their own RNA polymerase, meaning their transcription is partially independent of the nucleus, a lifestyle which the ancestral phycodnavirus likely employed. Coccolithovirus is highly divergent from the rest of *Phycodnaviridae*, and in future may be reassigned as a subfamily [43] or family [32].

0.2.3 Genus Prasinovirus

The prasinoviruses infect prasinophytes (phylum Chlorophyta, class Prasinophyceae, [68]) which are common unicellular green algae and important marine primary producers. Prasinophytes are the most basal lineage of green algae and terrestrial plants [53]. Up to 25 % of the daily host population can be lysed by

prasinoviruses [53]. The first report of phycodnavirus isolation was of prasinoviruses from *Micromonas pusilla*. Notable features of Prasinovirus genomes include unusually long ORFans which occupy 10-15 % of *Bathycoccus* virus genomes, a viral heat shock protein which may delay cell autolysis, and infection synchronisation with the diurnal rhythms of their hosts [54]. Many Prasinovirus genes are acquired from prasinophytes, other eukaryotes, and bacteria, giving prasinoviruses highly flexible and diverse genomes [69]. Prasinoviruses encode seven to eight MCPs per genome (most viruses encode only one MCP) and genes involved in glycosylation and nitrogen metabolism, and their DNA polymerases contain inteins which may facilitate viral recombination [53].

0.2.4 Genus Prymnesiovirus

Prymnesiophytes (phylum Haptophyta) are mostly marine unicellular algae with a global distribution, can form blooms, and have calcified scales. Prymnesioviruses strongly influence the ecology of *Chrysochromulina* and *Phaeocystis* (both can form harmful algal blooms), with subsequent impacts on algal seasonal dynamics, biogeochemical cycling, and secondary production [70, 71]. The complex evolutionary relationships of *Mimiviridae* and *Phycodnaviridae* are especially apparent in the NCLDVs infecting prymnesiophytes, as they are infected by both families [72]; mimiviruses with highly reduced genomes (group 1 Phaeocystis globosa viruses, PgVs, ~470 kb genomes, [73, 74]; Aureococcus anophagefferens virus, AaV, and Chrysochromulina ericina virus, CeV), and Prymnesiovirus phycodnaviruses (Chrysochromulina brevifilum virus PW1, CbV-PW1, and group 2 PgVs, ~170 kb genomes, [33, 75]).

0.2.5 Genus Raphidovirus

Raphidoviruses infect raphidophytes, which are mostly marine unicellular algae (class Raphidophyceae, Heterokonta) which form blooms including harmful red tides. The only known raphidoviruses infect *Heterosigma akashiwo*, the type species being Heterosigma akashiwo virus 01 (HaV01). The raphidoviruses display the most gene losses of any member of *Phycodnaviridae* or *Mimiviridae* (since divergence from the *Phycodnaviridae/Mimiviridae* ancestor) and may be a distinct viral lineage within *Phycodnaviridae* [33].

0.3 Genus Phaeovirus

Phaeoviruses infect the multicellular brown algae (class Phaeophyceae, Stramenopila) and are the only known phycodnaviruses to employ a latent infection strategy (Table 0.1; Table 0.2), which is shown in Figure 0.2 and images of the infection are shown in Figure 0.3. The type species is Ectocarpus siliculosus virus 1 (EsV-1).

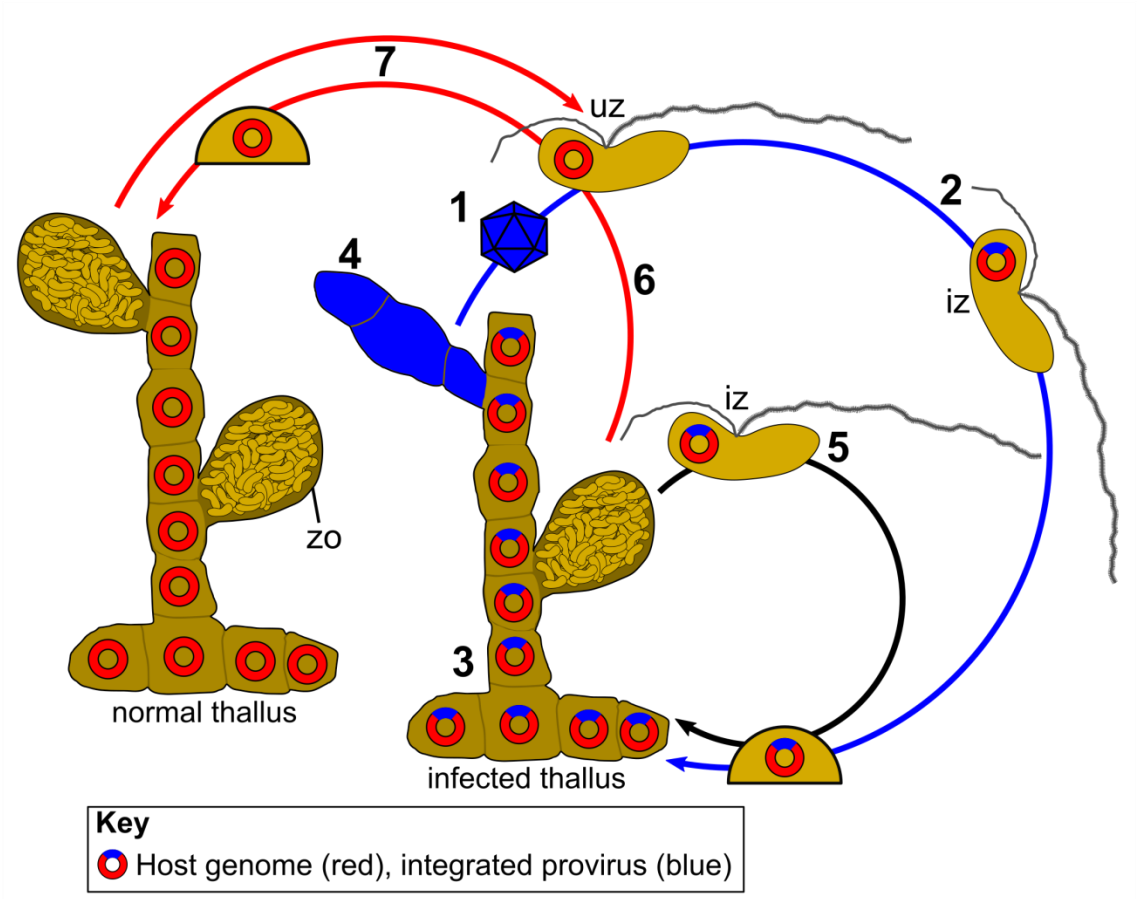

Figure 0.2: The Phaeovirus infection cycle. (**1**; **blue arrow**) Phaeovirus virion infects uninfected zoids (**uz**) (zoid = flagellated reproductive cell, such as spore or gamete). Zoids are produced by zoidangia (**zo**). Zoids settle and develop into walled initial cells (**semi-circles**) which develop via mitosis into multicellular thalli. Only the zoids are susceptible to infection, as they lack cell walls and phaeoviruses lack cell wall degrading enzymes [49, 60]. (**2**; **blue arrow**) The viral core enters the nucleus and an integrated Phaeovirus genome (**provirus**; **key**) is inserted into the genome of the infected zoid (**iz**) [60, 76]. This does not normally cause cell lysis. (**3**) The provirus is copied with every mitosis, which results in an **infected thallus** (sporophytes, gametophytes, or parthenosporophytes) with a provirus copy in every cell [76]. (**4**) The thallus appears normal until environmental or cellular factors induce the expression of the provirus, which occurs almost exclusively in zoidangia, but sometimes occurs in vegetative cells [77]. Viral expression interrupts the early development of zoidangia, causing high viral DNA replication in the nucleus, followed by nuclear and plastid degeneration and cytoplasmic virion assembly. These zoidangia (**4**) are deformed, stain intensely with DAPI, lack chlorophyll, and release 10^6 virions in response to the same environmental triggers of zoid release (changes in salinity and temperature [52, 77]). (**5**) (**black arrow**) Infected thalli produce infected zoids which vertically transmit the infection via proviruses to the next generation. (**6**; **red arrows**) Meiosis segregates a Phaeovirus provirus to one daughter chromosome, which eliminates the provirus from 50% of the meiotic zoids (meiospores). (**7**) This can result in virus-free host life cycles [78, 79]. However, all zoids can be re-infected by virions (**1**; **blue arrow**); some phaeoviruses (subgroup B) can infect already infected zoids, leading to multiple infections.

Qualitatively the extent of virus symptoms appears to be highly variable in Ectocarpales hosts, ranging from asymptomatic to simultaneous virion/zoid production, to sterile macroalgal which only produce virions [77, 80]. Only the phaeoviruses EsV-1 and EfasV-1 replicate in both the gametangia (organs that produce gametes via mitosis) and sporangia (organs that produce meiospores via meiosis), whilst the rest replicate only in the sporangia (Table 0.3, [49]). Phaeovirus symptoms can increase at lower or higher temperatures (12-15 ^{o}C versus 18-20 ^{o}C, [81–83]). Microscopy of wild Ectocarpales showed highly variable rates of visible Phaeovirus symptoms (1-25 % of individuals of *Hincksia*, *Ectocarpus*, and *Feldmannia*; [82–84]), whilst PCR of a Phaeovirus gene (capsid protein gp1) showed a higher infection rate of 50-100 % in *Ectocarpus*, which indicates that unexpressed Phaeovirus infections are common [85, 86]. The abundance of unexpressed Phaeovirus infections indicates that virion production, and therefore horizontal transmission, is low. The high infection rates of phaeoviruses must be achieved by the vertical transmission of latent proviruses (Figure 0.2). Variation in environmental conditions may favour vertical or horizontal transmission, especially if those conditions favour host asexual or sexual reproduction (which many brown algae can switch between). For example, a Phaeovirus provirus is segregated to one daughter chromosome during meiosis, meaning that 50 % of the next generation will be virus free (Figure 0.2, [78, 79]). To counteract this elimination of proviruses in sexually reproducing hosts, phaeoviruses may need to horizontally infect new hosts. In contrast, asexually reproducing hosts will reliably transmit latent proviruses to their progeny, reducing the need for horizontal transmission.

The impacts of phaeoviruses on host fitness are currently unknown. Phaeovirus infection had no negative effects on the growth or photosynthesis of *E. siliculosus* [87], but reduced the photosynthesis, chlorophyll content, and possibly growth of *Feldmannia* [88]. Impairment of host reproduction by phaeoviruses is a general observation and virtually no host impacts have been studied quantitatively [49]. Though *Feldmannia* can asexually reproduce after sterilisation by phaeoviruses, it is unknown how sterilisation would impact brown algae with different life histories [89, 90].

Phaeovirus infects seven species of brown algae, all belonging to four families of the order Ectocarpales, and it is the only phycodnavirus genus in which a single virus can infect multiple host families (Table 0.3). For example, EsV can infect *Feldmannia simplex* to cause symptoms and establish latency, but cannot produce virions [91, 92]. Similarly, Ectocarpus fasciculatus virus (EfasV) can infect *E. siliculosus* (but EsV cannot infect *E. fasciculatus*, [91]) and *Myriotrichia clavaeformis* [93], producing symptoms but not virions. However, EsV infection of *Kuckuckia kylinii* produced virions which could re-infect the original *E. siliculosus* host [94]. Inter-species infections have the potential to facilitate viral recombination and gene transfer between brown algal species, but their consequences in brown algae are unknown.

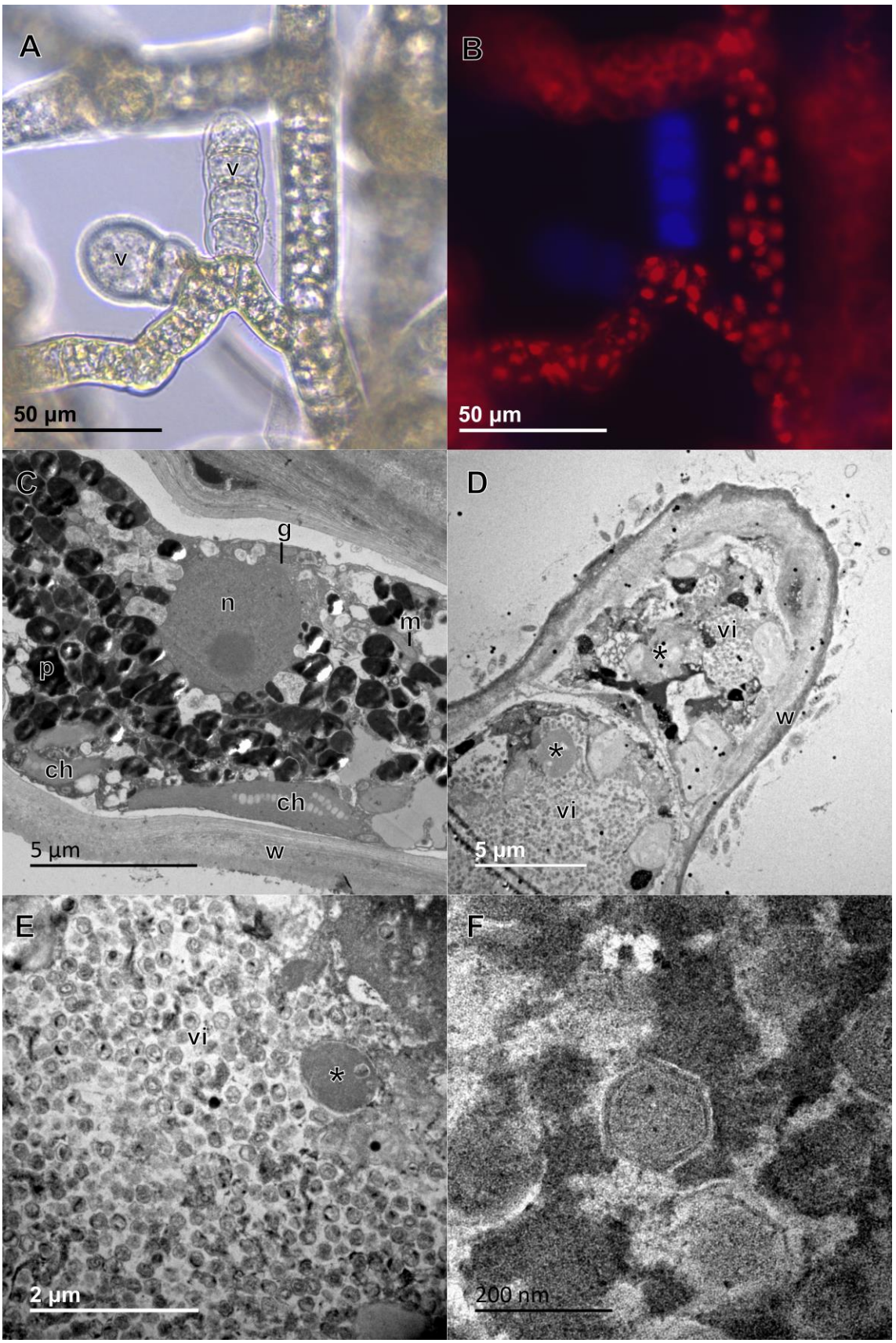
A
v
v
50 µm
B
50 µm
C
g
n
m
p
ch
ch
5 µm
w
D
vi
*
w
*
vi
5 µm
E
vi
*
2 µm
F
200 nm

Figure 0.3: Microscopic images of a Phaeovirus infection the Ectocarpales brown algae *Pylaiella littoralis*. Optical microscopy: (**A**) Virion-filled cells have grey and homogenous contents (**v**). Epifluorescent microscopy: (**B**) DAPI staining excited by UV light shows these cells to be completely filled with DNA (**blue**; this is DNA within the virions) and the absence of chlorophyll (**red**). Transmission electron microscopy: (**C**) Healthy brown algal cell with nucleus (**n**), chloroplasts (**ch**), mitochondria (**m**), golgi apparatus (**g**), physodes (**p**; dark vesicles), and thick cell wall (**w**); (**D** and **E)** virus infected brown algal cell with degenerated organelles (*****), masses of virions occupying the cytoplasm (**vi**; the darker nucleoprotein cores can be seen in some of the virions), and a thin cell wall (**w**); (**F**) Phaeovirus virions in the brown algal cytoplasm, showing the hexagonal cross-sections typical of icosahedral virions.

0.3.1 Phaeovirus Evolution

Based on concatenated phylogeny of DNA polymerase and major capsid protein (MCP), Ectocarpales phaeoviruses are split into two subgroups (Table 0.3); subgroup A consisting of one virus genotype, which infects *Ectocarpus*, *Pylaiella*, *Myriotrichia*, and *Hincksia*, and subgroup B, which consists of multiple viral genotypes and infects only *Feldmannia*. The genomes of subgroup B are smaller (from 240-336 kb in A to 155-220 kb in B), allowing the subgroup B phaeoviruses to exploit a more acute infection strategy, whereas subgroup A viruses have retained a more persistent strategy (Table 0.3, [95, 96]). The subgroup B phaeoviruses also have evolved at a similar rate to lytic phycodnaviruses (possibly facilitated by the loss of a DNA proofreading gene), giving them twice the DNA polymerase divergence rate of subgroup A and as a result, more variants [95]. Another consequence of subgroup B's infection strategy is multiple infections, the most extreme example being eight variants of latent phaeoviruses in a *Feldmannia simplex* genome. This is an exception to the superinfection exclusion hypothesis which posits that closely related viruses will exclude each other from infecting the same host [97]. It is unknown whether the subgroup A/B division is the result of subgroup A jumping hosts to *Feldmannia* or if it is the result of divergence from a common Phaeovirus ancestor that infected an ancient member of Ectocarpales.

0.3.2 Phaeovirus Genomes

The three sequenced phaeoviral genomes have the largest size range of all known *Phycodnaviridae* and highly divergent genes and structures (Table 0.3); Ectocarpus siliculosus virus 1 (EsV-1), Feldmannia species virus 158 (FsV-158), and Feldmannia irregularis virus 1 (FirrV-1). FsV-158 has the smallest genome of any phycodnavirus and has 81 less genes than EsV-1 [48, 98]. FsV-158 has lost the second most genes out of all *Mimiviridae* or *Phycodnaviridae* [33] and has retained only 10 out of 31 core genes (EsV-1 has 16 out of 31), which is the smallest known set of core genes able to make a functional NCLDV [98]. Phaeoviruses have the least compact phycodnavirus genomes (one gene per 900-1000 bp in most phycodnaviruses versus one gene per 1450 bp in EsV-1), with only 67 % of the EsV-1 genome encoding proteins. EsV-1 also has the highest GC content than chloroviruses or coccolithoviruses (52 % versus ~40 %) and lacks their introns and tRNAs [39].

Notable features of the EsV-1 genome include a large integrase-like protein and lysogeny regulators (likely involved in latency; [47]) a capsid protein (gp1) which resembles an alginate synthesis protein (mannuronan C-5-epimerases), and unique hybrid histidine kinases homologous to cellular enzymes of two-component signalling pathways (may alter the cell environment to facilitate infection; [99]). Phaeovirus genomes are highly divergent; for example EsV-1 (231 genes) and FirrV-1 (156 genes) share only 93 genes with very different orders. Despite infecting closely related hosts using similar infection strategies, these viruses have experienced high recombination since their divergence [37].

Table 0.3: Virion size, genomes, host range, evolutionary strategies of Ectocarpales Phaeovirus subgroups A and B. ND = no data; genome not sequenced.

Virus	Virion diameter (nm)	Genome size (kb)	Host family	Replication	No. of genotypes	Ref.
Subgroup A: Single infections, Persistent, K-selected, evolutionary strategy						
Ectocarpus siliculosus virus 1 (EsV-1)	130-150	336	Ectocarpaceae	Sporangia and gametangia	1	[49, 100, 101]
Ectocarpus fasciculatus virus 1 (EfasV-1)	135-140	320 (ND)	Ectocarpaceae	Sporangia and gametangia	1	[49, 50, 101]
Pylaiella littoralis virus 1 (PlitV-1)	130-170	280 (ND)	Acinetosporaceae	Sporangia	1	[49, 52, 101]
Hincksia hincksiae virus 1 (HincV-1)	140-170	240 (ND)	Acinetosporaceae	Sporangia	1	[49, 50, 101]
Myriotrichia clavaeformis virus 1 (MclaV-1)	170-180	320 (ND)	Chordariaceae	Sporangia	1	[49, 50, 101]
Subgroup B: Multiple infections, Acute, *r*-selected, evolutionary strategy						
Feldmannia simplex virus 1 (FlexV-1)	120-150	220 (ND)	Acinetosporaceae	Sporangia	8	[49, 50, 101]
Feldmannia irregularis virus 1 (FirrV-1)	140-167	158-178	Acinetosporaceae	Sporangia	3	[48, 49, 101]
Feldmannia species virus 158 (FsV-158)	150	170	Acinetosporaceae	Sporangia	2	[49, 98, 101]

0.3.3 Phaeovirus Host Genome Integration

Known phaeoviruses most likely persist as integrated proviruses, as EsV-1 DNA co-migrates with high molecular weight host DNA, indicating genome integration [76]. The mechanisms of this integration are not well understood, for example; it is unknown whether integration occurs at a specific or random site. FsV integrates at specific sites of the host genome [102], but this has not been studied in other phaeoviruses. It is also unknown whether phaeoviruses integrate as a single intact viral sequence or as multiple fragments throughout the host genome.

A single EsV-1-like provirus is integrated in the genome of *Ectocarpus siliculosus* (strain Ec32) with terminal repeat positions, which indicate that the provirus was

inserted as a circular genome. The provirus is 310 kb long (EsV-1 is 336 kb), has a GC content of 51 % (EsV-1 is 51 %, *E. siliculosus* genome is 53.6 %), shares 75 % of EsV-1 genes (173 out of 231 of EsV-1 orthologs), and has its lost histidine protein kinases and gained a FirrV-1-like gene. Provirus Ec32 has all EsV-1 NCLDV core genes and most key life cycle genes [103], but its integrase (3.4 kb, 97 % shared DNA identity with EsV-1 integrase) has undergone an unexplained relocation to another site in the host genome and been replaced by another integrase (70% shared DNA identity with EsV-1 integrase). Viral sequences were rare elsewhere in the *E. siliculosus* genome, which suggests there are barriers to phaeoviral gene transfer to brown algal genomes [103]. Unexpectedly, the provirus Ec32 was not functional; it was transcriptionally silent and did not produce virions, even under stress or at any life history stage, despite a lack of host suppression by RNA silencing of viral DNA [103]. This may be due to the loss of key genes, such as integrase or histidine kinases, as was observed in FsV with a large (>50 kb) repetitive insert in its protein kinase which prevented viral expression [104]. However, untested environmental or cell factors may have been capable of inducing virion production.

In contrast to strain Ec32, the *E. siliculosus* strain NZVicZ14 produces functional EsV-1 virions but its only known provirus is scattered throughout the host genome as short fragments (average length 35 kb), three of which totalled ~150 kb [105]. This suggests that phaeoviruses employ a novel and complex system of recombination, possibly using a large integrase/recombinase protein, to reassemble fragmented proviruses into complete viral genomes to be packaged into virions. A similar mechanism (post-transcription, horizontal recombination of RNA or DNA) has been proposed for the reverse-transcribing dsDNA viruses of plants (*Caulimoviridae*), which can reconstruct functional and infectious virus genomes from multiple EVEs spread

throughout the host genome, as well as from intact proviruses [106]. Such recombination may also explain the ability of FsV to produce virions with different genomes sizes depending on temperature (more 158 kb at 18-20 ^{o}C, more 178 kb at 5-10 ^{o}C; [90]). However, the provirus fragments identified did not comprise a complete EsV-1 genome and were highly dissimilar to the EsV-1 genome. It is therefore possible that the observed infection actually originated from an intact and functional provirus elsewhere in the genome of strain NZVicZ14.

It remains unknown whether Phaeovirus proviruses integrate as single or multiple fragments, because of the contradictory observations of an intact, but non-functional, provirus in strain Ec32 and a fragmented, but possibly functional, provirus in strain NZVicZ14. The unique evolutionary patterns, genomes, and integration of phaeoviruses are not well understood, but they suggest these unusual pathogens may play unexpected roles in brown algal biology, such as contributing novel genes and regulatory functions to their hosts.

0.4 Comparing the Viruses of Macroalgae and Plants

"Seaweeds are not wet trees and marine herbivores are not soggy insects" - Hay & Steinberg 1992 [107].

It has been previously argued that because marine macroalgae (red, Rhodophyta; green, Chlorophyta; and brown, Phaeophyceae; also known as seaweeds) and terrestrial plants (Embryophyta) have distinct evolutionary histories, biochemistry, morphology, and environments, they therefore have evolved distinct interactions with herbivores [107]. This is also likely true of their viruses, in other words; the viruses of marine macroalgae are probably not just 'soaked plant viruses'. The large evolutionary distance between the Archaeplastida (land plants, green and red macroalgae) and the

brown macroalgae (Stramenopila, SAR clade) may have driven the evolution of especially distinct virus-host relationships.

The major types of viruses are not uniformly distributed across host lineages, which probably reflects independent viral origins and close virus-host evolutionary relationships [108]. For example, the largest animal virus group (~38 %) has dsDNA genomes and most plant viruses (66.7 %) have ssRNA genomes, but no true (non-reverse transcribing, RT) dsDNA genomes (Table 0.4, [109]).

In contrast to plant viruses, most (67 %, Table 0.4) algal viruses have dsDNA genomes, mainly the NCLDV family *Phycodnaviridae* which infect distantly related algal lineages including green algae, haptophytes, and stramenopiles. Other algal virus groups include *Bacilladnaviridae* (ssDNA viruses of diatoms; Stramenopila), *Bacillarnavirus* (ssRNA viruses of diatoms), *Dinornavirus* (ssRNA viruses of dinoflagellates; Alveolata), *Marnaviridae* (ssRNA viruses of raphidophytes; Stramenopila), *Sedoreovirinae* (dsRNA viruses of chlorophytes), and *Pseudoviridae* (RT ssRNA viruses of chlorophytes) [40].

Plant viruses comprise about 42 % of all known viruses, with about 92 genera in 21 families [40, 109]. Though there may be over 100,000 species of algae [110], there are only a few hundred algal viruses described formally or mentioned in the literature [37]. Only 9 viruses have been described for the ~11,000 species of macroalgae (Table 0.4), which all belong to the genus Phaeovirus (*Phycodnaviridae*) and infect brown macroalgae. For macroalgal viruses, there are large knowledge gaps even in basic areas, such as what types of viruses infect macroalgae, what infection strategies they employ, what host impacts they have, or how macroalgal viruses are transmitted.

0.4.1 Viruses in Macroalgae

All the available evidence of viral infection in macroalgae is summarised in Table 0.5 (pre-2011) and Table 0.6 (post 2011). These data are comprised of transmission electron microscopy (TEM) observations of virus-like particles (VLPs), viral sequences isolated from macroalgae, and integrated viral sequences (endogenous viral elements, EVEs) in macroalgal genomes. Most VLPs in red macroalgae were small (<80 nm) and icosahedral; and therefore not distinctive enough to be identified. In contrast, the large (typically >150 nm) icosahedral VLPs reported in several brown and one green macroalgae likely belong to the distinctive NCLDVs.

Phaeoviruses infecting the order Ectocarpales are almost the only known macroalgal viruses and most VLPs observed in brown algae resembled phaeoviruses. Some of these observations suggest novel Phaeovirus infection strategies, such as replication in *Botrytella micromora* zoids (Ectocarpales; 170 nm VLPs [111]), *Ectocarpus fasciculatus* zoids within zoidangia (Ectocarpales; 170 nm VLPs, [112]), and *Halosiphon tomentosa* zoids (Stschapoviales; 170 nm VLPs, [113]). Damaging the cell walls by gently scraping adult *B. micromora* increased the infection rate of a putative Phaeovirus, and the infection may have spread between neighbouring cells [111]. In *Streblonema* (Ectocarpales), VLPs were observed frequently in vegetative cells (135-150 nm; [114]). These observations suggest that Phaeovirus infection strategies are more variable than is currently known. Outside of their currently known brown algal host range, phaeoviruses may replicate in other life history stages or cells (such as zoids or vegetative cells) or infect hosts through routes other than the zoids (such as damaged cell walls or connections between cells).

The only other VLPs observed in brown algae were filamentous VLPs that resembled ssRNA plant viruses of the genera *Tobamovirus* (25 by 280 nm) and *Potyvirus* (25 by 700-900 nm) in *Ecklonia radiata* (Laminariales, [115]).

Since a 2011 review ([101], Table 0.5), there have been only seven publications reporting viruses in macroalgae (Table 0.6; excluding 2 publications resulting from this thesis). These reports include VLPs and sequences of RNA viruses in red macroalgae (Rhodophyta) and *Phycodnaviridae* EVEs in the genomes and transcriptomes of red and brown macroalgae. No VLPs or viral sequences have been reported in green macroalgae (Chlorophyta) since 2011.

The sequence data provide a broader picture; NCLDV EVEs were common in brown macroalgae (1-10 EVEs per species from six orders, [116]) and in another study, all species screened (3/3) contained at least one NCLDV core gene [31]. The stramenopile lineage (to which the brown algae belong) contained the most NCLDV-positive organisms (19/66, [31]), but the green and red macroalgae contained few NCLDV EVEs [116] and neither contained NCLDV core genes (0/0 green and 0/2 red) [31]. Only two plants (out of ~110 genomes and 786 transcriptomes) contained NCLDV EVEs [31, 117]. This suggests that brown macroalgae are widely infected by NCLDVs, whereas the NCLDV EVEs in red macroalgae and plants may be remnants of ancient infections. The few metagenome studies of macroalgae found RNA virus sequences (mostly dsRNA) in 13 red macroalgae species (Table 0.6). These dsRNA were most closely related to the fungi-infecting genus *Totivirus* (family *Totivridiae*; infects protozoans and fungi).

In plants, most EVEs originate from *Caulimoviridae* (RT dsDNA, 68 species) and *Geminiviridae* (ssDNA, 447 species); whilst most brown macroalgal EVEs are from phaeoviruses. This means that plant and brown macroalgal genomes may have had distinct interactions with their respective viruses, leading to different consequences

for virus and host evolution. For example, caulimovirus and geminivirus EVEs probably integrate by random recombination of virus and host DNA during double-strand break repair in the nucleus, but phaeovirus EVEs are integrated by virus-encoded integrases as part of the viral life cycle [49, 118, 119].

There has been a single viral metagenome study of brown algae. Kelp (*Ecklonia radiata*) affected by a bleaching disease had an elevated abundance of *Circoviridae*-like sequences, possibly elevated due to bleaching-associated grazing by circovirus-infected invertebrates, as circoviruses are only known to infect animals. *Phycodnaviridae* sequences were equally present in healthy and bleached kelps and were the second most abundant viral group after bacteriophages. Most of the *Phycodnaviridae* sequences were related to EsV-1, but not described in any further detail [120].

Viral expression in macroalgae has been reported by a single study which was a transcriptome of the kelp *S. japonica*. 10.21 % of expressed genes in *S. japonica* sporophytes were of viral origin; in addition, 8.9 % of genes expressed differentially between sporophyte maturity stages were also of viral origin [121]. No disease phenotype was observed and the identities of these viral transcripts were not reported.

There are currently no formally described RNA viruses of any macroalgae, but RNA virus sequences have been identified in viral metagenomes of red macroalgae. Sequences and VLPs of ssRNA viruses (*Picornavirales*-like; viruses of plants, animals, and diatoms) and dsRNA viruses (*Totivirus*-like; viruses of fungi) have been detected in the red macroalgae *Delisea pulchra* [122]. *Totivirus* sequences have also been detected in *Chondrus crispus* and possibly eight other red macroalgae species [123]. However, whether these viruses infect red macroalgae or associated organisms is unknown.

There are two reports of possible viral disease in red macroalgae; green spot disease in *Pyropia* spp. (GSD; cell lysis leading to holes, complete disintegration of blade, and mortality, [124]) and galls in *Bostrychia simpliciuscula* [125].

In summary, the available evidence suggests that: 1) plants are infected by ssRNA and no true dsDNA viruses, 2) brown macroalgae and other stramenopile groups are infected by NCLDVs (dsDNA), 3) red macroalgae are infected by dsRNA viruses related to fungi viruses, and 4) Archaeplastida (plants, red and green macroalgae) was infected by NCLDVs in the past. Expanding this limited view of macroalgal virology would likely reveal novel evolutionary relationships between viruses and photosynthetic, multicellular hosts.

Table 0.4: Virus types present in Embryophyta (plants), Chlorophyta, Rhodophyta, and Phaeophyceae. References: (A) virus numbers [40, 109]; (B) reports (see Tables 0.5 and 0.6); multicellular species numbers: plants [126]; green, red, and brown macroalgae [110]. RT= reverse transcribing.

	Embryophyta (plants)	**Chlorophyta (green macroalgae)**	**Rhodophyta (red macroalgae)**	**Phaeophyceae (brown macroalgae)**
No. of multicellular species	~391,000	~2,000	~7,000	~2,000
(A) Virus species recognised by the ICTV				
dsDNA (%)	0	87.5	0	100
ssDNA (%)	23.4	0	0	0
dsRNA (%)	3.9	4.2	0	0
ssRNA (%)	66.7	0	0	0
RT (%)	1.7 (ssRNA) 4.5 (dsDNA)	8.3 (ssRNA)	0	0
Total % of all known viruses (n)	42 (1325)	0.76 (24)	0 (0)	0.29 (9)
% of multicellular host species with known viruses	0.34	0	0	0.45
(B) Uncharacterised reports of viruses in macroalgae				
Number of macroalgae species in which virus-like particles (VLPs)have been observed				
Unknown	-	1	8	0
dsDNA	-	0	0	11 (Phaeovirus)
ssDNA	-	0	0	0
dsRNA	-	1	1	0
ssRNA	-	0	1	2
RT (%)	-	0	0	0
Number of macroalgae species found to contain viral nucleic acids				
Unknown	-	0	0	1
dsDNA	-	12 (NCLDVs)	16 (NCLDVs)	14 (NCLDVs)
ssDNA	-	0	0	0
dsRNA	-	0	12	0
ssRNA	-	0	1	0
RT (%)	-	0	0	0

Table 0.5: Reports of virus-like particles (VLPs) and virus sequences found in macroalgae. Adapted from "Viruses of Seaweeds", Chapter 8 of Studies in Viral Ecology: Microbial and Botanical Host Systems, Volume 1 [101] with permission from https://www.wiley.com/en-gb. Copyright Wiley-Blackwell 2011. All rights reserved.

Phylum	Class	Order	Family	Species	Virus classification, genome type	Virion diameter or dimensions (nm) and morphology	Virus sequence data	Ref.
Charophyta	Charophyceae	Charales	Characeae	*Chara* sp.	Unclassified, *Furovirus*-like, ssRNA	18x532, rod shaped	ND	[127]
Chlorophyta	Chlorophyceae	Chaetophorales	Uronemataceae	*Uronema gigas*	Unclassified	390, icosahedral, tailed	ND	[128]
	Ulvophyceae	Bryopsidales	Bryopsidaceae	*Bryopsis* spp.	Unclassified, dsRNA	25-40, icosahedral	dsRNA	[129]
Rhodophyta	Porphyridiophyceae	Porphyridiales	Porphyridiaceae	*Porphyridium purpureum*	Unclassified	40, spherical/icosahedral	ND	[130]
	Florideophyceae	Batrachospermales	Batrachospermaceae	*Sirodotia suecica*	Unclassified	50-60, icosahedral	ND	[131]
		Gracilariales	Gracilariaceae	*Gracilaria epihippisora*	Unclassified	80, icosahedral	ND	[132]
		Acrochaetiales	Acrochaetiaceae	*Audouinella saviana*	Unclassified	40x1000, rod shaped	ND	[133]

Table 0.5 (continued)

Phylu	Class	Order	Family	Species	Virus classification, genome type	Virion diameter or dimensions (nm) and morphology	Virus sequence data	Ref.
Ochrophyta	Phaeophyceae	Ectocarpales	Ectocarpaceae	*Ectocarpus siliculosus*	EsV-1, Phaeovirus, dsDNA	130-150, icosahedral	336 kb genome, fully sequenced	[100]
				Ectocarpus fasciculatus	EfasV-1, Phaeovirus, dsDNA	135-140, icosahedral	320 kb genome, ND	[50]
			Acinetosporaceae	*Feldmannia simplex*	FlexV-1, Phaeovirus, dsDNA	120-150, icosahedral	220 kb genome, ND	[50]
				Feldmannia irregularis	FirrV-1, Phaeovirus, dsDNA	140-167, icosahedral	180 kb genome, fully sequenced	[48]
				Feldmannia sp.	FsV-158, Phaeovirus, dsDNA	150, icosahedral	170 kb genome, fully sequenced	[98]
				Hincksia hincksiae	HincV-1, Phaeovirus, dsDNA	140-170, icosahedral	240 kb genome, ND	[50]
				Pylaiella littoralis	PlitV-1, Phaeovirus, dsDNA	130-170, icosahedral	280 kb genome, ND	[52]
			Chordariaceae	*Myriotrichia clavaeformis*	MclaV-1, Phaeovirus, dsDNA	170-180, icosahedral	320 kb genome, ND	[50]
				Streblonema sp.	Unclassified, Phaeovirus-like	135-150, icosahedral	ND	[114]
				Botrytella micromora	Unclassified, Phaeovirus-like	170, icosahedral	ND	[111]

Table 0.5 (continued)

Phylum	Class	Order	Family	Species	Virus classification, genome type	Virion diameter or dimensions (nm) and morphology	Virus sequence data	Ref.
Ochrophyta	Phaeophyceae	Stschapoviales	Halosiphonaceae	*Halosiphon tomentosa*	Unclassified, Phaeovirus-like	170, icosahedral	ND	[113]
		Laminariales	Lessoniaceae	*Ecklonia radiata*	Unclassified, *Tobamovirus*-like, ssRNA	25x280	ND	[115]
					Unclassified, *Potyvirus*-like, ssRNA	25x700-900	ND	

Table 0.6: Reports of virus-like particles (VLPs) and virus sequences found in macroalgae, since the 2011 review [101].

Phylum	Class	Order	Family	Species	Virus classification, genome type	Virion size (nm) and morphology	Virus sequence data	Ref.
Rhodophyta	Bangiophyceae	Bangiales	Bangiaceae	*Pyropia/ Porphyra* sp.	Unclassified, dsRNA	ND	Viral metagenome	[123]
				Pyropia spp.: *P. dentata* *P. tenera*	Unclassified	100, spherical, dark stained	ND	[124]
				Pyropia yezoensis	Unclassified	100, spherical, dark stained	ND	[124]
					Phycodnaviridae	ND	8 EVEs	[116]
				Laurencia pinnatifida	Unclassified, dsRNA	ND	Viral metagenome	[123]
				Neosiphonia japonica	*Phycodnaviridae*	ND	1 EVEs	[116]
				Polysiphonia elongata	Unclassified, dsRNA	ND	Viral metagenome	[123]
	Cyanidiophyceae	Cyanidiales	Cyanidiaceae	*Cyanidioschyzon merolae*	*Phycodnaviridae*	ND	6 EVEs	[116]

Table 0.6 (continued)

Phylum	Class	Order	Family	Species	Virus classification, genome type	Virion size (nm) and morphology	Virus sequence data	Ref.
Rhodophyta	Florideophyceae	Bonnemaisoniales	Bonnemaisoniaceae	*Delisea pulchra*	Unclassified *Picornavirales*, ssRNA	30, hexagonal, *Picornavirales*-like	Viral metagenome	[122]
					Unclassified, *Totivirus*-like, dsRNA	40, hexagonal, *Totivirus*-like		
		Ceramiales	Rhodomelaceae	*Bostrychia simpliciuscula*	Unclassified	70-75, spherical, dark stained	ND	[125]
					Unclassified	70-75, hexagonal		
	Bangiophyceae	Gigartinales	Dumontiaceae	*Dumontia contorta*	Unclassified, dsRNA	ND	Viral metagenome	[123]
				Dumontia simplex	*Phycodnaviridae*	ND	1 EVEs	[116]
			Endocladiaceae	*Gloiopeltis furcata*	*Phycodnaviridae*	ND	1 EVEs	[116]
			Gigartinaceae	*Chondracanthus acicularis*	Unclassified, dsRNA	ND	Viral metagenome	[123]
				Chondrus crispus	*Phycodnaviridae*	ND	2 EVEs	[116]
					Unclassified, *Totivirus*-like, dsRNA	ND	Viral metagenome	[123]

Table 0.6 (continued)

Phylum	Class	Order	Family	Species	Virus classification, genome type	Virion size (nm) and morphology	Virus sequence data	Ref.
Rhodophyta	Bangiophyceae	Gigartinales	Gigartinaceae	*Mazzaella japonica*	*Phycodnaviridae*	ND	2 EVEs	[116]
			Phyllophoraceae	*Ahnfeltiopsis flabelliformis*	*Phycodnaviridae*	ND	2 EVEs	[116]
				Mastocarpus stellatus	Unclassified, dsRNA	ND	Viral metagenome	[123]
			Solieriaceae	*Eucheuma denticulatum*	*Phycodnaviridae*	ND	1 EVEs	[116]
			Furcellariaceae	*Furcellaria lumbricalis*	Unclassified, dsRNA	ND	Viral metagenome	[123]
		Gracilariales	Gracilariaceae	*Gracilaria* spp.: *G. blodgettii* *G. chouae* *G. lemaneiformi* *G. vermiculophylla*	*Phycodnaviridae*	ND	1-4 EVEs per species	[116]

Table 0.6 (continued)

Phylum	Class	Order	Family	Species	Virus classification, genome type	Virion size (nm) and morphology	Virus sequence data	Ref.
Rhodophyta	Bangiophyceae	Halymeniales	Halymeniaceae	*Grateloupia catenata*	*Phycodnaviridae*	ND	2 EVEs	[116]
				Grateloupia chiangii	*Phycodnaviridae*	ND	3 EVEs	[116]
				Grateloupia turuturu	*Phycodnaviridae*	ND	1 EVEs	[116]
					Unclassified, dsRNA	ND	Viral metagenome	[123]
		Palmariales	Palmariaceae	*Palmaria palmata*	Unclassified, dsRNA	ND	Viral metagenome	[123]

Table 0.6 (continued)

Phylum	Class	Order	Family	Species	Virus classification, genome type	Virion size (nm) and morphology	Virus sequence data	Ref.
Ochrophyta	Phaeophyceae	Desmarestiales	Desmarestiaceae	*Desmarestia viridis*	*Phycodnaviridae*	ND	5 EVEs	[116]
		Dictyotales	Dictyotaceae	*Dictyopteris undulata*	*Phycodnaviridae*	ND	4 EVEs	[116]
		Ectocarpales	Chordariaceae	*Cladosiphon okamuranus*	Phaeovirus	ND	5 NCLDV core genes	[31]
			Ectocarpaceae	*Ectocarpus siliculosus*	*Phycodnaviridae*	ND	172 EVEs	[116]
					Phaeovirus	ND	5 NCLDV core genes	[31]
			Scytosiphonaceae	*Colpomenia sinuosa*	*Phycodnaviridae*	ND	6 EVEs	[116]
				Scytosiphon lomentaria	*Phycodnaviridae*	ND	10 EVEs	[116]
		Fucales	Sargassaceae	*Sargassum* spp.: *S. fusiforme* *S. hemiphyllum* *S. horneri* *S. integerrimum* *S. thunbergii* *S. vachellianum*	*Phycodnaviridae*	ND	3-5 EVEs Per species	[116]
		Ishigeales	Ishigeaceae	*Ishige okamurai*	*Phycodnaviridae*	ND	3 EVEs	[116]

Table 0.6 (continued)

Phylum	Class	Order	Family	Species	Virus classification, genome type	Virion size (nm) and morphology	Virus sequence data	Ref.
Ochrophyta	Phaeophyceae	Laminariales	Lessoniaceae	*Ecklonia radiata*	Unclassified, *Circoviridae*-like, ssDNA	ND	Viral metagenome	[120]
					Unclassified, Phaeovirus-like	ND		
			Laminariaceae	*Saccharina japonica*	Phaeovirus	ND	1 NCLDV core gene	[31]
					Phycodnaviridae	ND	1 EVEs	[116]
					Unclassified	ND	8.9-10.21 % of transcripts were of viral origin	[121]
				Saccharina sculpera	*Phycodnaviridae*	ND	5 EVEs	[116]

0.4.2 Independent Evolution of Plant and Macroalgal Viruses

Most major virus lineages (+ and - sense ssRNA, dsRNA, ssDNA, dsDNA, and RT) probably originated before the origin of eukaryotes or their major supergroups, because most major virus groups infect multiple eukaryotic supergroups [134, 135]. Assuming that the early ancestors of Archaeplastida and the SAR clade were exposed to the same major virus lineages; have distinct virus-host relationships evolved in the plant and macroalgal lineages?

Complex multicellularity has evolved independently in land plants, green macroalgae, red macroalgae, and brown macroalgae. Brown macroalgae are very distantly related to Archaeplastida and are the only members of the SAR clade with complex multicellularity. Brown macroalgae have become important to evolutionary and molecular biology due to their unique signalling systems, halogen metabolism, photosynthesis pathways and pigments, cell walls, carbohydrate synthesis and storage,

lipid metabolism, and cell cycles [136–139]. Like their hosts, the viruses of these lineages may have also evolved independently, especially when comparing the brown macroalgae with Archaeplastida.

At some point during the transition from unicellular green algae to plants, NCLDVs may have been excluded from land plants [117]. Viruses cannot pass through intact cell walls, so they must bypass this barrier by using 1) vectors, 2) virus-encoded cell wall degrading enzymes, 3) entering through already damaged cell walls or 4) vertical transmission via host reproduction [109]. Most (~75 %) NCLDV hosts may be from aquatic environments, possibly because virus particles as large as those of NCLDVs may not be able to disperse effectively in terrestrial environments [31]. These two limitations could have excluded NCLDVs from land plants as they evolved walled dispersal stages and moved from aquatic to terrestrial habitats. The NCLDV-like sequences in lycophytes and bryophytes are probably remnants of NCLDV infections in green algae [117], whilst NCLDVs may continue to infect marine macroalgae due to their aquatic environments and unwalled dispersal stages (Table 0.7).

A key difference between plants and macroalgae is the complexity of their multicellularity. For example, the number of cell types decreases from land plants through brown macroalgae, red macroalgae, and finally green macroalgae (Table 0.7). In addition, all plant body plans are parenchymatous, whereas macroalgae can have simpler pseudoparenchymatous, filamentous or siphonous forms (Table 0.7).

Plasmodesmata and vascular tissue are structural features which have clear implications for viral infections. In plants, viruses can move short distances between adjacent cells through the plasmodesmata, often using virus-encoded proteins. Viruses usually move between cells to reach the vascular tissue, which rapidly carries viruses to many locations within the host. This long distance movement is vital for most plant

viruses, as it allows them to achieve more effective 'systemic' infections, rather than be restricted to the initially infected cells [109]. Similar short distance transport of viruses in red macroalgae would be restricted by the absence of plasmodesmata, whilst similar long distance transport of viruses would be restricted in most macroalgae, due to the absence of vascular tissue (Table 0.7). Long distance transport would be possible in some brown macroalgae which have vascular tissue (sieve tubes), such as kelps, but these sieve tubes are less extensive than the xylem and phloem of plants [140, 141]. This exemplifies how the independently-evolved multicellularity of plants and macroalgae may have created different virus-host interactions. Macroalgal viruses may have evolved ways of achieving systemic infections not known in plant viruses.

The presence or absence of vascular tissue also has implications for virus transmission between hosts. The vast majority of plant viruses bypass host cell walls using vectors, which are mostly specialist herbivorous insects which pierce the plant vascular tissue and suck out nutrition (piercing/sucking feeding mode). These vectors are highly effective because they mostly feed on specific plants (90 % of insect herbivores feed on around 3 plant families [142]) and they deliver viruses directly into the vascular tissue, which favours systemic infections. Their effectiveness is shown by the rarity of plant virus vectors with chewing feeding modes [109, 143]. In marine systems, insects are absent and the dominant marine herbivores include sea urchins, gastropods, crustaceans, and fish [107]. In contrast to insect herbivores, most marine herbivores are generalists which feed on 10 to >20 macroalgae families and also consume detritus and animals, usually by chewing or rasping feeding modes (Table 0.7; [107, 142]. Therefore, to use marine herbivores as vectors, macroalgal viruses may have evolved different strategies to plant viruses, such as novel ways of moving

between host cells or persisting in vectors. Alternatively, macroalgal viruses may be more reliant on other transmission routes, such as non-herbivore vectors, the abiotic environment, or latent proviruses.

0.4.3 Distinct Environments of Plant and Macroalgal Viruses

How have the contrasting abiotic and biotic environments of land plants and marine macroalgae shaped the evolution of their respective virus-host relationships? The routes of aquatic virus transmission are not well understood, especially those involving vectors. One of the few known examples of marine virus transmission vectors are planktonic crustaceans carrying EhVs over many kilometres [144]. Macroalgae are infected by a range of poorly understood pathogens including fungi, nematodes, oomycetes, protozoans, bacteria, and macroalgae [145–148]. Most of these pathogens have some mechanical or chemical means to penetrate cell walls and potentially act as viral vectors.

A notable interaction which is more common in marine versus terrestrial systems is epibiosis (organisms living attached to the surfaces of other organisms). Aquatic environments more reliably provide nutrients and prevent desiccation, which makes most available surfaces possible habitats for epibiotic organisms [149], whilst terrestrial epibiotes are restricted to humid climates [150]. This is why terrestrial epibiosis is restricted to a few groups (mosses, lichens, unicellular algae, and some seed plants), whilst most marine phyla have many members with epibiotic life history phases [150]. Macroalgae are colonised by diverse invertebrates, microbes, unicellular algae, and other macroalgae [151], which could transmit viruses by shedding adsorbed viruses near wounds or abrasions on macroalgae.

Transmission without vectors may be more important for macroalgal viruses. There only are a few examples of plant viruses being spread without vectors, such as clothing in cultivated systems, direct plant to plant contact, contact with virus-contaminated soil, fluids ejected from leaf pores (guttation), water in hydroponic systems [109], and possibly aquatic environments [109, 152]. About 25 % of plant viruses can infect the pollen or embryo and subsequently be transmitted through seeds; vertical transmission via genome integration is only known in the *Caulimoviridae* [109]. Phaeoviruses employ a latent infection strategy to infect brown macroalgae, but whether this is representative of macroalgal viruses is unknown.

One of the few examples of virus transmission by physical means is EhVs transmitted by seawater aerosols [153]. Aquatic virus transmission is not well understood, but aquatic systems are more favourable than terrestrial ones for virus transmission without vectors. This may be because pathogens can survive or remain infective longer in water than in air, and coastal organisms have more linear distributions (especially macroalgae, due to depth/light constraints or aquaculture practices) [154, 155]. Aquatic environments are also more favourable to the passive diffusion of viruses without adsorption onto vectors or abiotic particles. Favourable micro-currents in laboratory cultures can increase virus infection rates [156], but in natural environments this could be an unreliable transmission route for macroalgal viruses. If transmitted by diffusion or currents, the number of virions required to achieve sufficient infection rates increases as susceptible host density decreases. One analogous example of this is the pollination of seagrasses: when pollen was dispersed by passive diffusion alone, pollinations rates decreased once male and female flowers were >20 cm apart. The addition of small marine invertebrates allowed the pollination rate to remain unchanged, even in seagrass flowers 150 cm apart. This was because

the invertebrates moved actively between the seagrass flowers with pollen attached to their body surfaces [157]. For the viruses of macroalgae or aquatic plants, passive diffusion may be reliable when susceptible hosts are densely distributed and vectors may become more important when susceptible hosts are sparsely distributed.

If an algal virus is dispersed without a vector and lacks any cell wall-degrading enzymes (only known in Chlorovirus; [59]) or mechanisms, then it must randomly contact already damaged cell walls of its target host, which seems unlikely. This may be why the same environmental and cell factors induce Phaeovirus replication and host reproduction, to maximise the chance of viruses infecting susceptible unwalled host zoids (phaeoviruses cannot infect the walled adult cells) [158]. Random passive diffusion is therefore advantageous for phaeoviruses because they produce virions when susceptible host zoids are densely distributed. Without this synchronisation with host reproduction, the chance of virions encountering host zoids may be too low to maintain the virus-host relationship. Though phaeoviruses may not be representative of macroalgal viruses, they are an example of how the unique selective pressures of their marine environment and macroalgal hosts have led to novel viral evolutionary strategies which do not exist in terrestrial plants.

Table 0.7: The features of plants and macroalgae relevant to viral infection. This includes evolutionary lineages, divergence times (bya), habitat, morphological and life history traits, and associated organisms. References: Morphological traits - plants [159, 160], charophytes [140, 161], and macroalgae [140, 141]; number of cell types [162, 163]; life history dispersal stages [140, 160, 164]; main virus vectors [109]; grazer feeding modes and main grazer groups [107, 142, 165, 166]; Epibiotes [149–151, 167]; evolutionary divergence times: last common ancestor of eukaryotes, SAR clade, and Archaeplastida [168], Chromista [169], Ochrophyta [170], red and green macroalgae, charophytes, and all embryophyte land plants [160, 168], and brown macroalgae [171, 172]. Y = yes, N = no, ND = no data (found by this review), - = unknown, na = not applicable, M = male, F = female, P/S = piercing/sucking.

	Last common ancestor of eukaryotes 1.9-1.7 bya						
	SAR clade 1.5 bya	**Archaeplastida** 1.5 bya					
	Chromista ~0.75 bya						
	Ochrophytes ~0.5 bya			**Streptophytes** 1-0.8 bya			
					Embryophytes 0.47 bya		
	Phaeophytes (brown macroalgae) 0.26 bya	**Rhodophytes** (red macroalgae) 1.4-1.2 bya	**Chlorophytes** (green macroalgae) 1-0.8 bya	**Charophytes** (green macroalgae) 1-0.8 bya	**Bryophytes** (non-vascular, seedless plants 0.47 bya	**Lycophytes & Polypodiopsida** (vascular, seedless plants) 0.44 bya	**Spermatophytes** (vascular, seed plants) 0.4-0.3 bya
Primary habitat							
Terrestrial					Y	Y	Y
Freshwater				Y			
Marine	Y	Y	Y				
Morphology							
Siphonous			Y				
Filamentous	Y	Y	Y	Y			
Pseudo-parenchymatous	Y	Y	Y				
Parenchymatous (simple)[1]		Y	Y	Y			
Parenchymatous (complex)[2]	Y				Y	Y	Y
Vascular tissue	Y[3]					Y	Y
Plasmodesmata	Y		Y[4]	Y	Y	Y	Y
Average no. of cell types (range)	9 (3-14)	5 (1-9)	2 (1-3)	ND	23 (20-25)	23 (20-25)	63 (25-100)
Life history							
Dispersal medium of reproductive cells:							
Air					Y	Y	Y
Freshwater				Y	Y[5]	Y[5]	
Seawater	Y	Y	Y				
Do cell walls protect the reproductive cells?							
Male gametes	N	N[6]	N[7]	N[7]	N	N	Y[9]
Female gametes	N	Y[8]	N[7]	Y[8]	Y[8]	Y[8]	Y[8]

Spores	N	N	N	na	Y	Y	na
Associated organisms							
Main virus vectors	-	-	-	-	-	-	P/S insects
Grazer feeding modes	*Generalist*: Chewing Rasping P/S[10]			ND	*Specialist*: Chewing Rasping	*Specialist*: Chewing Rasping P/S	*Specialist*: Chewing Rasping P/S
Main grazer groups	Fish, sea urchins, gastropods, crustaceans			ND	Insects, mammals, gastropods		
Epibiotes	Bacteria, protozoans, diatoms, macroalgae, bryozoans, echinoderms, sponges, worms, crustaceans, ascidians, cnidarians			ND	Unicellular algae, lichens, mosses, seed plants		

Table 0.7 Footnotes:
[1] Cells are arranged in 1-2 rows.
[2] Cells are differentiated into multiple specialised tissues.
[3] A minority of brown macroalgae (such as the Laminariales) have vascular tissue (called sieve tubes).
[4] A minority of green macroalgae consist of a single large multinucleate cell (siphonous).
[5] The male gametes of seedless plants swim through rain or melt water.
[6] Cells are covered with a layer of mucilage comprised of sulfated polysaccharides.
[7] In some species, these cells are covered with a layer of calcified scales.
[8] Reproductive cells are unwalled, but retained inside walled reproductive structures on adult.
[9] Male plant gametes are unwalled, but protected by walled gametophyte (pollen).
[10] The only known piercing/sucking macroalgal herbivores are the ascoglossan gastropods, which feed on siphonous (see [4]) green macroalgae.

0.4.4 Human Influences on the Viruses of Plants and Macroalgae

Since the 'Green Revolution' of the middle twentieth century, large scale agriculture has changed the environment for plant viruses in various ways, such as novel interactions between cultivated and natural systems, or the transportation of plants, vectors, and viruses outside of their native ranges. Viruses cause major losses of terrestrial crops and various methods are used to control plant viruses, such as reducing insect vectors with pesticides [109]. Many plant viruses have adapted to cultivated plants, as these hosts are often genetically uniform and densely spaced. This has resulted in the selection of more virulent viruses, leading to the emergence of

many destructive viral diseases in agriculture, exemplified by the increasing levels of disease from wild, to semi-wild, to cultivated plant populations [173].

The 'Blue Revolution' of aquaculture is currently ongoing and includes a transition from Asia-dominated aquaculture and wild harvest practices to global, large scale macroalgal aquaculture [174]. Global macroalgal aquaculture production has more than doubled since 2000 and currently comprises about 30 % of global marine aquaculture production [175, 176]. However, this is still only 0.3 % of the annual production of terrestrial agriculture [175]. The domestication of macroalgae is also in its early stages, but similar problems have emerged as with cultivated plants, such as decreased genetic diversity and disease emergence (either unknown, bacterial, or protist pathogens, [145, 177, 178]. Further novel macroalgal diseases and interactions between wild and cultivated macroalgae have been predicted to emerge [179]. Whether the intensification of cultivation will alter virus relationships with macroalgae in similar ways as seen in plants is a major knowledge gap in understanding of sustainable cultivation systems and viral evolution.

The majority of wild plant viruses may be symptomless [180, 181] and have been overlooked by 120 years of plant virology in favour of the disease-causing viruses of economically important crops, which are the majority of known plant viruses [40, 182] [183]. Over 40 years of genetic and biochemical studies of plants and their viruses have provided detailed understanding of their mechanisms and host interactions [109]. These fields are less developed for algae, but are advancing quickly. These are important, but early stage, developments for the future of macroalgal domestication, conservation, disease control, and genetic modification [184]. Macroalgal virology has yet to begin in earnest (Tables 1.4-1.6) and must be expanded to meet the challenge of emerging viral diseases in ecosystems and expanding macroalgal aquaculture.

0.5 The Brown Macroalgae

The brown algae (kingdom Chromista which is synonymous with Heterokonta or stramenopiles, phylum Ochrophyta/Heterokonta, class Phaeophyceae; [185] are macroalgae which diverged from the Plantae lineage (plants, green and red algae) 1.5 billion years ago [186] and since then the brown algae and Plantae have independently evolved complex multicellularity. This has given brown algae unique metabolism, physiology, cellular structures, cell walls, polysaccharides, and developmental processes [136, 137]. Brown algae diverged from their closest relatives (class Schizocladiophyceae) around 260 Ma (Figure 0.5; [171, 172]). The first (basal) brown algal orders had isomorphic life histories and the derived orders (10/17 of brown algal orders) with heteromorphic life histories evolved later during the 'Brown Algal Crown Radiation' 110-155 Ma (BACR; Figure 0.5; [172]). Brown algal evolution has many unresolved relationships and their evolution in general is not well understood [171]. There are currently around 2,000 recognised species and 300 genera of brown algae [110].

0.5.1 Brown Macroalgal Morphology

Brown macroalgal morphologies range from uniseriate filaments (filamentous) or compacted filaments (pseudoparenchymatous), to differentiated tissues (parenchymatous). Growth occurs from the meristem, which is either terminal (at the ends) or intercalary (at the middle or base). The stramenopile chloroplast of brown algae has four membranes and originated from a secondary endosymbiotic event [187, 188]. The thylakoids have three layers and a girdle lamella and most species lack pyrenoids (storage extension of the chloroplast). The endoplasmic reticulum envelops the chloroplasts (multiple or singular per cell) and nucleus. The photosynthetic

pigments are fucoxanthin, carotenes, violaxathin, and chlorophylls *a*, *c*, and c_1. The main carbohydrates used for storage are laminaran (contains glucose and mannitol) and for cell walls are alginates, fucoidan/fucan (sulfated polysaccharides), and cellulose. Alginates may provide flexible structural support and desiccation resistance, whilst sulfated polysaccharides may provide desiccation resistance and defence. The cell walls have channels called plasmodesmata which connect the cytoplasms of neighbouring cells. Brown algae have small membrane-bound vacuoles called physodes which contain phenolic compounds possibly used in defence against herbivores, oxidative stress, and UV radiation [187].

0.5.2 Brown Macroalgal Ecology

Brown algae are almost exclusively marine, often dominating intertidal and subtidal coastal zones worldwide, in polar, cold to warm temperate, and sub-tropical waters. They usually live attached to rocks, but also artificial structures, other macroalgae, and some species are free-floating [187].

The only characterised macroalgal viruses infect the order Ectocarpales, a group of ~775 species in 203 genera [110], which are small filamentous, pseudoparenchymatous, or parenchymatous macroalgae. The Ectocarpales member *Ectocarpus siliculosus* is a model organism for molecular and genetic studies of brown algae [103, 189], as it has a short life history (three months; Figure 0.4), is easily genetically crossed, and has a smaller genome than other brown algae (200 Mb vs 640 Mb in *Laminaria digitata*; [190]). The genus *Ectocarpus* is distributed worldwide in temperate marine waters from the high intertidal to the sublittoral and sometimes occurs in freshwater and brine environments. Wild *Ectocarpus* can grow up to 30 cm in length and colonise a range of surfaces including other macroalgae and artificial

materials, making it a common fouling species [137, 189]. Though their ecology is not well studied, small brown algae are important primary producers; for example a single bloom of *Colpomenia* (Ectocarpales) may have exported 0.2-0.8 % of the daily oceanic carbon flux [191].

The closest relatives to Ectocarpales are kelp of the order Laminariales (Figure 0.5; diverged 76-107 Ma; [172]). Kelp can refer to any large brown algae, but here it refers to the order Laminariales, which comprises ~144 species in 61 genera [110]. Kelp sporophytes have the greatest size (1-50 metres long), complexity, and longevity (1-25 years) of any macroalgal thalli [187, 192]. Kelp sporophytes are differentiated into outer meristoderm, inner cortex, central medulla, and (in derived kelp) vascular tissues. The sporophyte body plan is further differentiated into a blade (analogous to leaves), stipe (analogous to stem), and secured to substrate by a holdfast. Growth occurs from an intercalary meristem (at junction of stipe and blade) and the meristoderm (thickens the sporophyte) and sporophytes reach maturity after 1-6 years [193, 194]. The kelp life history is shown in Figure 0.4; per m^{-2} per yr^{-1}, 3 mature kelp sporophytes produce 20 billion meiospores, which become 1 million gametophytes, which finally generate one mature sporophyte (example is of *L. digitata*; [195]). Unless carried by currents, kelp have very limited dispersal and the meiospores must settle at high densities to achieve fertilisation (1-10 per mm^2; [196]). Kelp are self-fertile [197] and synchronise meiospore release which may reduce inbreeding [196, 198]. In laboratory cultures, kelp hybrids can be produced by intergeneric crosses, but whether such hybrids occur naturally is unknown [199].

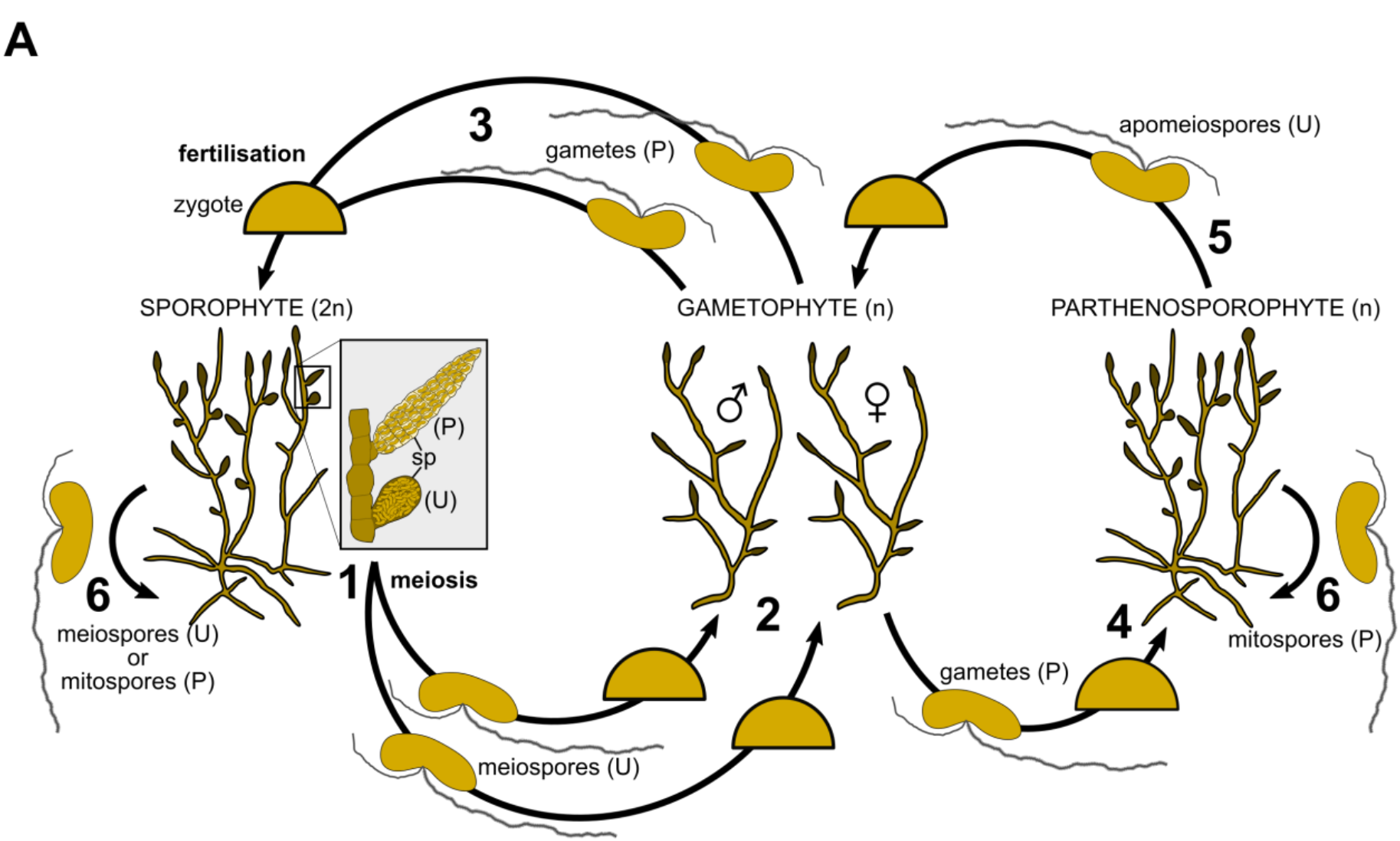
A
fertilisation
zygote
3
gametes (P)
apomeiospores (U)
5
SPOROPHYTE (2n)
GAMETOPHYTE (n)
PARTHENOSPOROPHYTE (n)
(P)
sp
(U)
♂
♀
6
meiospores (U)
or
mitospores (P)
1
meiosis
2
4
gametes (P)
6
mitospores (P)
meiospores (U)

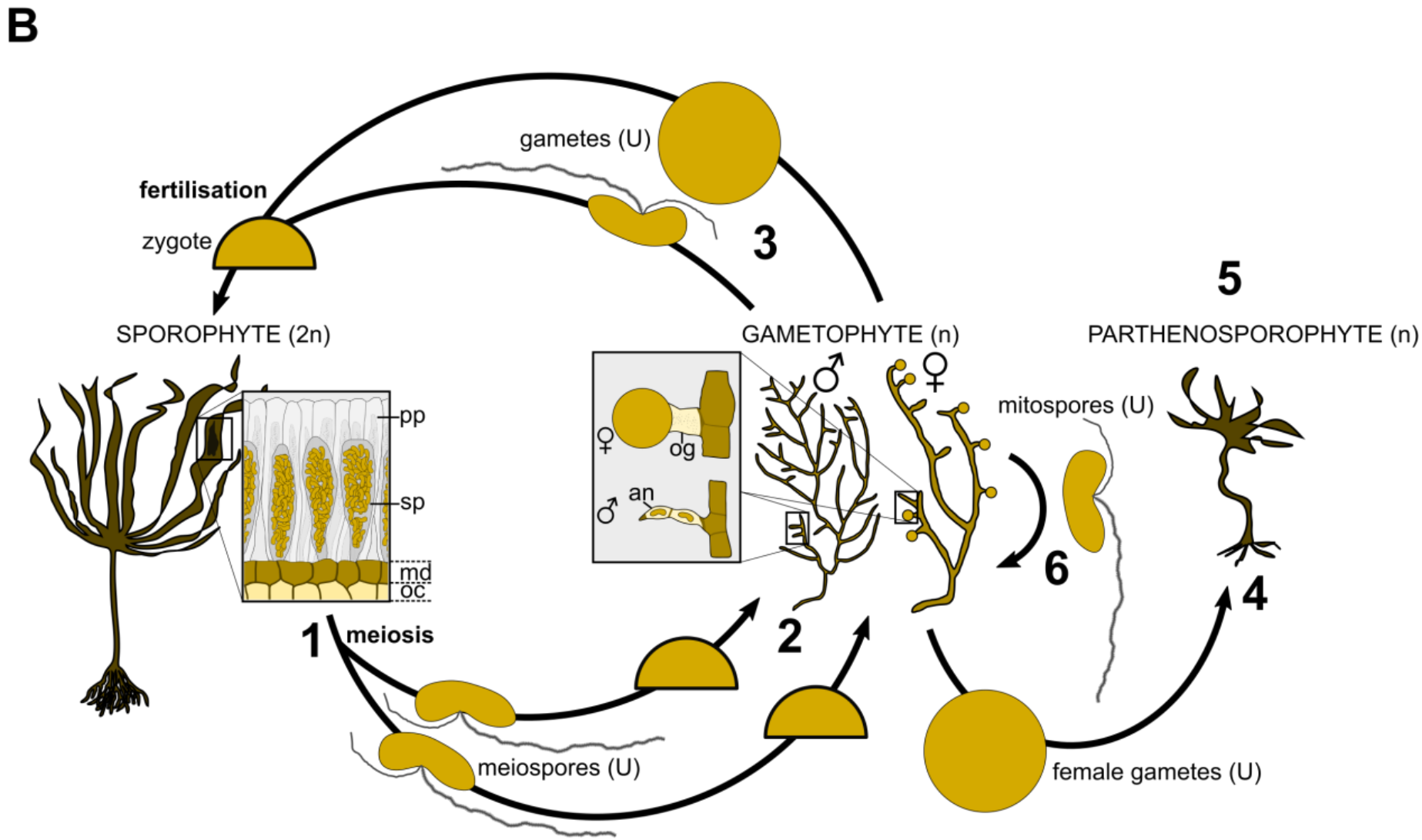
B
gametes (U)
fertilisation
zygote
3
5
SPOROPHYTE (2n)
GAMETOPHYTE (n)
PARTHENOSPOROPHYTE (n)
pp
sp
md
oc
og
an
mitospores (U)
6
4
1
meiosis
2
meiospores (U)
female gametes (U)

Figure 0.4: Life histories of (**A**) *Ectocarpus siliculosus* (Ectocarpales) and (**B**) *Laminaria digitata* (Laminariales). Brown macroalgal life histories alternate between diploid **sporophyte** and haploid **gametophyte** generations. The morphologies of gametophyte and sporophyte generations in *E. siliculosus* are similar (isomorphic, slightly heteromorphic; most Ectocarpales are heteromorphic), whilst in all kelp species they are very different (heteromorphic) [171]. Both *Ectocarpus* generations are uniseriate filamentous thalli, whilst kelp have uniseriate filamentous gametophytes and parenchymatous sporophytes [187]. Brown algae have free-swimming reproductive cells (collectively called zoids), which are produced in sporangia or gametangia (these reproductive organs are collectively called zoidangia). Zoids are generated by unilocular (**(U)**; single compartment) or plurilocular (**(P)**; multiple compartments) zoidangia. Meiosis generates **meiospores** (n), mitosis generates **gametes** (n) and **mitospores** (n or 2n), and apomeiosis (non-reductive meiosis) generates **apomeiospores** (n). All zoids (including gametes post-fertilisation) settle and develop into initial cells with cell walls (**semi-circles**) which develop via mitosis into multicellular thalli.
Sexual cycles (1-3): (**1**) Meiosis occurs in the sporangia (**sp**) of the diploid sporophyte, which produces meiospores. Kelp sporangia form dark areas on the blade; they are protected by sterile filamentous paraphyses (**pp**) and they emerge from the thallus surface, with the meristoderm (**md**) and outer cortex (**oc**) just below. (**2**) The meiospores settle and develop into multicellular, haploid gametophytes. Most brown algal orders, including the Ectocarpales and Laminariales, have separate sexes in the gametophytes (dioicy), but some orders have hermaphroditic gametophytes (monoicy), separate sexes in sporophytes (dioecy), or hermaphroditic sporophytes (monoecy) [171, 200]. (**3**) The gametophytes produce gametes and their fertilisation generates a diploid **zygote** which develops into the sporophyte [187]. In *E. siliculosus,* like most Ectocarpales, the male and female gametes have similar morphologies (isogamous). All Laminariales have antheridia (**an**) that produce small flagellated male gametes which are attracted by pheromones to large non-motile female gametes (oogamous) produced by oogonia (**og**) [171, 187].
Asexual cycles (4-6): Many brown algae can also reproduce asexually if they are fragmented, as the resultant short filaments can regrow into whole thalli. This occurs in kelp gametophytes [201] and any *Ectocarpus* thalli [137]. (**4**) Unfertilised *Ectocarpus* gametes (male or female) can develop into haploid parthenosporophytes, which is common in brown macroalgae [187]. The unfertilised female gametes of kelp can develop into parthenosporophytes [199, 202]. (**5**) *Ectocarpus* parthenosporophytes can generate apomeiospores which develop into gametophytes [203]. Most kelp only produce small, short-lived, and sterile parthenosporophytes which do not occur often naturally. They likely do not continue the life cycle [199, 202]. (**6**) *Ectocarpus* parthenosporophytes and sporophytes can also reproduce asexually via mitospores. A small portion of *Ectocarpus* meiospores can also develop directly into sporophytes [140, 203]. In kelp, only the gametophytes reproduce asexually via mitospores [204].

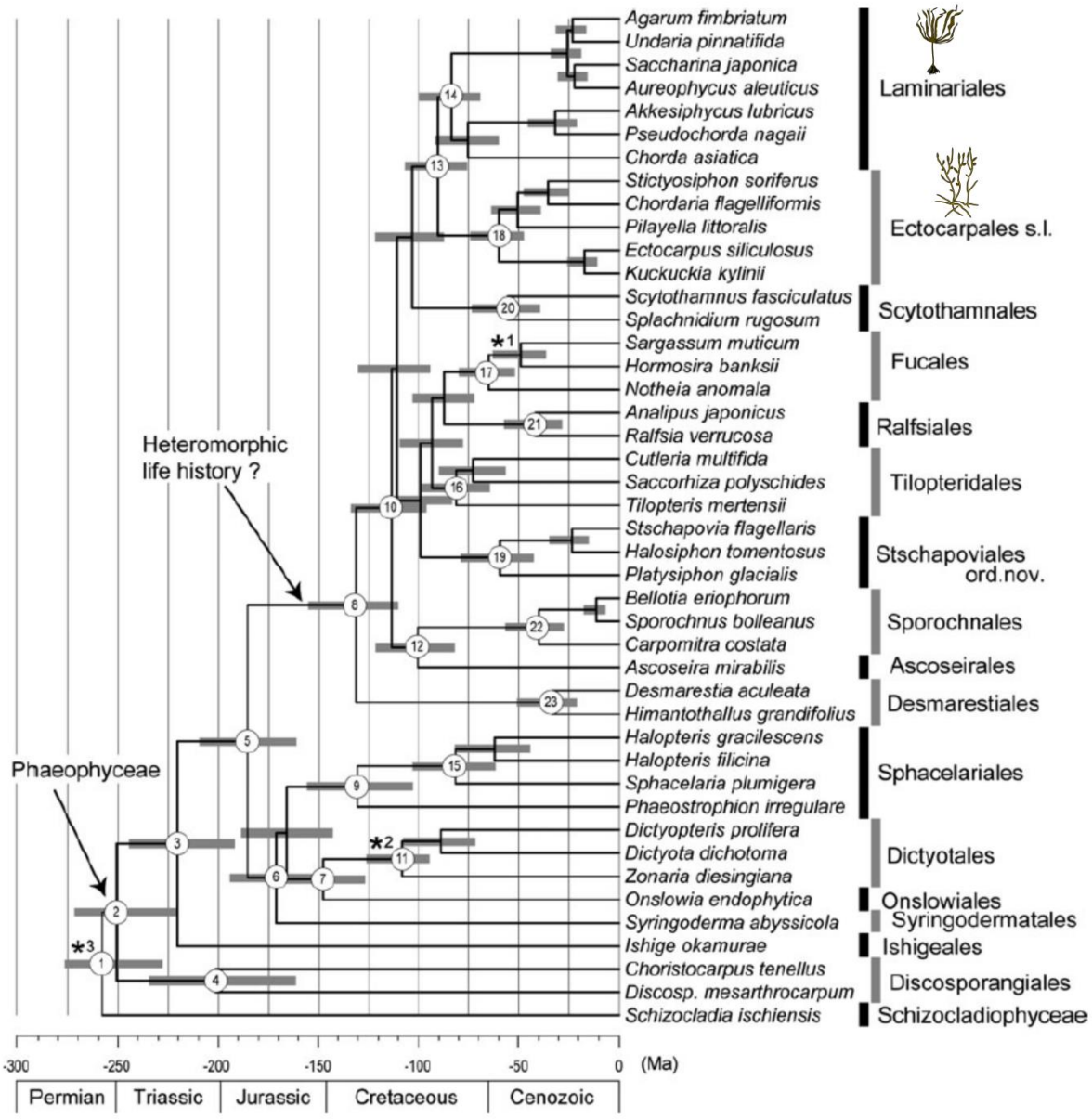

Figure 0.5: Time tree derived from relaxed molecular clock method. Horizontal bars indicate 95% credible intervals of divergence time estimates. Asterisks on nodes correspond to calibration points. Asterisks 1 and 2 indicate calibration points with fossils and minimum time constraints used for nodes were 13 and 99.6 Ma, respectively. Asterisk 3 shows calibration point based on previous molecular clock study. See [172] for asterisk references and estimated ages and their 95% credible intervals of node number labels. Reprinted from "Molecular phylogeny of two unusual brown algae, *Phaeostrophion irregulare* and *Platysiphon glacialis*, proposal of the Stschapoviales ord. nov. and Platysiphonaceae fam. nov., and a re-examination of divergence times for brown algal orders", Volume 51, Kawai et al. 2015, 918-928 [172] with permission from https://www.wiley.com/en-gb, under the Creative Commons Attribution Non-Commercial No Derivatives 4.0 International Public License. Copyright John Wiley & Sons, Inc. 2016. All rights reserved.

0.5.3 Kelp Evolution

The evolutionary study of kelp has begun to combine morphological and genetic data, which has led to the division and merging of various kelp species [205, 206]. Genetic molecular clock methods are especially useful to kelp evolutionary biology because of their morphological plasticity and lack of a fossil record [206, 207]. It is apparent that kelp have undergone complex radiations and geographical movements [205]. The main hypothesised events of kelp evolution are summarised in Figure 0.6, most of which have not been tested with time-calibrated phylogeny.

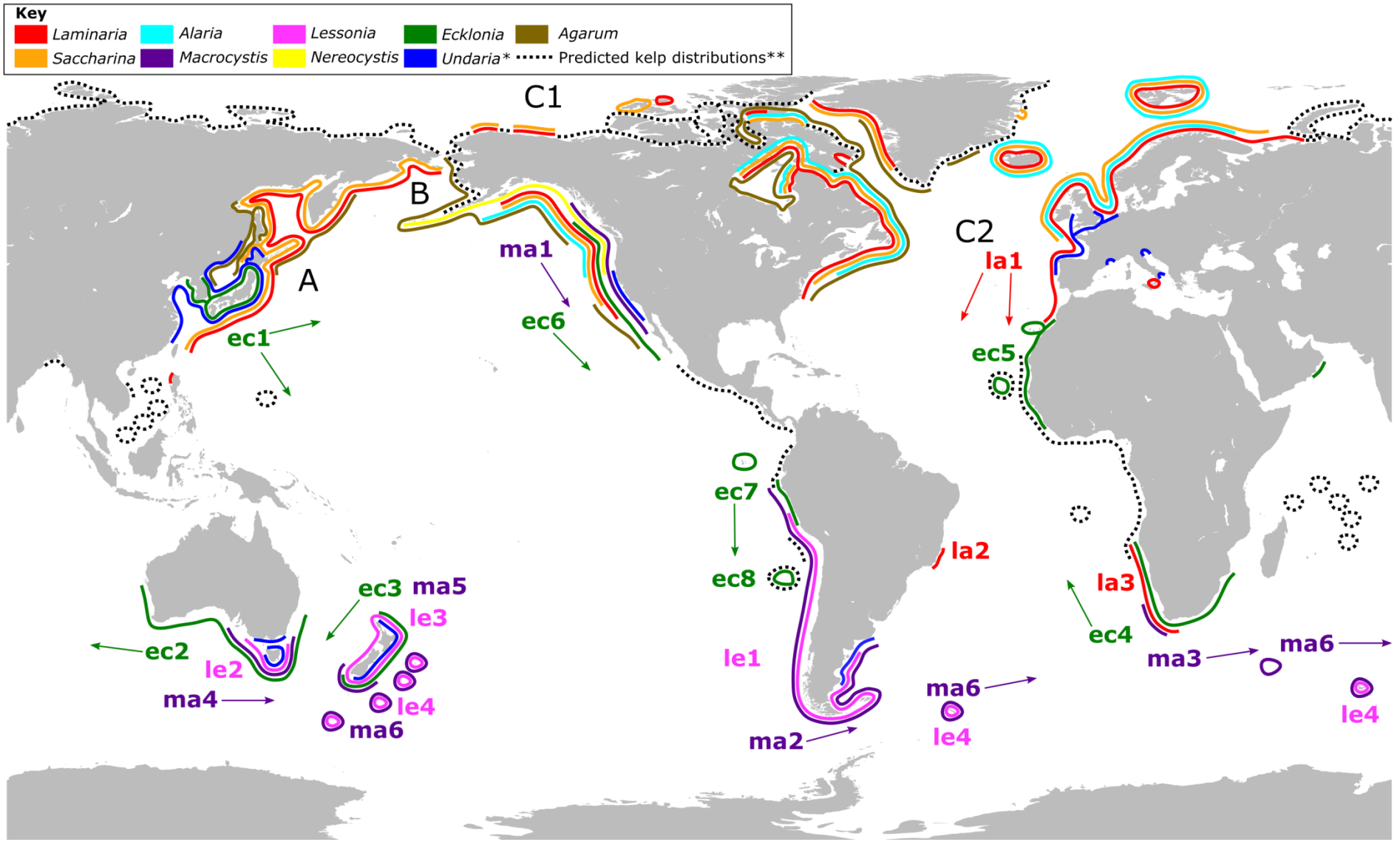
Key
Laminaria
Alaria
Lessonia
Ecklonia
Agarum
Saccharina
Macrocystis
Nereocystis
Undaria*
Predicted kelp distributions**
C1
B
A
C2
ma1
ec6
ec1
la1
ec5
ec7
ec8
la2
la3
ec4
ec3
ma5
le3
ec2
le2
ma4
le4
ma6
le1
ma2
ma6
le4
ma3
ma6
le4

Figure 0.6: Geographical distribution of major kelp genera and the hypotheses (H) of major events in kelp evolution. Arrows indicate general direction of kelp migration. Key details meaning of colours and dotted lines. All codes and letters are detailed below.

(**A**) *H: 90.5 Ma, the Laminariales and Ectocarpales diverged* [172] *in the cold temperate NW Pacific* [206]*, and the first (basal) kelp families evolved at around 75 Ma* [172]*:*

- The basal Laminariales families are Akkesiphycaceae, Chordaceae, and Pseudochordaceae (ACP) [172, 206] and 6/7 ACP species exist in Japan [206].

(**B**) *H: ~25 Ma, the later (derived) kelp families diverged from ACP* [172] *in the warm temperate NW and NE Pacific, before separation by cooling of the Bering Sea* [206]*:*

- The derived Laminariales families are Agaraceae, Alariaceae, Aureophycaceae [208], Laminariaceae, and Lessoniaceae (AAALL). Most AAALL species and endemism occurs in in the NW and NE Pacific [206].

(**C1**) *H: 3.5-5.3 Ma, the Bering Strait opened, which allowed derived kelp to colonise the warm-temperate Arctic and later (**C2**) the cold-temperate N Atlantic* [206, 209]*.*

- Arctic cooling prevented further colonisation, as few kelp can exist in both temperate and Arctic waters [206]. Arctic and Atlantic kelp are distinct, but both include *Laminaria*, *Saccharina*, *Alaria,* and *Agarum*. Only these genera colonised the Atlantic via the Bering Strait and are species rich and have species complexes due to their recent Atlantic diversification [206].
- *Laminaria solidungula* is endemic to the Arctic and is basal to Atlantic cold temperate *Laminaria* species [206, 209].
- *Laminaria* colonised N Atlantic at 5.43 Ma and Mediterranean at 2.07 Ma and by 3.44 Ma diverged into N (*L. hyperborea* and *L. digitata*) and S (*L. rodriguezii*, *L. ochroleuca*, *L. abyssalis*, and *L. pallida*) Atlantic clades [209].
- The *Saccharina latissima* species complex colonized the Atlantic 1.22-1.68 Ma, creating isolated populations which have not yet undergone speciation [210].

*(**ec1-8 la1-3**, **le1-4**, **ma1-6**) H: Kelp have migrated (by drifting or cool water 'stepping stones') from the N to S Hemisphere 6 times and vice versa 1 time* [206, 211]*.*

- *Macrocystis* drifted from California (**ma1**) to S America (**ma2**), S Africa (**ma3**), Australia (**ma4**), New Zealand (**ma5**), and subantarctic islands (**ma6**) [206].
- *Ecklonia* from Japan (**ec1**) to Australia (**ec2**) and New Zealand (**ec3**), S Africa (**ec4**), and back to the N Hemisphere at N Africa and NE Atlantic islands (**ec5**). *Ecklonia* (formerly *Eisenia*, [212]) from Japan (**ec1**) to N America (**ec6**), Peru and Galapagos (**ec7**), and Chilean islands (**ec8**) [206].
- *Laminaria* at 1.34 Ma from S Atlantic (**la1**) to Brazil (**la2**; *L. abyssalis*) and at 0.87 Ma from S Atlantic (**la1**) to S Africa and Namibia (**la3**; *L. pallida*) [209].
- *Lessonia*, the only kelp genus endemic to S Hemisphere [206], diverged at 18 Ma after crossing the equator and then underwent speciation in S America at 4.6 Ma and Australasia at 3.4 Ma [205]. *Lessonia* migrated, in unknown order, to S America (**le1**), Australia (**le2**), New Zealand (**le3**), and subantarctic islands (**le4**) [206].

Other references: distributions of kelp [151, 213], N and SE Pacific *Ecklonia* (formerly *Eisenia*) [214–216]; S Hemisphere *Lessonia* and *Macrocystis* [217]; Arctic *Alaria*, *Laminaria*, and *Saccharina* [218]; Galapagos *Ecklonia*, *Laminaria* at Brazil and the Philippines [211]; and *Agarum* [219].* Range outside NW Pacific is of invasive *Undaria pinnatifida* [220]. ** Kelp distributions predicted based on habitat requirements; Arctic kelp are probably *Alaria*, *Laminaria*, and *Saccharina* [218]; tropical kelp live in deep water (30-200 m) and are probably *Laminaria*, *Ecklonia*, or *Lessonia* [211].

0.5.4 Kelp Ecology

Kelp (order Laminariales) form perennial forests or beds on 25 % of the world's coastlines, primarily on Arctic and temperate coastlines from the lower intertidal to the subtidal zones [213, 221, 222]. Kelp forests rarely exist where minimum average monthly seawater temperatures are above 20 °C, but they can occur in the tropics (Figure 0.6) if either shallow temperate waters are created within tropical waters by upwelling, if tropical waters are clear enough to allow enough light penetration to cooler depths at which kelp can survive, or if temperatures are stable all year at the upper limit of kelp temperature tolerance [206, 211].

Kelp ecosystems are among the most productive in the world [223, 224] and they provide complex habitat for diverse invertebrates [151, 167], smaller macroalgae [225, 226], deposit and filter feeders [225], microbial communities [227], grazers [228], and vertebrates [229, 230]. This high secondary productivity is fuelled by the rapid 'conveyer belt' of kelp growth, which continuously sheds organic matter from the decaying blade ends. Currents carry kelp detritus, which exports carbon to ecosystems hundreds of kilometres away, from the land to the deep sea [231, 232].

Macroalgae have high net primary production (NPP) per area (420 g C m^{-2} yr^{-1}, [233]; 1210 g C m^{-2} yr^{-1} for kelp, [234, 235]) compared to other marine macrophytes (seagrasses, mangroves, and salt marshes; 278-440 g C m^{-2} yr^{-1}; [236]) and terrestrial plants (31-787 g C m^{-2} yr^{-1}, [235]). Macroalgae have higher global NPP (1.5 versus 0.27 Pg C yr^{-1}, [236]) and global carbon burial (0.17 versus 0.15 Pg C yr^{-1}, [233, 236]) than seagrasses, mangroves, and salt marshes combined. This is mainly because macroalgae cover a larger area (3.4 versus 0.75 million km^2, [233, 236]).

Though macroalgae cover only 0.94 % of the global ocean surface (kelp cover 0.09 %, [233, 237], globally they contribute 2.5 % (1.5 Pg C yr^{-1}) of ocean NPP ([35, 233, 236, 238]; 0.17 Pg C yr^{-1} of this is from kelp [235, 237]), 40.5 % of the ocean carbon burial (0.17 Pg C yr^{-1}; [233, 239, 240]), and 30.4 % of the carbon exported from the coastal to the open ocean (0.73 Pg C yr^{-1}; 0.14 Pg C yr^{-1} of which is from kelp; [232, 241]).

0.5.5 Human Utilisation of Kelp Resources

Kelp are ecologically and economically important as they provide a range of benefits including fisheries, iodine cycling [242–244], tourism, scientific research, nitrogen cycling [245], carbon sequestration [234], climate regulation, coastal protection through alteration of hydrodynamics [246], nutrient cycling, and cultural and economic importance [247–252]. The harvesting and farming of macroalgae is especially important in providing new income sources for impoverished communities [252, 253].

99 % of cultivated kelp is produced for food [175, 254], whilst wild kelp are harvested primarily for industrial chemicals such as alginates [175, 255]. Less than 1% of kelp production is for emerging purposes including environmental bioremediation [236, 256], renewable bioenergy (unlike terrestrial bioenergy sources, macroalgae do not compete with food crops for land and freshwater, they require no pesticides or fertilisers; [257–259]), cosmetics [260], nutrition [261], and medical applications [262, 263]. Though currently not recognised, farmed macroalgae could help mitigate climate change by being significant carbon sinks [237, 264].

Global kelp aquaculture production has increased 2.3 times since 2000 and currently comprises about 20% of global marine aquaculture and 30% of all macroalgal

aquaculture production (Table 0.8). Harvesting of wild macroalgae has remained constant due to ecological constraints and overexploitation [177, 265]. However, macroalgal industries are in their infancy, as they produce only 0.3 % of the annual production of terrestrial agriculture [175].

Currently, over 95 % of cultured and harvested macroalgae are produced in Asia [174] and 99 % of cultured kelp are either *Saccharina japonica* (26% of all aquaculture macroalgae) or *Undaria pinnatifida* (6.7 % of all aquaculture macroalgae; Table 0.8). Though kelp aquaculture is expanding globally [175], such as with *Saccharina* and *Laminaria* spp. in Europe [265, 266] and *Macrocystis pyrifera* in Chile [267], most macroalgal production outside of Asia is wild-harvested (Table 0.8).

Table 0.8: Summary of global macroalgal production (aquaculture and wild harvest) in 2016. Values are metric tonnes in fresh weight and numbers in parentheses are % of total global macroalgal production [176].

Category	**Aquaculture**	**Wild harvest**	**Total global production**
All kelp	10289003 (33.36)	369274 (1.19)	10658277 (34.55)
Undaria pinnatifida	2069682 (6.71)	2679 (0.008)	2072361 (6.718)
Saccharina japonica	8219210 (26.65)	58111 (0.188)	8277321 (26.838)
Alaria esculenta	76 (<0.001)	0 (0)	76 (<0.001)
Macrocystis pyrifera	1 (<0.001)	35093 (0.114)	35094 (0.115)
Saccharina latissima	33 (<0.001)	0 (0)	33 (<0.001)
Laminaria digitata	0 (0)	49413 (0.16)	49413 (0.16)
Lessonia spp.	0 (0)	49802 (0.16)	49802 (0.16)
Laminaria hyperborea	0 (0)	68291 (0.22)	68291 (0.22)
Macroalgae	30050655 (97.45)	785992 (2.55)	30,836,647

0.5.6 Anthropogenic Impacts on Kelp Resources and Ecosystems

By 2100, the global mean surface temperature is predicted to be 2-4 ^{o}C higher than preindustrial temperatures [268]. The upper layers of the ocean have warmed by 0.1 ^{o}C per decade since around 1950 [269, 270], however some regions are warming hotspots such as the Northeast Atlantic which has warmed by 0.3-0.8 ^{o}C per decade [271]. Anthropogenic changes in marine temperatures, pH, and oxygenation are projected to have a range of impacts including increased disease prevalence, distribution shifts, and decreased primary productivity [272].

Over the last 50 years, 38 % percent of kelp ecoregions globally have decreased in kelp abundance, but with large variation between localities (in 27 % and 35 % of regions, kelp abundance has increased and not changed, respectively) due to complex interactions influencing kelp responses to change. This is a different scenario from most terrestrial and other marine foundation species, which have declined more consistently across the globe [222]. Globally, across hundreds of kilometres of coastline, kelp ecosystems are being replaced by algal turfs (structurally simple mats of low-lying algae; [273–276]) and impoverished barrens due to overgrazing by sea urchins [277] or tropical herbivorous fish migrating into warming temperate waters [278].

Another major consequence of human impacts is kelp distribution shifts. The invasive *Undaria pinnatifida* has been introduced around the world (35-50 km-year; [220, 279, 280]). Possible anthropogenic cooling of waters in South Africa may have driven the rapid eastward expansion of *Ecklonia maxima* (36.5 km/year, [280]) into the range of *Ecklonia radiata* [281]. *Macrocystis pyrifera* and Australian *E. radiata* have declined dramatically due to warming (95 % cover reduction and 88 km/year, respectively; [280]). Warm temperate *Laminaria ochroleuca* (2.5-5.4 km/year, [282])

has expanded into the warming Northeast Atlantic where the cold temperate *L. digitata*, *L. hyperborea*, and *Alaria esculenta* are retreating northwards [192]. Northwards moving local extinctions of Northeast Atlantic *L. digitata* are predicted to occur from 2050 to 2100 [283]. These shifts are expected to reduce the ecosystem services provided by kelp, for example; kelp forests exported 0.5 times less carbon in warmed waters [284].

The main anthropogenic factors which are driving these changes in kelp ecosystems are climate change, pollution and eutrophication, coastal development, [192, 213, 222], and increasingly frequent storms and heat waves [285, 286]. These abiotic factors cause losses of kelp by altering complex biotic interactions such as competition and grazing, which is why the recovery of kelp ecosystems varies so widely [276]. These impacts are expected to threaten kelp aquaculture by reducing growth [287] and increasing disease [145, 177, 179, 288–290].

0.5.7 Viruses: A Major Knowledge Gap in Kelp Biology

Since known phaeoviruses are temperature sensitive [77, 88], elevated sea temperatures could led to more disease caused by phaeoviruses. This could include more frequent inhibition of reproduction, possibly causing reduced recovery of kelp ecosystems. Invasive plant spread can be facilitated by leaving their viruses behind in their native range [291] or by spreading novel viruses to native competitors [292]. Viruses could play similar roles for macroalgal range shifts driven by anthropogenic influences.

Controlling disease is a major issue for the sustainable future of macroalgal aquaculture [145, 177, 293]. Disease is facilitated by cultivation due to the reduced genetic diversity of domesticated organisms, high stock density, crop to wild disease

spread, and the favouring of horizontal over vertical viral transmission [145, 177, 179, 294]. To date, with the exception of Ectocarpales phaeoviruses and possibly green spot disease in *Pyropia* red macroalgae [124], no macroalgal disease has ever been linked to a virus (Table 0.5 and Table 0.6). Currently, the major causes of disease in marine macroalgal aquaculture are epiphytes, bacteria, and oomycetes [145, 179]. However, as previously unknown viruses have emerged to become important pathogens of crops [295] and marine animals [296], there is potential for viruses to emerge as important macroalgal viruses in the future.

The brown algae are the only lineage to have evolved complex multicellularity [103] within the SAR clade, which is one of the most diverse major eukaryotic groups [188, 297]. Since phaeoviruses are related to phycodnaviruses which infect unicellular eukaryotes, then comparative genomics of novel phaeoviruses could reveal how phycodnaviruses have adapted to infect multicellular hosts. Furthermore, the widespread and latent phaeoviruses could offer a unique system for exploring the deeper evolutionary relationships of virus and host, as integrated viral sequences (EVEs) evolve at the rate of the host and can be compared to exogenous viruses [298]. For example; to test whether phaeoviral EVE ages correlate with the proposed timing of the diversification of the derived kelp families in the North Pacific [281], or how the dynamics of expansion and reduction in phaeoviral EVEs over long evolutionary timescales compare to hypotheses regarding NCLDV genome evolution [16].

Almost nothing is known of viruses and their roles in the ecology, health, and evolution of macroalgae [96]. Basic knowledge is missing, such as macroalgal virus host range, disease, genetics, distribution, and infection cycles. These knowledge gaps should be addressed, especially since macroalgal ecosystems are in decline and macroalgal aquaculture is expanding. Before viruses can be accounted for in the

conservation, utilization, and evolutionary study of macroalgae, basic research on macroalgal viruses is needed.

0.6 Aims

One basic research need is to screen brown algae outside of the order Ectocarpales for phaeoviruses. Given that they are closely related to the Ectocarpales and are ecological and economic important, the order Laminariales is a good option for phaeoviral screening.

The objective of this study is to investigate the evolutionary relationships, symptoms, host impacts, host range, distribution, and genomics of phaeoviruses which infect the order Laminariales (kelp).

The specific objectives are as follows:

1) Assess laboratory cultured kelp gametophytes (primarily *Laminaria digitata*) for Phaeovirus-like symptoms resembling those known in the Ectocarpales. This will involve optical, epifluorescent, and transmission electron microscopy. This may show what infection strategies kelp phaeoviruses employ and establish a model with which proceed with for some of the following aims.

2) Screen kelp sporophytes using PCR for the Phaeovirus core genes MCP across a wide range of species from around the world, followed by sequencing and phylogenetic analyses to investigate the evolutionary relationships of the phaeoviruses of the Laminariales and Ectocarpales. This may reveal a broader evolutionary history for the phaeoviruses and what strategies they use to infect kelp.

3) Compare the frequency of symptoms between kelp gametophytes cultured at different temperatures and the reproductive success between infected and virus-free gametophytes. This may show how Phaeovirus infections impacts kelp.

4) Isolate Phaeovirus virions from laboratory cultured kelp gametophytes and use next generation sequencing to acquire a Phaeovirus genome. Screen all of the available brown algal genomes in databases for integrated Phaeovirus sequences. This should allow comparisons between the genes or genomes of kelp phaeoviruses with other *Phycodnaviridae*.

CHAPTER 1 MICROSCOPY OF KELP PHAEOVIRUSES

1.1 Abstract

Phaeoviruses are latent dsDNA viruses that insert their genomes into those of their brown algal (Phaeophyceae) hosts. Currently, these viruses are described in only the order Ectocarpales, which is comprised of small and short-lived macroalgae. Here we report morphological evidence of a novel Phaeovirus, Laminaria digitata virus 1 (LdV-1), which infects the kelp (order Laminariales) *Laminaria digitata*, an ecologically and commercially important group of macroalgae. Epifluorescence and TEM observations indicated that LdV-1, the type species of subgroup C, may use a latent infection strategy and targets the host nucleus for its genome replication, followed by gradual degradation of the chloroplast and assembly of virions in the cytoplasm of both vegetative and reproductive cells. However, the potential biological impact of Phaeovirus infection in kelp remains unknown.

1.2 Introduction

Kelp (order Laminariales) belong to the brown algae (class Phaeophyceae) and are the largest marine photosynthetic organisms, engineering temperate rocky coastlines into complex habitats comparable to terrestrial forests and supporting extensive marine ecosystems and industries [221]. They are the dominant producers of biomass in coastal temperate waters [232], influencing water movement [246], and

biogeochemistry [243]. Global aquaculture and harvesting of kelp are sources of food, industrial chemicals, biofuel, fertiliser, and pharmaceuticals [258, 299].

Kelp are closely related to the order Ectocarpales, which are small brown algae that often co-occur with kelp [137, 172, 190]. The Ectocarpales are host to the only described macroalgal viruses (genus Phaeovirus), which are comprised of nine virus species infecting seven Ectocarpales species. Phaeoviruses are eukaryotic algal viruses (family *Phycodnaviridae*; [37]) with large (150-350 kb), complex dsDNA genomes [39, 40], and are Nucleo-Cytoplasmic Large DNA viruses (NCLDV) alongside *Poxviridae*, *Asfarviridae*, *Iridoviridae*, *Ascoviridae*, and *Mimiviridae*. The well-studied type species of Phaeovirus is Ectocarpus siliculosus virus 1 (EsV-1), which infects *Ectocarpus siliculosus* using a persistent strategy, integrating its genome into the genome of the host [60, 76]. Phaeoviruses appear to infect only the short lived, wall-less life cycle stages (gametes and spores; hereafter collectively referred to as zoids). Mitosis of the zoids gives rise to adult multicellular macroalgae (gametophytes or sporophytes). Every host cell inherits a copy of the phaeoviral genome from the initially infected zoid. In vegetative cells, the phaeoviral genome remains latent and is only expressed in reproductive structures (gametangia or sporangia). Infected host organs produce densely-packed virions instead of zoids. The extent of host reproduction inhibition varies widely from partial to complete sterilisation, depending on temperature and light conditions [82]. Released phaeoviruses infect the next generation of zoids, and a proportion of the zoids will have already vertically inherited the latent phaeoviral genome [50, 91].

The diversity of macroalgal viruses has not been thoroughly explored, as there are only nine formally described viruses [40] for the approximately 13.5 thousand described macroalgae species, around 2000 of which are brown algae [110]. In brown

macrolagae, there have been microscopic observations of virus-like particles (VLPs) resembling phaeoviruses in eleven brown algal species, one of which was not Ectocarpales (Table 0.5, [101]). These VLPs have diameters of 120-180 nm and hexagonal cross-sections which indicate icosahedral morphology, darkly stained nucleocapsid cores, and multiple capsid layers which may be internal lipid membranes. The infection cycles and impacts on host morphology has been described in detail for several of these phaeoviruses, such as EsV-1 [49, 50, 52, 77, 81, 93, 111, 113, 114]. Phaeovirus infection is visible by optical microscopy, because viral replication fills the cells with virus particles which appear as grey, homogenous material that occupies the entire cytoplasm [77]. Virus-filled cells are easily visualised by epifluorescent microscopy with red chlorophyll autofluorescence (red; 640 nm) and DAPI stain (blue; 340 nm), under which infected cells are completely filled with DAPI-fluorescent DNA (the DNA within the virus particles), and lack any chlorophyll.

To address the lack of detailed observations of Phaeovirus infections in brown algal groups beyond the Ectocaprales, we assessed gametophytes of the ecologically and commercially important kelp species, *Laminaria digitata* (Hudson) J.V. Lamouroux. We focused on an *L. digitata* gametophyte strain which PCR has previously revealed to contain a Phaeovirus gene for major capsid protein (MCP). Optical microscopy, fluorescent microscopy with chlorophyll autofluorescence and DAPI-staining, and transmission electron microscopy (TEM) revealed Phaeovirus-like morphologies in *L. digitata*) gametophytes. This is the first detailed description of a putative Phaeovirus infection in any species of kelp.

1.3 Materials and Methods

1.3.1 Gametophyte strains

Three unialgal gametophyte strains from which Phaeovirus MCP was previously amplified by PCR [300] were selected for this study: *Laminaria digitata* Perharidy 2010 number 30 male (LdigPH10-30m), *Laminaria digitata* Perharidy 2010 number 31 female (LdigPH10-31f), *Laminaria digitata* Perharidy 2010 number 22 female (LdigPH10-22f). In addition, one MCP-negative gametophyte strain was examined: *Laminaria digitata* Perharidy 2010 number 21 male (LdigPH10-21m). These gametophytes were collected on the 11.8.10 from the low intertidal zone at low tide from Perharidy, Roscoff, France.

1.3.2 Gametophyte Isolation and Culture

All kelp gametophytes were isolated as follows [301, 302]: sori tissue was cut out from mature kelp sporophytes and left in sealed tubes overnight at 4 ^{o}C. The following day, the sori were cut with a razor blade into ~2x2 mm cubes. For each sporophyte, a sterile cover slip was placed on top of a drop of sterile seawater in a petri dish. Several sterile seawater drops were placed on each cover slip. In autoclaved seawater, per sporophyte, the cubes were pipetted up and down repeatedly with the pipette tip pressed against the bottom of the petri dish, forcing the water out (this creates shear forces which removes diatoms or protists on the kelp cubes). A single sori cube was pipetted into each drop on the cover slips, then additional seawater droplets were added, and the dishes sealed with parafilm to reduce desiccation. The dishes were turned upside down carefully in a small arc movement and left overnight or for 8 hours. During this time, the meiospores are released from the sori and settle onto the cover slip (most unwanted debris or ogranisms will sink and be washed away in the next step). The following day, each cover slip was removed and rinsed with

sterile seawater, then broken in half and placed into tubes or dishes filled with culture media. The settled meiospores develop via mitosis into male or female gametophytes, which are distinguishable by their cell sizes and frequency of branches.

Gametophytes were cultured in half strength Provasoli's enriched seawater (PES, [302]) and a 16:8 light dark cycle at 15 ^{o}C, with PES media changing every 4 weeks. All gametophytes were kept under red light (covered with red translucent plastic) to inhibit gametogenesis, allowing long term vegetative growth. Once the resultant gametophyte mixes were visible to the naked eye, they could be gently ground up and male and female filaments picked out and placed in well plates. These individual filaments grow into unialgal cultures. All gametophyte cultures were transferred to 10-20 mL culture dishes or tubes once visible to the naked eye.

1.3.3 Optical and Epifluorescence Microscopy of Gametophytes

To visualise any DNA-filled cells, gametophytes were stained with 1 µg/ml of 4',6-Diamidino-2-phenylindole (DAPI; Sigma Aldrich) for 1-2 h in darkness, then washed 3 times with sterile seawater [52]. Samples were viewed under x 60 to x 100 oil objective on a Leica DMi8 epilfuorescent microscope and excited using 488 (640 nm emission; red, chlorophyll) and 340 nm (461 nm emission; blue, DAPI) wavelengths. The DAPI and autofluorescence channels were overlaid in post-processing for the Figures.

1.3.4 Tranmission Electron Microscopy of Gametophytes

L. digitata gametophyte thalli (~1 mm^3) were fixed for 2 hours at room temperature in a solution of 65 % half-strength PES media, 2.5 % glutaraldehyde, 1 % caffeine, and 0.05 M sodium cacodylate. The fixed thalli were then washed 3 times for

10 mins in the same buffer solution with glutaraldehyde replaced with an equal volume of distilled water. Postfixation of thalli was by 1 % osmium tetraoxide in sodium cacodylate solution for 2 hours at room temperature, then washed 2 times for 10 mins in sodium cacodylate solution and the sample dehydrated in an increasing ethanol series from 30 % up to absolute ethanol at 15 mins each step. Samples were infiltrated with increasing concentrations (30, 50, 70, 100, 100 %) of high viscosity agar resin in ethanol overnight, with final embedding in 100 % resin at 70 ^{o}C. Ultrathin sections (~70 nm) were cut with a diamond knife and mounted on copper grids. The sections were stained with 2 % uranyl acetate solution and a 4 % lead citrate solution. Virus particles were filtered from culture media by a 2-step process. Firstly, the media was pump-filtered through Supor-450 membrane disc 0.45 µm filters to remove larger material such as gametophytes and bacteria, and then the filtrate was ultrafiltered using Amicon Ultra-15 Centrifugal Filter Devices 30 kDA (according to the manufacturer's instructions) to concentrate virus particles. A drop of ultrafiltrate was added onto a Formvar-coated copper grid for 10 mins, then distilled water for 10 seconds, then saturated (2 %) uranyl acetate solution for 10 mins, and distilled water for a final 10 seconds. All imaging was performed on a JEOL 1200 EX II transmission electron microscope at 120 kV at varying magnifications from x 10,000 to x 100,000.

1.4 Results

1.4.1 Microscopy of Phaeovirus-like symptoms in Kelp

The *L. digitata* strain LdigPH10-30m gametophyte culture showed consistent Phaeovirus infection-like symptoms (Figure 1.1 a-n), alongside normal growth and gametogenesis (Figure 1.1 a). Gametangia formed preferentially on short side branches (Figure 1.1 a), with one to several spermatozoids developing in each (~5 µm

in diameter, arrowhead Figure 1.1 a). The gametes were ejected through a mucilaginous cap, leaving empty translucent gametangia (white arrow, Figure 1.1 a). Female *L. digitata* gametophyte strains (LdigPH10-31f and LdigPH10-22f) showed similar phaeoviral infection symptoms (Figure 1.1). Healthy gametophyte cells have a large nucleus that can be visualised through DAPI staining and epifluorescence microscopy (discrete and localised blue fluorescence, white arrowheads Figure 1.1 b, c); these are often closely associated with chloroplasts (large irregular red auto-fluorescent structures, Figure 1.1 a-c) distributed around the cell periphery (Figure 1.1 e). Heavily DAPI stained cells were associated with many opaque and not translucent cells (Figure 1.1 b-d). It has been previously reported that similar cells in Ectocarpales were a result of viral infection and that the phaeovirus DNA genomes could be detected through DAPI staining [77]. DAPI-filled cells were not observed in the MCP-negative strain LdigPH10-21m (data not shown).

Transmission electron microscopy (TEM) of the *L. digitata* strain LdigPH10-30m suggests that LdV-1, similar to phaeovirus infections in Ectocarpales, in male (Figures 1.5 and 1.6) and female (Figure 1.3) *L. digitata* gametophytes. Targets the nucleus resulting in the eventual degeneration (Figure 1.1 f & g) as the cytoplasm fills with long tubular structures (arrows; Figure 1.1 h, i, k), followed by the development of virus-like particles (VLPs) (Figure 1.1 f-l). Simultaneously, the chloroplasts detached from the cell periphery and lost their internal structure and pigmentation (Figure 1.1 f). After nuclear and chloroplast degeneration, more fully formed VLPs were visible in the cytoplasm (Figure 1.1 j-l). VLPs were 80-150 nm in diameter, with a 60-100 nm granular core (Figure 1.1 l & n). The VLPs appeared round to hexagonal and may have icosahedral capsids, as known in other phaeoviruses. Mature VLPs were observed in

ultrafiltered gametophyte culture medium (Figure 1.1 m & n) showing a structure similar to intracellular VLPs.

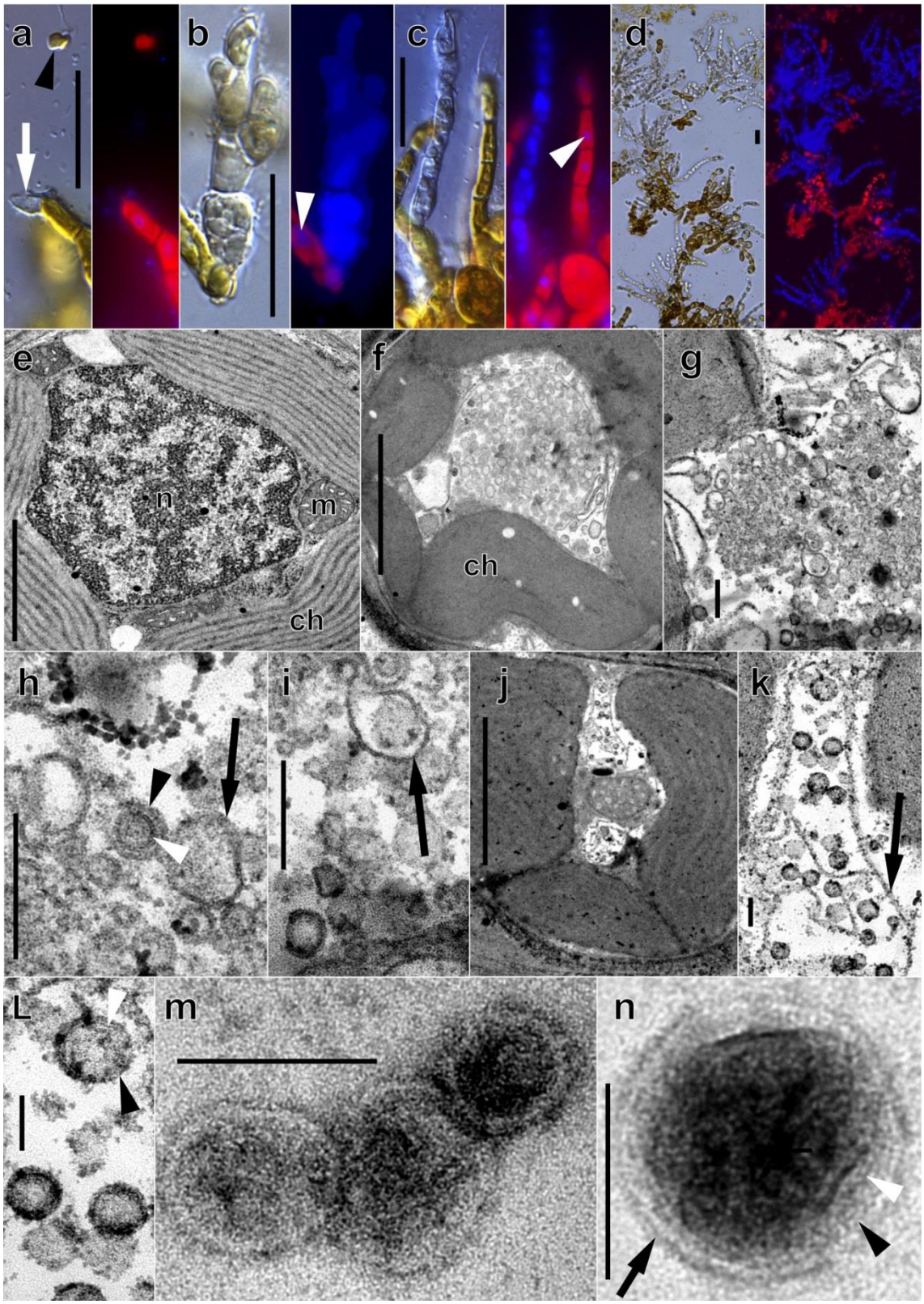

Figure 1.1: Optical and epifluorescence (**a-d**, DAPI stained) and transmission electron (**e-n**) micrographs of Laminaria digitata gametophyte strain LdigPH10-30m, infected by putative Phaeovirus Laminaria digitata virus 1 (LdV-1). (**a**) Spermatozoid (**arrowhead**) released from antheridium (**white arrow**), (**b & c**). Deformed opaque structures with high DAPI blue fluorescence in contrast to normal nuclei (**white arrowheads**). (**d**) High prevalence of DAPI-fluorescent filaments. (**e**) Cross-section of healthy vegetative cell showing chloroplast (**ch**), nucleus (**n**), and mitochondria (**m**). (**f-l**) VLP formation in vegetative gametophyte cells. Chloroplasts detached from cell periphery, loss of internal structure, appearance of tubular structures (**arrows**) and various stages of VLP assembly showing internal membranes (**white arrowheads**) and capsids (**arrowheads**). (**m & n**) VLPs isolated from extracellular medium and visualised by negative staining, showing capsid (**arrow**), internal membrane (**arrowhead**), and nucleoprotein core (**white arrowhead**). Scale bars: 25 µm (**a-d**), 2 µm (**e, f, j**), 200 nm (**g, h, i**), and 100 nm (**k, l, m, n**).

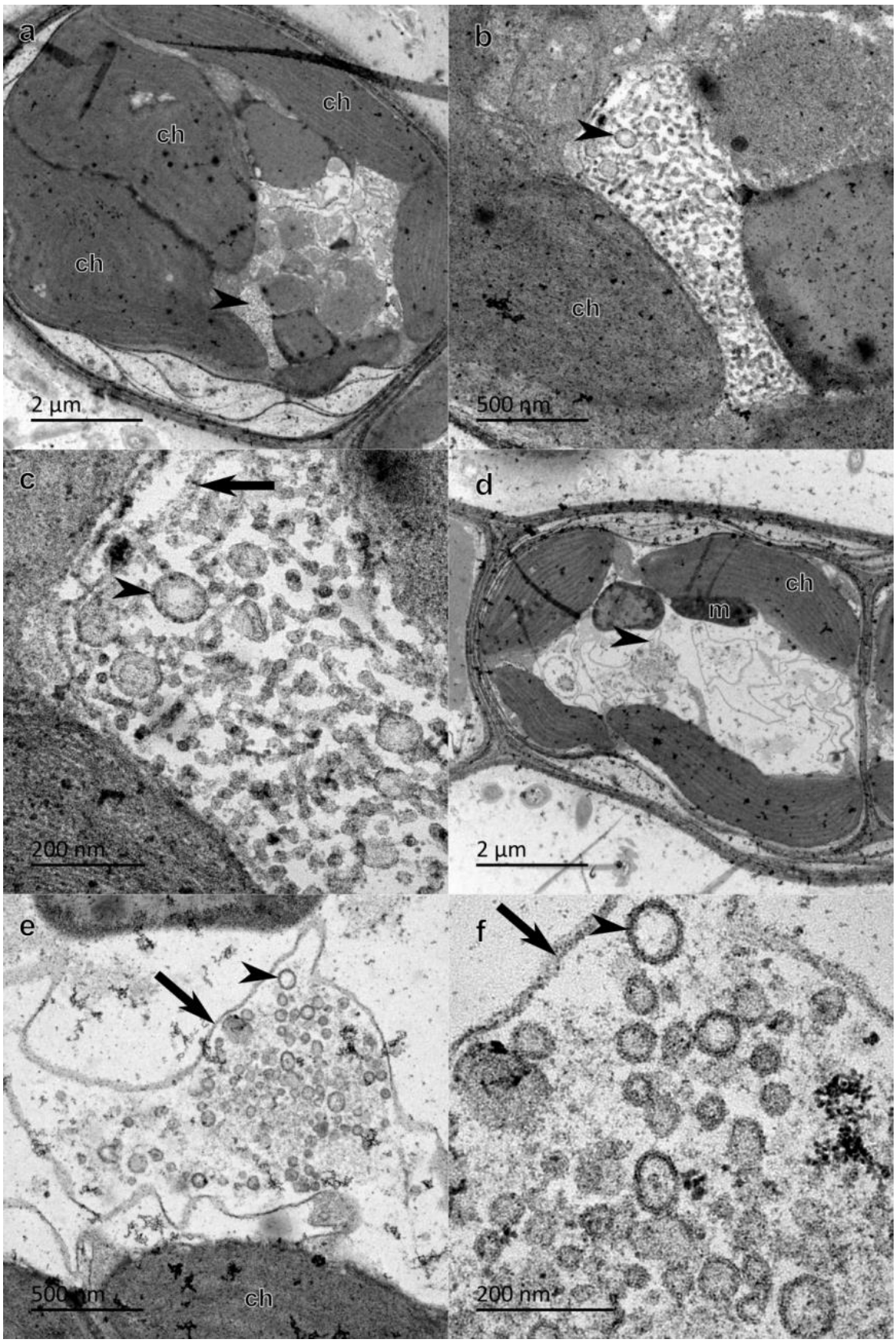
a
ch
ch
ch
2 µm
b
ch
500 nm
c
200 nm
d
ch
m
2 µm
e
500 nm
ch
f
200 nm

Figure 1.2: Transmission electron micrographs (**a-f**) of the vegetative cells of male *Laminaria digitata* gametophyte strain LdigPH10-30m with VLPs (**arrowheads**) and associated tubules (**arrows**). (**a-c**) Three magnifications of a cell with VLPs and tubules. (**d-f**) Three magnifications of a cell with early VLP formation and tubules, mitochondria (**m**), degraded chloroplasts (**ch**) detached from cell periphery, and no nucleus. Scale bars are labelled with lengths.

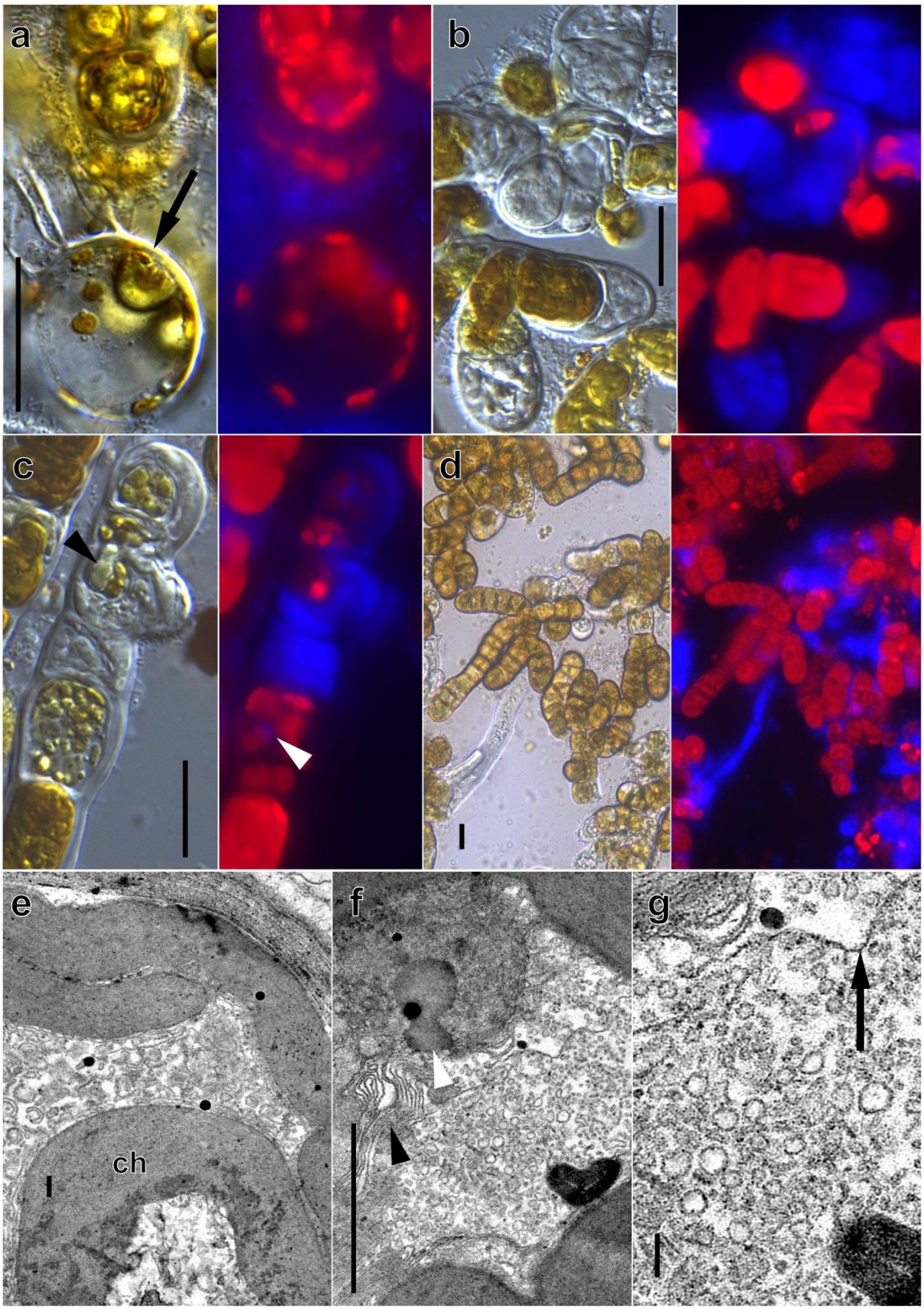
a
b
c
d
e
ch
f
g

Figure 1.3: Light and epifluorescence (**a-d**, DAPI stained) and transmission electron (**e-g**) micrographs of female *Laminaria digitata* gametophyte strains LdigPH10-31f (**b-g**) and LdigPH10-22f (**a**). (**a**) Normal female gamete (arrow), (**b**) Deformed opaque structures with high DAPI blue fluorescence, (**c**) deformed structure with partially degraded chloroplasts (**arrowhead**) and opaque, DAPI-fluorescent material in contrast to healthy nuclei (**white arrowhead**), and (**d**) prevalent putative virus-filled structures in female gametophyte culture. Cross-sections of vegetative cells showing (**e**) degraded chloroplasts (**ch**) which have detached from cell periphery and lost internal structure, (**f**) VLP formation in vegetative gametophyte cells with putative degraded chloroplast (**arrowhead**) and nucleus (**white arrowhead**), and appearance of tubular structures (**arrow**) and early stages of VLP assembly in cytoplasm. Scale bars: 25 µm (**a-d**), 2 µm (**e & f**), and 200 nm (**g**).

1.5 Discussion

Our microscopy observations in kelp resemble those of EsV-1 infections in *Ectocarpus* as previously described [77]. However, kelp phaeoviruses seem to be often expressed in vegetative cells (Figure 1.1 d & e). The replication of phaeoviruses in kelp gametophytes is in contrast to the Ectocarpales phaeoviruses, which all replicate in the sporophyte (only EsV-1 and EfasV-1 also replicate in the gametophyte) [49]. Due to culture of kelp gametophytes under red light to maintain vegetative growth, which is not required for Ectocarpus, this may have altered Phaeovirus symptoms. For example, the infection may have been mostly observed in vegetative cells because no reproductive cells were available. It would have been desirable to have imaged the gametophytes without DAPI staining to identify any background blue autofluorescence. Image quality could also have been improved through the use of DNA stains (such as Sybr green) which are excited by non-UV wavelengths, hence reducing any background blue autofluorescence.

The Phaeovirus MCP-positive gametophyte strains LdigPH10-30m (infected by LdV-1), LdigPH10-31f, and LdigPH10-22f consistently showed Phaeovirus-like infection symptoms (Figure 1.1; Figure 1.2; Figure 1.3). These putative Phaeovirus-filled cells were not observed in the MCP PCR-negative strain LdigPH10-21m (data not shown).

Similar symptoms were also observed in MCP PCR-positive gametophytes of *Laminaria hyperborea* and *Saccharina latissima* (data not shown). Light and epifluorescent microscopy showed symptoms similar to the latent Phaeovirus infection of Ectocarpales, such as in *Ectocarpus siliculosus* [77] and *Pilayella littoralis* [52]. The opaque, DAPI-stained material in kelp gametophytes may be dense masses of Phaeovirus particles (Figures 1.5-1.7). A latent infection strategy is also supported by the co-existence of infected and functionally reproductive filaments, which is consistent with the partial reproductive inhibition seen in Ectocarpales phaeoviruses [82]. All microscopic observations suggest nucleo-cytoplasmic replication, forming virions in unilocular gametangia (Figure 1.1 b-c), association with tubular structures (Figure 1.1 h & k), at least one internal lipid membrane, similar virion size (phaeoviruses are 120-150 nm; absence of darkly stained cores indicates these may not be fully mature virions), and irregular icosahedral morphology (Figure 1.1 h-l; [40, 77]. Mature VLPs were observed in the ultrafiltered gametophyte culture media, showing the similar size (80-150 nm) and structure as the VLPs seen within kelp gametophyte cells (Figure 1.1 m & n).

Kelp gametangia usually form on the ends of lateral branches and each contains a single gamete, which makes it difficult to distinguish infected reproductive and vegetative cells, but both cell types were probably infected (Figures 1.5-1.7). In *Ectocarpus*, for example, vegetative and reproductive cells expressing Phaeovirus infection are easily distinguished because the macroalga forms lateral reproductive plurilocular organs. During Pilayella littoralis virus 1 (PlitV-1) infection, sporangia development is interrupted at the 16-32 plurilocular cell stage; the nuclei disintegrate whilst DAPI-fluorescent viral DNA fills the plurilocular compartments [52]. We observed the nuclei of kelp gametophytes becoming enlarged and intensely DAPI-

fluorescent, followed by loss of chlorophyll fluorescence. This suggests that kelp Phaeovirus replication may also interrupt host reproduction, disrupting the nuclei and then the chloroplasts. The apparent Phaeovirus expression in the vegetative cells (Figure 1.1 b-d) affected entire filaments, which suggests that kelp phaeoviruses could be more virulent than those of the Ectocarpales. Whilst effects of host reproduction, growth, and biochemical composition have yet to be studied, clearly the reproduction of kelp gametophytes could be impaired by the proposed viral infection (Figure 1.1 d).

We considered whether the observed infection could be caused by other macroalgal pathogens. For example, bacterial infection by *Alteromonas* has been documented in *Saccharina japonica* gametophytes [303]. Bacteria-infected gametophytes show cell wall projections, swelling, loss of pigmentation and chloroplasts, and empty cells. After two weeks entire infected cultures were extensively bleached with disintegration visible to the naked eye. The proposed Phaeovirus infection did not induce mortality or bleaching, even after one year. The infection replaced normal cellular structures with opaque material, rather than empty cells with wall projections. DAPI confocal microscopy also shows the masses of dsDNA observed to be too uniform to be bacteria (Figure 1.1 b & c; Figure 1.3 a-d); thus, the observed morphologies were probably not caused by bacteria.

Brown algae are also host to intracellular eukaryotic parasites such as plasmodiophorids. *Ectocarpus siliculosus* is infected by the plasmodiophorid *Maullinia ectocarpii*, which forms abnormal host sporangia filled with plasmodia spores [60]. Plasmodia sporangia form several hundred large spores (~4.6 by ~2.3 µm) which move vigorously inside sporangia and transform into cysts that move by extending pseudopodia. DAPI stained *M. ectocarpii* spores have distinct fluorescent nuclei, lateral sporangia which, under TEM, are full of parasite cells with clear nuclei, vacuoles, and

host-parasite boundaries. *Laminaria digitata* cultures formed abnormal cells lacking internal movement, and DAPI-binding material too dense to be individual plasmodia nuclei (Figure 1.1 b & c). No parasite cells were observed within the gametophytes with TEM, and such large motile spores would be obvious when observing gametophyte cultures. Also, an intense selection process to establish stable host-parasite cultures, but our observations seem too common and naturally stable (no additional culture maintenance beyond subculturing and media changes) to be a plasmodiophorid parasite.

This study did not look for Phaeovirus symptoms in the sporophyte sori, which are comprised of the sporophyte reproductive structures (sporangia). It is reasonable to expect that phaeoviruses may replicate in the sporophyte sporangia, near any newly released zoospores, which are wall-less and free-swimming. Another limitation was that only a single Phaeovirus MCP PCR-negative gametophyte was examined. Due to the possibility of divergent phaeoviruses undetected by PCR, a negative MCP PCR result does not mean that a brown alga is not infected. A greater range of molecular tools such as primers are needed to test whether these observed symptoms and Phaeovirus infection are causally linked.

1.5.1 Conclusions

Three gametophytes strains of *Laminaria digitata* were proposed to be infected by phaeoviruses, including the putative Phaeovirus Laminaria digitata virus 1 (LdV-1). LdV-1 may employ a similar latent infection cycle as the phaeoviruses of Ectocarpales. LdV-1 replication appears to occur in the reproductive and vegetative cells, initially degrading the nucleus, before completion in the cytoplasm, followed by the degradation of the chloroplasts. The resulting virus particles are around 115 nm in

diameter, with icosahedral morphology, a darkly stained nucleoprotein core, and at least 1 internal lipid membrane. Further detailed characterisation of kelp Phaeovirus infection cycles are needed, such as of the sites of replication and cell entry, host impacts, and viral evolutionary strategies.

CHAPTER 2 THE DISTRIBUTION AND HOST RANGE OF KELP PHAEOVIRUSES

2.1 Abstract

Two sister orders of the brown macroalgae (class Phaeophyceae), the morphologically complex Laminariales (commonly referred to as kelp) and the morphologically simple Ectocarpales, are natural hosts for dsDNA viruses (family *Phycodnaviridae*, genus Phaeovirus) that persist as proviruses in the genomes of their hosts. Previously, major capsid protein (MCP) and DNA polymerase concatenated gene phylogeny have split the phaeoviruses into two subgroups, A and B (both infecting Ectocarpales), whilst MCP based phylogeny places the kelp phaeoviruses in subgroup C. Here we used MCP PCR to better understand the host range of phaeoviruses by screening a further 96 individuals of 11 kelp species. Kelp sporophyte samples were collected from their various natural coastal habitats spanning five continents: Africa, Asia, Australia, Europe, and South America. Our phylogenetic analyses showed that while most of the kelp phaeoviruses, including one from *Macrocystis pyrifera*, belonged to the previously designated subgroup C, new lineages of Phaeovirus in 3 kelp species, *Ecklonia maxima, Ecklonia radiata, Undaria pinnatifida*, grouped instead

with subgroup A. Overall, 26 % kelp were positive for Phaeovirus MCP and only intra-subgroup phaeoviral infections were observed in kelp. We conclude that Phaeovirus infection is a widely occurring phenomenon and that phaeoviruses have diversified with their hosts at least since the divergence of the Laminariales and Ectocarpales.

2.2 Introduction

The brown algae (class Phaeophyceae, kingdom Chromista) are mostly marine macroalgae which have evolved complex multicellularity independently from terrestrial plants, red and green algae, animals, and fungi [103]. The order Ectocarpales is comprised of small and short-lived brown algae, with little ecological or economic information regarding them [137]. The sister order to the Ectocarpales is the order Laminariales (kelp) [172]. In contrast to the Ectocarpales, kelp are large, perennial macroalgae which form complex forests that dominate temperate and subpolar rocky coastlines, from the lower intertidal to the subtidal zones [213, 221, 222]. Kelp can also occur in the tropics where sea temperatures are cool enough [211]. Kelp ecosystems are highly productive and complex [223, 224], and they support high biodiversity [151, 225, 227–230, 304] and are involved in biogeochemical cycles [226, 231, 232, 234, 242–245]. These roles result in socioeconomic benefits including fisheries, tourism, coastal protection and environmental remediation [236, 256], and cultural heritage [247, 248, 250]. Kelp aquaculture production is expanding rapidly (increased by 2.3 times since 2000 [176]), as it is an increasingly important source of food, fertiliser,

industrial chemicals [175], renewable bioenergy, and medical applications [252, 257, 262].

Kelp ecosystems and aquaculture are mainly threatened by global climate change, pollution, and overgrazing due to trophic cascades [192, 213, 222, 287]. Climate change may favour novel and more virulent macroalgal pathogens [288–290]. This is a major issue for aquaculture, which is already experiencing losses to various poorly understood macroalgal diseases [145, 177].

The viruses of macroalgae are poorly understood [96, 101], with the exception of Ectocarpus siliculosus virus 1, genus Phaeovirus in the family *Phycodnaviridae* [98, 100]. Nine viruses are currently assigned to the genus Phaeovirus [40]. The phaeoviruses host range include multiple species within the Ectocarpales and kelp lineages [100, 305], but the biology and ecology of kelp phaeoviruses is largely unknown. Phaeoviruses employ a unique latent infection strategy, which begins with the virus infecting the wall-less, free-swimming reproductive algal cells (spores and gametes). The phaeoviral genome is then integrated into the host genome [76]. As the host develops into a mature macroalga, every cell inherits a copy of the phaeoviral genome via mitosis [60, 79]. The genome remains latent except in the host reproductive organs (sporangia and gametangia), which become filled with virus particles [52, 77]. In addition to infection by virus particles, the macroalgae hosts are infected vertically by inheritance of the latent phaeoviral genome.

Concatenated phylogeny of DNA polymerase and major capsid protein (MCP) genes split the Ectocarpales phaeoviruses into two subgroups: subgroup A consisting of one virus genotype, which infects *Ectocarpus*, *Pylaiella*, *Myriotrichia*, and *Hincksia*, and subgroup B, which consists of multiple viral genotypes and infects only *Feldmannia*. The genomes of subgroup B are smaller (from 240-336 kb in A to 155-220

kb in B) and lost a DNA proofreading gene, allowing the subgroup B phaeoviruses to exploit a more acute infection strategy, whereas subgroup A viruses have retained a more persistent strategy [95]. The Phaeovirus subgroup C has been defined based solely on the MCP gene found in the kelp species *Laminaria digitata* (Hudson) J.V. Lamoroux, *Laminaria hyperborea* (Gunnerus) Foslie, and *Saccharina latissima* (Linnaeus) C.E.Lane, C.Mayes, Druehl & G.W.Saunders) [305].

Originally, the extent of viral infection in natural Ectocarpales populations was estimated using light and electron microscopy [77, 84]. However PCR has revealed that *Ectocarpus* spp. are infected by phaeoviruses at rates of 40-100 % [85, 86], and 23.2-64.7 % of kelp individuals collected from European waters are infected by phaeoviruses [305]. The only other reports of viruses in kelp are virus-like particles in *Ecklonia radiata* [115], phaeoviral MCPs integrated in the genome of *Saccharina japonica* [31, 306], and a viral metagenome from *Ecklonia radiata* [120].

In order to improve our understanding of viruses in the biology and ecology of kelp, a key first step is to investigate the geographical and host range of kelp phaeoviruses. To address this, we screened 96 kelp samples from 11 species from Africa, Asia, Australia, Europe, and South America. All available data on the distribution and host range of phaeoviruses was compiled, which included *Ectocarpus crouaniorum* Thuret in Le Jolis (from high to mid intertidal), *Ectocarpus siliculosus* (Dillwyn) Lyngbye (from mid-intertidal to subtidal)*, Ectocarpus fasciculatus* Harvey (from low intertidal to subtidal; [137, 307]), *Ecklonia cava* Kjellman, *Ecklonia kurome* Okamura, *Ecklonia maxima* (Osbeck) Papenfuss, *Ecklonia radiata* (C.Agardh) J.Agardh, *Ecklonia stolonifera* Okamura, *Laminaria ochroleuca* Bachelot de la Pylaie, *Laminaria pallida* Greville, *Lessonia spicata* (Suhr) Santelices, *Macrocystis pyrifera* (Linnaeus) C.Agardh, *Saccharina japonica* (Areschoug) C.E.Lane, C.Mayes, Druehl & G.W.Saunders, and

Undaria pinnatifida (Harvey) Suringar. We present a summary of the broad prevalence of phaeoviruses in 2 major orders of brown algae including previous phaeoviral PCR screen data (Chapter 2; [85, 86, 300]). We describe the phylogeny of novel Phaeovirus MCPs found in the kelp species *E. maxima*, *E. radiata*, *M. pyrifera*, and *U. pinnatifida*.

2.3 Materials and Methods

2.3.1 Sampling and DNA extraction

Epiphyte-free, clean meristematic tissue was cut from kelp sporophytes (diploid) and stored in silica gel. 10-20 mg dry weight of sporophyte material was frozen in liquid nitrogen and homogenized with pestle and mortar. This was followed by DNA extraction with either a NucleoSpin® Plant II (Machery-Nagel, Düren, Germany) kit according to the manufacturer's instructions or a CTAB-SDS DNA extraction method [308]. The DNA samples provided [209, 212] were extracted using this CTAB-SDS method.

2.3.2 Phaeovirus prevalence map

The map and pie charts (Figure 2.1, Table 2.1; Figure A.2.1; Table A.2.1) were constructed using QGIS 3.0.0 (https://qgis.org/en/site/) and visualised using Inkscape 0.92 (https://inkscape.org/). In total we included 96 kelp sporophytes from 26 sites (8 countries) comprised of *Ecklonia cava*, *Ecklonia kurome*, *Ecklonia maxima*, *Ecklonia radiata*, *Ecklonia stolonifera*, *Laminaria ochroleuca*, *Laminaria pallida*, *Lessonia spicata*, *Macrocystis pyrifera*, *Saccharina japonica*, and *Undaria pinnatifida*. Figure 2.1 also includes PCR screen data from other studies comprised of 909 unialgal Ectocarpales strains from 39 sites (3 countries) comprised of *Ectocarpus crouaniorum,*

Ectocarpus siliculosus, and *Ectocarpus fasciculatus* [300], 116 kelp samples from Europe [305]; 63 *Laminaria digitata*, 14 *Laminaria hyperborea*, 39 *Saccharina latissima*), 97 Ectocarpales isolates from a broad range of coasts (*Ectocarpus siliculosus*, *Ectocarpus fasciculatus*; [86]), and a further 570 isolates of *Ectocarpus* spp. from the North Atlantic and South Pacific ([85]; Figure 2.1, Table 2.1; Figure A.2.1, Table A.2.1).

2.3.3 PCR and sequencing

The *mcp* primers used were designed based on a consensus of EsV-1, FirrV-1, FsV-158, and the *E. siliculosus* genome provirus (Figure 2.3; [95]). The MCP primer sequences were: forward primer CVGCGTACTGGGTGAACGC and reverse primer AGTACTTGTTGAACCAGAACGG. All PCRs were performed using Promega Gotaq® Flexi DNA polymerase kit according to the manufacturer's instructions (Promega, Madison, WI, USA), with the addition of 1 µL of 0.8 mg/mL bovine serum albumin (BSA) per 25 µL reaction. PCR conditions were as following: Initial extension of 95 ^{o}C for 5 min, then 40 cycles of 95 ^{o}C for 1 min (step 1), 55 ^{o}C for 30 sec (step 2), and 72 ^{o}C for 30 sec (step 3), and a final extension of 72 ^{o}C for 10 min. All PCR products were Sanger sequenced by Source Bioscience (Nottingham, UK; accessions in Table A.2.1).

2.3.4 Phylogenetic analysis and tree construction

For phylogenetic analysis we used the protein sequences translated from MCP gene fragments amplified from kelp and Ectocarpales (Figure 2.2, Figure 2.4) and from the MCP genes of known *Phycodnaviridae* and *Mimiviridae* (Figure 2.5, see Table A.2.1 and Table A.2.2 for all accession numbers). Only the conserved *mcp* region aligned with the *mcp* fragment found in kelp and Ectocarpales was used to construct Figure

2.5. The additional sequences in Figure 2.5 were obtained using the GenBank blastp algorithm and selecting the sequence with the highest homology to phaeoviral MCP within each available genome of *Phycodnaviridae* and *Mimiviridae*. All translated amino acid sequences were aligned using MUSCLE using MEGA7 [309]. Bayesian inference analysis was performed using MrBayes v3.2 [310], stopping the analysis once the number of generations was over 300,000 and once the posterior probabilities no longer changed with each generation. Trees were visualised using Inkscape 0.92 and Dendroscope 3 [311] and rooted using MCP from the poxvirus *Fowlpox virus* (*Poxviridae*). The Phaeovirus MCPs reported in the genome of S. *japonica* [31] were compared to MCPs from other kelp species. *Saccharina japonica* MCPs were found with the GenBank blastn algorithm searching the *S. japonica* genome using MCP genes from EsV-1, FsV-158, and FirrV-1. MCP ORFs were identified from the *S. japonica* genome scaffolds using Artemis [312]. MCPs from phaeoviral genomes were aligned with MCPs from *S. japonica* and the MCP primers (Figure 2.3) to examine their homology.

2.4 Results

2.4.1 Prevalence of phaeoviruses in the Laminariales

PCR detected a phaeoviral MCP fragment in four of eleven kelp species tested. This amplified MCP fragment was 181 bp to 214 bp. There was a positive result in 15.6 % of the kelp sporophytes studied (15 out of 96; Figure 2.1, Table 2.1, Table A.2.1). Phaeoviral MCP was found in 25 % of *E. maxima* (4 out of 16, South Africa), 25 % of *E. radiata* (5 out of 20, South Africa), 20 % of *M. pyrifera* (1 out of 5, Chile), and 100 % of *U. pinnatifida* (5 out of 5, South Korea). Phaeoviral MCP was not found in *E. cava* (out

of 2, Japan), *E. kurome* (out of 5, Japan), *E. stolonifera* (out of 1, Japan), *L. ochroleuca* (out of 16, UK and Portugal), *L. pallida* (out of 16, South Africa, Namibia), *L. spicata* (out of 5, Chile), and *S. japonica* (out of 5, South Korea). Including previous data, the overall phaeoviral infection rate of kelp was 26 % (56 out of 212 individual sporophytes).

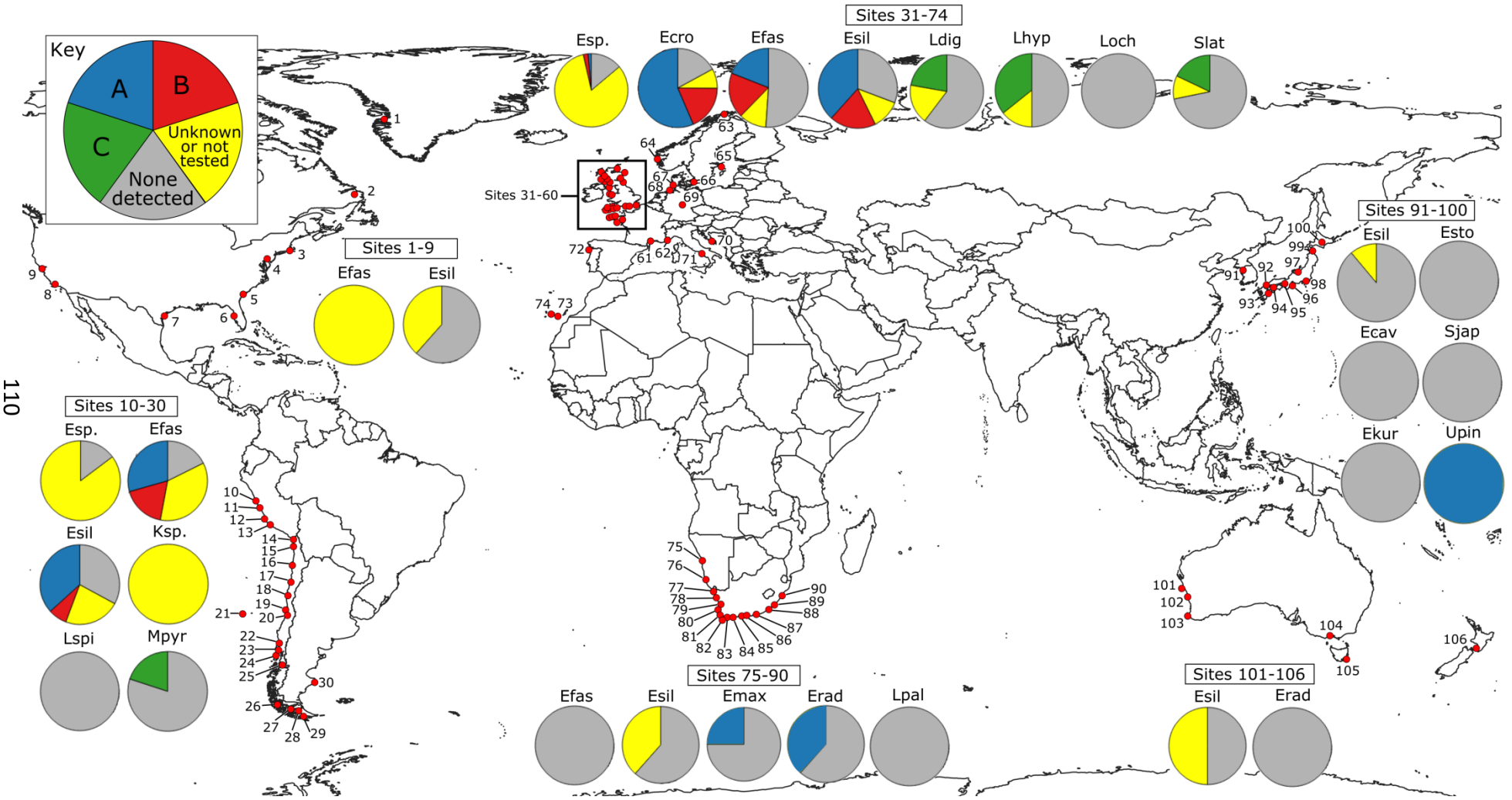
Key
A
B
C
Unknown or not tested
None detected
Sites 1-9
Efas
Esil
Sites 10-30
Esp.
Efas
Esil
Ksp.
Lspi
Mpyr
Sites 31-60
Sites 31-74
Esp.
Ecro
Efas
Esil
Ldig
Lhyp
Loch
Slat
Sites 75-90
Efas
Esil
Emax
Erad
Lpal
Sites 91-100
Esil
Esto
Ecav
Sjap
Ekur
Upin
Sites 101-106
Esil
Erad

Figure 2.1: World map of Phaeovirus subgroups (see Key) and prevalence in kelps (this study) and Ectocarpales (previously available data). Red points are sites. Pie charts show viral prevalence and subgroup per species at given site range. See Figure A.2.1 for map of sites 31-60. See Table A.2.1 for site key and full sample details and Figure A.2.1 for sites 31-60. See Table 2.1 for sample sizes. Species abbreviations: *Ecklonia cava* (Ecav), *Ecklonia kurome* (Ekur), *Ecklonia maxima (Emax), Ecklonia radiata* (Erad), *Ecklonia stolonifera* (Esto), *Ectocarpus crouaniorum* (Ecro), Ectocarpus fasciculatus (Efas), *Ectocarpus siliculosus* (Esil), *Ectocarpus* species (Esp.), *Kuckuckia* sp. (Ksp.), *Laminaria digitata* (Ldig), *Laminaria hyperborea* (Lhyp), *Laminaria ochroleuca* (Loch), *Laminaria pallida* (Lpal), *Lessonia spicata* (Lspi), *Macrocystis pyrifera* (Mpyr), *Saccharina japonica* (Sjap), *Saccharina latissima* (Slat), and *Undaria pinnatifida* (Upin).

Table 2.1: Summary of phaeoviral infections detected with PCR in kelp sporophytes, kelp gametophytes, and Ectocarpales. See Table A.2.1 for site names key and full sample details. Includes data from this study and previous studies [85, 86, 300].

Host species	Subgroup A	Subgroup B	Subgroup C	Unknown subgroup	Subgroup not tested	Total hosts sampled	No. not infected	No. infected	Sites
Ecklonia cava	0	0	0	0	0	2	2	0	96, 98
Ecklonia kurome	0	0	0	0	0	5	5	0	93, 97
Ecklonia maxima	0	0	0	4	0	16	12	4	77, 79, 80, 82-84
Ecklonia radiata	0	0	0	5	0	20	15	5	76, 84-86, 88, 89, 101-103, 105
Ecklonia stolonifera	0	0	0	0	0	1	1	0	99
Ectocarpus crouaniorum	163	52	0	23	0	235	49	186	31-35, 37, 40-43, 47, 50-56, 58, 62
Ectocarpus fasciculatus	49	46	0	28	3	219	121	98	4, 13, 14, 17, 19, 21, 22, 26, 32-34, 36, 38-52, 54-57, 59, 68, 73, 81
Ectocarpus siliculosus	232	107	0	56	42	555	216	339	1-19, 21, 23, 25, 27-33, 36, 40, 43, 44, 46, 47, 50, 52-57, 59-71, 73, 81, 87, 90, 92, 94, 95, 100, 104, 106
Ectocarpus sp.	4	6	0	2	490	579	84	502	24, 34, 36, 39, 40, 46, 53, 74
Kuckuckia sp.	0	0	0	1	0	1	0	0	14
Laminaria digitata	0	0	14	11	0	63	38	25	46, 56
Laminaria hyperborea	0	0	5	0	0	14	9	5	46, 56
Laminaria ochroleuca	0	0	0	0	0	16	16	0	46, 72
Laminaria pallida	0	0	0	0	0	16	16	0	75, 77-80, 82, 83
Lessonia spicata	0	0	0	0	0	5	5	0	20
Macrocystis pyrifera	0	0	1	0	0	5	4	1	20
Saccharina japonica	0	0	0	0	0	5	5	0	91
Saccharina latissima	0	0	7	4	0	39	28	11	46, 56
Undaria pinnatifida	0	0	0	5	0	5	0	5	91

2.4.2 Phylogeny of phaeoviruses based on novel kelp MCP fragments

Subgroup B viruses were grouped together, but with low support (0.66; Figure 2.2). In a previous study, concatenated MCP and DNA polymerase phylogeny placed *M. clavaeformis* 2 in subgroup A [95], but this study's analysis placed it in subgroup B

(Figure 2.2). Ectocarpales subgroup A viruses were closely related, but not within a supported node (Figure 2.2). Phaeoviral MCP from *U. pinnatifida*, *E. maxima*, and *E. radiata* fell within subgroup A (0.72 and 0.78; Figure 2.2). *P. littoralis* 1 was most similar to the kelp subgroup A viruses (0.78; Figure 2.2). *F. simplex* 8 was previously placed by concatenated MCP and DNA polymerase phylogeny as an intermediate between subgroups A and B [95], but this study's analysis placed it with the subgroup A kelp phaeoviruses (0.72; Figure 2.2). MCP from *L. digitata*, *L. hyperborea*, *S. latissima*, and *M. pyrifera* were assigned to subgroup C with low support (0.6) and were more closely related to subgroup B than A (1.0; Figure 2.2). MCPs from the genome of *S. japonica* were divergent from subgroups B and C, and were defined as subgroup D (1.0; Figure 2.2). Out of 59 amino acids, the subgroup A was distinguished from subgroups B, C, and D by 2 amino acids (100% conserved sites 9 and 22; Figure 2.4). Subgroup B had 3 amino acids different from the other subgroups (100 % conserved site 4; partially conserved sites 19 and 47; Figure 2.4). Subgroup C was distinguished from the other subgroups by 5 amino acids (partially conserved sites 2, 24, 34, 35, and 44; Figure 2.4). Subgroup D was the most divergent, with 7 amino acids different from the other subgroups (100 % conserved sites 6, 7, 16, 17, 26, 29, 33; Figure 2.4).

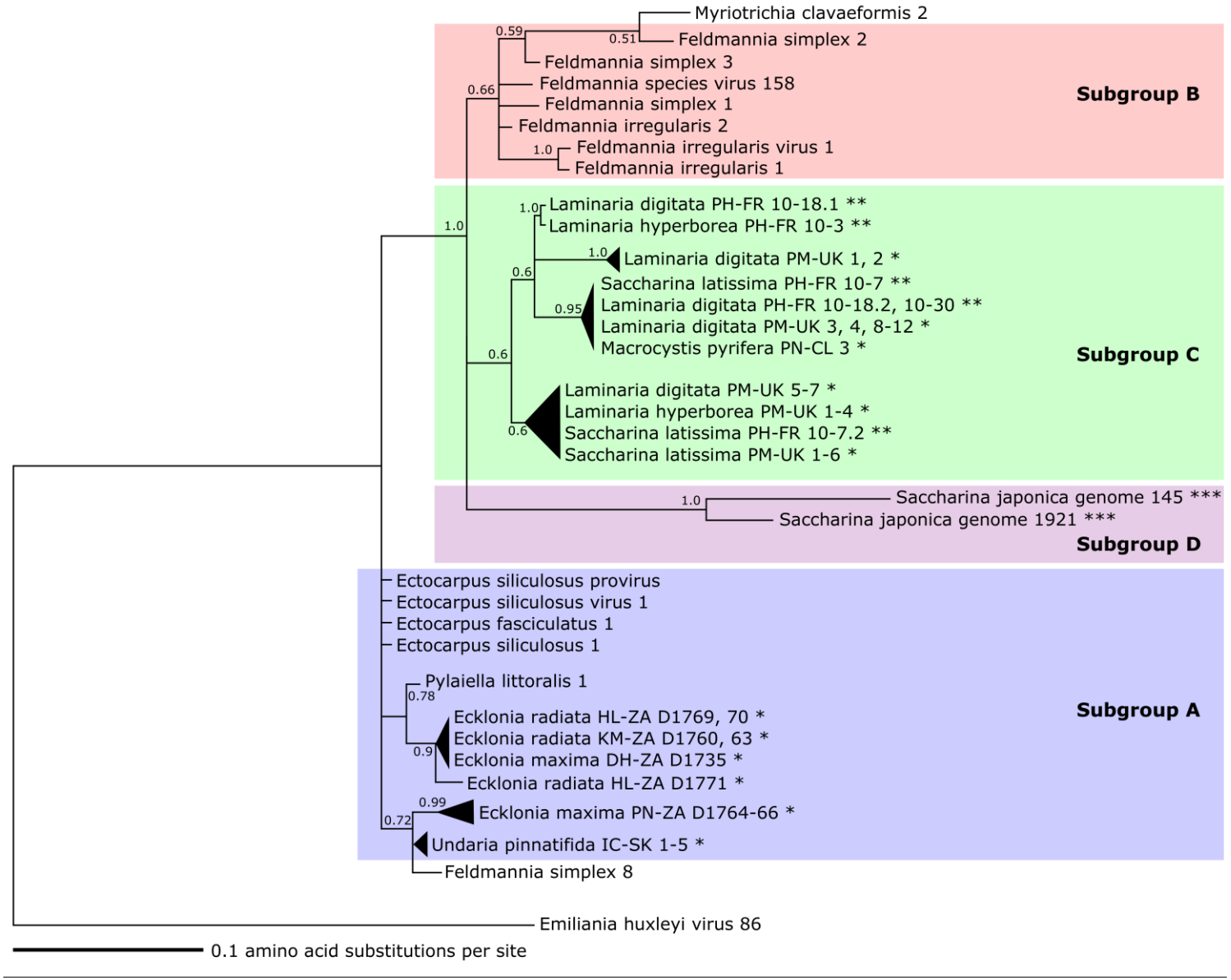
Myriotrichia clavaeformis 2
Feldmannia simplex 2
Feldmannia simplex 3
Feldmannia species virus 158
Feldmannia simplex 1
Feldmannia irregularis 2
Feldmannia irregularis virus 1
Feldmannia irregularis 1
Subgroup B
Laminaria digitata PH-FR 10-18.1 **
Laminaria hyperborea PH-FR 10-3 **
Laminaria digitata PM-UK 1, 2 *
Saccharina latissima PH-FR 10-7 **
Laminaria digitata PH-FR 10-18.2, 10-30 **
Laminaria digitata PM-UK 3, 4, 8-12 *
Macrocystis pyrifera PN-CL 3 *
Laminaria digitata PM-UK 5-7 *
Laminaria hyperborea PM-UK 1-4 *
Saccharina latissima PH-FR 10-7.2 **
Saccharina latissima PM-UK 1-6 *
Subgroup C
Saccharina japonica genome 145 ***
Saccharina japonica genome 1921 ***
Subgroup D
Ectocarpus siliculosus provirus
Ectocarpus siliculosus virus 1
Ectocarpus fasciculatus 1
Ectocarpus siliculosus 1
Pylaiella littoralis 1
Ecklonia radiata HL-ZA D1769, 70 *
Ecklonia radiata KM-ZA D1760, 63 *
Ecklonia maxima DH-ZA D1735 *
Ecklonia radiata HL-ZA D1771 *
Ecklonia maxima PN-ZA D1764-66 *
Undaria pinnatifida IC-SK 1-5 *
Feldmannia simplex 8
Subgroup A
Emiliania huxleyi virus 86
0.1 amino acid substitutions per site

Figure 2.2: Phylogeny of partial Phaeovirus MCP amplified by PCR from Ectocarpales and kelps. Subgroups A (**blue**) and B (**red**) are labelled as previously defined [95], subgroup C (**green**) by [305], and subgroup D (**purple**). Scale units are the number of amino acid substitutions per site. Triangles are collapsed branches. Node values are Bayesian inference proportions. Root is the outgroup Emiliania huxleyi virus 86. Kelp life history stages are labelled sporophyte (*****), gametophyte (******), kelp gamete (*******). Country codes; Chile (CL), France (FR), South Korea (SK), United Kingdom (UK), South Africa (ZA). Sites codes; De Hoop (DH), Hluleka (HL), Incheon (IC), Kei Mouth (KM), Perharidy (PH), Piedras Negras (PN), Plymouth (PM), Port Nolloth (PN). See Figure 2.3 (*S. japonica*) and Table A.2.1 for accession numbers and sample details, and Figure 2.4 for alignment.

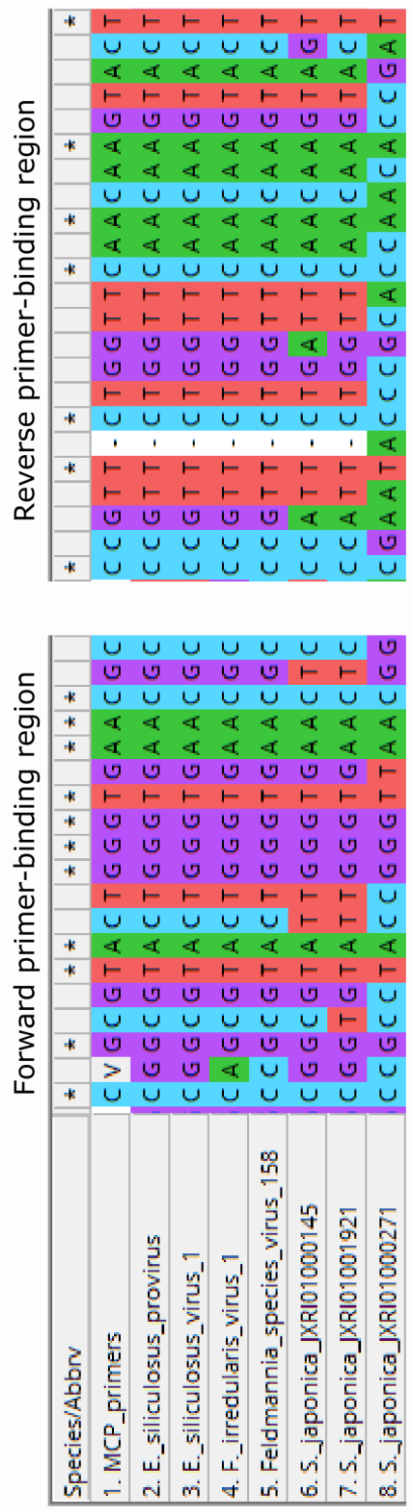

Figure 2.3: Multiple nucleotide sequence alignment of phaeoviral MCP primers, phaeoviral MCP, and *S. japonica* MCP. Region between the primers is the partial MCP sequence used in phylogenetic analysis (Figure 2.2). Conserved sites are indicated by asterisks.

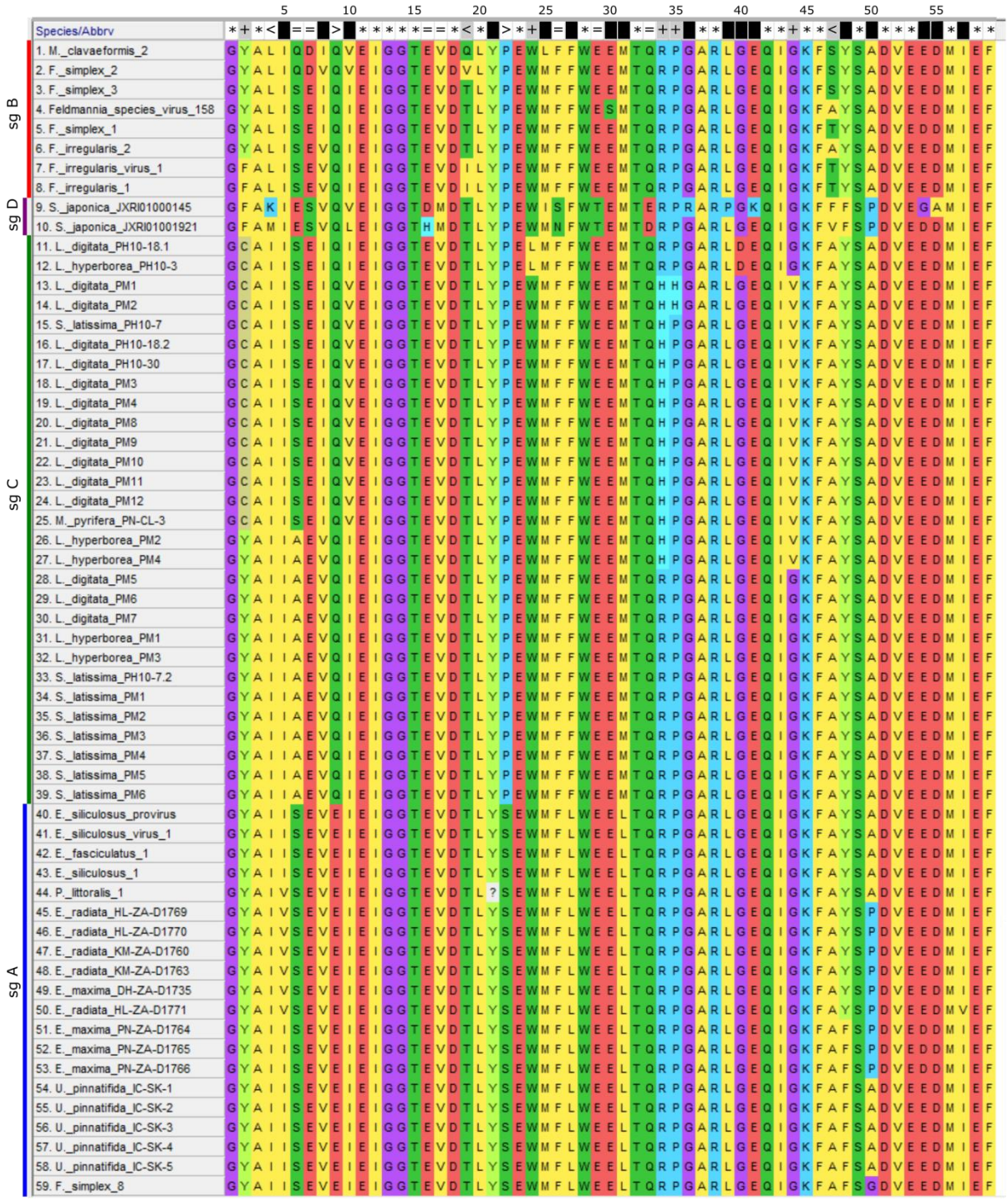

Figure 2.4: Multiple amino acid sequence alignment of Phaeovirus MCP fragments used in phylogenetic analysis. Colours represent the amino acids as labelled. This alignment was the basis of Figure 2.2. sg = subgroup. Sites conserved across all subgroups are labelled (*****). Sites conserved within subgroups are labelled for subgroups B (**<**), A (**>**), D (**=**), C (**+**) and level of conservation within subgroup; none (**black**), partial (**grey**), 100% (**white**).

2.4.3 Phylogeny of *Phycodnaviridae* and *Mimiviridae* based on MCP fragments

Phylogeny based on the MCP region orthologous to the conserved 59 amino acid MCP fragment found in kelp could distinguish *Phycodnaviridae* genera and *Mimiviridae* (Figure 2.5). All phaeoviral MCPs fall within the Phaeovirus genus, including the MCPs from *S. japonica*. Most phycodnavirus members are grouped together into their previously defined genera with high support (0.9 Bayesian inference value *Chlorovirus*, 1.0 Bayesian inference value *Prasinovirus*, 0.93 Bayesian inference value *Prymnesiovirus*), and members of *Mimiviridae* are grouped together (1.0 Bayesian inference value) except *Cafeteria roenbergensis virus*. The other exception was the grouping of *Coccolithovirus* and Phaeovirus together (0.83 Bayesian inference value), but with large evolutionary distance between these 2 genera.

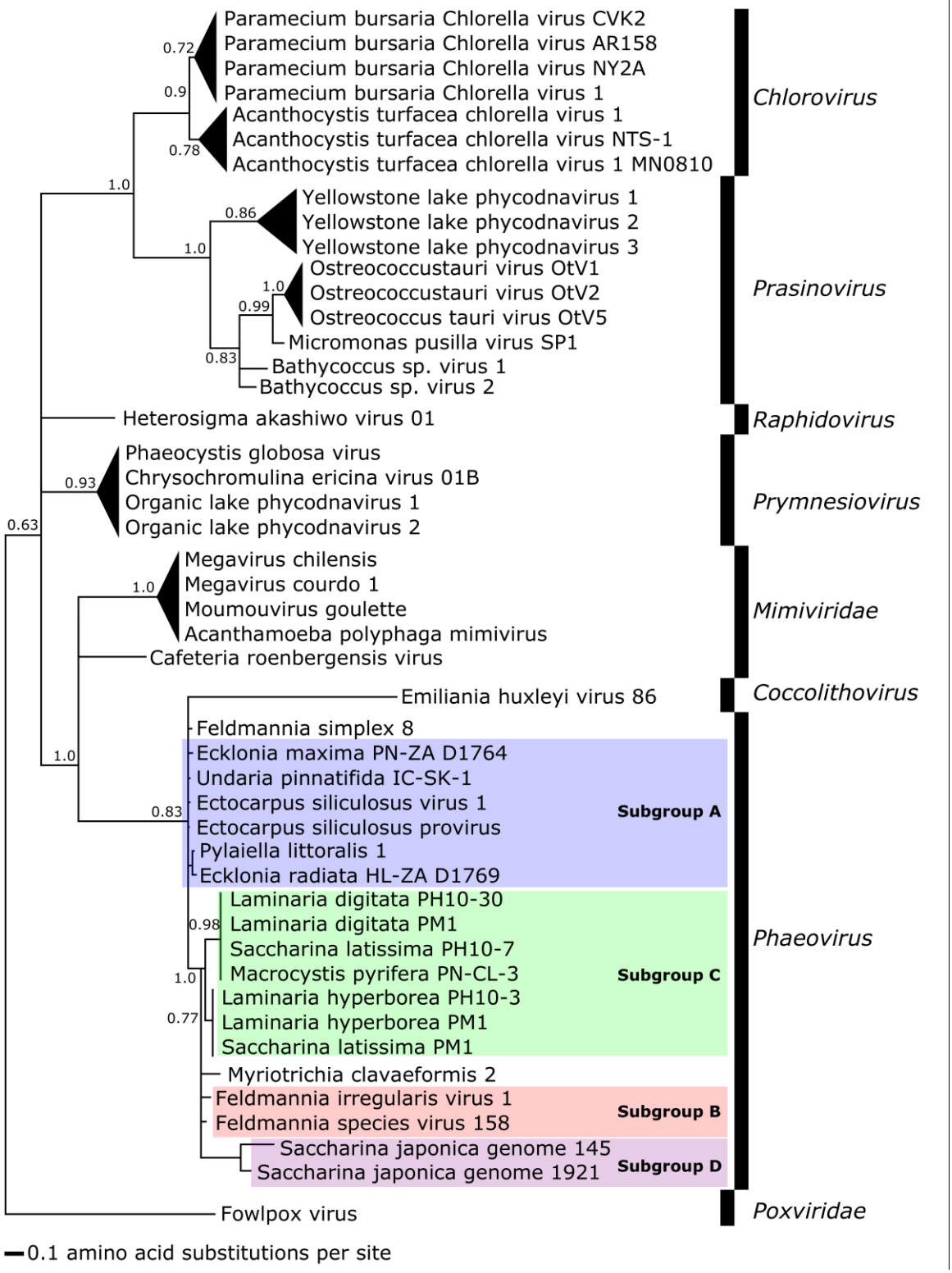
Paramecium bursaria Chlorella virus CVK2
Paramecium bursaria Chlorella virus AR158
Paramecium bursaria Chlorella virus NY2A
Paramecium bursaria Chlorella virus 1
Acanthocystis turfacea chlorella virus 1
Acanthocystis turfacea chlorella virus NTS-1
Acanthocystis turfacea chlorella virus 1 MN0810
Chlorovirus
Yellowstone lake phycodnavirus 1
Yellowstone lake phycodnavirus 2
Yellowstone lake phycodnavirus 3
Ostreococcustauri virus OtV1
Ostreococcustauri virus OtV2
Ostreococcus tauri virus OtV5
Micromonas pusilla virus SP1
Bathycoccus sp. virus 1
Bathycoccus sp. virus 2
Prasinovirus
Heterosigma akashiwo virus 01
Raphidovirus
Phaeocystis globosa virus
Chrysochromulina ericina virus 01B
Organic lake phycodnavirus 1
Organic lake phycodnavirus 2
Prymnesiovirus
Megavirus chilensis
Megavirus courdo 1
Moumouvirus goulette
Acanthamoeba polyphaga mimivirus
Cafeteria roenbergensis virus
Mimiviridae
Emiliania huxleyi virus 86
Coccolithovirus
Feldmannia simplex 8
Ecklonia maxima PN-ZA D1764
Undaria pinnatifida IC-SK-1
Ectocarpus siliculosus virus 1
Ectocarpus siliculosus provirus
Pylaiella littoralis 1
Ecklonia radiata HL-ZA D1769
Subgroup A
Laminaria digitata PH10-30
Laminaria digitata PM1
Saccharina latissima PH10-7
Macrocystis pyrifera PN-CL-3
Subgroup C
Laminaria hyperborea PH10-3
Laminaria hyperborea PM1
Saccharina latissima PM1
Myriotrichia clavaeformis 2
Feldmannia irregularis virus 1
Feldmannia species virus 158
Subgroup B
Saccharina japonica genome 145
Saccharina japonica genome 1921
Subgroup D
Phaeovirus
Fowlpox virus
Poxviridae
0.72
0.9
0.78
1.0
0.86
1.0
1.0
0.99
0.83
0.93
0.63
1.0
1.0
0.83
0.98
1.0
0.77
0.1 amino acid substitutions per site

Figure 2.5: Phylogeny of partial Phaeovirus MCP amplified by PCR from kelps. These sequences were aligned with other *Phycodnaviridae* (*Coccolithovirus*, Phaeovirus, *Raphidovirus*, *Prymnesiovirus*, *Prasinovirus*, *Chlorovirus*) and *Mimiviridae*. Subgroups A (**blue**) and B (**red**) are labelled as previously defined [95], subgroup C (**green**) as by [305], and subgroup D (**purple**). Scale units are the number of amino acid substitutions per site. Triangles are collapsed branches. Node values are Bayesian inference proportions. Root is the out-group Fowlpox virus. See Figure 2.3 (*S. japonica*) and Table A.2.1 and Table A.2.2 for accession numbers and sample details.

2.4.4 Phaeovirus MCP from *Saccharina japonica*

Both JXRI01001921 and JXRI01000145 MCPs were included in this study's phylogeny (Figure 2.2, Figure 2.5) as they contained the conserved MCP region found in Ectocarpales and kelp (Figure 2.4, Figure 2.3). The JXRI01000271 MCP was too short to be included in the phylogenetic analysis. The three phaeoviral MCP orthologs in the *S. japonica* genome had distinct structures. The JXRI01001921 MCP was a 458 amino acid ORF, with an MCP primer binding site which mismatched our primers by thee bases (forward primer) and two bases (reverse primer). The MCP primer binding sites of EsV-1, FirrV-1, and FsV-158 matched every base of both primers (Figure 2.3). JXRI01000145 MCP was a 439 amino acid non-ORF containing seven stop codons, with an MCP primer binding site which mismatched our primers by two bases (forward primer) and two bases (reverse primer; Figure 2.3). JXRI01000271 MCP was 47 amino acids within a 263 amino acid ORF, with an MCP primer binding site which mismatched our primers by four bases (forward primer) and did not contain the reverse primer binding site.

2.5 Discussion

Including data from our previous study [305], 26 % of kelp individuals were positive for Phaeovirus MCP. Novel phaeoviral MCPs were found in 4 species of kelp (Figure 2.1, Table 2.1; *M. pyrifera*, *E. maxima*, *E. radiata*, and *U. pinnatifida*). Including *S. japonica* [31], *L. digitata*, *L. hyperborea*, and *S. latissima* [305], this expands the Phaeovirus host range to 8 kelp species in 5 genera and includes the most species-rich genera of the Laminariales, which contain 44 % of all kelp species (63 out of 143 Laminariales species; *Laminaria*, *Saccharina*, *Ecklonia* [110]). It is therefore not unreasonable to expect phaeoviral infection to be present throughout the entire kelp order. Basal kelp taxa such as the family Chordaceae [172] should be assessed to test whether phaeoviral infection is ancient within the Laminariales. Furthermore, kelp phaeoviruses are geographically widespread, being present in kelp species from Europe (UK, France), South America (Chile), Asia (South Korea), and Africa (South Africa). Kelp phaeoviral subgroups are likewise geographically widespread, with subgroup C being present in Europe and South America (Figure 2.1) and subgroup A being present in Africa and Asia (Figure 2.1).

The subgroup A and B viruses (Figure 2.2) were not grouped as previously defined [95] and showed the MCP fragment alone to be an unreliable marker for assigning viral subgroups. Phylogenetic analysis including other core viral genes would more reliably reflect the evolutionary relationships of kelp phaeoviruses. Compared to equivalent MCP regions from members of *Phycodnaviridae* and *Mimiviridae*, the MCP fragment from kelp (Figure 2.4) showed mostly appropriate phylogeny of NCLDVs [20, 313], with good support for the assignment of these kelp viruses to Phaeovirus (Figure 2.5).

We hypothesise that *Laminaria*, *Saccharina*, and *Macrocystis* phaeoviruses (subgroup C; [305]) have smaller genomes and broader host range (as they are close to subgroup B) than *Undaria* and *Ecklonia* viruses (subgroup A). MCP from Chilean *M. pyrifera* was most closely related to MCP from *L. digitata* and *S. latissima* (0.95, subgroup C; Figure 2.2), suggesting a viral lineage with a host range of at least three kelp genera. In contrast, MCP from the very closely related *S. latissima* and *S. japonica* [314] were assigned to different subgroups (Figure 2.2; subgroups C and D), suggesting divergent phaeoviruses within closely related host species. The extent to which phaeoviruses co-diverge with their kelp hosts is unclear, but could reveal novel understanding of viral evolution, especially regarding the shifts between horizontal (transmission via virus particles) and vertical (transmission via genome integration; may have greater degree co-divergence with host). However, it is worth noting that phylogeny based on multiple core NCLDV genes would more reliably represent the evolutionary relationships of kelp phaeoviruses, but first kelp Phaeovirus genomes sequences must be acquired.

These kelp MCPs are only a hint of Phaeovirus prevalence and diversity, as the negative MCP PCR results may be due to divergent phaeoviruses with low affinity for our MCP primers, which may help explain the lower infection rate of 26 % in kelp versus 63 % in Ectocarpales (Figure 2.1). For example: the absence of MCP in the *S. japonica* samples may have been false negatives, as our primers would not have amplified the phaeoviral MCPs in the *S. japonica* genome (Figure 2.3; [31, 306]). Furthermore, these primers evidently have a higher affinity for the MCP of phaeoviruses in UK *L. digitata*, *L. hyperborea*, and *S. latissima* sporophytes, which had an infection rate of 64.7 % [305]. The presence of MCP in the *S. japonica* genome [31], in addition to apparent Mendelian inheritance of phaeoviral MCP in kelp

gametophytes [305], suggests that kelp phaeoviruses employ a latent infection strategy involving provirus integration into the host genome. Overall, 63 % of Ectocarpales were infected by Phaeovirus, which is within the range of previous approximations of 40 to 100 % (Figure 2.1, Table 2.1; [85, 86]).

Human impacts on kelp ecosystems [213] and aquaculture [287] are expected to threaten the ecological and economic roles of kelp [222, 283]. These threats include climate change, pollution, overexploitation, and overgrazing leading to barren grounds [192, 213, 222, 315]. In the future of aquaculture, macroalgae are expected to have reduced performance in warmer, more acidic oceans [287] and experience losses from a range of eukaryotic and bacterial pathogens [145, 177, 179, 288–290]. Viruses however, are largely absent from our understanding of macroalgal ecology and performance [96]. We have shown evidence of phaeoviral infection in 5 kelp genera of major ecological and economic importance (*Saccharina*, *Laminaria*, *Macrocystis*, *Undaria*, and *Ecklonia*) and the impact of phaeoviral infection on these genera should be further investigated.

2.5.1 Conclusions

We expand the Phaeovirus host range to a total of eight kelp species including the most species-rich genera and their geographical range to five continents. These novel MCPs from kelp may represent new members of the genus Phaeovirus. Phaeoviral infections may be present in the entire kelp order, a group of ecologically and economically important marine macroalgae. However, we lack the molecular tools to thoroughly study the diversity and evolutionary relationships of kelp phaeoviruses.

CHAPTER 3 VARIABILITY OF KELP PHAEOVIRUS SYMPTOMS AND HOST IMPACTS

3.1 Abstract

There are general observations of Phaeovirus infections being temperature sensitive and impairing host reproduction. However, these hypotheses have not been tested in non-Ectocarpales brown algae or with quantitative methods. To test temperature sensitivity, the cultivation temperature of one Phaeovirus MCP-positive (LdigPH10-30m) and one Phaeovirus MCP-negative (LdigPH10-21m) gametophyte culture were increased from 15 to 18 ^{o}C and the occurrence of virus-producing (DAPI-

filled) cells was counted. At 18 ^{o}C, DAPI-filled cells became 2.7-3.4 times more common. However the virus-negative culture expressed symptoms and was found to be MCP positive (in contrast to previous PCRs), meaning that Phaeovirus temperature sensitivity in kelp remains unclear. To test the impact of phaeoviruses on kelp reproduction, DAPI-filled cells were counted in gametophyte crosses, to test whether crosses with more common DAPI-filled cells produced fewer sporophytes. No correlation was found between the number of DAPI-filled cells and that of sporophytes produced. However, the fact that only one virus negative gametophyte (determined by MCP PCR) was in the crosses and the use of mixed gametophyte cultures, meant that the relationship between Phaeovirus infection and sporophyte reproduction could not be tested.

3.2 Introduction

The extent of Phaeovirus symptoms is highly variable in Ectocarpales hosts. In wild populations, Phaeovirus symptoms were visualised with optical microscopy and found to vary from 1 to 25 % of macroalgae individuals (of several genera: *Hincksia*, *Ectocarpus*, and *Feldmannia*; [82–84]), though PCR of a Phaeovirus gene (capsid protein gp1) showed an infection rate of 50-100 % in *Ectocarpus* [85, 86]. One of the few factors known to increase Phaeovirus symptoms are shifts in temperature between 12-15 and 18-20 ^{o}C [77, 82, 83].

An infected individual may have both normal (spore/gamete producing) and deformed (virion producing) reproductive organs, or exclusively one or the other. A general hypothesis is that virion-producing organs displace those which produce host spores/gametes and subsequently reduce host reproduction [77, 80]. Whilst phaeoviruses have been observed in general to sterilise or reproductively impair their Ectocarpales hosts, essentially no quantitative methods have been used to test whether Phaeovirus infection impacts host reproduction [49]. What little is known of Phaeovirus host impacts does not show a clear picture. For example, whilst brown algae such as *Ectocarpus* and *Feldmannia* can be sexually sterilised by phaeoviruses [77, 89, 90], they can continue to propagate themselves via asexual reproduction (mitospores, apomeiospores or fragmentation of vegetative cells). Many Ectocarpales, such as *Ectocarpus*, can reproduce asexually through several routes [137]. Their unfertilised gametes (male or female) can develop into haploid parthenosporophytes which can produce apomeiospores which can develop into fertile sporophytes [187, 203]. Their parthenosporophytes and sporophytes can also reproduce asexually via mitospores. A small portion of *Ectocarpus* meiospores can even develop directly into sporophytes [140, 203] and fragmented Ectocarpus can regenerate whole thalli from short filaments.

It is unknown how sterilisation could impact brown algae with different life histories, such as kelp which have more limited asexual reproduction than many Ectocarpales such as *Ectocarpus* or *Feldmannia*. For example, unlike many Ectocarpales, kelp can only reproduce asexually via the fragmentation of gametophytes [201] or mitospores produced by gametophytes [204], and they cannot produce fertile parthenosporophytes [199, 202].

The aim was to test the hypothesis that as the number of Phaeovirus-filled cells changes in response to a change in temperature. The culture temperature was increased from 15 to 18 ^{o}C for one Phaeovirus MCP-positive (LdigPH10-30m) and one Phaeovirus MCP-negative (LdigPH10-21m) and the number of DAPI-filled (proposed to be filled by Phaeovirus virions) cells per 100 healthy cells were recorded using epifluorescent microscopy. To test the hypothesis that increased Phaeovirus symptoms decrease host reproduction (sporophyte production), a second set of *L. digitata* gametophytes (n=12, LdigPM 1-12) were crossed (gametophytes produce gametes which fertilise to form sporophytes) and the number of DAPI-filled cells per 100 healthy cells and the number of sporophytes per 100 mm^2 of gametophytes were recorded. The infection status of the sporophytes LdigPM 1-12 was determined by MCP PCR before isolating gametophytes LdigPM 1-12 from them.

3.3 Methods and materials

3.3.1 Sample collection and culture

Similar sized *Laminaria digitata* sporophytes with mature sori were collected from the low intertidal zone at low tide in Plymouth May 2018 (LdigPM518-1 to LdigPM518-12) and in Perharidy 2010 (LdigPH10).

All kelp gametophytes were isolated as follows: sori tissue was cut out from mature kelp sporophytes and left in sealed Eppendorf tubes overnight at 4 ^{o}C. The following day, the sori from individual sporophytes was cut with a razor blade into ~2 mm^3 cubes and >24 cubes were transferred to plastic petri dishes. In ~20 mL of autoclaved seawater, the cubes from each sporophyte were pipetted up and down repeatedly with the pipette tip pressed against the bottom of the petri dish, forcing

the water out and creating shear forces, which remove diatoms and protists from the cubes. The cubes were transferred to well-plates and cultured in 2 mL culture media and the plate was sealed with parafilm. After 8 hours, the sori cubes were removed. The settled meiospores develop via mitosis into a mix of male and female gametophytes.

Gametophytes were cultured in half strength Provasoli's enriched seawater (PES; [302]) on a 16:8 light dark cycle at 15 ^{o}C, with PES media changing every 6 weeks. To test virus induction by temperature, cultures of LdigPH10-30m (MCP positive) and LdigPH10-21m (MCP negative) were each kept at both 15 and 18 ^{o}C. These temperatures were chosen as changes from 15 to 18 ^{o}C have been shown to change Phaeovirus symptom occurrence [77, 82, 83]. All gametophyte crosses were kept at 15 ^{o}C. The gametophyte crosses (for the first 6 weeks) and temperature experiment gametophytes were kept under red light (covered with red translucent plastic; 22.2 µmol m^{-2} s^{-1}) to inhibit gametogenesis, allowing long term vegetative growth. After seven weeks, the gametophyte crosses were kept in white light (54.8 µmol m^{-2} s^{-1}) to induce sporophyte production.

3.3.2 Gametophyte crosses

The gametophytes from twelve sporophytes were crossed with themselves (one replicate per cross) and with the eleven other gametophytes (two replicates per cross). Two equal sized sori cubes were placed in each well plate to create cultures of gametophytes from two sporophytes (or one sporophyte for the self-crosses). Kelp can be self-crossed because they are self-fertile [197]. Self-crosses were performed as a control to which the out-crosses can be compared.

3.3.3 Microscopic observations of gametophytes

During culture in white light, the gametophyte crosses were examined weekly with optical microscopy (Nikon TMS optical microscope) at x 2.5 magnification and any sporophytes present were counted. The coverage of gametophytes in each well plate was estimated by eye as very low (~1% = 0.001 mm^2), low (~25% = 19.42 mm^2), medium (~50% = 106.91 mm^2), high (~75% = 194.4 mm^2), or very high (~100% = 213.81 mm^2). At the end of the experiment, for each well plate, the maximum number of sporophytes and maximum gametophyte area in mm^2 was used to calculate the number of sporophytes produced per mm^2 of gametophytes.

After twelve weeks of culture, each well plate was DAPI stained and examined with epifluorescent microscopy (Leica DMi8 epilfuorescent microscope) and excited using 640 nm (red, chlorophyll) and 340 nm (blue, DAPI) wavelengths at x10 magnification, to visualise DNA and chlorophyll. Five images were taken per well plate, at the same positions (quadrants and centre). The numbers of red autofluorescent cells (healthy cells with chlorophyll) and blue DAPI fluorescent cells (putative virus-filled cells) were counted automatically in ImageJ (method from https://www.unige.ch/medecine/bioimaging/files/3714/1208/5964/CellCounting.pdf). This method was also used to test whether the number of DAPI cells was different between gametophytes *Laminaria digitata* Perharidy 2010 number 30 male (LdigPH10-30m) and *Laminaria digitata* Perharidy 2010 number 21 male (LdigPH10-21m) grown at 15 versus 18 ^oC. Temperature experiment replication at 15 ^oC: LdigPH10-21m n=5 and LdigPH10-30m n=6. At 18 ^oC: LdigPH10-21m n=4 and LdigPH10-30m n=7.

3.3.4 DNA Extraction and MCP PCR

Epiphyte-free, clean meristematic tissue from kelp sporophytes *Laminaria digitata* Plymouth May 2018 number 1 to *Laminaria digitata* Plymouth May 2018

number 12 (LdigPM518-1 to LdigPM518-12) was cut out and stored in silica gel. Fresh gametophytes were taken from culture dishes for DNA extraction of LdigPH10-30m and LdigPH10-21m. 10–20 mg dry weight of sporophyte or 100-200 mg wet weight of gametophyte material was frozen with liquid nitrogen and homogenized with pestle and mortar. This was followed by DNA extraction with the NucleoSpin® Plant II (Machery-Nagel, Düren, Germany) kit, according to the manufacturer's instructions.

MCP PCR was performed on sporophytes LdigPM518-1 to LdigPM518-12 (proxy for gametophyte infection, as a Phaeovirus-infected sporophyte produces infected gametophytes) and gametophytes LdigPH10-30m and LdigPH10-21m. The degenerate primers used were designed previously [95] based on a consensus of sequences from EsV-1, FirrV-1, FsV-158, and the *E. siliculosus* genome provirus [48, 98, 100, 103]. These primers were for 3 viral genes encoding MCP. Additionally, LSU d1d2 PCRs were performed on MCP-negative samples to ensure these were not false negatives caused by non-amplifiable DNA. All PCRs performed using Promega Gotaq® Flexi DNA polymerase kit according to the manufacturer's instructions, with additional 0.8 mg/ml bovine serum albumin (BSA). All primers and PCR cycling conditions are detailed in Table 4.2. PCR products were run on 1.5-2 % agarose gels at 100 V.

3.4 Results

3.4.1 Temperature induction

Unexpectedly, LdigPH10-21m had DAPI-filled cells and with similar frequency to LdigPH10-30m at 15 °C. At 18 versus 15 °C, DAPI-filled cells were 3.4 and 2.7 times more common in LdigPH10-21m and LdigPH10-30m, respectively. However, the increase in DAPI-filled cells was not significant due to large variation between replicates, particularly at 18 °C (Figure 3.1).

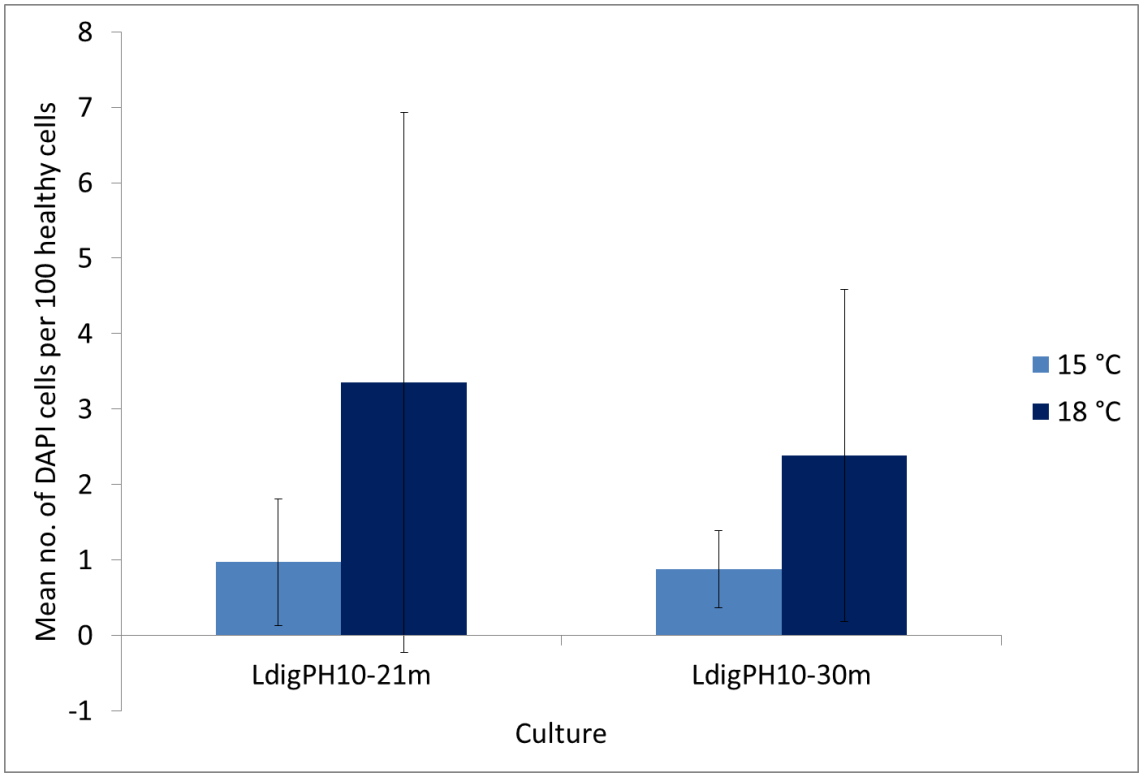

Figure 3.1: Mean number of DAPI-filled cells per 100 healthy cells. Gametophytes LdigPH10-30m and LdigPH10-21m kept at 15 and 18 °C on a 16:8 light dark cycle under 22.2 µmol m^{-2} s^{-1} red light. The error bars represent standard deviation; at 15 °C: LdigPH10-21m n=5 and LdigPH10-30m n=6. At 18 °C: LdigPH10-21m n=4 and LdigPH10-30m n=7.

3.4.2 Gametophyte crosses

For all gametophyte crosses, there was no correlation between the maximum number of sporophytes produced per 100 mm^2 of gametophytes and the mean

number of DAPI-filled cells per 100 healthy cells (Figure 3.2). When comparing specific gametophytes, no correlation was observed for any cross (Figure 3.3 and Figure 3.4).The only MCP negative culture (LdigPM518-5) did not produce significantly more sporophytes.

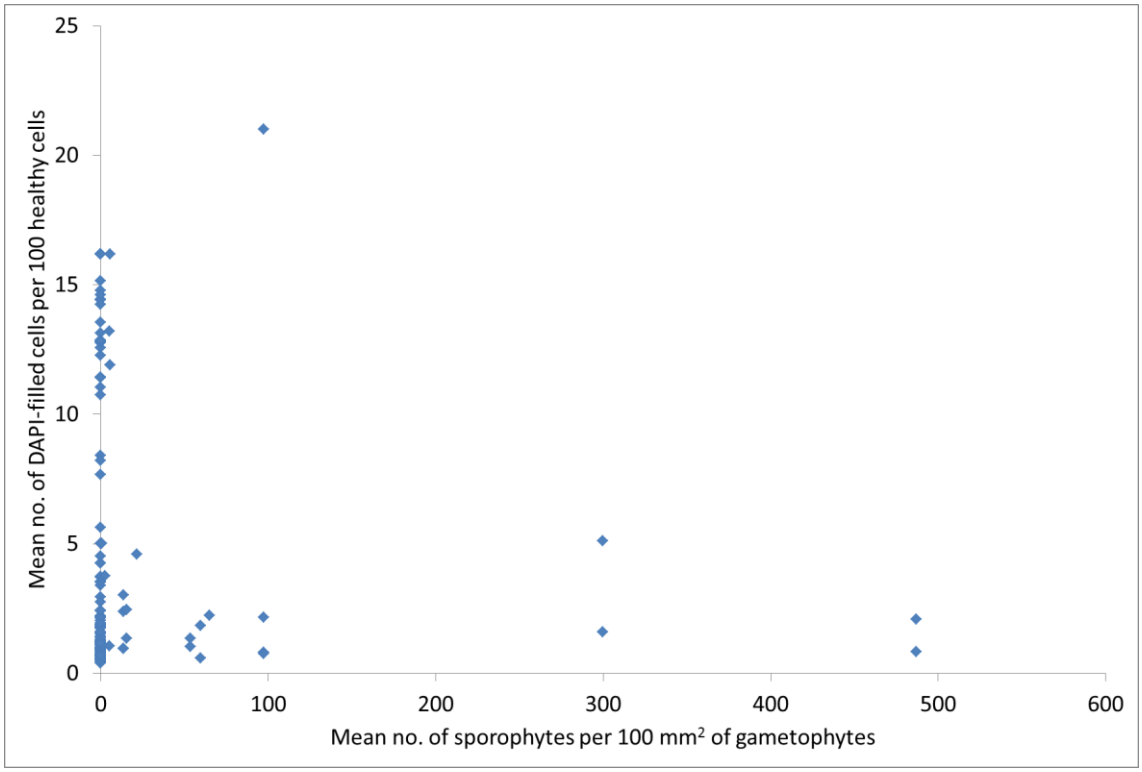

Figure 3.2: All crosses of LdigPM518, strains 1-12 (144 data points). Means of the maximum number of sporophytes produced per 100 mm^2 of gametophytes, plotted against the mean number of DAPI-filled cells per 100 healthy cells. Each data point (self-crosses n=1, all other crosses n=2) represents a unique gametophyte cross (LdigPM518-1 x LdigPM518-1, LdigPM518-1 x LdigPM518-2, etc).

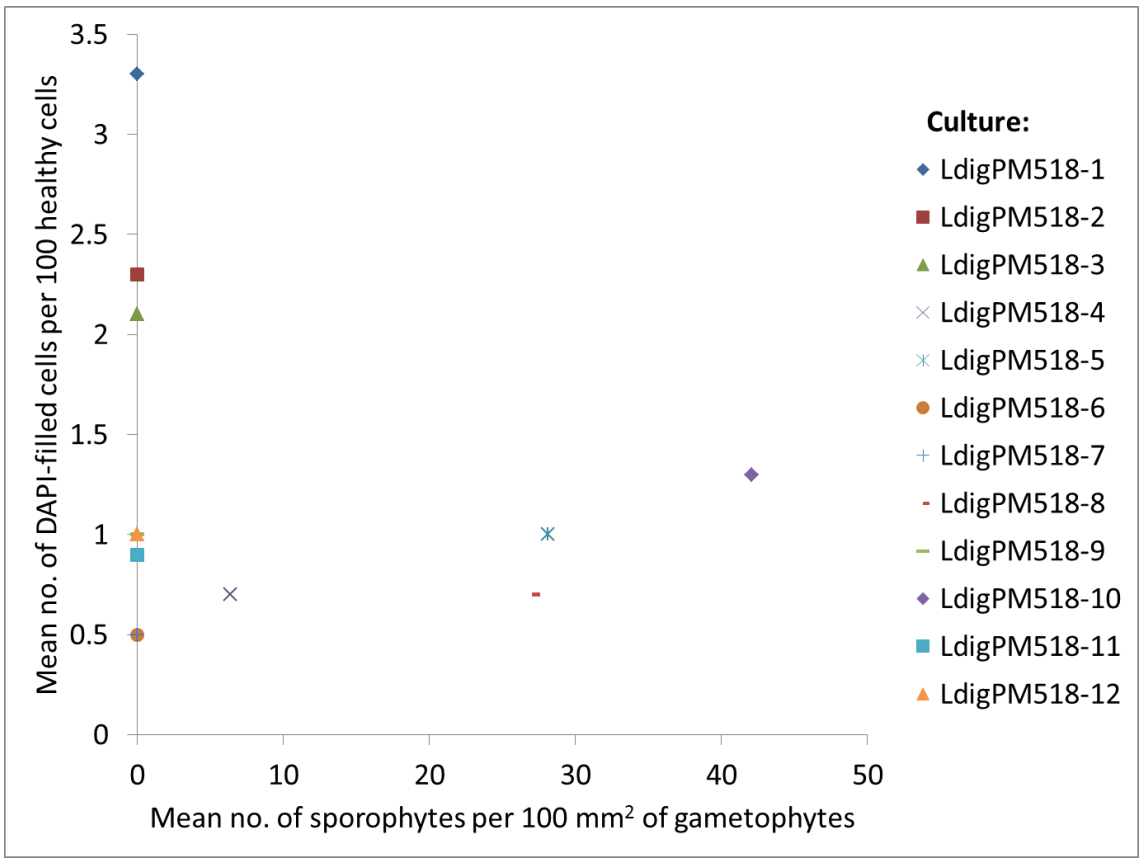

Figure 3.3: Self-crosses of LdigPM518, strains 1-12. The maximum number of sporophytes produced per 100 mm^2 of gametophytes, plotted against the mean number of DAPI-filled cells per 100 healthy cells (n=1). The legend indicates the culture self-crossed.

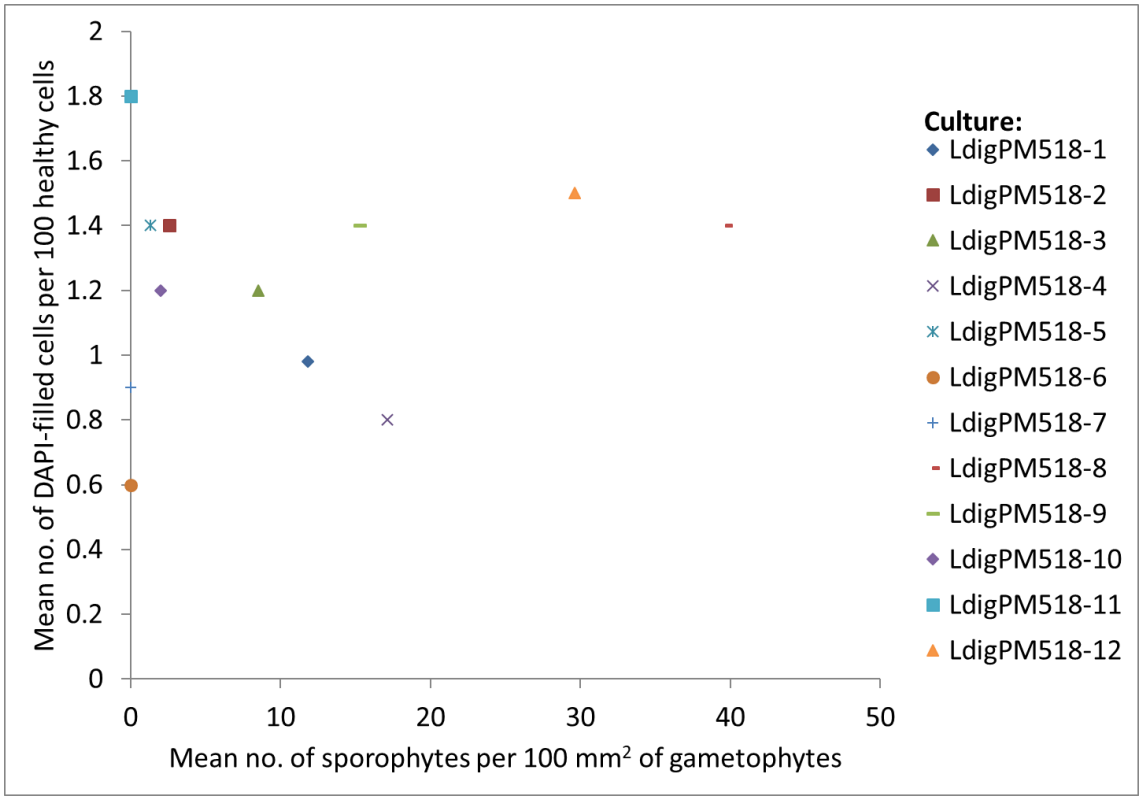

Figure 3.4: Crosses of LdigPM518, strains 1-12 (except self-crosses). Means (n=11) of the maximum number of sporophytes produced per 100 mm^2 of gametophytes, plotted against the mean number of DAPI-filled cells per 100 healthy cells. The legend indicates the culture crossed with the other 11 cultures.

3.4.3 MCP PCR

Except for LdigPM518-5, all LdigPM518 were positive for Phaeovirus MCP. Previously, LdigPH10-30m and LdigPH10-21m were tested by MCP PCR and found to be virus positive and negative, respectively. Repeating the PCR revealed that LdigPH10-21m had become MCP positive.

3.5 Discussion

The 2.7-3.4 times increase (Figure 3.1) in the frequency of DAPI-filled cells at 18 versus 15 ^{o}C was unsupported due to the large variability of DAPI cell occurrence (error bars; Figure 3.1) and the lack of a virus negative control because of the unexpected presence of DAPI-filled cells and Phaeovirus MCP in LdigPH10-21m. Why this culture became MCP positive is unclear; possibilities include viral cross infection from another culture, which would mean kelp phaeoviruses can infect walled cells, perhaps if cell walls are damaged as seen in *Botrytella micromora* (Ectocarpales; [111]). Perhaps the virus was previously integrated into too few vegetative cells (due to host elimination or initiation of a new infection) to be detected and has since then spread throughout the

host. This would mean that kelp Phaeovirus genomes can somehow move between host cells, which is known in plant viruses [109].

It was hypothesised that increased frequency of DAPI-filled cells would mean decreased host reproduction (fewer sporophytes), as virion production was expected to displace gamete production. No correlations were observed in any gametophyte crosses, in either all 144 possible crosses (Figure 3.2 , Figure 3.3, and Figure 3.4). Unfortunately, these cross experiments could not truly test the impact of virus infection on host reproduction, because of two unrecorded factors: the Mendelian segregation of integrated phaeoviruses and variation of gametophyte recruitment. Mendelian segregation means that the gametophytes from an infected sporophyte could be mostly virus-free or infected. This means that the portion of virus-infected gametophytes in all crosses was unknown; a portion could have been in fact virus-free crosses. In outcrosses, gametophyte recruitment variation means that one strain could dominate the culture and in fact be a self-cross. Variation in gametophyte sex ratios would also influence reproduction, but this was not accounted for. Ideally, this experiment would be performed with unialgal, unisex gametophyte cultures of known virus-infection state, and crossed with equal starting biomasses in all crosses. The MCP PCRs should be performed on the unialgal gametophytes to account for homo/heterozygosity of integrated Phaeoviruses. In future, the Mendelian inheritance of Phaeoviruses should be studied in kelp, as it has in *Ectocarpus* [78].

It may also have been better to use DNA stains such as Sybr green and a DAPI-free control to account for background fluorescence due to temperature stress induced cell changes. In future, the extent of virus infection could also be assessed with transcriptomics to compare virus expression with observed symptoms.

3.5.1 Conclusions

At 18 ^{o}C, around 3 % of cells at most were DAPI-filled (Figure 3.1) and in most crosses (115 out of 144), less than 5 % of cells were DAPI-filled (Figure 3.2).

The hypothesis that kelp phaeoviruses are temperature sensitive was not sufficiently tested due to lack of replication and a true negative control.. The confounding factors caused by using gametophyte mixes isolated directly from sporophytes prevented the testing of the hypothesis that increased frequency of Phaeovirus symptoms reduce kelp gametophyte reproduction.

CHAPTER 4 GENOMICS AND MULTI-GENE PHYLOGENY OF KELP PHAEOVIRUSES

4.1 Abstract

The genus Phaeovirus (family *Phycodnaviridae*) are nucleo-cytoplasmic large DNA viruses (NCLDVs) which employ a latent infection strategy in brown algae (class Phaeophyceae) of the orders Ectocarpales and Laminariales (kelp). Despite the evolutionary, economic, and ecological importance of their hosts, the available sequence data of kelp phaeoviruses is restricted to a single gene, namely the major capsid protein gene *mcp*. Next generation sequencing was performed on Phaeovirus MCP PCR-positive and symptomatic gametophytes of the kelp *Laminaria digitata*. The resulting data, along with 3 kelp genomes (*Ecklonia radicosa*, *Saccharina japonica*, and *Undaria pinnatifida*) and 1 kelp viral metagenome (*Ecklonia radiata*), were mapped to the reference genomes of the Ectocarpales phaeoviruses Ectocarpus siliculosus virus 1 (EsV-1) and Feldmannia species virus 158 (FsV-158). We present a range of sequences orthologous to Phaeovirus ORFs which were identified in *L. digitata* (10 orthologs), *E. radicosa* (24), *S. japonica* (9), and *U. pinnatifida* (87). It was hypothesised that these Phaeovirus orthologs originate from a partial genome of Laminaria digitata virus 1 (LdV-1; orthologs to 4.3 % of EsV-1 ORFs; unknown if integrated or from virions), integrated genomes (unclear if partial or complete) from Saccharina japonica virus (SjV; orthologs to 3 % of EsV-1 ORFs) and Ecklonia radicosa virus (ErcV; orthologs to 7.4 % of EsV-1 ORFs), and a putative complete integrated genome of Undaria pinnatifida virus (UpV; orthologs to 36.4 % of EsV-1 ORFs). We expand the set of core NCLDV

genes described in kelp phaeoviruses from one to nine, which is 56 % of the 16 core genes known in phaeoviruses. Core genes included the functions of viral DNA replication, integration and transposition, transcription, nucleotide metabolism, protein synthesis, and capsid structure. Single and concatenated core gene phylogeny placed these viral sequences in Phaeovirus, with LdV-1 in subgroup A or C, SjV in subgroup D, and ErcV and UpV in subgroup A. The putative functions of several other kelp Phaeovirus orthologs provide new insights into the biology of phaeoviruses and their kelp hosts, such as the evolution of Phaeovirus transposases, and revealed that kelp phaeoviruses also encode histidine kinases, host development and defence proteins, and potassium ion channel components.

4.2 Introduction

Laminaria digitata virus 1 (LdV-1), as indicated by PCR of the Major Capsid Protein (*mcp*) gene and transmission electron microscopy (TEM) of virions is a putative member of the dsDNA genus Phaeovirus [305], in the family *Phycodnaviridae* and the Nucleo-cytoplasmic Large DNA Viruses (NCLDVs). Phaeoviruses infect the brown algae (class Phaeophyceae), but they have only been described in detail in the order Ectocarpales, as exemplified by the type species, Ectocarpus siliculosus virus 1 (EsV-1, [100]) amplification of Phaeovirus MCP has expanded the Phaeovirus host range to a total of 8 Laminariales (kelp) species [316], which are among the first non-Ectocarpales brown algae shown to be infected by phaeoviruses.

LdV-1 and the other phaeoviruses of kelp are expected to employ a latent infection strategy like that of the Ectocarpales phaeoviruses (see Section 0.3). This is supported by the PCR amplification of Phaeovirus MCP from healthy kelp sporophyte

and gametophyte tissue, i.e. the MCP PCR amplified the gene in host genomes, not virions [305, 316]. Furthermore, around 50 % of unialgal gametophytes (haploid) from MCP PCR-positive sporophytes (diploid) were found to be MCP PCR-negative, which indicates that a latent virus genome (provirus) has been removed from half of the gametophyte generation by meiotic segregation of chromosomes, as seen in EsV [78, 79]. Latency in kelp phaeoviruses is also supported by the presence of Phaeovirus MCPs integrated into the genome of the kelp *Saccharina japonica* [31].

Phaeoviruses are a major knowledge gap for virology, phycology, conservation efforts, and aquaculture. Though only nine species of Phaeovirus are described and only from a single order of brown algae, phaeoviruses display many unique but poorly understood features. The enigmatic features of phaeoviruses include contradictory genome integration mechanisms (EsV provirus is either a single contiguous sequence; [103], or multiple sequences scattered throughout the genome; [105]), genome reduction (Feldmannia species virus 158, FsV-158, has a genome around half the size of EsV-1; 155 versus 336 kb; [98, 100], novel acute (*r*-selected, subgroup B) versus persistent (*K*-selected, subgroup A) evolutionary dynamics [95], and multiple infections (up to eight distinct viruses integrated into a single host genome; [95]) which challenge the superinfection exclusion hypothesis [97].

Brown algae are members of the SAR clade, which makes them only distantly related to the Archaeplastida (plants and green and red macroalgae, [168, 186]). In addition, they have evolved complex multicellularity independently [103]. These factors suggest that phaeoviruses are a major knowledge gap for evolutionary biology.

To further investigate the enigmatic latent phaeoviruses, we attempted to acquire novel Phaeovirus sequence data from 1) various cellular fractions of *Laminaria digitata* gametophytes, which contained both host and virion derived Phaeovirus DNA,

and 2) from Phaeovirus DNA integrated into three of the currently available kelp genome sequences (*Ecklonia radicosa*, *Saccharina japonica*, and *Undaria pinnatifida*) and 3) one viral metagenome from the kelp *Ecklonia radiata*. We report a set of Phaeovirus orthologs identified in *L. digitata*, and the genomes of *E. radicosa*, *S. japonica*, and *U. pinnatifida*. These orthologs are putatively from a partial Laminaria digitata virus 1 (LdV-1; Chapter 1) genome, integrated genomes of unclear completeness from Saccharina japonica virus (SjV) and Ecklonia radicosa virus (ErcV), and a complete integrated genome of Undaria pinnatifida virus (UpV). These orthologs included nine NCLDV core genes: VV D5-type ATPase (UpV), VV A18-type helicase (UpV), VV D6R-type helicase (LdV-1), PCNA (UpV), VLTF2 (UpV), RRLS (SjV, UpV), RRSS (UpV), VV A32-type ATPase (ErcV, UpV), and MCP (LdV-1, SjV, UpV). Single and concatenated phylogenetic analyses of these core genes placed LdV-1 in subgroup A or C, SjV in subgroup D, and ErcV and UpV in subgroup A, which mostly agrees with previous analyses [305, 316]. The putative functions of the Phaeovirus orthologs identified in these proposed phaeoviruses provide new insights into the biology of phaeoviruses and their kelp hosts.

4.3 Methods and materials

4.3.1 Gametophyte culture conditions

Gametophytes were cultured in half strength Provasoli's enriched seawater (PES; [302]) on a 16:8 light dark cycle at 15 ^{o}C and 18 ^{o}C, with PES media changing every 4 weeks. Gametophytes were kept in red light (covered with red translucent plastic; 22.2 µmol m^{-2} s^{-1}).

4.3.2 Sample preparation for DNA extraction and virion isolation

To separate the culture media and biomass, the cultures were passed through 0.45 µm filters with a vacuum pump. The gametophyte biomass wet weight was recorded and the biomass was ground with a pestle and mortar in liquid nitrogen.

To increase the chances of virus DNA recovery, the homogenised gametophyte material was split into three fractions by centrifugation: the bulk of the cellular material (cell debris pellet, CDP, 1 and 2; Table 4.1), isolated nuclei and chloroplasts (organelle pellet, OP, 3 and 4; Table 4.1), and isolated virions (virus fraction, VF, 5 and 6, Table 4.1). This was performed as follows: to inhibit organelle disruption, the chloroplasts and nuclei were isolated in modified STE (mSTE) buffer: 0.01 M $MgCl_2$ and 0.04 M Tris-HCl (pH 7.8) with an addition of 0.01 M EDTA and 0.4 M sucrose [317, 318]. 500 mg of brown algal material was added per 1.5 mL of mSTE buffer and re-suspended. An equal volume of 2 mm glass beads was added to each Eppendorf tube, vortexed for 1 min, and disrupted at 2500 rpm (Biospec Products Mini-Beadbeater-1) for 40 sec and placed on ice before and after the disruption. The homogenised samples were centrifuged at 200 x g for 20 min. The pellet was kept for DNA extraction (cell debris pellet). The supernatant was centrifuged at 3700 x g for 20 min and the pellet re-suspended (this was repeated twice). The pellet was kept for DNA extraction (organelle pellet). The supernatant was kept for DNA extraction (virus fraction).

Virion isolation was also performed on the culture media in which the gametophytes were kept (MV, 7-9; Table 4.1). The culture media was filtered through a 0.2 µm Quixstand benchtop hollow fibre cartridge pump, which reduced the volume to around 150 mL. The culture media was then concentrated to around 200 µL with a 30 kDa Amicon ultracentrifuge filter according to the manufacturer's instructions.

Table 4.1: Details of samples sequenced. ND = no data (sequencing failed).

Sample Code	Sample description	DNA (ng/µL)	MCP PCR	LSU d1d2 PCR	Illumina Sequenced
1_15_5L_CDP	15 °C, 5 L culture cell debris pellet	91.2	+	+	Y
2_18_5L_CDP	18 °C, 5 L culture cell debris pellet	352	+	-	Y
3_15_5L_OP	15 °C, 5 L culture organelle pellet	14.3	+	+	Y
4_18_5L_OP	18 °C, 5 L culture organelle pellet	412.8	+	+	Y (ND)
5_15_5L_VF	15 °C, 5 L culture virus fraction	62.9	-	-	Y (ND)
6_18_5L_VF	18 °C, 5 L culture virus fraction	45.3	-	-	Y (ND)
7_15_5L_MV	15 °C, 5 L culture media virus isolate	3.6	-	-	N
8_18_5L_MV	18 °C, 5 L culture media virus isolate	<0.1	-	+	N
9_15_10L_MV	15 °C, 10 L culture media virus isolate	30	-	+	N

4.3.3 DNA extraction

For all samples (Table 4.1), DNA was extracted using the Nucleospin Plant II Midi kit (Machery-Nagel), according to the manufacturer's instructions with the following modifications. For the virus fractions and culture media virus isolates, 1 µl of RQ1 RNase-free DNase and 9 µl RQ1 buffer (Promega) were added per 90 µL of viral fraction, and incubated at 37 °C for 30 min. The reaction was terminated with1 µL of DNase stop solution per 100 µL of reaction mix and incubation at 65 °C for 10 min. Next, 1 % β-mercaptoethanol was added and the mix incubated at 37 °C for 30 min. This was followed by the initial 65 °C for 60 min incubation step of the kit's instructions with the addition of 0.5 mg mL^{-1} of proteinase K.

For the cell debris and organelle pellets, 1 % β-mercaptoethanol was added to the buffer PL1 step and incubated at 37 °C for 30 min. This was followed by the initial 65 °C for 60 min incubation step of the kit's instructions with the addition of 0.5 mg mL^{-1} of proteinase K.

DNA was quantified by PicoGreen and Nanodrop. The presence of Phaeovirus was tested with MCP PCR and the presence of PCR inhibitors was tested with PCR of the D1-D2 region of the large subunit ribosomal gene (Table 4.2).

Table 4.2: PCR cycling conditions.

Major capsid protein	268	1.5	2	95, 300	95, 60	55, 30	72, 30	40	72, 600	CVGCGTACTGGGTGAACGC	AGTACTTGTTGAACCAGAACGG

	Large subunit ribosomal D1D2
Product size (bp)	600-800
[Mg^{2+}] (mM)	1.5
For/rev primer (pmol/µl)	2
Initial (°C, sec)	95, 300
Step 1 (°C, sec)	95, 30
Step 2 annealing (°C, sec)	60, 60
Step 3 extension (°C, sec)	72, 60
Cycles of steps 1-3	35
Final elongation (°C, sec)	72, 300
For primer sequence	-
Rev primer sequence	-

4.3.4 Next Generation Sequencing

MiSeq paired-end 2 x 300 bp (Illumina), 300 cycles, version 3 chemistry. Nextera XT library creation standard scale. Each technology was used on the samples as detailed in Table 4.1.

Table 4.3: Datasets used in the analyses. References: *Ecklonia radicosa* genome [319], *Saccharina japonica* genome [306], and *Ecklonia radiata* viral metagenome [120].

Dataset [Accession]	Sequencing technology	No. of sequences	No. of nucleotides	Average sequence length	Format
1_15_5L_CDP	Illumina Miseq	10216904	3075288104	301	Paired reads
2_18_5L_CDP	Illumina Miseq	13555832	4080305432	301	Paired reads
3_15_5L_OP	Illumina Miseq	9567132	2879706732	301	Paired reads
Ecklonia radicosa genome [PRJDB6405]	Illumina Miseq	29956280	3739438584	125	Paired reads
Saccharina japonica genome [JXRI00000000.1]	Illumina Miseq	13327	543425876	40776	Scaffolds
Undaria pinnatifida genome	Illumina Miseq	112333	168154505	1497	Paired end contigs

[SRR2976377]					
Ecklonia radiata viral metagenome [SRX3446198]	Illumina Miseq	542742	79319267	146	Contigs of paired reads
Ecklonia radiata viral metagenome [SRX3446199]	Illumina Miseq	1142971	166660233	146	Contigs of paired reads
Ecklonia radiata viral metagenome [SRX3446200]	Illumina Miseq	504250	73775745	146	Contigs of paired reads
Ecklonia radiata viral metagenome [SRX3446201]	Illumina Miseq	772410	112927229	146	Contigs of paired reads
Ecklonia radiata viral metagenome [SRX3446202]	Illumina Miseq	605515	88778690	147	Contigs of paired reads
Ecklonia radiata viral metagenome [SRX3446203]	Illumina Miseq	1045902	153230741	147	Contigs of paired reads

4.3.5 Sequence assembly and annotation

All sequence analysis steps were performed with Geneious Prime 2019.0.4 (https://www.geneious.com). The ends of all sequence reads were trimmed where there was a >5 % chance of error per base, based on the base call quality. Two methods were applied to detect phaeovirus-like sequences. In method A, reads were mapped to a Phaeovirus reference genome (repeated for EsV-1; NC_002687 and FsV-158; NC_011183) at Medium Sensitivity/Fast with up to 5 iterations. In method B, reads were further verified using BLASTn searches restricted to EsV-1 and FsV-158. The consensus sequences of reads aligned with Phaeovirus ORFs by mapping (method A) or BLASTn (method B) were extracted and annotated as the corresponding Phaeovirus ORF. The identity of the consensus sequences was analysed using BLASTn (assembly method A only) and BLASTx. Consensus sequences with phaeoviruses as their top protein (BLASTx) search hits (Bit-Scores above 100) were annotated as potential Phaeovirus genes or partial genes and with putative function/features (Table 4.4).

4.3.6 Sequence analysis and phylogeny

Proteins which contained at least one conserved domain of a core NCLDV gene [98] were aligned using ClustalW with the corresponding proteins of NCLDVs (*Poxviridae*, *Iridoviridae*, *Phycodnaviridae*, *Asfarviridae*, and *Mimiviridae*). Maximum likelihood phylogenetic trees were constructed from both single and concatenated protein alignments using the Geneious Prime PhyML plugin (http://www.atgc-montpellier.fr/phyml/) with the LG substitution model and 100 bootstraps. The trees were visualised using Inkscape 0.92 (https://inkscape.org/en/).

4.4 Results

4.4.1 Presence of putative Phaeovirus orthologs

A total of ten different Phaeovirus orthologs were present in the Illumina-sequenced *L. digitata* samples 1_15_5L_CDP (ten orthologs), 2_18_5L_CDP (three orthologs), and 3_15_5L_OP (three orthologs) (Table 4.4). In all three *L. digitata* samples, *mcp* was present and more Phaeovirus orthologs were detected when assembled to EsV-1 (seven orthologs) versus FsV-158 (four orthologs). No Phaeovirus orthologs were present in the MinION-sequenced samples. Culture temperature may have increased the number of Phaeovirus orthologs at 15 versus 18 ^{o}C (ten orthologs in 1_15_5L_CDP versus three in 2_18_5L_CDP; Table 4.4).

The kelp genomes contained the following numbers of different Phaeovirus orthologs (Table 4.4), with the number of those orthologs assembled to EsV-1 versus FsV-158 (in parentheses): *Ecklonia radicosa* 24 (16 versus 9), *Saccharina japonica* 9 (6 versus 6), and *Undaria pinnatifida* 87 (85 versus 11). No Phaeovirus orthologs were found in the viral metagenome of *Ecklonia radiata*.

A total of 104 different Phaeovirus orthologs were found for all the kelp sequence data tested. Of these, 37 were orthologs of genes with known or putative functions, which included nine NCLDV core genes (Table 4.5). The most commonly found core gene was *mcp*, which was present in all three LdV samples, SjV, and UpV. Subsequent phylogenetic analyses were based on these nine NCLDV core genes (Figures 4.1-4.7).

Table 4.4: Sequences identified in LdV-1, ErcV, SjV, and UpV which were orthologs of ORFs (based on amino acid sequences) in the phaeoviruses EsV-1, EsV provirus, FsV-158, and FirrV-1. (A) and (B) indicate the method used for the assembly of orthologs. See Appendices Tables A.4.1 and A.4.2 for full details of all Phaeovirus BLAST hits.

Annotation reference	**EsV-1 ortholog(s)**	**EsV provirus ortholog(s)**	**FsV-158 ortholog(s)**	**FirrV-1 ortholog(s)**	**Putative Function/Features**
1_15_5L_CDP to EsV-1 (A)					
23	23				Helicase (VV D6R)
24	24	24			Unknown
116	116	116	59	B50	Major capsid protein
210, 211	210, 211	210			Unknown
231	231	231			Unknown
1_15_5L_CDP to EsV-1 (B)					
145269 - 146699	116	116	59	B50	Major capsid protein
196773 - 197924	170	155, 170			Transposase (DDE domain; IS4 family)
222390 -	155, 170	155, 170			Transposase (DDE domain; IS4 family)

223541					
298428 - 299969	210, 211	210			Unknown
300736 - 303096	213	213	13		Integrase (phage integrase family)
332508 - 333659	231	231			Unknown
1_15_5L_CDP to FsV-158-1 (A)					
59	116	116	59	B50	Major capsid protein
1_15_5L_CDP to FsV-158-1 (B)					
1212 - 2438			2		Transposase (OrfB_Zn_ribbon superfamily)
2383 - 3063			3		Integrase/resolvase (Serine Recombinase family)
52791 - 54098	116	116	59	B50	Major capsid protein
2_18_5L_CDP to EsV-1 (A)					
116	116	116	59	B50	Major capsid protein
2_18_5L_CDP to EsV-1 (B)					
145269 - 146699	116	116	59	B50	Major capsid protein
298428 - 299969	210, 211	210	4, 75	A33	Unknown
2_18_5L_CDP to FsV-158 (A)					
59	116	116	59	B50	Major capsid protein
2_18_5L_CDP to FsV-158 (B)					
52791 - 54098	116	116	59	B50	Major capsid protein
3_15_5L_OP to EsV-1 (B)					
145269 - 146699	116	116	59	B50	Major capsid protein
3_15_5L_OP to FsV-158 (B)					
1212 - 2438			2		Transposase (OrfB_Zn_ribbon superfamily)
52791 - 54098	116	116	59	B50	Major capsid protein
E. *radicosa* to EsV-1 (A)					
7		7			Unknown
7		7			Unknown

Table 4.4 (continued)

Annotation reference	**EsV-1 ortholog(s)**	**EsV provirus ortholog(s)**	**FsV-158 ortholog(s)**	**FirrV-1 ortholog(s)**	**Putative Function/Features**
17	17				Unknown (Ankyrin repeats)
26	26		87	A12	Viral ATPase (VV A32-type ATPase)
29	29				Helicase (Superfamily I)
129	129				Adenine DNA methylase
153	153	153		E5	Unknown
155		170			Transposase (DDE domain; IS4 family)
170	155, 170	155, 170			Transposase (DDE domain; IS4 family)
182	182				Replication factor C-Archaeae small subunit (ATPase)
231	231	231			Unknown
157, 175	157, 175				Unknown
160	160	210, 211	72		Unknown
E. *radicosa* to EsV-1 (B)					
17330 - 18466	7	7			Unknown

196773 - 197924	155, 170	155, 170			Transposase (DDE domain; IS4 family)
199080 - 199757	210, 211	210, 211			Unknown
222390 - 223541	155, 170	155, 170			Transposase (DDE domain; IS4 family)
253899 - 254879	182				Replication factor C-Archaeae small subunit (ATPase)
268569 - 269711	155, 170	155, 170			Transposase (DDE domain; IS4 family)
30668 - 34069	17				Unknown (Ankyrin repeats)
58289 - 59161	26		87	A12	Viral ATPase (VV A32-type ATPase)
E. *radicosa* to FsV-158 (A)					
3			3		Integrase/resolvase (Serine Recombinase family)
96		180	96	A20	Ribonucleotide reductase large subunit
70, 135			135		Unknown
E. *radicosa* to FsV-158 (B)					
1212 - 2438			2		Transposase (OrfB_Zn_ribbon superfamily)
2383 - 3063			3		Integrase/resolvase (Serine Recombinase family)
33011 - 34882		164	38	B30	NosD copper-binding protein & precursor
93295 - 95616		180	96	A20	Ribonucleotide reductase large subunit
S. japonica to EsV-1 (B)					
145269 - 146699		116	59	B50	Major capsid protein
18439 - 20712	178/222			M1	Transposase (OrfB_Zn_ribbon superfamily)
201313 - 201933	158	158	136	G2	Protein lysine methyltransferase
220067 - 222340	178/222			M1	Transposase (OrfB_Zn_ribbon superfamily)
222390 - 223541	155, 170	155, 170			Transposase (DDE domain; IS4 family)
248410 - 250707				A20	Ribonucleotide reductase large subunit
268569 - 269711	155, 170	155, 170			Transposase (DDE domain; IS4 family)
S. japonica to FsV-158 (B)					

Table 4.4 (continued)

Annotation reference	**EsV-1 ortholog(s)**	**EsV provirus ortholog(s)**	**FsV-158 ortholog(s)**	**FirrV-1 ortholog(s)**	**Putative Function/Features**
134578 - 135201	158	158	136	G2	Protein lysine methyltransferase
145492 - 146463			146		Unknown
2383 - 3063			3	P1	Integrase/resolvase (Serine Recombinase family)
3270 - 4646	211		4		Unknown
52791 - 54098	116	116	59	B50	Major capsid protein
93295 - 95616			96	A20	Ribonucleotide reductase large subunit
U. pinnatifida to EsV-1 (A)					
29	29				Helicase (Superfamily I)
30	30	30			Unknown
36	36	36			Unknown
42	42	42	117	A43	Unknown
43	43	43	118		Unknown
45	45	45	121	A46	Unknown

56	56	56	46	B38	Unknown
67	67	67	39	B32	Unknown
68	68	68			Unknown
70	70	70	42		Unknown
71	71	71			Unknown
76	76	76	18	B10, I1	Unknown
91	91	91	108	A30	Unknown
109	109		34	B27	Superfamily III helicase (viral) (VV D5-type ATPase)
114	114	114			Unknown (Ankyrin repeats)
116	116	116	59	B50	Major capsid protein
117	117	117			Putative antirepressor of the lysogenic cycle
125	125	125			Unknown
126	126	126			Exonuclease (DEDDh 3'-5' exonuclease domain)
131	131	131			Unknown
132	132	132	80	A6	Proliferating cell nuclear antigen
133	133	133			Unknown
172	172	172	132		Ubiquitin ligase
U. pinnatifida to EsV-1 (B)					
100261 - 101223	71	71			Unknown
102474 - 104003	74	74			Unknown
104041 - 105222	75				Cysteine protease C1A
105297 - 106166	76	76	18	I1	Unknown
106169 - 107170	77	77	19	B11	Unknown
107251 - 108126	78				Unknown
108100 - 108534	79	79			Unknown
108596 - 109240	80	80			Heat shock protein 40 (DnaJ super family: DnaJ/Hsp40)

Table 4.4 (continued)

Annotation reference	**EsV-1 ortholog(s)**	**EsV provirus ortholog(s)**	**FsV-158 ortholog(s)**	**FirrV-1 ortholog(s)**	**Putative Function/Features**
109978 - 110892	82	82			Protein kinase (Pkinase superfamily)
110936 - 111721	83	83			UDP-glucose/GDP-mannose dehydrogenase
114900 - 115874	87	87			Replication factor C-Archaeae small subunit (ATPase)
118751 - 120406	91	91	108	A30	Unknown
125039 - 125923	96	96			Very late transcription factor 2
125984 - 126961	97, 98	97, 98			Unknown
128037 - 128306	99	99			Unknown
128758 - 129720	101	101	28	B20	Very late transcription factor 3
135055 - 136875	109		34	B27	Superfamily III helicase (viral) (VV D5-type ATPase)
138875 - 140626	112				Viral hybrid histidine kinase
140674 - 141000	113				Viral phosphoshuttle (histidine-containing phosphotransfer domain)

141087 - 142181	114	114			Unknown (Ankyrin repeats)
145269 - 146699	116	116	59	B50	Major capsid protein
155049 - 155492	124	124			Unknown
155574 - 156134	125	125			Unknown
156149 - 156769	126	126			Exonuclease (DEDDh 3'-5' exonuclease domain)
157195 - 158454	128	128	94	A19	Ribonucleotide reductase small subunit
161005 - 161910	132	132	80	A6	Proliferating cell nuclear antigen
161911 - 162972	133	133			Unknown
165925 - 166356	137	137	101	O1	Unknown
166394 - 167602	138	138			Replication factor C-Archaeae large subunit (ATPase)
167599 - 168423	139	139			Oligoribonuclease (DnaQ-like 3'-5' exonuclease domain superfamily)
168542 - 169369	140	140			Unknown
169378 - 170004	141	141			Unknown
170007 - 171344	142	142			Ubiquitin ligase
179752 - 180714	149	149			Unknown
194450 - 196723	178/222				Transposase (OrfB_Zn_ribbon superfamily)
196773 - 197924	155, 170	155, 170			Transposase (DDE domain; IS4 family)
199080 - 199757	210/211	210/211			Unknown
211615 - 213702	164	164			NosD copper-binding protein
217194 - 218375	169	169			Thaumatin-like protein (glycoside hydrolase family 64)
220067 - 222340	178/222				Transposase (OrfB_Zn_ribbon superfamily)
222390 - 223541	155, 170	155, 170			Transposase (DDE domain; IS4 family)

Table 4.4 (continued)

Annotation reference	**EsV-1 ortholog(s)**	**EsV provirus ortholog(s)**	**FsV-158 ortholog(s)**	**FirrV-1 ortholog(s)**	**Putative Function/Features**
232829 - 236530	171				Unknown
236917 - 239346	172	172			Ubiquitin ligase
243546 - 244310	176	176	147		von Willebrand factor (type A)
248410 - 250707	180	180			Ribonucleotide reductase large subunit
253899 - 254879	182	182			Replication factor C-Archaeae small subunit (ATPase)
254986 - 255393	183	183			Unknown
255485 - 256198	184	184			Unknown
259449 - 260423	187	187			Replication factor C-Archaeae small subunit (ATPase)
268569 - 269711	155, 170	155, 170			Transposase (DDE domain; IS4 family)
275146 - 276396	199	199			Unknown (ankyrin repeats)
293009 - 293626	207	207	139	C7	Unknown

295172 - 296371	209	209			Unknown
296503 - 298032	210, 211	210			Unknown
298428 - 299969	210, 211	210	4, 135		Unknown
321504 - 321878	223				Potassium channel pore region
321942 - 322916	224				Replication factor C-Archaeae small subunit (ATPase)
325898 - 327883	226				Glycoprotein-1 (putative capsid protein)/ mannuronan C-5-epimerase
42136 - 43974	23				Helicase (VV D6R)
58289 - 59161	26		87	A12	Viral ATPase (VV A32-type ATPase)
60675 - 62702	29				Helicase (Superfamily I)
63677 - 64435	31				Unknown (Ankyrin repeats)
65100 - 67328	34				Phage-related protein (COG5412 super family)
68781 - 69413	37				Unknown
72084 - 73547	40	40			Unknown
73599 - 74072	41	41	116	A42	Unknown
74069 - 74593	42	42			Unknown
75843 - 77543	45	45			Unknown
78090 - 78410	47	47			Unknown
79165 - 80433	50	50			Unknown
80854 - 81222	52	52			Unknown
81236 - 81796	53	53			Unknown
83273 - 84919	56	56	46	B38	Calcium binding protein 1
87711 - 88136	59	59			Unknown
90438 - 91031	63	63			Unknown
94110 - 95543	66	66			Helicase (DEAD/H-like, Superfamily II)
95964 - 98036	68	68			Unknown

Table 4.4 (continued)

Annotation reference	**EsV-1 ortholog(s)**	**EsV provirus ortholog(s)**	**FsV-158 ortholog(s)**	**FirrV-1 ortholog(s)**	**Putative Function/Features**
U. pinnatifida to FsV-158 (B)					
105428 - 105649			110		Unknown
109479 - 109877	41	41	116	A42	Unknown
133324 - 134460	210, 211	210	4, 135	P1	Unknown
20971 - 21651	96	96	22	I5	Very late transcription factor 2
24052 - 24963	101		28	B20	Very late transcription factor 3
28433 - 30262	109		34	B27	Superfamily III helicase (viral) (VV D5-type ATPase)
33011 - 34882		164	38	B30	NosD copper-binding protein & precursor
52791 - 54098	116	116	59	B50	Major capsid protein
63668 - 64714	211	210, 211	72, 135		Unknown
78029 - 78889	132	132	80	A6	Proliferating cell nuclear antigen
91664 - 92692	128	128	94	A19	Ribonucleotide reductase small subunit

Table 4.5: Putative Phaeovirus proteins encoded by LdV-1 and kelp genomes (ErcV, SjV, and UpV). Core NCLDV proteins are underlined. LdV-1 (1)= 1_15_5L_CDP, LdV-1 (2)= 2_18_5L_CDP, LdV-1 (3)= 3_15_5L_OP.

Putative Function	LdV-1 (1)	LdV-1 (2)	LdV-1 (3)	ErcV	SjV	UpV	EsV-1	FsV-158	FirrV-1
DNA replication, recombination, repair, and modification									
ATPase (VV D5-type)						Y	109	34	B27
Adenine DNA methylase				Y			129	37	B29
Exonuclease (DEDDh 3'-5' exonuclease domain)						Y	126		
Helicase (Superfamily I)				Y		Y	29		
Helicase (VV A18-type)						Y	66		
Helicase (VV D6R-type)	Y					Y	23		
Proliferating cell nuclear antigen						Y	132	80	A6
Replication factor C-Archaea large subunit (ATPase)						Y	138	105	A26
Replication factor C-Archaea small subunit (ATPase)				Y			182		
Integration and transposition									
Integrase (phage integrase family)	Y						213	13	B4
Integrase/resolvase (Serine Recombinase family)				Y	Y			3	
Transposase (DDE domain; IS4 family)	Y			Y	Y	Y	155, 170		
Transposase (OrfB_Zn_ribbon superfamily)	Y		Y	Y	Y	Y		2	
Transcription									
Oligoribonuclease (DnaQ-like domain)						Y	139	77	A3
Very late transcription factor 2						Y	96	22	B14/15
Very late transcription factor 3						Y	101	28	B20
Nucleotide metabolism									
Ribonucleotide reductase large subunit (RRLS)				Y	Y	Y	180	96	A20
Ribonucleotide reductase small subunit (RRSS)						Y	128	94	A19
Viral ATPase (VV A32-type)				Y		Y	26	87	A12
Protein and lipid synthesis, modification, and degradation									
Cysteine protease C1A						Y	75	126	A48
Protein lysine methyltransferase					Y		158	136	G2
Ubiquitin ligase						Y	142, 172	132	D5
Signalling									
Protein kinase (Pkinase superfamily)						Y	82		
Viral hybrid histidine kinase						Y	112		
Viral phosphoshuttle						Y	113		
Miscellaneous									
Calcium binding protein 1						Y	56	46	B38
Glycoprotein-1						Y	226		
Heat shock protein 40 (DnaJ super family)						Y	80		
Major capsid protein	Y	Y	Y		Y	Y	116	59	B50
NosD copper-binding protein				Y		Y	164	38	B30
Phage-related protein (COG5412 super family)						Y	34		
Potassium channel pore region						Y	223		
Putative antirepressor of the lysogenic cycle						Y	117		

Thaumatin-like protein						Y	10	169	
UDP-glucose/GDP-mannose dehydrogenase						Y	83		
von Willebrand factor (type A)						Y	176	147	

4.4.2 Phylogenetic analyses

LdV-1 was supported as a subgroup A Phaeovirus by Figures 4.2B (100 bootstrap) and 4.6B (100 bootstrap). However, LdV-1 was also supported as its own subgroup, most closely related to subgroup D by Figures 4.3A (100 and 91 bootstraps) and 4.7 (unsupported bootstrap). For the partial MCP region (Figure 4.7), 1_15_5L_CDP (FB) and 3_15_5L_OP (EB) were highly divergent from the phaeoviruses, suggesting that the most accurate assembly was 1_15_5L_CDP (FA and EB). ErcV was supported as a subgroup A Phaeovirus by Figures 4.1B (95 bootstrap). SjV was supported as the sole member of subgroup D (defined in chapter 2) by Figures 4.3A (100 bootstrap), 4.4A (84 bootstrap), 4.6C (68 bootstrap), and 4.7 (80 bootstrap). UpV was well supported as a subgroup A Phaeovirus by Figures 4.1A (99 bootstrap), 4.1B (95 bootstrap), 4.2A (100 bootstrap), 4.3B (82 bootstrap), 4.4A (74 bootstrap), 4.4B (99 bootstrap), 4.4C (96 bootstrap), 4.5A (100 bootstrap), 4.5B (100 bootstrap), 4.6A (100 bootstrap), 4.6B (100 bootstrap), 4.6C (100 bootstrap), and 4.7. UpV was placed in its own distinct subgroup by Figures 4.2B (100 bootstrap) and 4.3A (86 bootstrap).

In all single protein trees (except VLTF2; Figure 4.3B) including the subgroup B viruses, Phaeovirus and the subgroups A and B are strongly supported. The concatenated protein trees distinguish the NCLDV families which good support (Figure 4.5), except those in Figure 4.6, which suggest that *Phycodnaviridae* was polyphyletic.

A

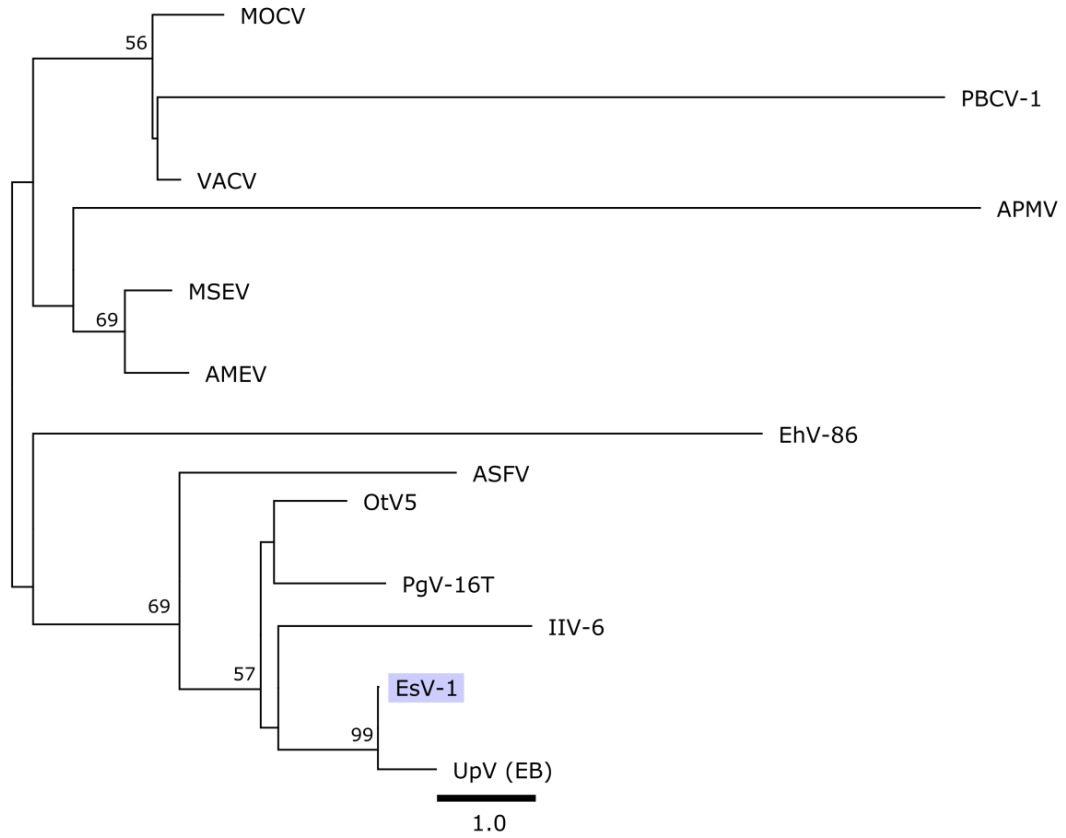
MOCV
56
PBCV-1
VACV
APMV
MSEV
69
AMEV
EhV-86
ASFV
OtV5
PgV-16T
69
IIV-6
57
EsV-1
99
UpV (EB)
1.0

B

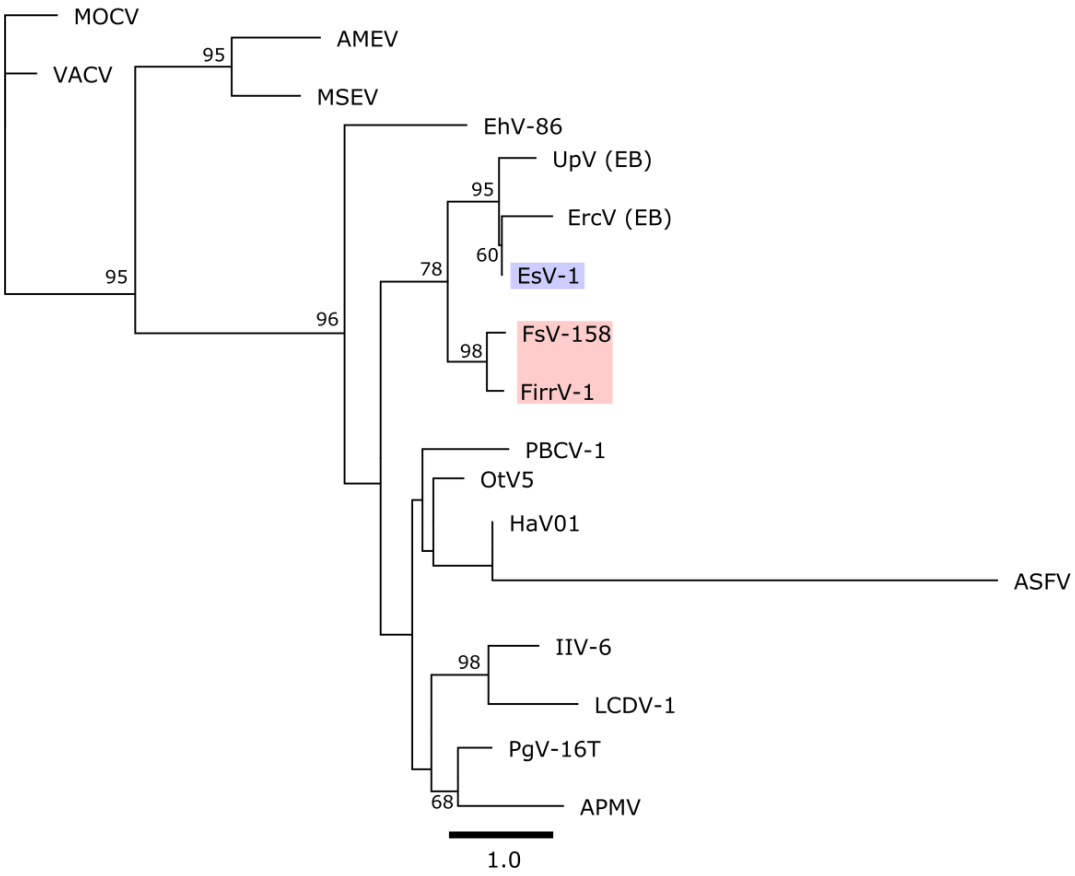
MOCV
AMEV
95
VACV
MSEV
EhV-86
UpV (EB)
95
ErcV (EB)
60
78
EsV-1
95
96
FsV-158
98
FirrV-1
PBCV-1
OtV5
HaV01
ASFV
IIV-6
98
LCDV-1
PgV-16T
68
APMV
1.0

Figure 4.1: Maximum likelihood phylogenetic tree of (A) VV A18-type helicase and (B) VV A32-type ATPase. Assembly method labelled as follows: EsV-1 method A (EA), EsV-1 method B (EB), FsV-158 method A (FA), FsV-158 method B (FB). This study's LdV-1 samples labelled as 1_15_5L_CDP, 2_18_5L_CDP, and 3_15_5L_OP. The abbreviations for viruses are as follows: MOCV, Molluscum contagiosum virus; VACV, Vaccinia virus; MSEV, Melanoplus sanguipes entomopoxvirus; AMEV, Amsacta moorei entomopoxvirus; IIV-6, Invertebrate iridescent virus 6; LCDV-1, Lymphocystis disease virus 1; ASFV, African swine fever virus; APMV, Acanthamoeba polyphaga mimivirus; PgV-16T, Phaeocystis globosa virus 16T; EhV-86, Emiliania huxleyi virus 86; HaV01, Heterosigna akashiwo virus 1; OtV5, Ostreococcus tauri virus 5; PBCV-1, Paramecium bursaria virus 1; EsV-1, Ectocarpus siliculossu virus 1; FsV-158, Feldmannia species virus 158; FirrV-1, Feldmannia irregularis virus 1; ErcV, Ecklonia radicosa virus; SjV, Saccharina japonica virus; UpV, Undaria pinnatifida virus. Node values are maximum likelihood bootstrap values (values <50 not shown). Trees rooted with the *Poxviridae* (MOCV, VACV, MSEV, AMEV). See Appendices Figures A.4.1 and A.4.2 for sequence alignments and GenBank Accession numbers. Scale units are the number of amino acid substitutions per site.

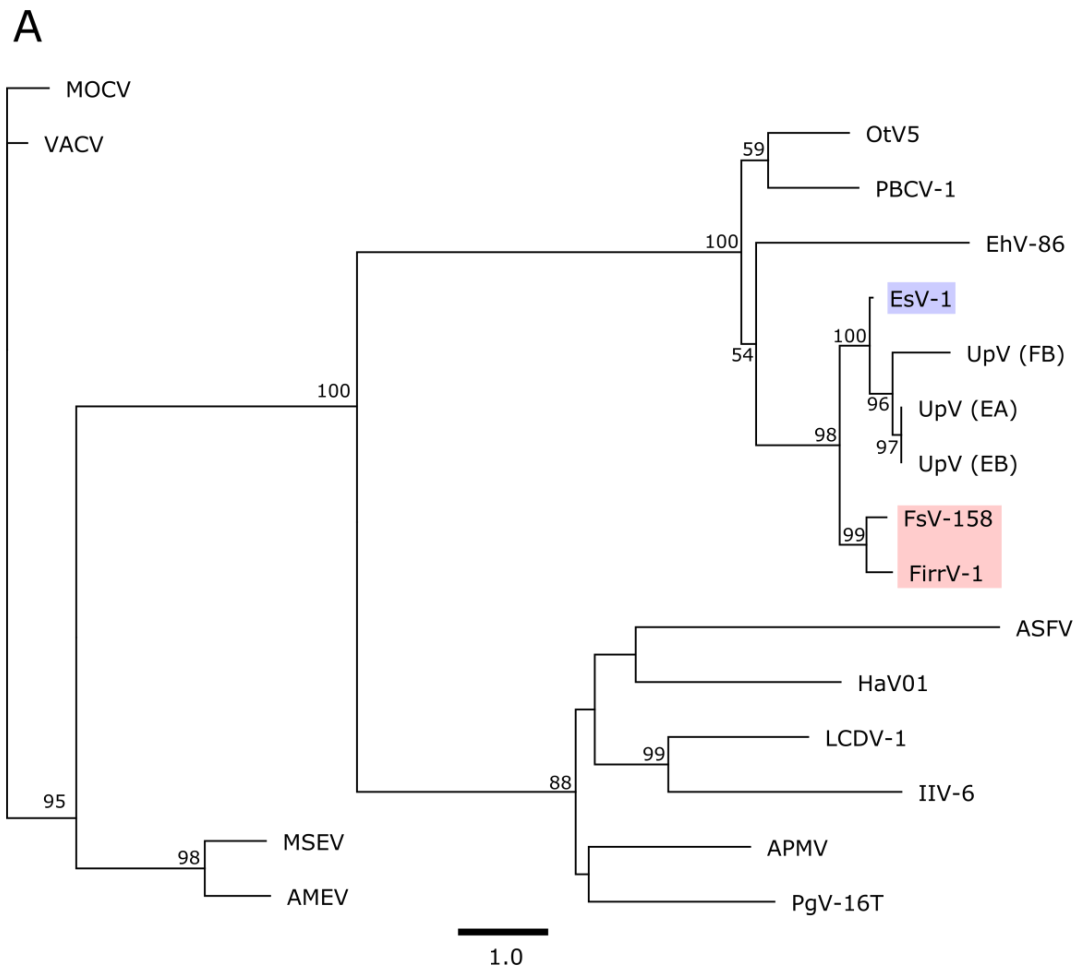
A
MOCV
VACV
OtV5
PBCV-1
EhV-86
EsV-1
UpV (FB)
UpV (EA)
UpV (EB)
FsV-158
FirrV-1
ASFV
HaV01
LCDV-1
IIV-6
APMV
PgV-16T
MSEV
AMEV
59
100
54
100
96
97
98
99
100
99
88
95
98
1.0

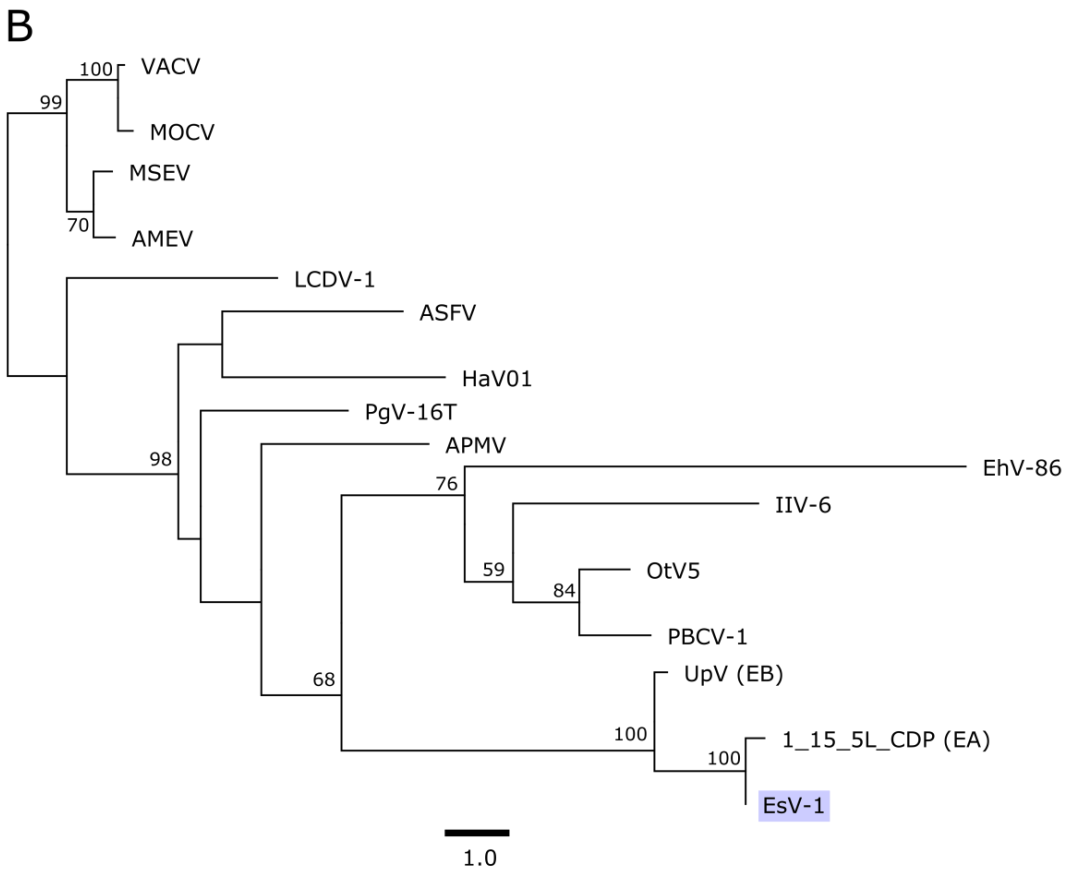
B
VACV
MOCV
MSEV
AMEV
LCDV-1
ASFV
HaV01
PgV-16T
APMV
EhV-86
IIV-6
OtV5
PBCV-1
UpV (EB)
1_15_5L_CDP (EA)
EsV-1
100
99
70
98
76
59
84
68
100
100
1.0

Figure 4.2: Maximum likelihood phylogenetic tree of (A) VV D5-type ATPase and (B) VV D6R-type helicase. Assembly method labelled as follows: EsV-1 method A (EA), EsV-1 method B (EB), FsV-158 method A (FA), FsV-158 method B (FB). This study's LdV-1 samples labelled as 1_15_5L_CDP, 2_18_5L_CDP, and 3_15_5L_OP. The abbreviations for viruses are as follows: MOCV, Molluscum contagiosum virus; VACV, Vaccinia virus; MSEV, Melanoplus sanguipes entomopoxvirus; AMEV, Amsacta moorei entomopoxvirus; IIV-6, Invertebrate iridescent virus 6; LCDV-1, Lymphocystis disease virus 1; ASFV, African swine fever virus; APMV, Acanthamoeba polyphaga mimivirus; PgV-16T, Phaeocystis globosa virus 16T; EhV-86, Emiliania huxleyi virus 86; HaV01, Heterosigna akashiwo virus 1; OtV5, Ostreococcus tauri virus 5; PBCV-1, Paramecium bursaria virus 1; EsV-1, Ectocarpus siliculossu virus 1; FsV-158, Feldmannia species virus 158; FirrV-1, Feldmannia irregularis virus 1; ErcV, Ecklonia radicosa virus; SjV, Saccharina japonica virus; UpV, Undaria pinnatifida virus. Node values are maximum likelihood bootstrap values (values <50 not shown). Trees rooted with the *Poxviridae* (MOCV, VACV, MSEV, AMEV). See Appendices Figures A.4.3 and A.4.4 for sequence alignments and GenBank Accession numbers. Scale units are the number of amino acid substitutions per site.

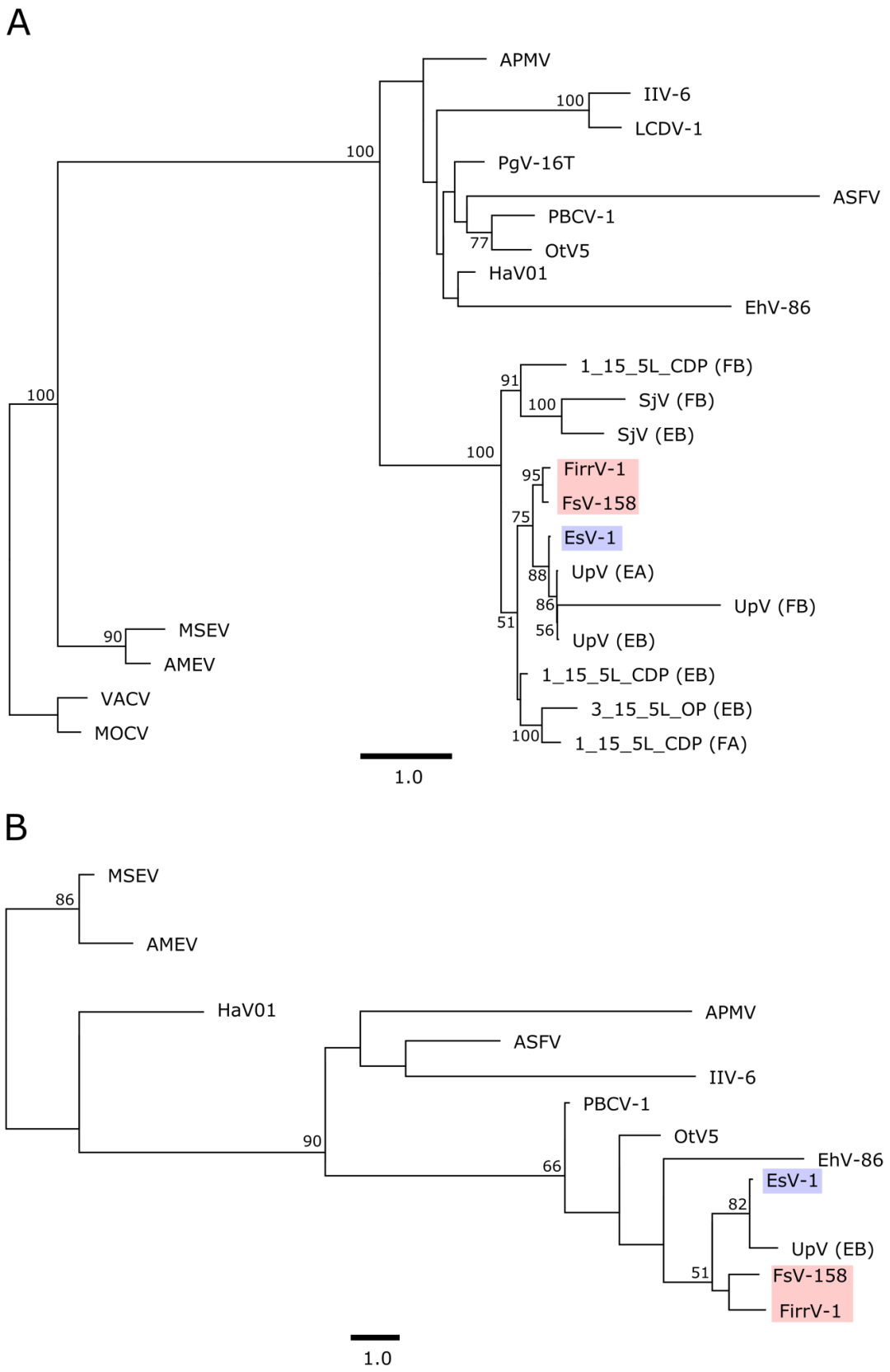
A
APMV
IIV-6
LCDV-1
PgV-16T
ASFV
PBCV-1
OtV5
HaV01
EhV-86
1_15_5L_CDP (FB)
SjV (FB)
SjV (EB)
FirrV-1
FsV-158
EsV-1
UpV (EA)
UpV (FB)
UpV (EB)
1_15_5L_CDP (EB)
3_15_5L_OP (EB)
1_15_5L_CDP (FA)
MSEV
AMEV
VACV
MOCV
100
100
100
100
91
100
100
95
75
88
86
56
51
90
100
1.0
B
MSEV
AMEV
HaV01
APMV
ASFV
IIV-6
PBCV-1
OtV5
EhV-86
EsV-1
UpV (EB)
FsV-158
FirrV-1
86
90
66
82
51
1.0

Figure 4.3: Maximum likelihood phylogenetic tree of (A) MCP and (B) VLTF2. Assembly method labelled as follows: EsV-1 method A (EA), EsV-1 method B (EB), FsV-158 method A (FA), FsV-158 method B (FB). This study's LdV-1 samples labelled as 1_15_5L_CDP, 2_18_5L_CDP, and 3_15_5L_OP. The abbreviations for viruses are as follows: MOCV, Molluscum contagiosum virus; VACV, Vaccinia virus; MSEV, Melanoplus sanguipes entomopoxvirus; AMEV, Amsacta moorei entomopoxvirus; IIV-6, Invertebrate iridescent virus 6; LCDV-1, Lymphocystis disease virus 1; ASFV, African swine fever virus; APMV, Acanthamoeba polyphaga mimivirus; PgV-16T, Phaeocystis globosa virus 16T; EhV-86, Emiliania huxleyi virus 86; HaV01, Heterosigna akashiwo virus 1; OtV5, Ostreococcus tauri virus 5; PBCV-1, Paramecium bursaria virus 1; EsV-1, Ectocarpus siliculossu virus 1; FsV-158, Feldmannia species virus 158; FirrV-1, Feldmannia irregularis virus 1; ErcV, Ecklonia radicosa virus; SjV, Saccharina japonica virus; UpV, Undaria pinnatifida virus. Node values are maximum likelihood bootstrap values (values <50 not shown). Trees rooted with the *Poxviridae* (MOCV, VACV, MSEV, AMEV). See Appendices Figures A.4.5 and A.4.6 for sequence alignments and GenBank Accession numbers. Scale units are the number of amino acid substitutions per site.

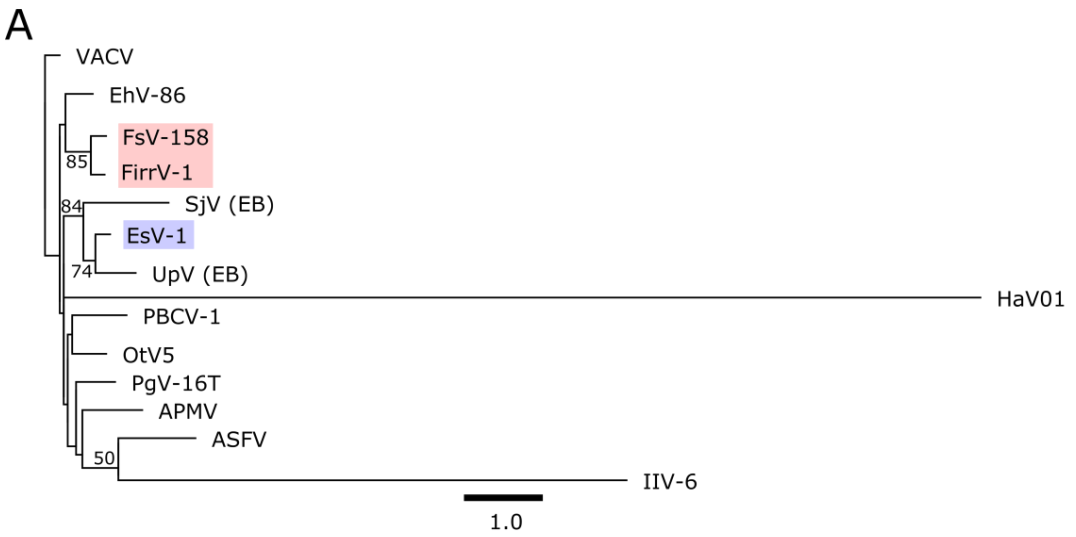
A
VACV
EhV-86
FsV-158
FirrV-1
85
84
SjV (EB)
EsV-1
74
UpV (EB)
HaV01
PBCV-1
OtV5
PgV-16T
APMV
ASFV
50
IIV-6
1.0

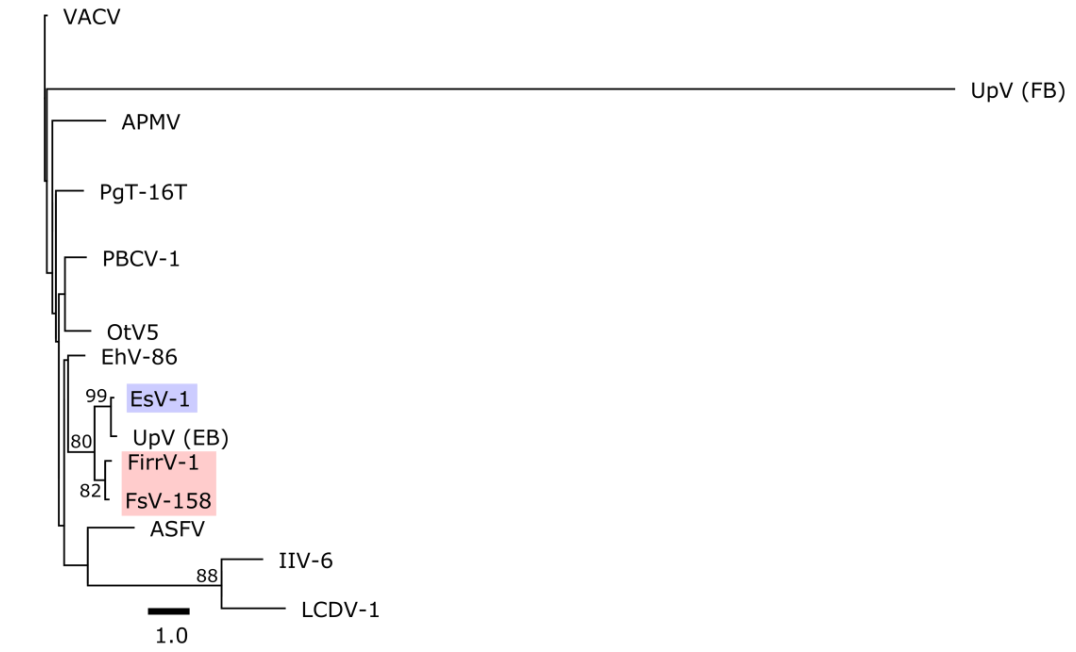
B
VACV
UpV (FB)
APMV
PgT-16T
PBCV-1
OtV5
EhV-86
99
EsV-1
80
UpV (EB)
FirrV-1
82
FsV-158
ASFV
IIV-6
88
LCDV-1
1.0

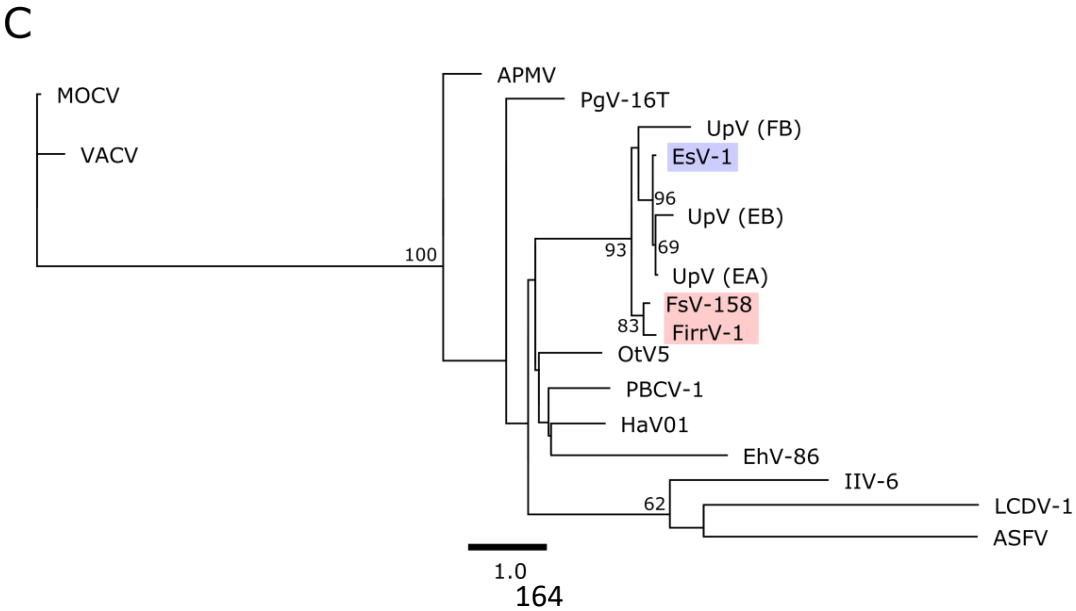
C
MOCV
VACV
APMV
PgV-16T
UpV (FB)
EsV-1
96
UpV (EB)
100
93
69
UpV (EA)
FsV-158
83
FirrV-1
OtV5
PBCV-1
HaV01
EhV-86
IIV-6
62
LCDV-1
ASFV
1.0

Figure 4.4: Maximum likelihood phylogenetic tree of (A) Ribonucleotide reductase large subunit, (B) ribonucleotide reductase small subunit, and (C) PCNA. Assembly method labelled as follows: EsV-1 method A (EA), EsV-1 method B (EB), FsV-158 method A (FA), FsV-158 method B (FB). This study's LdV-1 samples labelled as 1_15_5L_CDP, 2_18_5L_CDP, and 3_15_5L_OP. The abbreviations for viruses are as follows: MOCV, Molluscum contagiosum virus; VACV, Vaccinia virus; MSEV, Melanoplus sanguipes entomopoxvirus; AMEV, Amsacta moorei entomopoxvirus; IIV-6, Invertebrate iridescent virus 6; LCDV-1, Lymphocystis disease virus 1; ASFV, African swine fever virus; APMV, Acanthamoeba polyphaga mimivirus; PgV-16T, Phaeocystis globosa virus 16T; EhV-86, Emiliania huxleyi virus 86; HaV01, Heterosigna akashiwo virus 1; OtV5, Ostreococcus tauri virus 5; PBCV-1, Paramecium bursaria virus 1; EsV-1, Ectocarpus siliculossu virus 1; FsV-158, Feldmannia species virus 158; FirrV-1, Feldmannia irregularis virus 1; ErcV, Ecklonia radicosa virus; SjV, Saccharina japonica virus; UpV, Undaria pinnatifida virus. Node values are maximum likelihood bootstrap values (values <50 not shown). Trees rooted with the *Poxviridae* (MOCV, VACV, MSEV, AMEV). See Appendices Figures A.4.7, A.4.8, and A.4.9 for sequence alignments and GenBank Accession numbers. Scale units are the number of amino acid substitutions per site.

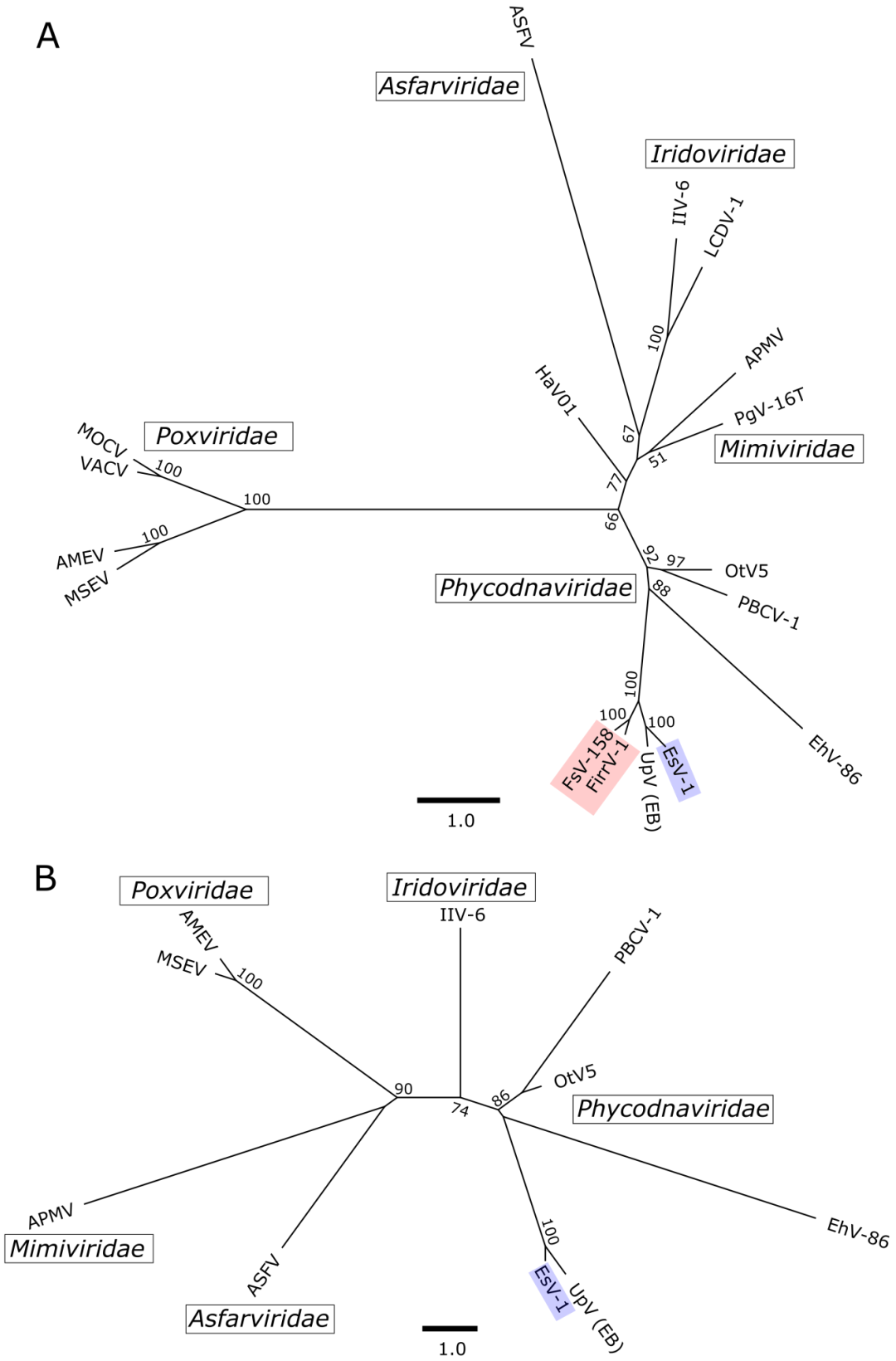
A
ASFV
Asfarviridae
Iridoviridae
IIV-6
LCDV-1
100
APMV
HaV01
PgV-16T
67
Mimiviridae
51
77
MOCV
Poxviridae
VACV
100
100
66
AMEV
100
92
97
OtV5
MSEV
Phycodnaviridae
88
PBCV-1
100
100
100
EhV-86
FsV-158
FirrV-1
UpV (EB)
EsV-1
1.0
B
Poxviridae
Iridoviridae
AMEV
IIV-6
MSEV
100
PBCV-1
90
OtV5
86
74
Phycodnaviridae
APMV
EhV-86
Mimiviridae
100
ASFV
EsV-1
UpV (EB)
Asfarviridae
1.0

Figure 4.5: Concatenated maximum likelihood phylogenetic tree of (A) VV D5-type ATPase, VV A32-type ATPase, and MCP, (B) VV A18-type helicase, VV D6R-type helicase, and VLTF2. Assembly method labelled as follows: EsV-1 method A (EA), EsV-1 method B (EB), FsV-158 method A (FA), FsV-158 method B (FB). This study's LdV-1 samples labelled as 1_15_5L_CDP, 2_18_5L_CDP, and 3_15_5L_OP. The abbreviations for viruses are as follows: MOCV, Molluscum contagiosum virus; VACV, Vaccinia virus; MSEV, Melanoplus sanguipes entomopoxvirus; AMEV, Amsacta moorei entomopoxvirus; IIV-6, Invertebrate iridescent virus 6; LCDV-1, Lymphocystis disease virus 1; ASFV, African swine fever virus; APMV, Acanthamoeba polyphaga mimivirus; PgV-16T, Phaeocystis globosa virus 16T; EhV-86, Emiliania huxleyi virus 86; HaV01, Heterosigna akashiwo virus 1; OtV5, Ostreococcus tauri virus 5; PBCV-1, Paramecium bursaria virus 1; EsV-1, Ectocarpus siliculossu virus 1; FsV-158, Feldmannia species virus 158; FirrV-1, Feldmannia irregularis virus 1; ErcV, Ecklonia radicosa virus; SjV, Saccharina japonica virus; UpV, Undaria pinnatifida virus. Node values are maximum likelihood bootstrap values (values <50 not shown). Tree is not rooted. Scale units are the number of amino acid substitutions per site. Boxes indicate virus families.

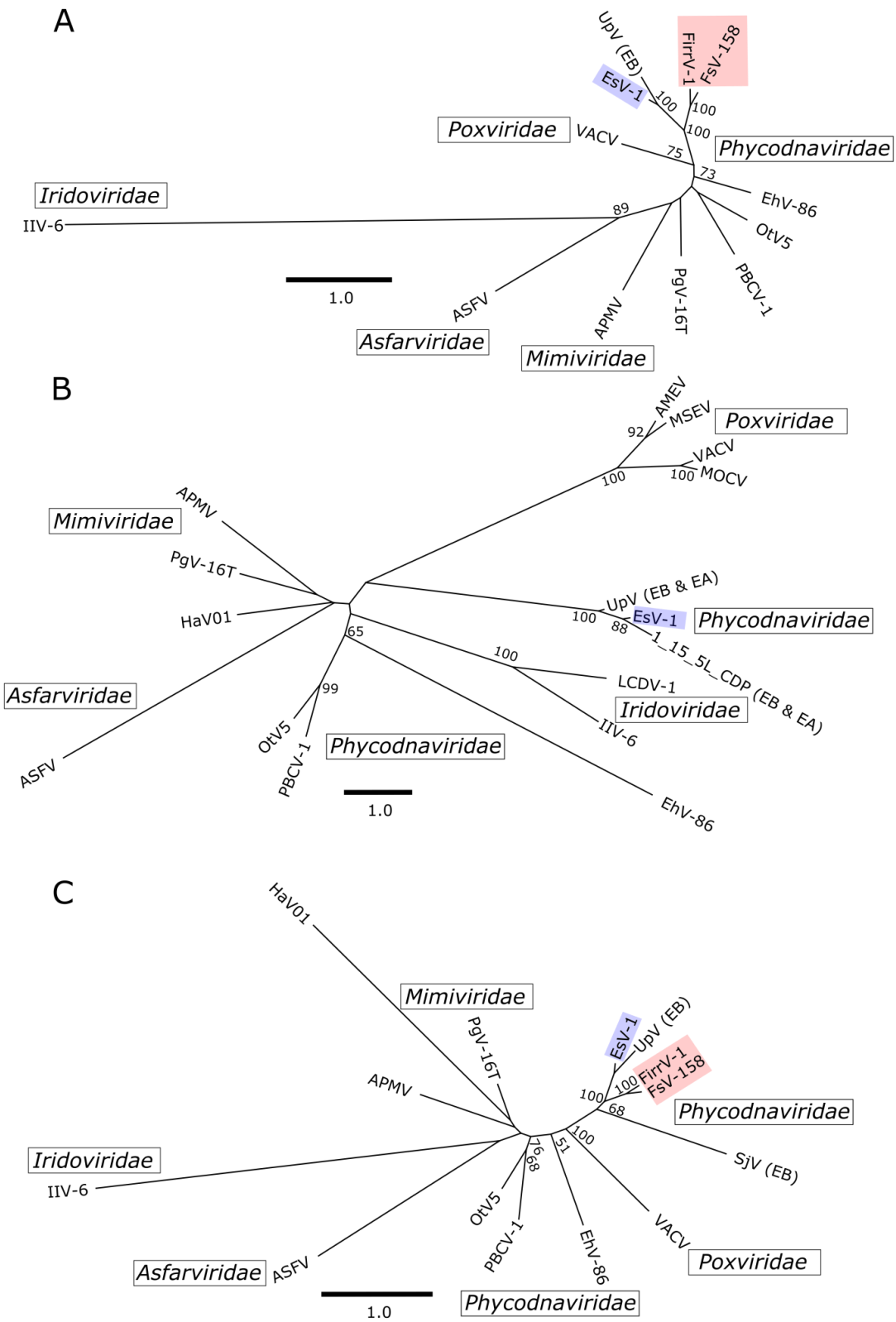
A
UpV (EB)
EsV-1
FirrV-1
FsV-158
100
100
100
Poxviridae
VACV
75
Phycodnaviridae
73
EhV-86
OtV5
PBCV-1
PgV-16T
APMV
Iridoviridae
IIV-6
89
1.0
ASFV
Asfarviridae
Mimiviridae
B
AMEV
MSEV
92
Poxviridae
VACV
100
100
MOCV
APMV
Mimiviridae
PgV-16T
HaV01
UpV (EB & EA)
100
EsV-1
88
Phycodnaviridae
1_15_5L_CDP (EB & EA)
65
100
LCDV-1
Iridoviridae
IIV-6
Asfarviridae
99
OtV5
PBCV-1
Phycodnaviridae
ASFV
1.0
EhV-86
C
HaV01
Mimiviridae
PgV-16T
EsV-1
UpV (EB)
APMV
FirrV-1
FsV-158
100
100
Phycodnaviridae
68
Iridoviridae
IIV-6
100
51
SjV (EB)
68
OtV5
PBCV-1
EhV-86
VACV
Poxviridae
Asfarviridae
ASFV
1.0
Phycodnaviridae

Figure 4.6: Concatenated maximum likelihood phylogenetic tree of (A) ribonucleotide reductase large subunit, ribonucleotide reductase small subunit, and PCNA. (B) MCP and VV D6R-type helicase. (C) Ribonucleotide reductase large subunit and MCP. Assembly method labelled as follows: EsV-1 method A (EA), EsV-1 method B (EB), FsV-158 method A (FA), FsV-158 method B (FB). This study's LdV-1 samples labelled as 1_15_5L_CDP, 2_18_5L_CDP, and 3_15_5L_OP. The abbreviations for viruses are as follows: MOCV, Molluscum contagiosum virus; VACV, Vaccinia virus; MSEV, Melanoplus sanguipes entomopoxvirus; AMEV, Amsacta moorei entomopoxvirus; IIV-6, Invertebrate iridescent virus 6; LCDV-1, Lymphocystis disease virus 1; ASFV, African swine fever virus; APMV, Acanthamoeba polyphaga mimivirus; PgV-16T, Phaeocystis globosa virus 16T; EhV-86, Emiliania huxleyi virus 86; HaV01, Heterosigna akashiwo virus 1; OtV5, Ostreococcus tauri virus 5; PBCV-1, Paramecium bursaria virus 1; EsV-1, Ectocarpus siliculossu virus 1; FsV-158, Feldmannia species virus 158; FirrV-1, Feldmannia irregularis virus 1; ErcV, Ecklonia radicosa virus; SjV, Saccharina japonica virus; UpV, Undaria pinnatifida virus. Node values are maximum likelihood bootstrap values (values <50 not shown). Tree is not rooted. Scale units are the number of amino acid substitutions per site. Boxes indicate virus families.

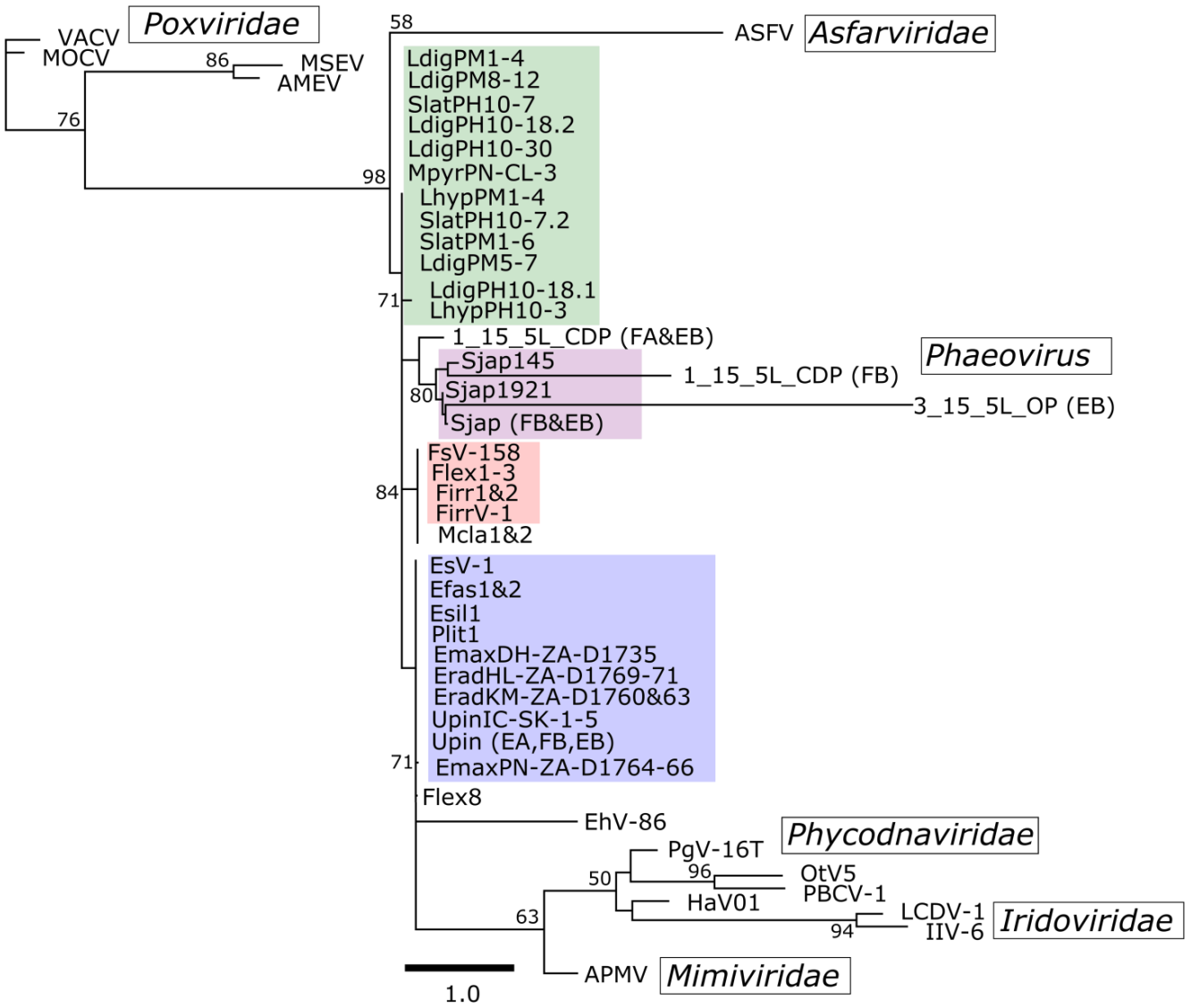
Poxviridae
VACV
MOCV
86
MSEV
AMEV
76
98
58
ASFV
Asfarviridae
LdigPM1-4
LdigPM8-12
SlatPH10-7
LdigPH10-18.2
LdigPH10-30
MpyrPN-CL-3
LhypPM1-4
SlatPH10-7.2
SlatPM1-6
LdigPM5-7
71
LdigPH10-18.1
LhypPH10-3
1_15_5L_CDP (FA&EB)
Sjap145
1_15_5L_CDP (FB)
Phaeovirus
80
Sjap1921
3_15_5L_OP (EB)
Sjap (FB&EB)
FsV-158
Flex1-3
Firr1&2
FirrV-1
84
Mcla1&2
EsV-1
Efas1&2
Esil1
Plit1
EmaxDH-ZA-D1735
EradHL-ZA-D1769-71
EradKM-ZA-D1760&63
UpinIC-SK-1-5
Upin (EA,FB,EB)
71
EmaxPN-ZA-D1764-66
Flex8
EhV-86
Phycodnaviridae
PgV-16T
50
96
OtV5
PBCV-1
HaV01
63
LCDV-1
94
IIV-6
Iridoviridae
APMV
Mimiviridae
1.0

Figure 4.7: Maximum likelihood phylogenetic tree of partial MCP. Assembly method labelled as follows: EsV-1 method A (EA), EsV-1 method B (EB), FsV-158 method A (FA), FsV-158 method B (FB). This study's LdV-1 samples labelled as 1_15_5L_CDP, 2_18_5L_CDP, and 3_15_5L_OP. The abbreviations are as follows: MOCV, Molluscum contagiosum virus; VACV, Vaccinia virus; MSEV, Melanoplus sanguipes entomopoxvirus; AMEV, Amsacta moorei entomopoxvirus; IIV-6, Invertebrate iridescent virus 6; LCDV-1, Lymphocystis disease virus 1; ASFV, African swine fever virus; APMV, Acanthamoeba polyphaga mimivirus; PgV-16T, Phaeocystis globosa virus 16T; EhV-86, Emiliania huxleyi virus 86; HaV01, Heterosigna akashiwo virus 1; OtV5, Ostreococcus tauri virus 5; PBCV-1, Paramecium bursaria virus 1; EsV-1, Ectocarpus siliculossu virus 1; Esil, Ectocarpus siliculosus virus; Efas, Ectocarpus fasciculatus virus; Plit, Pylaiella littoralis virus; FsV-158, Feldmannia species virus 158; FirrV, Feldmannia irregularis virus; Flex, Feldmannia simplex virus; ErcV, Ecklonia radicosa virus; SjV, Saccharina japonica virus; UpV, Undaria pinnatifida virus; Ldig, *Laminaria digitata*; Lhyp, *Laminaria hyperborea*; Slat, *Saccharina latissima*; Sjap, *Saccharina japonica*; Mpyr, *Macrocystis pyrifera*; Erad, *Ecklonia radiata*; Emax, *Ecklonia maxima*; Upin, *Undaria pinnatifida*. Node values are maximum likelihood bootstrap values (values <50 not shown). Tree rooted with the *Poxviridae* (MOCV, VACV, MSEV, AMEV). See Appendices Figure A.4.10 for sequence alignments and GenBank Accession numbers. Scale units are the number of amino acid substitutions per site. Boxes indicate virus families. Colours indicate Phaeovirus subgroup: blue, subgroup A; red, subgroup B; green, subgroup C; purple, subgroup D.

4.4.3 Nucleotide metabolism

UpV encodes several enzymes for the synthesis of nucleotides (ribonucleotide reductase small subunit, ribonucleotide reductase large subunit, and VV A32-type ATPase; Table 4.5), ErcV encodes 2 (ribonucleotide reductase large subunit and VV A32-type ATPase; Table 4.5), and SjV encodes 1 (ribonucleotide reductase large subunit; Table 4.5).

4.4.4 Integration and transposition

An ortholog of the conserved integrase of phaeoviruses was only found in LdV-1. 1 LdV-1, ErcV, SjV, UpV may share the DDE domain, IS4 family transposases (ORFs 155 and 170) with EsV-1. However, these same viruses and may also share an OrfB zinc ribbon transposase (ORF2) with FsV-158. Additionally, ErcV and SjV may share an integrase/resolvase (ORF3) with FsV-158 (Table 4.5).

4.4.5 Roles in brown algal biology

A single ortholog of the EsV-1 ORF7 was found in ErcV (Table 4.5) and contained the conserved cysteine and histidine motif of the EsV-1-7 repeats in the IMM protein of *Ectocarpus siliculosus* [320], but with a large insert within the motif (Figure 4.8). UpV contained a thaumatin-like protein ortholog. In plants, thaumatin-like protein is involved in the defence against pathogens [321]. This protein is also present in EsV-1, within a putative transposon, and is proposed to be advantageous to the host [100].

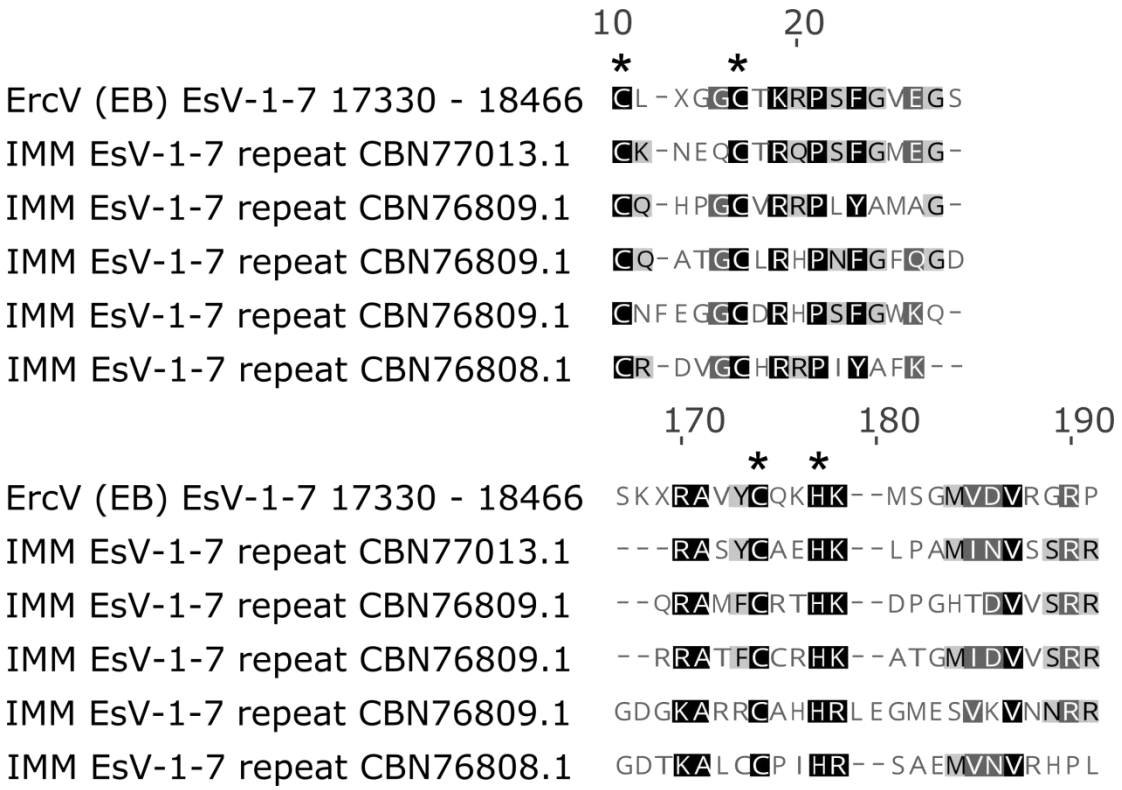

Figure 4.8: Alignment of EsV-1-7 ortholog from Ecklonia radicosa (ErcV) and the 5 EsV-1-7 repeat in the C-terminal region of the IMM protein [320]. The 3 conserved cysteine and 1 histidine residues are labelled with *. Between residues 28 and 167, there was a 138 amino acid insert in the ErcV EsV-1-7 ortholog. X= unknown amino acid. Amino acid highlighted as identical (black) or similar (grey; based on side chain group). Genbank accession numbers are included in labels.

4.4.6 Signalling

UpV had a viral histidine kinase ortholog (Table 4.5). Signalling kinases are a unique feature of phaeoviruses [48]. All histidine protein kinase and receiver conserved domains were identical between EsV-1-112 and the UpV ortholog, which including the conserved phosphoaccepting domains (Figure 4.9). Also present in UpV were a putative antirepressor of lysogeny and a DnaJ bacterial heat shock protein.

Histidine protein kinase domain

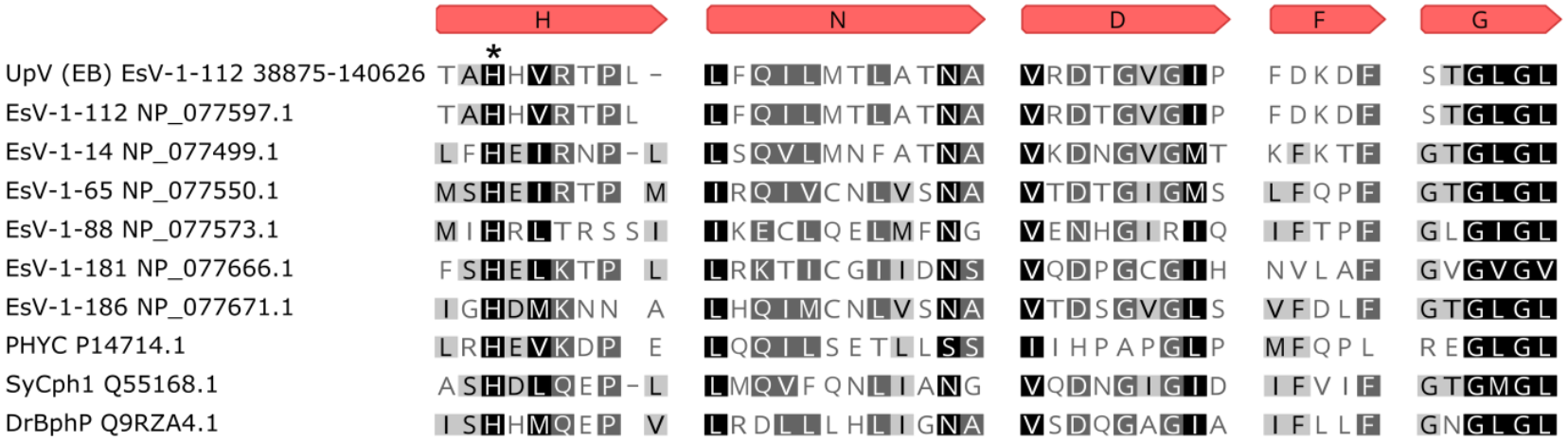

Receiver domain

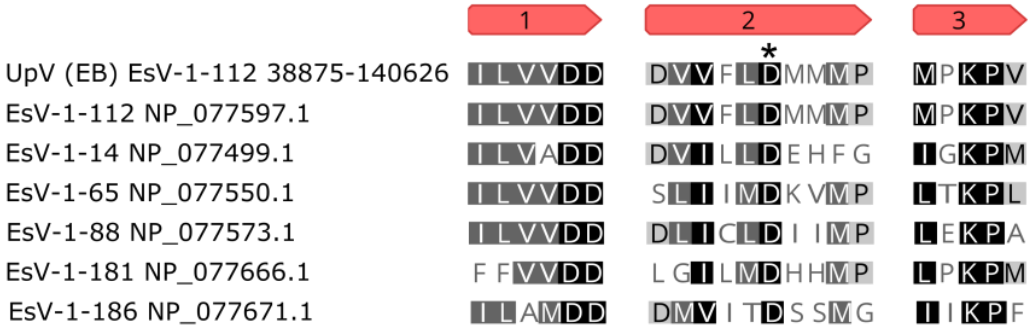

Figure 4.9: Alignment of the conserved histidine protein kinase (H, N, D, F, G) and receiver (1-3) domains of histidine kinases [100]. Alignment includes the EsV-1-112 ortholog from *Undaria pinnatifida* (UpV), the 6 viral histidine kinases encoded by EsV-1 (EsV-1-14, 65, 88, 112, 181, and 186; [100]) and histidine protein kinases from *Arabidopsis thaliana* phytochrome C (PHYC), *Synechocystis* sp. Cph1 (SyCph1), and *Deinococcus radiodurans* BphP (DrBphP). Phosphoaccepting amino acids are labelled with *. Amino acid highlighted as identical (black) or similar (grey; based on side chain group). Genbank accession numbers are included in labels.

4.4.7 Cell entry

An ortholog of EsV-1 glycoprotein 1 (gp1) was found in UpV. This protein was also orthologous to brown algal mannuronan C-5-epimerases (Table 4.5). UpV also encoded an ortholog of the potassium channel component encoded by EsV-1 [61, 100] and PBCV-1 [322]. The UpV ortholog was missing only 10 and 1 amino acids from the start and end of the sequence, respectively (Figure 4.10). The absent residues included 6 amino acids from TM0 (residues 5-10) and 1 PKC (residue 2). UpV and EsV-1 K+ channel component differed by 29 amino acids, 1 insert (residue 64), and 7 unknown amino acids in UpV (residues 66-68, 109-111, and 115) (Figure 4.10, [61]).

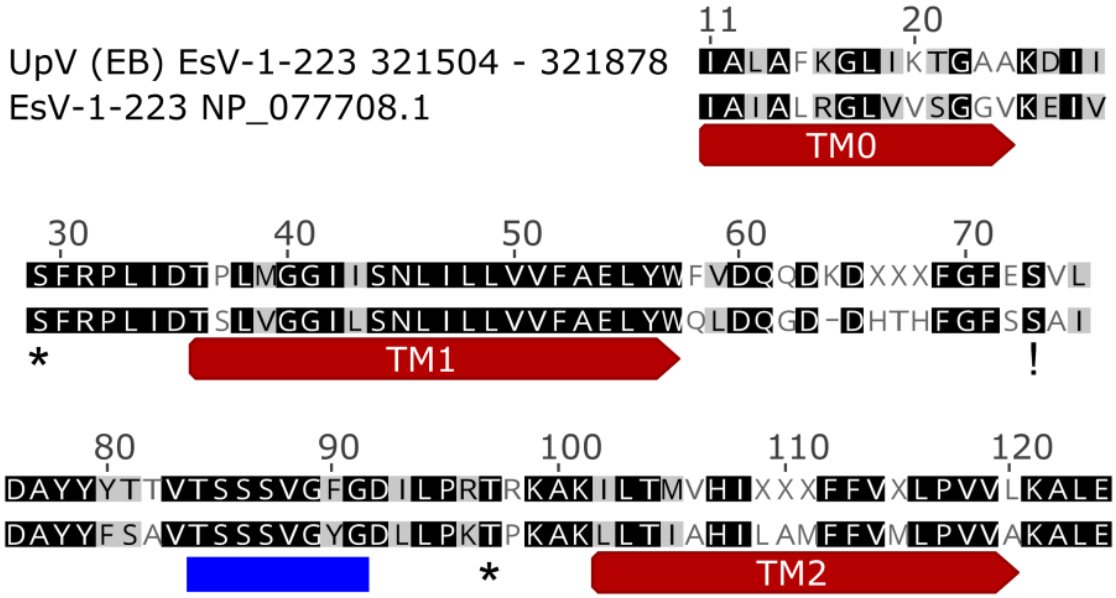

Figure 4.10: Alignment of the potassium ion channel component encoded by EsV-1 (EsV-1-223) and the EsV-1-223 ortholog from Undaria pinnatifida (UpV). Protein kinase C (PKC) are marked with *. Also indicated is the K+ channel signature sequence (blue rectangle), putative transmembrane domains (TM0, TM1, and TM2), and 1 casein kinase II phosphorylation site (!) [61]. X=unknown amino acid. Amino acid highlighted as identical (black) or similar (grey; based on side chain group). Genbank accession numbers are included in label.

4.5 Discussion

A total of ten different EsV-1/FsV-158 orthologs were identified from LdV-1 (Table 4.4), two of which were core NCLDV genes (MCP and VV D6R-type helicase; Table 4.5). This is equivalent to only 4.3 % of the 231 ORFs in the EsV-1 genome, which indicates that only a partial LdV-1 genome was obtained. Three times more Phaeovirus orthologs were recovered from the LdV-1 sample 1_15_5L_CDP (15^{o}C culture) versus 2_18_5L_CDP (18 ^{o}C culture) (Table 4.4), possibly due to the temperature sensitivity of Phaeovirus-like symptoms in the gametophyte strain which was host to LdV-1 (LdigPH10-30; Chapter 3). Whether these orthologs were isolated from virions trapped in the cellular debris or proviruses integrated in host genomes is unknown.

The 84 orthologs of EsV-1 ORFs found in *U. pinnatifida* cover 36.4 % (out of 231) of the ORFs in the EsV-1 genome. In comparison, 130 (56.3 %) and 93 (40.3 %) ORFs of EsV-1 are orthologous to FsV-158 [98] and FirrV-1 [48], respectively. These included orthologs to 9 out of the 16 NCLDV core genes encoded by EsV-1 (VV D5-type ATPase, VV A18-type helicase, VV D6R-type helicase, PCNA, VLTF2, RRLS, RRSS, VV A32-type ATPase, and MCP genes; Table 4.5; [98]). This suggests that this *U. pinnatifida* genome contained the most integrated Phaeovirus sequences.

Only seven EsV-1/FsV-158 orthologs were found in SjV including two core genes (MCP and ribonucleotide reductase large subunit genes). There are three *mcp* orthologs in the *S. japonica* genome [31], two of which are closely related and possibly full length; but one is only a partial *mcp* which is missing the conserved domain previously amplified by PCR [316]. In phaeoviruses, *mcp* is a single copy gene [48, 98, 100], which suggests that the *S. japonica* genome may contain multiple SjV proviruses, similar to the multiple infections of FsV [96]. This is noteworthy because it suggests that subgroup D (SjV) shares the acute evolutionary strategy of subgroup B [95]. It is possible that these SjV orthologs are remnants of ancient proviruses which have lost their functionality due to insertion or transposition events.

The 17 Phaeovirus orthologs present in *Ecklonia radicosa* included two core genes (ribonucleotide reductase large subunit and VV A32-type ATPase genes). Interestingly, ErcV was the only putative Phaeovirus for which *mcp* was not found (Table 4.5). This may be due to divergence, as Phaeovirus *mcp* can be amplified by PCR from *Ecklonia radiata* and *Ecklonia maxima* [316]. Such viral divergence may have been driven by host divergence, as *E. radicosa* occurs in Japan, and is in a distinct clade (within *Ecklonia*) from *E. maxima* and *E. radiata*, which occur in Australia and South Africa [212]. *E. radicosa* may contain a more divergent, integrated Phaeovirus genome.

Currently, we cannot tell whether viral orthologs or core genes were not detected because they were absent or simply too divergent to be assembled using known Phaeovirus reference genomes. One solution to this is to sequence virus genomes from sufficiently high concentrations of viral DNA isolated from virions. Due to the latent nature of phaeoviruses, this requires knowledge of which factors induce viral replication, such as culture temperature. In addition, as more fully assembled brown algal genomes become available, it will become possible to thoroughly explore the genomic context of integrated Phaeovirus DNA (fragmented versus contiguous, complete versus partial, virus encoded versus horizontally transferred to host).

Phylogeny of the full length (322-418 amino acids) MCP (Figure 4.3A) placed LdV-1 in its own distinct subgroup, which may be subgroup C as previously defined [305]. However, the partial LdV-1 MCP assembled by this study was placed in subgroup A and was not identical to the MCP PCR product of LdV-1 (LdigPH10-30; Figure 4.7). This ambiguity is likely the result of assembly without reference to long LdV-1 sequence reads, such as those created by MinION sequencing. Unfortunately, low virion recovery may have yielded insufficient quantities of viral DNA, which caused the MinION sequencing to fail. Ambiguities between the LdV-1 MCP sequences amplified by PCR and assembled from the Illumina data (this study) may explain the uncertain subgroup placement of LdV-1.

In contrast, SjV and UpV were unambiguously placed in subgroups D and A, respectively, which is in agreement with previous phylogeny based on partial MCP alone [316]. UpV was especially well supported as a subgroup A Phaeovirus by phylogeny of single (seven out of nine; Figures 4.1-4.4) and concatenated (three out of three; Figures 4.5 and 4.6) core genes. The placement of SjV in subgroup D was supported by a smaller set of single (two out of two; Figures 4.3A, 4.4A, and 4.7) and

concatenated core gene phylogeny (one out of one; Figure 4.6C), whilst ErcV was placed in subgroup A based on only 1 core gene (one out of one; Figure 4.1B). For both SjV and UpV, the partial MCP assembled by this study was identical or highly similar to those amplified by PCR previously (Figure 4.7; [316]). This may be because these viral orthologs were probably integrated into the host genome, which provided enough quantities of viral DNA for sequencing. The fact that the two *U. pinnatifida* MCPs were identical despite being from China (this study) and South Korea [316], suggests that UpV has a single genotype, as expected for subgroup A phaeoviruses [95].

NCLDVs (including all EsV-1, FsV-158, and FirrV-1) encode multiple deoxyribonucleotide enzymes to provide sufficient nucleotides to synthesise their large genomes [98], which suggests that UpV and ErcV have genomes within the typical size range of NCLDVs.

Phaeoviruses are the only NCLDVs known to integrate their genomes into their genome of the host, as demonstrated in EsV-1 [76, 105, 136] and FsV-158 [89, 102]. Integrase is responsible for the integration of a viral genome into a host genome, whilst viral transposases are responsible for DNA recombination within or between viruses and host genomes [39]. A conserved integrase (phage integrase family; Table 4.5) is shared by EsV-1, FsV-158, and FirrV-1 (ORFs 213, 13, and B4, respectively) and is probably responsible for Phaeovirus genome integration [98]. An ortholog of this integrase was found only in LdV-1, leaving open the question whether the other kelp phaeoviruses (ErcV, SjV, and UpV) employ different types of integrases.

FsV-158 alone has an OrfB zinc ribbon superfamily transposase (ORF2) and an integrase/resolvase (ORF3); these transposases are related to bacteriophages and mimiviruses and may have been inserted into the FsV-158 genome when it integrated into the host genome [98]. The putative presence of OrfB zinc ribbon transposase in

LdV-1, UpV, ErcV, and SjV and integrase/resolvase in ErcV and SjV suggests that the integration of these transposases did not occur in FsV-158 as proposed [98], but during an earlier transposition event in an ancestor of the Ectocarpales and kelp phaeoviruses.

EsV-1 also 2 transposases which it does not share with the other phaeoviruses (DDE domain, IS4 family transposases; [47, 98]). Surprisingly, LdV-1, UpV, ErcV, and SjV may have DDE domain, OrfB zinc ribbon, and integrase/resolvase transposases (Table 4.5). This suggests that these transposases were all present in a Phaeovirus ancestor, and were later lost during the divergence of EsV-1 and FsV-158 or the subgroups A and B. This emphasises the question of how and what evolutionary forces may have led to the differential retention of these different types of transposes across the phaeoviruses.

The IMM protein is responsible for the initial asymmetrical mitosis of the *E. siliculosus* sporophyte. This leads to a sporophyte which is composed of an apical (upright filaments which bear the reproductive organs) and basal cells (thick-walled, prostrate filaments which anchor the macroalga to its substrate). This developmental innovation is hypothesised to be an adaptation of the sporophyte to persist throughout winter and delay growth and reproduction until more favourable seasonal conditions. An *E. siliculosus* IMM mutant (*imm*) was found to develop symmetrically, leading to a sporophyte which developed apical cells immediately, and resulted in a reduced and structurally simple basal structure [320]. Surprisingly, the IMM gene shares a repeated motif with EsV-1 ORF7 (EsV-1-7). EsV-1-7 is present in multiple brown algal families including kelp, which suggests that EsV-1-7 was involved in a horizontal gene transfer event between brown algae and phaeoviruses, perhaps associated with the evolution of complex multicellularity in brown algae [320]. *S.*

japonica was previously found to contain EsV-1-7 orthologs [320], indicating that a more focused search could have revealed more EsV-1-7 orthologs in our kelp genomes. However, the single EsV-1-7 ortholog in E. *radicosa* expands on the known distribution of these horizontally transferred Phaeovirus/brown algal genes. The large insert in the IMM motif of ErcV EsV-1-7 (Figure 4.8) may be the result of the extensive gene loss and gain observed in this gene family, or possibly further transposition. The presence of EsV-1-7 raises the interesting question of what roles this gene family may play in kelp, as kelp have much larger, longer lived, and more complex sporophytes than *E. siliculosus*. In fact, most Phaeovirus genes (including those identified by this study) have no known function, highlighting the unexplored potential for Phaeovirus genes to play roles in host biology. The orthologs of the EsV-1-7 immediate upright gene [320] in ErcV and thaumatin-like protein [100] in UpV are examples of proteins which could also provide functions to their brown algal hosts. It may be hypothesised that by providing selective advantages to the host, latent phaeoviruses can increase their chances of being transmitted vertically, thus reducing the requirement for horizontal transmission via virions and the subsequent pathogeneses.

On the other hand, orthologs with important roles in the Phaeovirus infection cycle were also found. The viral hybrid histidine kinases are homologous to cellular enzymes of two-component signalling pathways and are proposed to alter the cell environment to facilitate infection [99]. The identical conserved domains of UpV and EsV-1-112 histidine kinases (Figure 4.9) indicated that UpV likely has a histidine kinase with the same putative function as in EsV-1 [99] and PBCV-1 [322]. Histidine kinase and the presence of protein interaction domains such as the antirepressor of lysogeny and the DnaJ heat shock protein suggest that, like EsV-1, UpV encodes various proteins for complex interactions with host proteins in order to control cellular events required for

the establishment, maintenance, and termination of the latent phase of Phaeovirus infection [100].

Gp1 is conserved in phaeoviruses [52, 86, 323] and localised in the capsid of EsV-1 [324]. The homology between gp1 and bacterial and brown algal mannuronan epimerases is hypothesised to modify or degrade alginate [100], which is a major component of brown algal cell walls. Indeed, similar homology is shared by a gp1 ortholog of UpV and brown algal mannuronan C-5-epimerases. The presence of a potassium channel component ortholog in UpV is also relevant to cell entry. In PBCV-1, the potassium ion channel is localised on the internal membrane of the virion. During cell entry, it depolarises the host cell membrane, possibly aiding viral DNA entry and preventing entry by other viruses [42]. Compared to EsV-1-223, the potassium channel ortholog of UpV shared almost all the conserved domains and functional regions of a potassium channel component, which included transmembrane and PKC domains, as well as a potassium channel signature sequence and a phosphorylation site (Figure 4.10). This suggests that UpV encodes a potassium channel component with a similar putative function to the potassium channel components of PBCV-1 and EsV-1. It is of interest whether alternative mechanisms of cell entry exist in other phaeoviruses, such as cell wall degradation, as opposed to the Ectocarpales phaeoviruses which exclusively infect the wall-less spores and gametes. It may also be evolutionarily important to understand why certain NCLDVs employ potassium channel components to enter host cells, whilst other related NCLDVs do not.

4.5.1 Conclusions

A partial genome was probably obtained for LdV-1, whilst the genomes of *Ecklonia radicosa* and *Saccharina japonica* may contain partial integrated genomes of ErcV and SjV, respectively. Alternatively, most of the genes of these viruses were maybe too divergent to be assembled to the currently available Phaeovirus genomes. The *Undaria pinnatifida* genome however, may contain a complete integrated genome of UpV. Future work should focus on isolating high concentrations of novel phaeoviruses, possibly through manipulating culture conditions, in combination with bioinformatics screening of assembled brown algal genomes for Phaeovirus sequences. The phylogenetic position of LdV-1 was ambiguous, in either subgroup A or C, whilst SjV belonged to subgroup D, and both Erc and UpV belonged to subgroup A. A variety of Phaeovirus orthologs with putative functions were identified with implications for the biology of kelp phaeoviruses and their hosts. These included NCLDV-sized genomes synthesised by multiple nucleotide metabolism genes, a Phaeovirus ancestor(s) with two types of transposases, virus-encoded proteins which may play roles in kelp development and pathogen defence, signalling proteins to manipulate the cellular environment, and carbohydrate degradation and membrane depolarisation to facilitate viral entry. The presence of Phaeovirus orthologs in these kelp genomes represent an intriguing knowledge gap in the evolutionary biology of brown algae and their viruses.

FINAL DISCUSSION

The aims of this PhD were fulfilled as follows: Aim 1: Microscopy (optical, fluorescent, and TEM) of *Laminaria digitata* gametophytes revealed cell morphologies

and virus-like particles (VLPs) that resembled those of latent Phaeovirus infections in the Ectocarpales. This putative Phaeovirus was named Laminaria digitata virus 1 (LdV-1).

Aim 2: Using Phaeovirus major capsid protein gene (*mcp*) primers, a broad PCR screen of kelp and subsequent phylogenetic analyses of *mcp* sequences revealed a broader range of kelp Phaeovirus distribution (Asia, Africa, Europe, and South America) and host species (an additional 4 species). The phylogeny showed the kelp Phaeovirus subgroups C and D were closely related to the subgroup B Ectocarpales phaeoviruses, whilst others were added to the subgroup A Ectocarpales phaeoviruses.

Aim 3: LdV-1 was further studied with optical and fluorescent microscopy, which revealed that Phaeovirus symptoms were 3 times more common at a culture temperature of 18 ^{o}C than 15 ^{o}C. However, no effect on host reproduction was observed.

Aim 4: Next Generation sequencing performed on the *L. digitata* strain infected with LdV-1 likely did not yield a complete virus genome. However, various Phaeovirus orthologs (including *mcp*) were found in *L. digitata* and three previously sequenced kelp genomes. Nine core NCLDV genes were found, which allowed detailed phylogeny placing the putative phaeoviruses LdV-1 in subgroup A or C, Saccharina japonica virus (SjV) in subgroup D, and Ecklonia radicosa virus (ErcV) and Undaria pinnatifida virus (UpV) in subgroup A. Overall, the phylogenetic inference trees of Chapters 2 and 4 were similar. Various non-core Phaeovirus orthologs revealed new insights into the occurrence and evolution of several transposases, a potassium ion channel component, a histidine kinase, and a host development protein. All findings are assimilated and discussed in detail below.

5.1 Phaeovirus infection cycle, symptom variability, and host impacts

The microscopy of infected *Laminaria digitata* gametophytes revealed morphologies resembling the Phaeovirus infections of the Ectocarpales. These symptoms could be observed consistently and across multiple virus positive strains. TEM observations also revealed cells with degraded nuclei and the presence of virus particles in the cytoplasm, indicating a replication cycle which began in the nucleus and completed in the cytoplasm, as is characteristic of an NCLDV. Phaeovirus-like infections were observed in several strains of *L. digitata*, but LdV-1 infecting strain LdigPH10-30m became the model for the host impact and genomic work. The putative and partial infection cycle of LdV-1 is shown in Figure 5.1.

Acquiring an image of virus particles took longer than anticipated due to the low of occurrence virus-filled cells in kelp gametophytes (<5% of cells on average, Chapter 3). The empty appearance of many VLPs in the cells, suggested that the infection was not imaged at peak virion maturity. There was a general observation that LdV-1 infection did not produce many virions, as indicated by low yields of NCLDV-sized particles (data not shown) and the low recovery of genomic LdV-1 DNA. The gametophyte culture conditions (e.g. red light or culture temperature) were possibly responsible; some of the first experiments should have been to test which conditions induced kelp Phaeovirus replication. In future, replication induction would improve the chances of recovering complete Phaeovirus genomes from virions.

A key difference with Ectocarpales phaeoviruses was that LdV-1 appeared to replicate more often in vegetative cells [77]. A kelp gametangium is a single cell which develops a single gamete, whereas in the known Ectocarpales hosts of phaeoviruses, the gametangia are multicellular organs which form multiple gametes. Since kelp gametophytes do not offer phaeoviruses the opportunity to hijack a gametangium

capable of producing 10^6 virus particles, LdV-1 may compensate for this by replicating more often in vegetative cells.

What impacts kelp phaeoviruses have on their hosts remain unclear. Future work should use unialgal, single sex gametophyte cultures of known virus infection states to reduce confounding factors caused by variable recruitment and sex ratios.However, the observations are still probably of Phaeovirus infections due to their striking similarity to Phaeovirus infections in the Ectocarpales [52, 77] and the lack of alternative explanations for gametophyte cells filled with homogenous DAPI-staining masses.

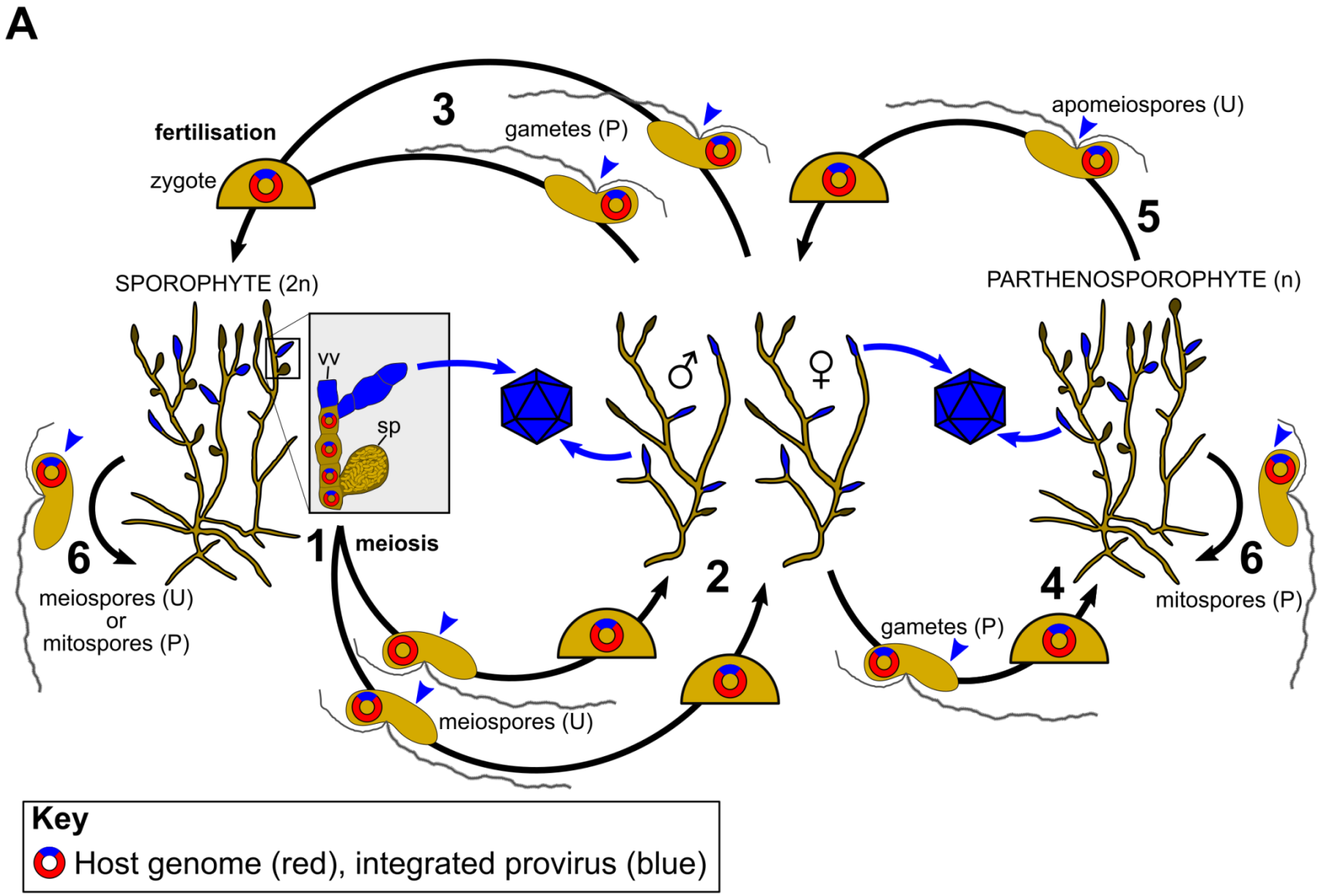
A
fertilisation
zygote
3
gametes (P)
apomeiospores (U)
5
SPOROPHYTE (2n)
PARTHENOSPOROPHYTE (n)
vv
sp
♂
♀
6
meiospores (U)
or
mitospores (P)
1
meiosis
2
meiospores (U)
4
gametes (P)
6
mitospores (P)
Key
Host genome (red), integrated provirus (blue)

B

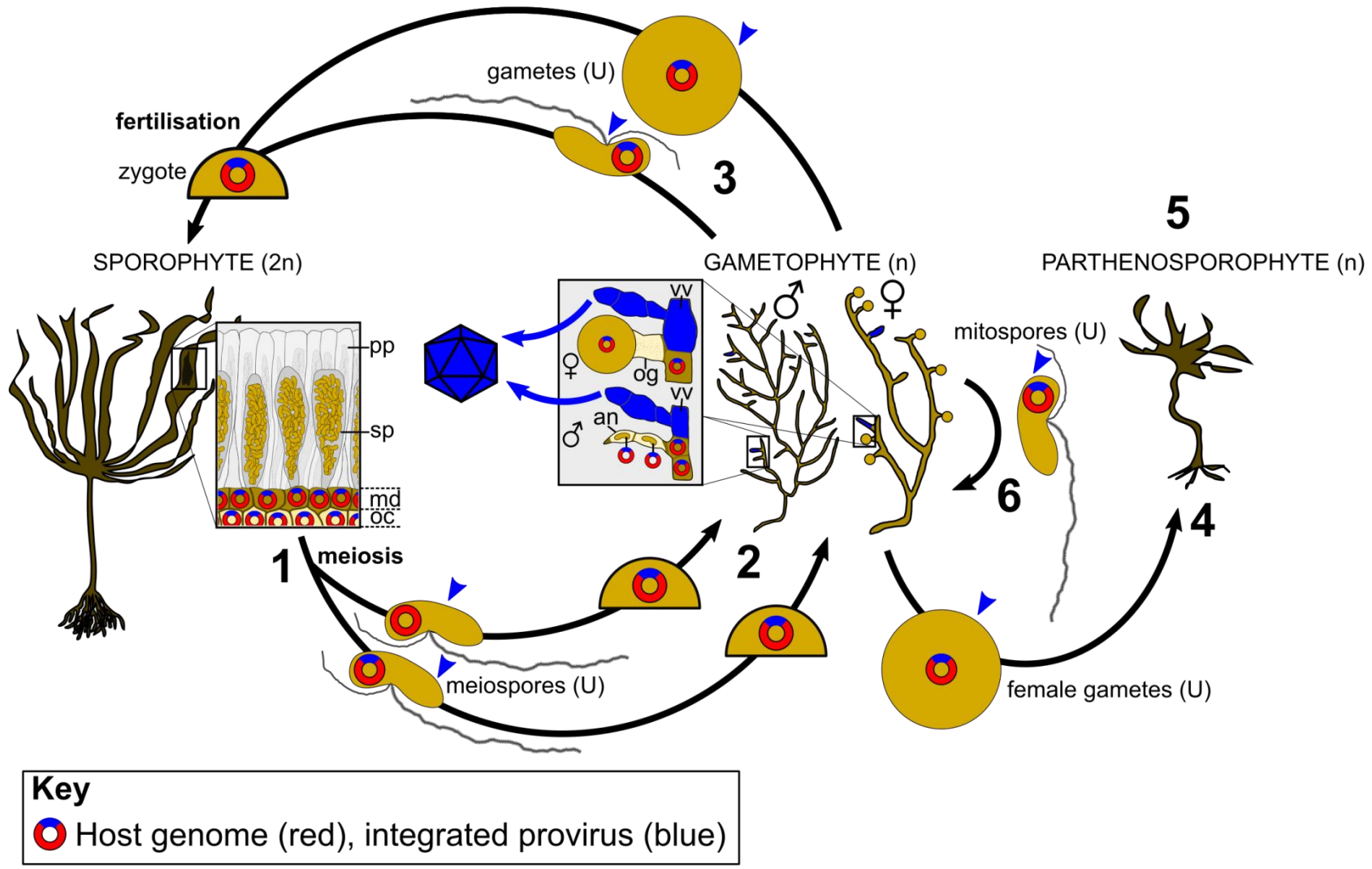
gametes (U)
fertilisation
zygote
3
5
SPOROPHYTE (2n)
GAMETOPHYTE (n)
PARTHENOSPOROPHYTE (n)
pp
sp
md
oc
vv
og
an
mitospores (U)
6
4
1
meiosis
2
meiospores (U)
female gametes (U)
Key
Host genome (red), integrated provirus (blue)

Figure 5.1: Life histories of (**A**) *Ectocarpus siliculosus* (Ectocarpales) and Ectocarpus siliculosus virus (EsV-1) and (**B**) *Laminaria digitata* (Laminariales) and Laminaria digitata virus 1 (LdV-1). Brown algae have free-swimming reproductive cells (zoids) which are produced by zoidangia (sporangia in sporophyte or gametangia in gametophyte. Zoidangia are unilocular (**(U)**; single compartment) or plurilocular (**(P)**; multiple compartments). Meiosis generates **meiospores** (n). Mitosis generates **gametes** (n) and **mitospores** (n or 2n). Apomeiosis (non-reductive meiosis) generates **apomeiospores** (n). All zoids (including gametes post-fertilisation) settle and develop into initial cells with cell walls (**semi-circles**) which develop via mitosis into multicellular thalli.
Phaeoviruses: Indicated are the brown algal life cycle stages which produce Phaeovirus virions (**blue arrows**) from cells with induced viral replication (**blue structures on sporophytes/gametophytes**). Note that vegetative cells can also produce virions (**vv**), but more often in kelp gametophytes. Unwalled cells which are susceptible to Phaeovirus infection are labelled with **blue arrowheads**. Kelp sporangia (**1**) are hypothesised to produce Phaeovirus virions. The host genome contains an integrated Phaeovirus genome (provirus). A copy of the provirus occurs in every cell of the multicellular thalli (sporophyte, gametophyte, parthenosporophyte) and is transmitted vertically by the reproductive life history stages as indicated (**Key**). Due to meiotic segregation, the provirus is removed from half of the meiospores (**1**; **Key**; [79]). Except for the sporophyte and gametophyte thalli, *L. digitata* life history stages have not been experimentally tested for Phaeovirus proviruses.
Sexual cycles (1-3): (**1**) Meiosis occurs in the sporangia (**sp**) of the diploid sporophyte, which produces meiospores. Kelp sporangia form dark areas on the blade; they are protected by sterile filamentous paraphyses (**pp**) and they emerge from the thallus surface, with the meristoderm (**md**) and outer cortex (**oc**) just below. (**2**) The meiospores settle and develop into multicellular, haploid gametophytes. Most brown algae, including the Ectocarpales and Laminariales, have separate sexes in the gametophytes (dioicy), but some have hermaphroditic gametophytes (monoicy), separate sexes in sporophytes (dioecy), or hermaphroditic sporophytes (monoecy) [171, 200]. (**3**) The gametophytes produce gametes and their fertilisation generates a diploid **zygote** which develops into the sporophyte [187]. In *E. siliculosus,* like most Ectocarpales, the male and female gametes have similar morphologies (isogamous). Laminariales are oogamous and their gametangia are referred to as: antheridia (**an**; produce small flagellated male gametes) and oogonia (**og**; large non-motile female gametes) [171, 187].
Asexual cycles (4-6): Many brown algae reproduce asexually by regrowth of fragmented thalli. This occurs in kelp gametophytes [201] and *Ectocarpus* [137]. (**4**) Unfertilised *Ectocarpus* gametes (male or female) can develop into haploid parthenosporophytes, which is common in brown macroalgae [187]. The unfertilised female gametes of kelp can develop into parthenosporophytes, but in most species they are small, infertile, and short-lived [199, 202]. (**5**) *Ectocarpus* parthenosporophytes can generate apomeiospores which develop into gametophytes [203]. Some kelp can produce parthenosporophytes with normal morphologies in laboratory conditions, but there is limited evidence of them successfully reproducing or occurring naturally [199, 202]. (**6**) *Ectocarpus* parthenosporophytes and sporophytes can also reproduce asexually via mitospores. A small portion of *Ectocarpus* meiospores can also develop directly into sporophytes [140, 203]. In kelp, only the gametophytes reproduce asexually via mitospores [204].

Ectocarpales which have been sexually sterilised by phaeoviruses can be maintained in culture because they continue to reproduce asexually [52, 77, 325]. Whether this strategy could be maintained in kelp is uncertain because kelp sporophytes cannot reproduce asexually; perhaps it is employed in persistent populations of kelp gametophytes with high rates of asexual reproduction. The known Ectocarpales hosts of phaeoviruses all have gametophytes with similar morphology to the sporophytes, whereas in kelp the sporophytes are far larger and more complex than the gametophytes. Future work should explore the infection strategy (if any) employed by phaeoviruses in the kelp sporophyte. Meiosis occurs in the sporophyte which eliminates an integrated Phaeovirus from half the meiospores [79, 305]. However, phaeoviruses maintain a widespread, common, and stable relationship with their kelp [305, 316] and Ectocarpales [85, 86] hosts. This is only possible if kelp phaeoviruses can counter meiotic elimination, possibly (like the *Ectocarpus* phaeoviruses) by releasing virions in close synchrony and proximity to the normal sporangia, to re-infect the meiospores. The alternative hypothesis is that the brown algal hosts infected with integrated proviruses have selective advantage(s) over virus-free hosts. Subsequently, the next generation becomes dominated by the competitively superior, infected kelp. In this strategy, phaeoviruses would rely mostly on vertical transmission and have a reduced need for horizontal transmission via virions, which means they have fewer negative effects on the host (because disease is a result of viral replication). Such symbiotic or mutualistic interactions are not well studied in viruses [181, 326] and would be a novel strategy for an algal virus. However, there are examples of plant viruses encoding proteins which can improve host drought tolerance [327], modify host root development in response to environmental nitrogen

availability [328], and deter herbivores [329]. Our study identified some Phaeovirus orthologs in kelp which may be hypothesised to benefit the host, such as thaumatin-like protein in UpV, which is hypothesised to enhance pathogen defences in the host [100]. The other example is an EsV-1-7 ortholog in ErcV which is homologous to repeats in a brown algal gene encoding the protein IMM. In *E. siliculosus*, IMM is required for the development of the sporophyte into upright and basal filaments [320]. This morphology allows the firm anchoring and overwintering of the sporophyte. Though IMM orthologs are present in *S. japonica*, their role in kelp biology is unknown [320]. How the horizontally transferred EsV-1-7 family has been utilized by brown algae with very different sporophyte morphologies and life histories (such as kelp and *E. siliculosus*) is an intriguing question. In our genomic sequence data and the available Phaeovirus genomes, the majority of Phaeovirus genes had no known function. In addition to novel viral functions, this viral gene pool may provide functions to brown algal hosts, whether by expression of active phaeoviruses or horizontal gene transfer.

Whether pathogenic or symbiotic, kelp phaeoviruses (and those of the Ectocarpales) may be finely tuned into the health and reproductive status of their host, perhaps through complex signalling processes such as two component signalling protein histidine kinases (UpV encoded orthologs), which are hypothesised to coordinate viral replication with the cellular environment and regulate Phaeovirus latency [99, 100]. For example, kelp Phaeovirus replication may only be induced by environmental or host factors when the host is reproductive or healthy, creating a virus-host relationship that can alternate between symbiosis and pathogenesis. Evidently, there is a need to investigate the complex mix of factors (such as host

morphology, longevity, fecundity, sexual system) which have shaped the infection strategies of phaeoviruses in different brown algal orders.

We propose that the phaeoviruses of kelp employ latent infection strategies. Previous evidence supporting this was that the *S. japonica* genome contained a Phaeovirus *mcp* [31] and that *mcp* is subject to Mendelian inheritance between the sporophyte and gametophyte generations in kelp [305]. This study showed the following evidence of latent Phaeovirus infections in kelp: the phaeovirus-like infection symptoms and no host mortality in kelp gametophytes which were isolated from Phaeovirus MCP-positive sporophytes [316] with normal morphologies (general observation, no data shown). Furthermore, a range of Phaeovirus orthologs were found which included Phaeovirus integrase in LdV-1 and various orthologs integrated into the genomes of two kelp species (*E. radicosa* and *U. pinnatifida*). Further work should determine the genomic context of integrated phaeoviruses in kelp, to determine whether they integrate as single or multiple sequences, or specific or random sites.

5.2 Kelp Phaeovirus host range, prevalence, and ecological and economic relevance

Previously, Phaeovirus was known to infect seven species of brown algae from four families of the order Ectocarpales, and a screen of eukaryotic genomes found NCLDV core genes in another Ectocarpales species and the kelp *Saccharina japonica* [31]. In addition, a previous MCP PCR screen found Phaeovirus MCP genes in *Laminaria digitata*, *Laminaria hyperborea*, and *Saccharina latissima* [300, 305].

Our MCP PCRs and genomic screening of kelp for Phaeovirus genes have expanded the known Phaeovirus host range to another five kelp species: *Ecklonia*

maxima, *Ecklonia radiata*, *Ecklonia radicosa*, *Macrocystis pyrifera*, and *Undaria pinnatifida* [316]. In total, nine kelp species are putative Phaeovirus hosts and they belong to three kelp families (Laminariaceae, Alariaceae, and Lessoniaceae), which reinforces the observation that phaeoviruses have the broadest interfamilial host range in the *Phycodnaviridae*. Evidently, phaeoviruses are widespread throughout taxa in the order Laminariales and possibly the entire brown algal class (Phaeophyceae).

Phaeoviruses also appear to be highly prevalent in kelp populations. Previous PCR screens found an infection prevalence of 50-100 % of across populations of *Ectocarpus* [85, 86] and 23.2-64.7 % for two populations of *L. digitata*, *L. hyperborea*, and *S. latissima* [305]. Per kelp species, our study found MCP in 20-100 % of kelp sporophytes and the infection prevalence from all available data and 9 kelp species was 26 % of sporophytes [316]. The apparent absence of Phaeovirus MCP in certain kelp species and the wide variation of Phaeovirus prevalence between kelp species were likely due to the MCP primers being coincidently specific to some kelp phaeoviruses, but not amplifying those which were more divergent from the Ectocarpales phaeoviruses. A key next step is to sequence kelp Phaeovirus genomes to allow the design of kelp Phaeovirus-specific primers, which would provide more representative insights into the diversity, phylogeny, and prevalence of kelp phaeoviruses. This approach should also be applied to a broader range of brown algal orders and phyla closely related to the brown algae.

Our study also showed that kelp phaeoviruses are geographically widespread. The known distribution of kelp phaeoviruses was previously limited to the UK and France (*L. digitata*, *L. hyperborea*, and *S. latissima*; [305]) and China (*S. japonica,* [31]).

This study has expanded the range to include Chile (*M. pyrifera*), Japan (*E. radicosa*), South Korea (*U. pinnatifida*), South Africa (*E. maxima* and *E. radiata*), and another region of China (*U. pinnatifida*).

5.3 Evolutionary history and implications of kelp phaeoviruses

Previously, the Ectocarpales phaeoviruses were split into two subgroups, subgroup A with larger genomes and a more persistent infection strategy and subgroup B with reduced genome sizes and a more acute strategy [95]. The kelp phaeoviruses of *L. digitata*, *L. hyperborea*, and *S. latissima* had previously been assigned to subgroup C (Table 5.1; [300, 305]). Our study added an *M. pyrifera* Phaeovirus to subgroup C and *Ecklonia maxima*, *E. radiata*, *E. radicosa,* and *Undaria pinnatifida* (two strains) phaeoviruses to subgroup A (Table 5.1; [316]). The putative Phaeovirus of *S. japonica* [31] was added to the new subgroup D (Table 5.1; [316]).

We hypothesise that the subgroup C and D phaeoviruses have undergone subgroup B type evolution and have therefore smaller genomes and may cause multiple infections within the same host, whereas the subgroup A kelp phaeoviruses have larger genomes and a more persistent infection strategy. The presence of three Phaeovirus MCPs in the *S. japonica* genome [31] suggests multiplicity of infection in subgroup D, but it is not known if these MCPs are active or remnant infections. The *U. pinnatifida* phaeoviruses from South Korea and China had highly similar MCPs, which is consistent with the single genotype trend of subgroup A.

Surprisingly, the Ectocarpales and kelp phaeoviruses were not divided into distinct subgroups, as some kelp phaeoviruses fell into the existing subgroup A. Instead, phaeoviruses infecting different brown algal orders may be subject to similar

selection pressures. This may have created a subgroup A/B-type divergence across phaeoviruses infecting multiple brown algal orders. Future studies should expand on the known diversity of kelp phaeoviruses and other brown algal orders, to test whether the subgroup A/B-type evolutionary pattern is a more general phenomenon in the phaeoviruses.

Table 5.1: Virion size, genomes, host range, evolutionary strategies of Phaeovirus subgroups A, B, C, and D. ND = no data; genome not sequenced. - = unknown.

Virus	Virion diameter (nm)	Genome size (kb)	Host order, family	Replication	No. of genotypes	Ref.
Subgroup A: Single infections, Persistent, K-selected, evolutionary strategy						
Ectocarpus siliculosus virus 1 (EsV-1)	130-150	336	Ectocarpales, Ectocarpaceae	Sporangia Gametangia	1	[49, 100, 101]
Ectocarpus fasciculatus virus 1 (EfasV-1)	135-140	320 (ND)	Ectocarpales, Ectocarpaceae	Sporangia Gametangia	1	[49, 50, 101]
Pylaiella littoralis virus 1 (PlitV-1)	130-170	280 (ND)	Ectocarpales, Acinetosporaceae	Sporangia	1	[49, 52, 101]
Hincksia hincksiae virus 1 (HincV-1)	140-170	240 (ND)	Ectocarpales, Acinetosporaceae	Sporangia	1	[49, 50, 101]
Myriotrichia clavaeformis virus 1 (MclaV-1)	170-180	320 (ND)	Ectocarpales, Chordariaceae	Sporangia	1	[49, 50, 101]
Ecklonia maxima (EmaxV)	-	-	Laminariales, Lessoniaceae	-	-	[316]
Ecklonia radiata (EradV)	-	-	Laminariales, Lessoniaceae	-	-	[316]
Ecklonia radicosa virus (ErcV)	-	-	Laminariales, Lessoniaceae	-	-	-
Undaria pinnatifida virus (UpV)	-	-	Laminariales, Alariaceae	-	-	-
Subgroup B: Multiple infections, Acute, *r*-selected, evolutionary strategy						
Feldmannia simplex virus 1 (FlexV-1)	120-150	220 (ND)	Ectocarpales, Acinetosporaceae	Sporangia	8	[49, 50, 101]
Feldmannia irregularis virus 1 (FirrV-1)	140-167	158-178	Ectocarpales, Acinetosporaceae	Sporangia	3	[48, 49, 101]
Feldmannia species	150	170	Ectocarpales,	Sporangia	2	[49,

virus 158 (FsV-158)			Acinetosporaceae			98, 101]
Subgroup C: Unknown evolutionary strategy						
Laminaria digitata virus 1 (LdV-1)	80-150	-	Laminariales, Laminariaceae	Gametangia Gametophyte vegetative cells	-	[305]
Laminaria hyperborea virus (LhypV)	-	-	Laminariales, Laminariaceae	Gametangia Gametophyte vegetative cells	-	[305]
Saccharina latissima (SlatV)	-	-	Laminariales, Laminariaceae	Gametangia Gametophyte vegetative cells	-	[305]
Macrocystis pyrifera virus (MpyrV)	-	-	Laminariales, Laminariaceae	-	-	[316]
Subgroup D: Unknown evolutionary strategy						
Saccharina japonica virus (SjV)	-	-	Laminariales, Laminariaceae	-	3	[31, 316]

Of the 16 Phaeovirus core genes, nine were identified in the kelp species studied. No genome sizes were acquired, but the presence of multiple deoxyribonucleotide synthesis in UpV and ErcV suggests that kelp phaeoviruses have large genome sizes typical of NCLDVs [98]. Without a complete kelp Phaeovirus genome isolated from virions (probably due to low virion recovery), the origin (host EVE or viral genome, provirus or virion, single or multiple sequences) of the Phaeovirus orthologs identified remains uncertain. It also means that novel or divergent genes present would not have been detected by PCR primers, BLAST searches or mapping, because they were based on Ectocarpales phaeoviruses. More complete genomes of kelp phaeoviruses may be acquired with the advancement of brown algal genomics and experimental biology to determine how to induce virion production in kelp gametophytes.

A variety of non-core genes with interesting functions were also identified for kelp phaeoviruses, several of which offered intriguing insights into Phaeovirus evolution. OrfB zinc ribbon superfamily and integrase/resolvase transposases may be encoded by kelp phaeoviruses (LdV-1, UpV, ErcV, and SjV) and may not be unique to

FsV-158. These transposases are related to those of bacteriophages and mimiviruses and were therefore hypothesised to have been horizontally acquired by FsV-158 [98]. However, I hypothesised that these transposases were acquired by an ancestor of the Ectocarpales and kelp phaeoviruses. This Phaeovirus ancestor may have also encoded DDE domain transposases, as suggested by their presence in kelp phaeoviruses (LdV-1, UpV, ErcV, and SjV). These findings suggest an unexplored evolutionary scenario in which, as phaeoviruses diverged with along with their brown algal hosts, they subsequently lost or retained different transposases. Some consequences of this could be the divergence of Phaeovirus recombination strategies or distinct horizontal transfer gene transfer events in certain brown algal taxa.

Two orthologs hypothesised to be involved in cell entry were found in UpV. One was a capsid protein which is also a mannuronan epimerase homolog (gp1) and the other was a potassium ion channel component. Previously, the only Phaeovirus with these genes was EsV-1 [61, 100, 324], which raises the question of why other phaeoviruses do not require these genes for cell entry as hypothesised. Clearly, there is a need to characterise the infection mechanisms of phaeoviruses, which may be more diverse than the current hypothesis of the infection of wall-less spores or gametes.

The kelp phaeoviruses present an intriguing system to study NCLDV evolution, because many kelp genera and species have diverged following migration events and have remained geographically isolated ever since, such as *Laminaria* spp., *Saccharina* spp., and *Ecklonia* spp. (Introduction Chapter, Figure 0.6). These various historical and ongoing changes in kelp distribution and evolution may reveal novel evolutionary dynamics in large DNA viruses, such as the selection pressures which drive NCLDV

genome reduction or the adjustment of viral replication to maintain stable host-virus relationship in a new environment and host population dynamics. If latent Phaeovirus infections are widespread in kelp, as our data suggest, then the molecular timing of endogenous viral elements (EVEs) left in kelp genomes by ancient Phaeovirus infections may provide insights into the deep time (possibly back to the origin of brown algae 250.7 Ma; [172]) evolution of NCLDVs [298]. Furthermore, they could also provide insights into host evolution, as the estimated timing of Phaeovirus EVE integration may coincide or contradict hypotheses of the timing of kelp evolutionary events (Introduction Chapter, Figure 0.6). *Laminaria* and *Saccharina* are two of the four kelp genera which colonised the Arctic and North Atlantic from the Pacific via the Bering Strait when it opened 3.5-5.3 Ma (Introduction Chapter, Figure 0.6; [206, 209]). Since then, they have diverged (3.44 Ma for *Laminaria*, [209]; 1.22-1.68 Ma for *Saccharina,* [210]) into distinct *Laminaria* and *Saccharina* species in the Pacific, Arctic, and Atlantic [206]. As an example, if Atlantic *Laminaria* spp. had a Phaeovirus EVE which was integrated around 3.44 Ma and was absent in Pacific *Laminaria* spp., this would support the estimated timing of *Laminaria* speciation in the Pacific and Atlantic. Since 83.8 Ma, kelp have diverged into families and species whilst colonising the Arctic, Atlantic (North and South), South Pacific, Indian, and Southern Oceans from the North Pacific [172, 206]. The recent migrations of kelp are also poorly understood, such as the widespread populations of *M. pyrifera* established by drifting across entire oceans and the invasive populations of *U. pinnatifida* established by human activities (Introduction Chapter, Figure 0.6). Combined with the fact that no other known NCLDVs employ genome integration, this exemplifies how phaeoviruses could be a unique system for studying the evolution of NCLDVs and their hosts over long time scales.

This study of kelp phaeoviruses is one of the few on any type of macroalgal viruses (Introduction Chapter, Tables 0.5 and 0.6; [101]), which exemplifies the lack of development in the field of macroalgal virology. Macroalgal viruses are a major evolutionary knowledge gap, especially those of brown algae, due to the large evolutionary distance between brown algae and plants. Phaeoviruses are large dsDNA viruses (NCLDVs) which infect aquatic photosynthetic organisms with complex multicellularity. Currently, virology has no similar virus-host system, because there are no true dsDNA viruses in plants [109], the viruses of red and green macroalgae are also mostly unknown (Introduction Chapter, Tables 0.5 and 0.6), and all known NCLDVs infect animals or unicellular eukaryotes [32, 40]. Furthermore, the study of the ecological dynamics and roles of aquatic viruses has advanced in unicellular algae [54, 63, 70, 330], but not in multicellular algae, which probably have distinct virus-host relationships from unicellular algae (Introduction Chapter, Tables 0.5 and 0.6). There are also no other known NCLDVs (except some iridoviruses, [40]) or algal viruses [37, 40] which employ a latent infection strategy. Therefore, this unique combination of virus and host groups, infection strategy, evolutionary history, and environment makes phaeoviruses a completely unique system of study that deserves detailed investigation.

6.1 Bibliography

1. Raoult D, Forterre P. Redefining viruses: lessons from Mimivirus. *Nat Rev Microbiol* 2008; **6**: 315–319.
2. Gibbs AJ, Calisher CH, Garcia-Arenal F (eds). Molecular basis of virus evolution. 1995. Cambridge University Press, Cambridge.
3. Short SM. The ecology of viruses that infect eukaryotic algae. *Environ Microbiol* 2012; **14**: 2253–2271.

4. Mackinder LCM, Worthy CA, Biggi G, Hall M, Ryan KP, Varsani A, et al. A unicellular algal virus, Emiliania huxleyi virus 86, exploits an animal-like infection strategy. *J Gen Virol* 2009; **90**: 2306–2316.
5. Hurst CJ (ed). Studies in Viral Ecology, Volume 1: Microbial and Botanical Host Systems. 2011. John Wiley & Sons, Hoboken, NJ, USA.
6. Hurst CJ (ed). Studies in Viral Ecology, Volume 2: Animal Host Systems. 2011. John Wiley & Sons, Hoboken, NJ, USA.
7. Koonin EV, Dolja VV. Virus World as an Evolutionary Network of Viruses and Capsidless Selfish Elements. *Microbiol Mol Biol Rev* 2014; **78**: 278–303.
8. Colson P, De Lamballerie X, Fournous G, Raoult D. Reclassification of giant viruses composing a fourth domain of life in the new order Megavirales. *Intervirology* 2012; **55**: 321–332.
9. De Castro IF, Volonté L, Risco C. Virus factories: biogenesis and structural design. *Cell Microbiol* 2013; **15**: 24–34.
10. Mutsafi Y, Zauberman N, Sabanay I, Minsky A. Vaccinia-like cytoplasmic replication of the giant Mimivirus. *Proc Natl Acad Sci* 2010; **107**: 5978–5982.
11. Abergel C, Legendre M, Claverie JM. The rapidly expanding universe of giant viruses: Mimivirus, Pandoravirus, Pithovirus and Mollivirus. *FEMS Microbiol Rev* 2015; **39**: 779–796.
12. Koonin EV, Krupovic M, Yutin N. Evolution of double-stranded DNA viruses of eukaryotes: From bacteriophages to transposons to giant viruses. *Ann N Y Acad Sci* 2015; **1341**: 10–24.
13. Blanc-Mathieu R, Ogata H. DNA repair genes in the Megavirales pangenome. *Curr Opin Microbiol* 2016; **31**: 94–100.
14. Iyer LM, Aravind L, Koonin EV. Common origin of four diverse families of large eukaryotic DNA viruses. *J Virol* 2001; **75**: 11720–11734.
15. Iyer LM, Balaji S, Koonin EV, Aravind L. Evolutionary genomics of nucleo-cytoplasmic large DNA viruses. *Virus Res* 2006; **117**: 156–184.
16. Filée J. Route of NCLDV evolution: The genomic accordion. *Curr Opin Virol* 2013; **3**: 595–599.
17. Wilhelm SW, Bird JT, Bonifer KS, Calfee BC, Chen T, Coy SR, et al. A student's guide to giant viruses infecting small eukaryotes: From Acanthamoeba to Zooxanthellae. *Viruses* 2017; **9**.
18. Williams TA, Embley TM, Heinz E. Informational gene phylogenies do not support a fourth domain of life for nucleocytoplasmic large DNA viruses. *PLoS One* 2011; **6**: e21080.
19. Yutin N, Wolf YI, Koonin EV. Origin of giant viruses from smaller DNA viruses not from a fourth domain of cellular life. *Virology* 2014; **466**–**467**: 38–52.
20. Yutin N, Colson P, Raoult D, Koonin EV. Mimiviridae: Clusters of orthologous genes, reconstruction of gene repertoire evolution and proposed expansion of the giant virus family. *Virol J* 2013; **10**.
21. Sharma V, Colson P, Chabrol O, Scheid P, Pontarotti P, Raoult D. Welcome to pandoraviruses at the 'Fourth TRUC' club. *Front Microbiol* 2015; **6**: 1–11.
22. Filée J. Genomic comparison of closely related Giant Viruses supports an accordion-like model of evolution. *Front Microbiol* 2015; **6**: 1–13.
23. Boyer M, Gimenez G, Suzan-Monti M, Raoult D. Classification and determination of possible origins of ORFans through analysis of nucleocytoplasmic large DNA viruses. *Intervirology* 2010; **53**: 310–320.
24. Tautz D, Domazet-Lošo T. The evolutionary origin of orphan genes. *Nat Rev*

Genet 2011; **12**: 692–702.
25. Legendre M, Fabre E, Poirot O, Jeudy S, Lartigue A, Alempic JM, et al. Diversity and evolution of the emerging Pandoraviridae family. *Nat Commun* 2018; **9**: 2285.
26. Sabath N, Wagner A, Karlin D. Evolution of viral proteins originated de novo by overprinting. *Mol Biol Evol* 2012; **29**: 3767–3780.
27. Long M, Vankuren N, Chen S, Vibranovski M. New gene evolution: little did we know. *Annu Rev Genet* 2013; **47**: 307–333.
28. Krupovic M, Bamford DH, Koonin EV. Conservation of major and minor jelly-roll capsid proteins in Polinton (Maverick) transposons suggests that they are bona fide viruses. *Biol Direct* 2014; **9**: 6.
29. Krupovic M, Koonin EV. Polintons: a hotbed of eukaryotic virus, transposon and plasmid evolution. *Nat Rev Microbiol* 2015; **13**: 105–115.
30. Krupovic M, Koonin EV. Multiple origins of viral capsid proteins from cellular ancestors. *Proc Natl Acad Sci* 2017; **114**: E2401–E2410.
31. Gallot-Lavallée L, Blanc G. A glimpse of nucleo-cytoplasmic large DNA virus biodiversity through the eukaryotic genomics window. *Viruses* 2017; **9**: 17.
32. Fischer MG. Giant viruses come of age. *Curr Opin Microbiol* 2016; **31**: 50–57.
33. Maruyama F, Ueki S. Evolution and phylogeny of large DNA viruses, Mimiviridae and Phycodnaviridae including newly characterized Heterosigma akashiwo virus. *Front Microbiol* 2016; **7**: 1942.
34. Guiry MD. How many species of algae are there? *J Phycol* 2012; **48**: 1057–1063.
35. Field CB. Primary production of the biosphere: integrating terrestrial and oceanic components. *Science (80-)* 1998; **281**: 237–240.
36. Brussaard CPD, Wilhelm SW, Thingstad F, Weinbauer MG, Bratbak G, Heldal M, et al. Global-scale processes with a nanoscale drive: the role of marine viruses. *ISME J* 2008; **0**: 1–4.
37. Wilson WH, Van Etten JL, Allen MJ. The Phycodnaviridae: The story of how tiny giants rule the world. *Curr Top Microbiol Immunol* 2009; **328**: 1–42.
38. Flaviani F, Schroeder DC, Balestreri C, Schroeder JL, Moore K, Paszkiewicz K, et al. A pelagic microbiome (viruses to protists) from a small cup of seawater. *Viruses* 2017; **9**: 47.
39. Dunigan DD, Fitzgerald LA, Van Etten JL. Phycodnaviruses: a peek at genetic diversity. *Virus Res* 2006; **117**: 119–132.
40. Lefkowitz EJ, Dempsey DM, Hendrickson RC, Orton RJ, Siddell SG, Smith DB. Virus taxonomy: the database of the International Committee on Taxonomy of Viruses (ICTV). *Nucleic Acids Res* 2018; **46**: D708–D717.
41. Jeanniard A, Dunigan DD, Gurnon JR, Agarkova IV, Kang M, Vitek J, et al. Towards defining the chloroviruses: A genomic journey through a genus of large DNA viruses. *BMC Genomics* 2013; **14**: 158.
42. Van Etten JL. Chlorovirus. In: Tidona C, Darai G (eds). *The Springer Index of Viruses*, 2nd ed. 2011. Springer-Verlag New York, New York, NY, pp 1243–1252.
43. Allen MJ, Schroeder DC, Holden MTG, Wilson WH. Evolutionary history of the Coccolithoviridae. *Mol Biol Evol* 2006; **23**: 86–92.
44. Nissimov JI, Pagarete A, Ma F, Cody S, Dunigan DD, Kimmance SA, et al. Coccolithoviruses: a review of cross-kingdom genomic thievery and metabolic thuggery. *Viruses* 2017; **9**: 52.
45. Wilson WH, Schroeder DC, Allen MJ, Holden MTG, Parkhill J, Barrell BG, et al. Complete genome sequence and lytic phase transcription profile of a

Coccolithovirus. *Science (80-)* 2005; **309**: 1090–1092.
46. Wilson WH, Allen MJ, Pagarete A. Coccolithovirus. In: Tidona C, Darai G (eds). *The Springer Index of Viruses*. 2011. Springer-Verlag New York, New York, NY, pp 1253–1258.
47. Van Etten JL, Graves M V., Müller DG, Boland W, Delaroque N. Phycodnaviridae - large DNA algal viruses. *Arch Virol* 2002; **147**: 1479–1516.
48. Delaroque N, Boland W, Müller DG, Knippers R. Comparisons of two large phaeoviral genomes and evolutionary implications. *J Mol Evol* 2003; **57**: 613–622.
49. Müller DG, Knippers R. Phaeovirus. In: Tidona C, Darai G (eds). *The Springer Index of Viruses*, 2nd ed. 2011. Springer-Verlag New York, New York, NY, pp 1259–1264.
50. Kapp M, Knippers R, Müller DG. New members of a group of DNA viruses infecting brown algae. *Phycol Res* 1997; **45**: 85–90.
51. Markey DR. A possible virus infection in the brown alga Pylaiella littoralis. *Protoplasma* 1974; **80**: 223–232.
52. Maier I, Wolf S, Delaroque N, Müller DG, Kawai H. A DNA virus infecting the marine brown alga Pilayella littoralis (Ectocarpales, Phaeophyceae) in culture. *Eur J Phycol* 1998; **33**: 213–220.
53. Weynberg KD, Allen MJ, Wilson WH. Marine prasinoviruses and their tiny plankton hosts: A review. *Viruses* 2017; **9**: 1–20.
54. Derelle E, Yau S, Moreau H, Grimsley NH. Prasinovirus attack of Ostreococcus is furtive by day but savage by night. *J Virol* 2018; **92**: e01703-17.
55. Suttle CA. Prasinovirus. In: Tidona C, Darai G (eds). *The Springer Index of Viruses*. 2011. Springer-Verlag New York, New York, NY, pp 1265–1268.
56. Suttle CA, Chan AM. Prymnesiovirus. In: Tidona C, Darai G (eds). *The Springer Index of Viruses*. 2011. Springer-Verlag New York, New York, NY, pp 1269–1274.
57. Nagasaki K, Yamaguchi M. Isolation of a virus infectious to the harmful bloom causing microalga Heterosigma akashiwo (Raphidophyceae). *Aquat Microb Ecol* 1997; **13**: 135–140.
58. Nagasaki K, Tomaru Y, Shirai Y. Raphidovirus. In: Tidona C, Darai G (eds). *The Springer Index of Viruses*. 2011. Springer-Verlag New York, New York, NY, pp 1275–1278.
59. Van Etten JL, Dunigan DD. Chloroviruses: not your everyday plant virus. *Trends Plant Sci* 2012; **17**: 1–8.
60. Maier I, Müller DG, Katsaros C. Entry of the DNA virus, Ectocarpus fasciculatus virus type 1 (Phycodnaviridae), into host cell cytosol and nucleus. *Phycol Res* 2002; **50**: 227–231.
61. Chen J, Cassar SC, Zhang D, Gopalakrishnan M. A novel potassium channel encoded by Ectocarpus siliculosus virus. *Biochem Biophys Res Commun* 2005; **326**: 887–893.
62. Van Etten JL, Agarkova I, Dunigan DD, Tonetti M, De Castro C, Duncan GA. Chloroviruses have a sweet tooth. *Viruses* 2017; **9**: 88.
63. Laber CP, Hunter JE, Carvalho F, Collins JR, Hunter EJ, Schieler BM, et al. Coccolithovirus facilitation of carbon export in the North Atlantic. *Nat Microbiol* 2018; **3**: 537–547.
64. Schroeder DC, Oke J, Malin G, Wilson WH. Coccolithovirus (Phycodnaviridae): Characterisation of a new large dsDNA algal virus that infects Emiliania huxleyi. *Arch Virol* 2002; **147**: 1685–1698.

65. Schatz D, Shemi A, Rosenwasser S, Sabanay H, Wolf SG, Ben-Dor S, et al. Hijacking of an autophagy-like process is critical for the life cycle of a DNA virus infecting oceanic algal blooms. *New Phytol* 2014; **204**: 854–863.
66. Mordecai GJ, Verret F, Highfield A, Schroeder DC. Schrodinger's cheshire cat: Are haploid Emiliania huxleyi cells resistant to viral infection or not? *Viruses* 2017; **9**: 51.
67. Martínez Martínez J, Schroeder DC, Larsen A, Bratbak G, Wilson WH. Molecular dynamics of Emiliania huxleyi and cooccurring viruses during two separate mesocosm studies. *Appl Environ Microbiol* 2007; **73**: 554–562.
68. Bellec L, Grimsley N, Moreau H, Desdevises Y. Phylogenetic analysis of new Prasinoviruses (Phycodnaviridae) that infect the green unicellular algae Ostreococcus, Bathycoccus and Micromonas. *Environ Microbiol Rep* 2009; **1**: 114–123.
69. Finke JF, Winget DM, Chan AM, Suttle CA. Variation in the genetic repertoire of viruses infecting Micromonas pusilla reflects horizontal gene transfer and links to their environmental distribution. *Viruses* 2017; **9**: 116.
70. Brussaard CPD, Kuipers B, Veldhuis MJW. A mesocosm study of Phaeocystis globosa population dynamics: I. Regulatory role of viruses in bloom control. *Harmful Algae* 2005; **4**: 859–874.
71. Brussaard CPD. Viral Control of Phytoplankton Populations-a Review. *J Eukaryot Microbiol* 2004; **51**: 125–138.
72. Mirza SF, Staniewski MA, Short CM, Long AM, Chaban Y V., Short SM. Isolation and characterization of a virus infecting the freshwater algae Chrysochromulina parva. *Virology* 2015; **486**: 105–115.
73. Santini S, Jeudy S, Bartoli J, Poirot O, Lescot M, Abergel C, et al. Genome of Phaeocystis globosa virus PgV-16T highlights the common ancestry of the largest known DNA viruses infecting eukaryotes. *Proc Natl Acad Sci* 2013; **110**: 10800–10805.
74. Brussaard CPD, Short SM, Frederickson CM, Suttle CA. Isolation and phylogenetic analysis of novel viruses infecting the phytoplankton. *Society* 2004; **70**: 3700–3705.
75. Johannessen TV, Bratbak G, Larsen A, Ogata H, Egge ES, Edvardsen B, et al. Characterisation of three novel giant viruses reveals huge diversity among viruses infecting Prymnesiales (Haptophyta). *Virology* 2015; **476**: 180–188.
76. Delaroque N, Maier L, Knippers R, Müller DG. Persistent virus integration into the genome of its algal host, Ectocarpus siliculosus (Phaeophyceae). *J Gen Virol* 1999; **80**: 1367–1370.
77. Müller DG, Kawai H, Stache B, Lanka S. A virus infection in the marine brown alga Ectocarpus siliculosus (Phaeophyceae). *Bot Acta* 1990; **103**: 72–82.
78. Müller DG. Mendelian segregation of a virus genome during host meiosis in the marine brown alga Ectocarpus siliculosus. *J Plant Physiol* 1991; **137**: 739–743.
79. Bräutigam M, Klein M, Knippers R, Müller DG. Inheritance and meiotic elimination of a virus genome in the host Ectocarpus siliculosus (Phaeophyceae). *J Phycol* 1995; **31**: 823–827.
80. Müller DG, Frenzer K. Virus infections in three marine brown algae: Feldmannia irregularis, F. simplex, and Ectocarpus siliculosus. *Fourteenth Int. Seaweed Symp.* 1993. Springer, pp 37–44.
81. Müller DG, Kapp M, Knippers R. Viruses in marine brown algae. *Adv Virus Res* 1998; **50**: 49–67.

82. Parodi ER, Müller DG. Field and culture studies on virus infections in Hincksia hincksiae and Ectocarpus fasciculatus (Ectocarpales, Phaeophyceae). *Eur J Phycol* 1994; **29**: 113–117.
83. Dixon NM, Leadbeater BS, Wood RK. Frequency of viral infection in a field population of Ectocarpus fasciculatus (Ectocarpales, Phaeopbyceae). *Phycologia* 2000; **39**: 258–263.
84. Müller DG, Stache B. Worldwide occurrence of virus-infections in filamentous marine brown algae. *Helgoländer Meeresuntersuchungen* 1992; **46**: 1–8.
85. Müller DG, Westermeier R, Morales J, Reina GG, del Campo E, Correa JA, et al. Massive prevalence of viral DNA in Ectocarpus (Phaeophyceae, Ectocarpales) from two habitats in the North Atlantic and South Pacific. *Bot Mar* 2000; **43**: 157–159.
86. Sengco MR, Bräutigam M, Kapp M, Müller DG. Detection of virus DNA in Ectocarpus siliculosus and E. fasciculatus (Phaeophyceae) from various geographic areas. *Eur J Phycol* 1996; **31**: 73–78.
87. Del Campo E, Ramazanov Z, Garcia-Reina G, Müller DG. Photosynthetic responses and growth performance of virus-infected and noninfected Ectocarpus siliculosus (Phaeophyceae). *Phycologia* 1997; **36**: 186–189.
88. Robledo DR, Sosa PA, Garcia-Reina G, Müller DG. Photosynthetic performance of healthy and virus-infected Feldmannia irregularis and F. simplex (Phaeophyceae). *Eur J Phycol* 1994; **29**: 247–251.
89. Henry EC, Meints RH. A persistent virus infection in Feldmannia (Phaeophyceae). *J Phycol* 1992; **28**: 517–526.
90. Ivey RG, Henry EC, Lee AM, Sharon LK, Krueger SK, Meints RH. A Feldmannia algal virus has two genome size-classes. *Virology* 1996; **220**: 267–273.
91. Müller DG, Brautigam M, Knippers R. Virus infection and persistence of foreign DNA in the marine brown alga Feldmannia simplex (Ectocarpales, Phaeophyceae). *Phycologia* 1996; **35**: 61–63.
92. Müller DG, Parodi E. Transfer of a marine DNA virus from Ectocarpus to Feldmannia (Ectocarpales, Phaeophyceae): aberrant symptoms and restitution of the host. *Protoplasma* 1993; **175**: 121–125.
93. Maier I, Rometsch E, Wolf S, Kapp M, Müller DG, Kawai H. Passage of a marine brown algal DNA virus from Ectocarpus fasciculatus (Ectocarpales, Phaeophyceae) to Myriotrichia clavaeformis (Dictyosiphonales, Phaeophyceae): infection symptoms and recovery. *J Phycol* 1997; **33**: 838–844.
94. Müller DG. Intergeneric transmission of a marine plant DNA virus. *Naturwissenschaften* 1992; **79**: 37–39.
95. Stevens K, Weynberg K, Bellas C, Brown S, Brownlee C, Brown MT, et al. A novel evolutionary strategy revealed in the phaeoviruses. *PLoS One* 2014; **9**: e86040.
96. Schroeder DC. More to Phaeovirus infections than first meets the eye. *Perspect Phycol* 2015; **2**: 105–109.
97. Abedon ST. Bacteriophage secondary infection. *Virol Sin* 2015; **30**: 3–10.
98. Schroeder DC, Park Y, Yoon HM, Lee YS, Kang SW, Meints RH, et al. Genomic analysis of the smallest giant virus - Feldmannia sp. virus 158. *Virology* 2009; **384**: 223–232.
99. Delaroque N, Wolf S, Müller DG, Knippers R. The brown algal virus EsV-1 particle contains a putative hybrid histidine kinase. *Virology* 2000; **273**: 383–390.
100. Delaroque N, Müller DG, Bothe G, Pohl T, Knippers R, Boland W, et al. The complete DNA sequence of the Ectocarpus siliculosus virus EsV-1 genome.

Virology 2001; **287**: 112–132.
101. Schroeder DC. Viruses of Seaweeds. In: Hurst C.J. (ed). *Studies in Viral Ecology: Microbial and Botanical Host Systems*. 2011. John Wiley & Sons, Hoboken, NJ, USA, pp 204–215.
102. Meints RH, Ivey RG, Lee AM, Choi T-J. Identification of two virus integration sites in the brown alga Feldmannia chromosome. *J Virol* 2008; **82**: 1407–13.
103. Cock JM, Sterck L, Rouzé P, Scornet D, Allen AE, Amoutzias G, et al. The Ectocarpus genome and the independent evolution of multicellularity in brown algae. *Nature* 2010; **465**: 617–621.
104. Lee AM, Ivey RG, Meints RH. Repetitive DNA insertion in a protein kinase ORF of a latent FSV (Feldmannia sp. virus) genome. *Virology* 1998; **248**: 35–45.
105. Delaroque N, Boland W. The genome of the brown alga Ectocarpus siliculosus contains a series of viral DNA pieces, suggesting an ancient association with large dsDNA viruses. *BMC Evol Biol* 2008; **8**: 110.
106. Chabannes M, Iskra-Caruana ML. Endogenous pararetroviruses - a reservoir of virus infection in plants. *Curr Opin Virol* 2013; **3**: 615–620.
107. Hay ME, Steinberg PD. The chemical ecology of plant-herbivore interactions in marine versus terrestrial communities, 2nd ed. *Herbivores: Their Interactions with Secondary Plant Metabolites Ecological and Evolutionary Processes* . 1992. Academic Press Limited, London.
108. Koonin E V., Wolf YI, Nagasaki K, Dolja V V. The Big Bang of picorna-like virus evolution antedates the radiation of eukaryotic supergroups. *Nat Rev Microbiol* 2008; **6**: 925–939.
109. Hull R. Plant Virology, 5th ed. 2014. Academic Press, London.
110. Guiry MD, Guiry GM. Algaebase. http://www.algaebase.org/. Accessed 1 May 2018.
111. Oliveira L, Bisalputra T. A virus infection in the brown alga Sorocarpus uvaeformis (Lyngbye) Pringsheim (Phaeophyta, Ectocarpales). *Ann Bot* 1978; **42**: 439–445.
112. Clitheroe SB, Evans L V. Viruslike particles in the brown alga Ectocarpus. *J Ultrasructure Res* 1974; **49**: 211–217.
113. Toth R, Wilce RT. Virus-like particles in the marine alga Chorda tomentosa Lyngbye (Phaeophyceae). *J Phycol* 1972; **8**: 126–130.
114. La Claire JW, West JA. Virus-like particles in the brown alga Streblonema. *Protoplasma* 1977; **93**: 127–130.
115. Easton LM, Lewis GD, Pearson MN. Virus-like particles associated with dieback symptoms in the brown alga Ecklonia radiata. *Dis Aquat Organ* 1997; **30**: 217–222.
116. Wang L, Wu S, Liu T, Sun J, Chi S, Liu C, et al. Endogenous viral elements in algal genomes. *Acta Oceanol Sin* 2014; **33**: 102–107.
117. Maumus F, Epert A, Nogué F, Blanc G. Plant genomes enclose footprints of past infections by giant virus relatives. *Nat Commun* 2014; **5**: 4268.
118. Hohn T, Richert-Pöggeler KR, Staginnus C, Harper G, Schwarzacher T, Teo HC, et al. Evolution of integrated plant viruses. In: Roossinck MJ (ed). *Plant Virus Evolution*. 2008. Springer-Verlag Berlin Heidelberg, Berlin, pp 53–81.
119. Staginnus C, Richert-Pöggeler KR. Endogenous pararetroviruses: two-faced travelers in the plant genome. *Trends Plant Sci* 2006; **11**: 485–491.
120. Beattie D, Lachnit T, Dinsdale E, Thomas T, Steinberg PD. Novel ssDNA viruses detected in the virome of bleached, habitat-forming kelp Ecklonia radiata. *Front*

Mar Sci 2018; **4**: 441.
121. Ding H, Guo L, Li X, Yang G. Transcriptome analysis of kelp Saccharina japonica unveils its weird transcripts and metabolite shift of main components at different sporophyte developmental stages*. *J Oceanol Limnol* 2019; **37**: 640–650.
122. Lachnit T, Thomas T, Steinberg P. Expanding our understanding of the seaweed holobiont: RNA viruses of the red alga Delisea pulchra. *Front Microbiol* 2016; **6**: 1489.
123. Rousvoal S, Bouyer B, López-Cristoffanini C, Boyen C, Collén J. Mutant swarms of a totivirus-like entities are present in the red macroalga Chondrus crispus and have been partially transferred to the nuclear genome. *J Phycol* 2016; **52**: 493–504.
124. Kim GH, Klochkova TA, Lee DJ, Im SH. Chloroplast virus causes green-spot disease in cultivated Pyropia of Korea. *Algal Res* 2016; **17**: 293–299.
125. West JA, Pueschel CM, Klochkova TA, Hoon Kim G, de Goër S, Zuccarello GC. Gall structure and specificity in Bostrychia culture isolates (Rhodomelaceae, Rhodophyta). *Algae* 2013; **28**: 83–92.
126. Kew Royal Botanic Gardens. State of the world's plants. 2017.
127. Skotnicki A, Gibbs A, Wrigley NG. Further studies on Chara corallina virus. *Virology* 1976; **75**: 457–468.
128. Dodds JA, Cole A. Microscopy and biology of Uronema gigas, a filamentous eucaryotic green alga, and its associated tailed virus-like particle. *Virology* 1980; **100**: 156–165.
129. Ishihara J, Pak JY, Fukuhara T, Nitta T. Association of particles that contain double-stranded RNAs with algal chloroplasts and mitochondria. *Planta* 1992; **187**: 475–482.
130. Chapman RL, Lang NJ. Virus-Like particles and nuclear inclusions in the red alga Porphyridium purpureum (Bory) Drew et Ross. *J Phycol* . 1973. , **9**: 117–122
131. Lee RE. Systemic viral material in the cells of the freshwater red alga Sirodotia tenuissima (Holden) Skuja. *J Cell Sci* 1971; **8**: 623–631.
132. Apt KE, Gibor A. The ultrastructure of galls on the red alga Gracilaria epihippisora. *J Phycol* 1991; **27**: 409–413.
133. Pueschel CM. Rod-shaped virus-like particles in the endoplasmic reticulum of Audouinella saviana (Acrochaetiales, Rhodophyta). *Can J Bot* 1995; **73**: 1974–1980.
134. Koonin EV, Dolja VV. Evolution of complexity in the viral world: the dawn of a new vision. *Virus Res* 2006; **117**: 1–4.
135. Koonin EV, Senkevich TG, Dolja VV. The ancient virus world and evolution of cells. *Biol Direct* 2006; **1**: 29.
136. Cock JM, Coelho SM, Brownlee C, Taylor AR. The Ectocarpus genome sequence: insights into brown algal biology and the evolutionary diversity of the eukaryotes. *New Phytol* 2010; **188**: 1–4.
137. Charrier B, Coelho SM, Le Bail A, Tonon T, Michel G, Potin P, et al. Development and physiology of the brown alga Ectocarpus siliculosus: two centuries of research. *New Phytol* 2008; **177**: 319–332.
138. Thomas F, Cosse A, Le Panse S, Kloareg B, Potin P, Leblanc C. Kelps feature systemic defense responses: insights into the evolution of innate immunity in multicellular eukaryotes. *New Phytol* 2014; **204**: 567–576.
139. Weinberger F. Pathogen-induced defense and innate immunity in macroalgae.

Biol Bull 2007; **213**: 290–302.
140. Lee RE. Phycology, 4th ed. 2008. Cambridge University Press, Cambridge.
141. Knoblauch J, Tepler Drobnitch S, Peters WS, Knoblauch M. In situ microscopy reveals reversible cell wall swelling in kelp sieve tubes: one mechanism for turgor generation and flow control? *Plant, Cell Environ* 2016; **39**: 1727–1736.
142. Poore AGB, Hill NA, Sotka EE. Phylogenetic and geographic variation in host breadth and composition by herbivorous amphipods in the family ampithoidae. *Evolution (N Y)* 2008; **62**: 21–38.
143. Andika IB, Kondo H, Sun L. Interplays between soil-borne plant viruses and RNA silencing-mediated antiviral defense in roots. *Front Microbiol* 2016; **7**: 1–13.
144. Frada MJ, Schatz D, Farstey V, Ossolinski JE, Sabanay H, Ben-Dor S, et al. Zooplankton may serve as transmission vectors for viruses infecting algal blooms in the ocean. *Curr Biol* 2014; **24**: 2592–2597.
145. Gachon CMM, Sime-Ngando T, Strittmatter M, Chambouvet A, Kim GH. Algal diseases: spotlight on a black box. *Trends Plant Sci* 2010; **15**: 633–640.
146. Andrews JH. The pathology of marine algae. *Biol Rev* 1976; **51**: 211–253.
147. Hancock L, Goff L, Lane C. Red algae lose key mitochondrial genes in response to becoming parasitic. *Genome Biol Evol* 2010; **2**: 897–910.
148. Heesch S, Peters AF. Scanning electron microscopy observation of host entry by two brown algae endophytic in Laminaria saccharina (Laminariales, Phaeophyceae). *Phycol Res* 1999; **47**: 1–5.
149. Wahl M. Marine epibiosis. I. Fouling and antifouling: some basic aspects. *Mar Ecol Prog Ser* 1989; **58**: 175–189.
150. Wahl M, Mark O. The predominantly facultative nature of epibiosis: experimental and observational evidence. *Mar Ecol Prog Ser* 1999; **187**: 59–66.
151. Teagle H, Hawkins SJ, Moore PJ, Smale DA. The role of kelp species as biogenic habitat formers in coastal marine ecosystems. *J Exp Mar Bio Ecol* 2017; **492**: 81–98.
152. Mehle N, Ravnikar M. Plant viruses in aqueous environment - survival, water mediated transmission and detection. *Water Res* 2012; **46**: 4902–4917.
153. Sharoni S, Trainic M, Schatz D, Lehahn Y, Flores MJ, Bidle KD, et al. Infection of phytoplankton by aerosolized marine viruses. *Proc Natl Acad Sci* 2015; **112**: 6643–6647.
154. McCallum H, Harvell D, Dobson A. Rates of spread of marine pathogens. *Ecol Lett* 2003; **6**: 1062–1067.
155. McCallum HI, Kuris A, Harvell CD, Lafferty KD, Smith GW, Porter J. Does terrestrial epidemiology apply to marine systems? *Trends Ecol Evol* 2004; **19**: 585–591.
156. Anekal SG, Zhu Y, Graham MD, Yin J. Dynamics of virus spread in the presence of fluid flow. *Integr Biol* 2009; **1**: 11–12.
157. Van Tussenbroek BI, Villamil N, Márquez-Guzmán J, Wong R, Monroy-Velázquez LV, Solis-Weiss V. Experimental evidence of pollination in marine flowers by invertebrate fauna. *Nat Commun* 2016; **7**: 12980.
158. Müller DG. Marine virioplankton produced by infected Ectocarpus siliculosus (Phaeophyceae). *Mar Ecol Prog Ser* 1991; **76**: 101–102.
159. Niklas KJ, Newman SA. The origins of multicellular organisms. *Evol Dev* 2013; **15**: 41–52.
160. Pires ND, Dolan L. Morphological evolution in land plants: new designs with old genes. *Philos Trans R Soc B Biol Sci* 2012; **367**: 508–518.

161. Bociąg K, Gałka A, Łazarewicz T, Szmeja J. Mechanical strength of stems in aquatic macrophytes. *Acta Soc Bot Pol* 2009; **78**: 181–187.
162. Lang D, Rensing SA. The evolution of transcriptional regulation in the Viridplantae and its correlation with morphological complexity. In: Ruiz-Trillo I, Nedelcu AM (eds). *Advances in Marine Genomics Volume 2*. 2015. Springer, Dordrecht, pp 301–333.
163. Bell G, Mooers AO. Size and complexity among multicellular organisms. *Biol J Linn Soc* 1997; **60**: 345–363.
164. Clayton MN. Propagules of marine macroalgae: structure and development. *Br Phycol J* 1992; **27**: 219–232.
165. Hay ME. The role of seaweed chemical defenses in the evolution of feeding specialization and in the mediation of complex interactions. In: Paul VJ (ed). *Ecological Roles of Marine Natural Products*. 1992. Comstock Publishing Associates, New York, NY, pp 93–118.
166. Hay ME, Duffy EJ, Fenical W. Host-plant specialization decreases predation on a marine amphipod: an herbivore in plant's clothing. *Ecology* 1990; **71**: 733–743.
167. Arnold M, Teagle H, Brown MP, Smale DA. The structure of biogenic habitat and epibiotic assemblages associated with the global invasive kelp Undaria pinnatifida in comparison to native macroalgae. *Biol Invasions* 2016; **18**: 661–676.
168. Parfrey LW, Lahr DJG, Knoll AH, Katz LA. Estimating the timing of early eukaryotic diversification with multigene molecular clocks. *Proc Natl Acad Sci* 2011; **108**: 13624–13629.
169. Cavalier-Smith T, Chao EE, Lewis R. Multiple origins of Heliozoa from flagellate ancestors: New cryptist subphylum Corbihelia, superclass Corbistoma, and monophyly of Haptista, Cryptista, Hacrobia and Chromista. *Mol Phylogenet Evol* 2015; **93**: 331–362.
170. Brown JW, Sorhannus U. A molecular genetic timescale for the diversification of autotrophic stramenopiles (Ochrophyta): Substantive underestimation of putative fossil ages. *PLoS One* 2010; **5**: 1–11.
171. Silberfeld T, Leigh JW, Verbruggen H, Cruaud C, de Reviers B, Rousseau F. A multi-locus time-calibrated phylogeny of the brown algae (Heterokonta, Ochrophyta, Phaeophyceae): investigating the evolutionary nature of the 'brown algal crown radiation'. *Mol Phylogenet Evol* 2010; **56**: 659–674.
172. Kawai H, Hanyuda T, Draisma SGA, Wilce RT, Andersen RA. Molecular phylogeny of two unusual brown algae, Phaeostrophion irregulare and Platysiphon Glacialis, proposal of the Stschapoviales ord. nov. and Platysiphonaceae fam. nov., and a re-examination of divergence times for brown algal orders. *J Phycol* 2015; **51**: 918–928.
173. Rodelo-Urrego M, Pagán I, González-Jara P, Betancourt M, Moreno-Letelier A, Ayllõn MA, et al. Landscape heterogeneity shapes host-parasite interactions and results in apparent plant-virus codivergence. *Mol Ecol* 2013; **22**: 2325–2340.
174. Kim JK, Yarish C, Hwang EK, Park M, Kim Y. Seaweed aquaculture: cultivation technologies, challenges and its ecosystem services. *Algae* 2017; **32**: 1–13.
175. Buschmann AH, Camus C, Infante J, Neori A, Israel Á, Hernández-González MC, et al. Seaweed production: overview of the global state of exploitation, farming and emerging research activity. *Eur J Phycol* 2017; **52**: 391–406.
176. FAO. Global Aquaculture Production. *Fishery Statistical Collections*. http://www.fao.org/fishery/statistics/global-aquaculture-production/query/en.

Accessed 5 Jun 2018.
177. Cottier-Cook EJ, Nagabhatla N, Badis Y, Campbell ML, Chopin T, Dai W, et al. Safeguarding the future of the global seaweed aquaculture industry. *United Nations University (INWEH) and Scottish Association for Marine Science Policy Brief* . 2016. Hamilton, Canada.
178. Wang G, Lu B, Shuai L, Li D, Zhang R. Microbial diseases of nursery and field-cultivated Saccharina japonica (Phaeophyta) in China. *Arch Hydrobiol Suppl Algol Stud* 2014; **145**: 39–51.
179. Loureiro R, Gachon CMM, Rebours C. Seaweed cultivation: potential and challenges of crop domestication at an unprecedented pace. *New Phytol* 2015; **206**: 489–492.
180. Roossinck MJ. Plant Virus Ecology. *PLoS Pathog* 2013; **9**: 9–11.
181. Roossinck MJ. Plants, viruses and the environment: ecology and mutualism. *Virology* 2015; **479–480**: 271–277.
182. Roossinck MJ. Lifestyles of plant viruses. *Philos Trans R Soc B Biol Sci* 2010; **365**: 1899–1905.
183. Roossinck MJ. Plant virus metagenomics: biodiversity and ecology. *Annu Rev Genet* 2012; **46**: 359–369.
184. Brodie J, Chan X, Clerck O De, Cock JM, Coelho SM, Gachon C, et al. The algal revolution. *Trends Plant Sci* 2017; **22**: 726–738.
185. Cavalier-Smith T. Kingdom Chromista and its eight phyla: a new synthesis emphasising periplastid protein targeting, cytoskeletal and periplastid evolution, and ancient divergences. *Protoplasma* 2018; **255**: 297–357.
186. Yoon HS, Hackett JD, Ciniglia C, Pinto G, Bhattacharya D. A molecular timeline for the origin of photosynthetic eukaryotes. *Mol Biol Evol* 2004; **21**: 809–818.
187. Kawai H, Henry EC. Phaeophyta. In: Archibald JM, Simpson AGB, Slamovits CH, Margulis L, Melkonian M, Chapman DJ, et al. (eds). *Handbook of the Protists*. 2016. Springer, Cham, Switzerland.
188. Grattepanche JD, Walker LM, Ott BM, Paim Pinto DL, Delwiche CF, Lane CE, et al. Microbial diversity in the eukaryotic SAR clade: illuminating the darkness between morphology and molecular data. *BioEssays* 2018; **40**: 1–12.
189. Coelho SM, Scornet D, Rousvoal S, Peters NT, Dartevelle L, Peters AF, et al. Ectocarpus: A model organism for the brown algae. *Cold Spring Harb Protoc* 2012; **7**: 193–198.
190. Peters AF, Marie D, Scornet D, Kloareg B, Cock JM. Proposal of Ectocarpus siliculosus (Ectocarpales, Phaeophyceae) as a model organism for brown algal genetics and genomics. *J Phycol* 2004; **40**: 1079–1088.
191. Dierssen HM, Zimmerman RC, Drake LA, Burdige DJ. Potential export of unattached benthic macroalgae to the deep sea through wind-driven Langmuir circulation. *Geophys Res Lett* 2009; **36**: L04602.
192. Smale DA, Burrows MT, Moore P, O'Connor N, Hawkins SJ. Threats and knowledge gaps for ecosystem services provided by kelp forests: a northeast Atlantic perspective. *Ecol Evol* 2013; **3**: 4016–4038.
193. Parke M. Studies on British Laminariaceae. I. growth in Laminaria saccharina (L.) Lamour. *J Mar Biol Assoc United Kingdom* 1948; **27**: 651–709.
194. Kain JM. The biology of Laminaria hyperborea VII. reproduction of the sporophyte. *J Mar Biol Assoc United Kingdom* 1975; **55**: 567–582.
195. Chapman ARO. Reproduction, recruitment and mortality in two species of Laminaria in southwest Nova Scotia. *J Exp Mar Bio Ecol* 1984; **78**: 99–109.

196. Reed DC, Anderson TW, Ebeling AW, Anghera M. The role of reproductive synchrony in the colonization potential of kelp. *Ecology* 1997; **78**: 2443–2457.
197. Raimondi PT, Reed DC, Gaylord B, Washburn L. Effects of self-fertilization in the giant kelp, Macrocystis pyrifera. *Ecology* 2004; **85**: 3267–3276.
198. Mohring MB, Wernberg T, Kendrick GA, Rule MJ. Reproductive synchrony in a habitat-forming kelp and its relationship with environmental conditions. *Mar Biol* 2013; **160**: 119–126.
199. Druehl LD, Collins JD, Lane CE, Saunders GW, Areschoug E. An evaluation of methods used to assess intergeneric hybridisation in kelp using Pacific Laminariales (Phaeophyceae). *J Phycol* 2005; **41**: 250–262.
200. Luthringer R, Cormier A, Ahmed S, Peters AF, Cock JM, Coelho SM. Sexual dimorphism in the brown algae. *Perspect Phycol* 2014; **1**: 11–25.
201. Destombe C, Oppliger LV. Male gametophyte fragmentation in Laminaria digitata: a life history strategy to enhance reproductive success. *Cah Biol Mar* 2011; **52**: 385–394.
202. Oppliger LV, Correa JA, Peters AF. Parthenogenesis in the brown alga Lessonia nigrescens (Laminariales, Phaeophyceae) from central Chile. *J Phycol* 2007; **43**: 1295–1301.
203. Bothwell JH, Marie D, Peters AF, Cock JM, Coelho SM. Role of endoreduplication and apomeiosis during parthenogenetic reproduction in the model brown alga Ectocarpus. *New Phytol* 2010; **188**: 111–121.
204. Liu X, Bogaert K, Engelen AH, Leliaert F, Roleda MY, De Clerck O. Seaweed reproductive biology: environmental and genetic controls. *Bot Mar* 2017; **60**: 89–108.
205. Martin P, Zuccarello GC. Molecular phylogeny and timing of radiation in Lessonia (Phaeophyceae, Laminariales). *Phycol Res* 2012; **60**: 276–287.
206. Bolton JJ. The biogeography of kelps (Laminariales, Phaeophyceae): A global analysis with new insights from recent advances in molecular phylogenetics. *Helgol Mar Res* 2010; **64**: 263–279.
207. Parker BC, Dawson EY. Fleshy seaweeds from California Miocene deposits. *Am J Bot* 1965; **52**: 643.
208. Kawai H. Recent advances in the phylogeny and taxonomy of Laminariales, with special reference to the newly discovered basal member Aureophycus. *Perspect Phycol* 2014; **1**: 27–40.
209. Rothman MD, Mattio L, Anderson RJ, Bolton JJ. A phylogeographic investigation of the kelp genus Laminaria (Laminariales, Phaeophyceae), with emphasis on the South Atlantic Ocean. *J Phycol* 2017; **53**: 778–789.
210. Luttikhuizen PC, van den Heuvel FHM, Rebours C, Witte HJ, van Bleijswijk JDL, Timmermans K. Strong population structure but no equilibrium yet: genetic connectivity and phylogeography in the kelp Saccharina latissima (Laminariales, Phaeophyta). *Ecol Evol* 2018; **8**: 4265–4277.
211. Graham MH, Kinlan BP, Druehl LD, Garske LE, Banks S. Deep-water kelp refugia as potential hotspots of tropical marine diversity and productivity. *Proc Natl Acad Sci* 2007; **104**: 16576–16580.
212. Rothman MD, Mattio L, Wernberg T, Anderson RJ, Uwai S, Mohring MB, et al. A molecular investigation of the genus Ecklonia (Phaeophyceae, Laminariales) with special focus on the Southern Hemisphere. *J Phycol* 2015; **51**: 236–246.
213. Steneck R, Graham MH, Bourque BJ, Corbett D, Erlandson JM. Kelp forest ecosystems: biodiversity, stability, resilience and future. *Environ Conserv* 2002;

29: 436–459.
214. Carr M, Reed D. Shallow Rocky Reefs and Kelp Forests. In: Mooney H, Zavaleta E (eds). *Ecosystems of California*, 1st ed. 2016. University of California Press, Oakland, CA, pp 311–336.
215. Fujita D. Management of kelp ecosystem in Japan. *Cah Biol Mar* 2011; **52**: 499–505.
216. Ramírez ME, Santelices B. Catálogo de las algas marinas bentónicas de la costa temperada del Pacífico de Sudámerica. *Monografías Biológicas N°5* . 1991. Universidad Católica de Chile, Santiago, Chile.
217. Huovinen P, Gómez I. Cold-temperate seaweed communities of the Southern Hemisphere. In: Wiencke C, Bischof K (eds). *Seaweed Biology. Ecological Studies*. 2012. Springer Berlin Heidelberg, Berlin, pp 293–313.
218. Filbee-Dexter K, Scheibling RE. Sea urchin barrens as alternative stable states of collapsed kelp ecosystems. *Mar Ecol Prog Ser* 2014; **495**: 1–25.
219. Boo GH, Lindstrom SC, Klochkova NC, Yotsukura N, Yang EC, Kim HG, et al. Taxonomy and biogeography of Agarum and Thalassiophyllum (Laminariales, Phaeophyceae) based on sequences of nuclear, mitochondrial, and plastid markers. *Taxon* 2011; **60**: 831–840.
220. Epstein G, Smale DA. Undaria pinnatifida: a case study to highlight challenges in marine invasion ecology and management. *Ecol Evol* 2017; **7**: 8624–8642.
221. Dayton PK. Ecology of kelp communities. *Annu Rev Ecol Syst* 1985; **16**: 215–245.
222. Krumhansl KA, Okamoto DK, Rassweiler A, Novak M, Bolton JJ, Cavanaugh KC, et al. Global patterns of kelp forest change over the past half-century. *Proc Natl Acad Sci* 2016; **113**: 13785–13790.
223. Mann HK. Seaweeds: their productivity and strategy for growth. *Science (80-)* 1973; **182**: 975–981.
224. Reed DC, Rassweiler AR, Arkema KK. Biomass rather than growth rate determines variation in net primary production by giant kelp. *Ecology* 2008; **89**: 2493–2505.
225. Leclerc JC, Riera P, Leroux C, Lévêque L, Davoult D. Temporal variation in organic matter supply in kelp forests: linking structure to trophic functioning. *Mar Ecol Prog Ser* 2013; **494**: 87–105.
226. Hyndes GA, Lavery PS, Doropoulos C. Dual processes for cross-boundary subsidies: incorporation of nutrients from reef-derived kelp into a seagrass ecosystem. *Mar Ecol Prog Ser* 2012; **445**: 97–107.
227. Newell R, Field J, Griffiths C. Energy balance and significance of microorganisms in a kelp bed community. *Mar Ecol Prog Ser* 1982; **8**: 103–113.
228. Bustamante RH, Branch GM, Eekhout S. Maintenance of an exceptional intertidal grazer biomass in South Africa: subsidy by subtidal kelps. *Ecology* 1995; **76**: 2314–2329.
229. Norderhaug KM, Christie H, Fosså JH, Fredriksen SP, Fossô JHO, Fredriksen SP, et al. Fish-macrofauna interactions in a kelp (Laminaria hyperborea) forest. *J Mar Biol Assoc United Kingdom* 2005; **85**: 1279–1286.
230. O'Connor KC, Anderson TW. Consequences of habitat disturbance and recovery to recruitment and the abundance of kelp forest fishes. *J Exp Mar Bio Ecol* 2010; **386**: 1–10.
231. Filbee-dexter K, Scheibling RE. Hurricane-mediated defoliation of kelp beds and pulsed delivery of kelp detritus to offshore sedimentary habitats. *Mar Ecol Prog Ser* 2012; **455**: 51–64.

232. Krumhansl KA, Scheibling RE. Production and fate of kelp detritus. *Mar Ecol Prog Ser* 2012; **467**: 281–302.
233. Krause-Jensen D, Duarte CM. Substantial role of macroalgae in marine carbon sequestration. *Nat Geosci* 2016; **9**: 737–742.
234. Abdullah MI, Fredriksen S, Christie H. The impact of the kelp (Laminaria hyperborea) forest on the organic matter content in sediment of the west coast of Norway. *Mar Biol Res* 2017; **13**: 151–160.
235. IUCN. The management of natural coastal carbon sinks. 2009. Gland, Switzerland.
236. Duarte CM, Losada IJ, Hendriks IE, Mazarrasa I, Marbà N. The role of coastal plant communities for climate change mitigation and adaptation. *Nat Clim Chang* 2013; **3**: 961–968.
237. Krause-Jensen D, Lavery P, Serrano O, Marba N, Masque P, Duarte CM. Sequestration of macroalgal carbon: the elephant in the blue carbon room. *Biol Lett* 2018; **14**: 20180236.
238. Behrenfeld MJ, Boss E, Siegel DA, Shea DM. Carbon-based ocean productivity and phytoplankton physiology from space. *Global Biogeochem Cycles* 2005; **19**: GB1006.
239. Seiter K, Hensen C, Zabel M. Benthic carbon mineralization on a global scale. *Global Biogeochem Cycles* 2005; **19**: GB1010.
240. Duarte CM, Middelburg JJ, Caraco N. Major role of marine vegetation on the oceanic carbon cycle. *Biogeosciences Discuss* 2004; **1**: 659–679.
241. Barrón C, Duarte CM. Global biogeochemical cycles from the coastal ocean. *Global Biogeochem Cycles* 2015; **29**: 1725–1738.
242. Allan JD, Williams PI, Najera J, Whitehead JD, Flynn MJ, Taylor JW, et al. Iodine observed in new particle formation events in the Arctic atmosphere during ACCACIA. *Atmos Chem Phys* 2015; **15**: 5599–5609.
243. Küpper FC, Carpenter LJ, McFiggans GB, Palmer CJ, Waite TJ, Boneberg E-M, et al. Iodide accumulation provides kelp with an inorganic antioxidant impacting atmospheric chemistry. *Proc Natl Acad Sci* 2008; **105**: 6954–6958.
244. Nitschke U, Dixneuf S, Schmid M, Ruth AA, Stengel DB. Contribution of living and degrading kelp to coastal iodine fluxes. *Mar Biol* 2015; **162**: 1727–1738.
245. Hamersley MR, Sohm JA, Burns JA, Capone DG. Nitrogen fixation associated with the decomposition of the giant kelp Macrocystis pyrifera. *Aquat Bot* 2015; **125**: 57–63.
246. Jackson GA, Winant CD. Effect of a kelp forest on coastal currents. *Cont Shelf Res* 1983; **2**: 75–80.
247. Vásquez JA, Zuñiga S, Tala F, Piaget N, Rodríguez DC, Vega JMA. Economic valuation of kelp forests in northern Chile: values of goods and services of the ecosystem. *J Appl Phycol* 2014; **26**: 1081–1088.
248. Bennett S, Wernberg T, Connell SD, Hobday AJ, Johnson CR, Poloczanska ES. The 'Great Southern Reef': social, ecological and economic value of Australia's neglected kelp forests. *Mar Freshw Res* 2015; **67**: 47–56.
249. Blamey LK, Bolton JJ. The economic value of South African kelp forests and temperate reefs: past, present and future. *J Mar Syst* 2018; **188**: 172–181.
250. Beaumont NJ, Austen MC, Mangi SC, Townsend M. Economic valuation for the conservation of marine biodiversity. *Mar Pollut Bull* 2008; **56**: 386–396.
251. Bertocci I, Araújo R, Oliveira P, Sousa-Pinto I. Potential effects of kelp species on local fisheries. *J Appl Ecol* 2015; **52**: 1216–1226.

252. Bjerregaard R. Seaweed aquaculture for food security, income generation and environmental health in tropical developing countries. 2016. Washington, DC, USA.
253. Rebours C, Marinho-Soriano E, Zertuche-González JA, Hayashi L, Vásquez JA, Kradolfer P, et al. Seaweeds: an opportunity for wealth and sustainable livelihood for coastal communities. *J Appl Phycol* 2014; **26**: 1939–1951.
254. Fleurence J. Seaweeds as Food. In: Fleurence J, Levine I (eds). *Seaweed in Health and Disease Prevention*, 1st ed. 2016. Academic Press, London, pp 149–167.
255. Bixler HJ, Porse H. A decade of change in the seaweed hydrocolloids industry. *J Appl Phycol* 2011; **23**: 321–335.
256. Marinho GS, Holdt SL, Birkeland MJ, Angelidaki I. Commercial cultivation and bioremediation potential of sugar kelp, Saccharina latissima, in Danish waters. *J Appl Phycol* 2015; **27**: 1963–1973.
257. Fasahati P, Saffron CM, Woo HC, Liu JJ. Potential of brown algae for sustainable electricity production through anaerobic digestion. *Energy Convers Manag* 2017; **135**: 297–307.
258. Kraan S. Mass-cultivation of carbohydrate rich macroalgae, a possible solution for sustainable biofuel production. *Mitig Adapt Strateg Glob Chang* 2013; **18**: 27–46.
259. Eide A. The right to food and the impact of liquid biofuels (agrofuels). *Right to Food Studies* . 2008. Rome.
260. Berthon JY, Nachat-Kappes R, Bey M, Cadoret JP, Renimel I, Filaire E. Marine algae as attractive source to skin care. *Free Radic Res* 2017; **51**: 555–567.
261. Macartain P, Gill CIR, Brooks M, Campbell R, Rowland IR. Nutritional value of edible seaweeds. *Nutr Rev* 2007; **65**: 535–543.
262. Smit AJ. Medicinal and pharmaceutical uses of seaweed natural products: a review. *J Appl Phycol* 2004; **16**: 245–262.
263. Holdt SL, Kraan S. Bioactive compounds in seaweed: functional food applications and legislation. *J Appl Phycol* 2011; **23**: 543–597.
264. Chung IK, Oak JH, Lee JA, Shin JA, Kim JG, Park K. Installing kelp forests/seaweed beds for mitigation and adaptation against global warming: Korean project overview. *ICES J Mar Sci* 2013; **70**: 1038–1044.
265. Stévant P, Rebours C, Chapman A. Seaweed aquaculture in Norway: recent industrial developments and future perspectives. *Aquac Int* 2017; **25**: 1373–1390.
266. Edwards M, Watson L. Cultivating Laminaria digitata. *Aquaculture Explained* . 2011.
267. Camus C, Infante J, Buschmann AH. Overview of 3 year precommercial seafarming of Macrocystis pyrifera along the Chilean coast. *Rev Aquac* 2016; **2014**: 1–17.
268. Pachauri R, Allen M, Barros V, Broome J, Cramer W, Christ R, et al. Climate change 2014: synthesis report. Contribution of working groups I, II and III to the fifth assessment report of the Intergovernmental Panel on Climate Change. 2014.
269. Solomon S, Qin D, Manning M, Chen Z, Marquis M, Averyt KB, et al. Contribution of working group I to the fourth assessment report of the Intergovernmental Panel on Climate Change. 2007.
270. Stocker TF, Qin D, Plattner GK, Tignor M, Allen SK, Boschung J, et al. Climate change 2013: the physical science basis, Working Group 1 (WG1) contribution to

the Intergovernmental Panel on Climate Change (IPCC) 5th Assessment Report (AR5). 2013.
271. Lima FP, Wethey DS. Three decades of high-resolution coastal sea surface temperatures reveal more than warming. *Nat Commun* 2012; **3**: 704.
272. Bijma J, Pörtner HO, Yesson C, Rogers AD. Climate change and the oceans - what does the future hold? *Mar Pollut Bull* 2013; **74**: 495–505.
273. Wernberg T, Smale DA, Tuya F, Thomsen MS, Langlois TJ, De Bettignies T, et al. An extreme climatic event alters marine ecosystem structure in a global biodiversity hotspot. *Nat Clim Chang* 2012; **3**: 78–82.
274. Moy FE, Christie H. Large-scale shift from sugar kelp (Saccharina latissima) to ephemeral algae along the south and west coast of Norway. *Mar Biol Res* 2012; **8**: 309–321.
275. Filbee-Dexter K, Feehan CJ, Scheibling RE. Large-scale degradation of a kelp ecosystem in an ocean warming hotspot. *Mar Ecol Prog Ser* 2016; **543**: 141–152.
276. Filbee-dexter K, Wernberg T. Rise of turfs: A new battlefront for globally declining kelp forests. *Bioscience* 2018; **68**: 64–76.
277. Ling SD, Scheibling RE, Rassweiler A, Johnson CR, Shears N, Connell SD, et al. Global regime shift dynamics of catastrophic sea urchin overgrazing. *Philos Trans R Soc B Biol Sci* 2015; **370**: 20130269–20130269.
278. Vergés A, Steinberg PD, Hay ME, Poore AGB, Campbell AH, Ballesteros E, et al. The tropicalization of temperate marine ecosystems: climate-mediated changes in herbivory and community phase shifts. *Proc R Soc B Biol Sci* 2014; **281**: 20140846.
279. South PM, Floerl O, Forrest BM, Thomsen MS. A review of three decades of research on the invasive kelp Undaria pinnatifida in Australasia: an assessment of its success, impacts and status as one of the world's worst invaders. *Mar Environ Res* 2017; **131**: 243–257.
280. Straub SC, Thomsen MS, Wernberg T. The dynamic biogeography of the Anthropocene: the speed of recent range shifts in seaweeds. In: Hu Z-M, Fraser C (eds). *Seaweed Phylogeography: Adaptation and Evolution of Seaweeds under Environmental Change*. 2016. Springer, Dordrecht, pp 63–93.
281. Bolton JJ, Anderson R, Smit A, Rothman M. South African kelp moving eastwards: the discovery of Ecklonia maxima (Osbeck) Papenfuss at De Hoop Nature Reserve on the south coast of South Africa. *African J Mar Sci* 2012; **34**: 147–151.
282. Smale DA, Wernberg T, Yunnie ALE, Vance T. The rise of Laminaria ochroleuca in the Western English Channel (UK) and comparisons with its competitor and assemblage dominant Laminaria hyperborea. *Mar Ecol* 2015; **36**: 1033–1044.
283. Raybaud V, Beaugrand G, Goberville E, Delebecq G, Destombe C, Valero M, et al. Decline in kelp in west Europe and climate. *PLoS One* 2013; **8**: e66044.
284. Pessarrodona A, Moore PJ, Sayer MDJ, Smale DA. Carbon assimilation and transfer through kelp forests in the NE Atlantic is diminished under a warmer ocean climate. *Glob Chang Biol* 2018; **24**: 4386–4398.
285. Byrnes JE, Reed DC, Cardinale BJ, Cavanaugh KC, Holbrook SJ, Schmitt RJ. Climate-driven increases in storm frequency simplify kelp forest food webs. *Glob Chang Biol* 2011; **17**: 2513–2524.
286. Wernberg T, Bennett S, Babcock RC, Bettignies T De, Cure K, Depczynski M, et al. Climate-driven shift of a temperate marine ecosystem. *Science (80-)* 2016; **353**: 169–172.

287. Chung IK, Sondak CFA, Beardall J. The future of seaweed aquaculture in a rapidly changing world. *Eur J Phycol* 2017; **52**: 495–505.
288. Kumar V, Zozaya-Valdes E, Kjelleberg S, Thomas T, Egan S. Multiple opportunistic pathogens can cause a bleaching disease in the red seaweed Delisea pulchra. *Environ Microbiol* 2016; **18**: 3962–3975.
289. Campbell AH, Harder T, Nielsen S, Kjelleberg S, Steinberg PD. Climate change and disease: bleaching of a chemically defended seaweed. *Glob Chang Biol* 2011; **17**: 2958–2970.
290. Egan S, Fernandes ND, Kumar V, Gardiner M, Thomas T. Bacterial pathogens, virulence mechanism and host defence in marine macroalgae. *Environ Microbiol* 2014; **16**: 925–938.
291. Mitchell CE, Power AG. Release of invasive plants from fungal and viral pathogens. *Nature* 2003; **421**: 625–627.
292. Borer ET, Hosseini PR, Seabloom EW, Dobson AP. Pathogen-induced reversal of native dominance in a grassland community. *Proc Natl Acad Sci* 2007; **104**: 5473–8.
293. Kim GH, Moon KH, Kim JY, Shim J, Klochkova TA. A revaluation of algal diseases in Korean Pyropia (Porphyra) sea farms and their economic impact. *Algae* 2014; **29**: 249–265.
294. Kennedy DA, Kurath G, Brito IL, Purcell MK, Read AF, Winton JR, et al. Potential drivers of virulence evolution in aquaculture. *Evol Appl* 2016; **9**: 344–354.
295. Oerke EC. Crop losses to pests. *J Agric Sci* 2006; **144**: 31–43.
296. Lafferty KD, Harvell CD, Conrad JM, Friedman CS, Kent ML, Kuris AM, et al. Infectious diseases affect marine fisheries and aquaculture economics. *Ann Rev Mar Sci* 2015; **7**: 471–496.
297. Del Campo J, Sieracki ME, Molestina R, Keeling P, Massana R, Ruiz-Trillo I. The others: our biased perspective of eukaryotic genomes. *Trends Ecol Evol* 2014; **29**: 252–259.
298. Aiewsakun P, Katzourakis A. Endogenous viruses: connecting recent and ancient viral evolution. *Virology* 2015; **479–480**: 26–37.
299. McHugh. Worldwide distribution of commercial resources of seaweeds including Gelidium. *Hydrobiologia* 1991; **221**: 19–29.
300. Stevens K. Multiplicity of viral infection in brown algae. 2013. University of Plymouth.
301. Müller DG. Isolation of gametophytes from field sporophytes. In: Lobban CS, Chapman DJ, Kremer BP (eds). *Experimental phycology: a laboratory manual*, 1st ed. 1988. Cambridge University Press, New York, NY, pp 249–250.
302. Coelho SM, Scornet D, Dartevelle L, Peters AF, Cock JM. How to cultivate Ectocarpus. *Cold Spring Harb Protoc* 2012.
303. Peng Y, Li W. A bacterial pathogen infecting gametophytes of Saccharina japonica (Laminariales, Phaeophyceae). *Chinese J Oceanol Limnol* 2013; **31**: 366–373.
304. Christie H, Norderhaug KM, Fredriksen S. Macrophytes as habitat for fauna. *Mar Ecol Prog Ser* 2009; **396**: 221–233.
305. McKeown DA, Stevens K, Peters AF, Bond P, Harper GM, Brownlee C, et al. Phaeoviruses discovered in kelp (Laminariales). *ISME J* 2017; **11**: 2869–2873.
306. Ye N, Zhang X, Miao M, Fan X, Zheng Y, Xu D, et al. Saccharina genomes provide novel insight into kelp biology. *Nat Commun* 2015; **6**: 6986.
307. Peters AF, van Wijk SJ, Cho GY, Scornet D, Hanyuda T, Kawai H, et al.

Reinstatement of Ectocarpus crouaniorum Thuret in Le Jolis as a third common species of Ectocarpus (Ectocarpales, Phaeophyceae) in Western Europe, and its phenology at Roscoff, Brittany. *Phycol Res* 2010; **58**: 157–170.
308. Maeda T, Kawai T, Nakaoka M, Yotsukura N. Effective DNA extraction method for fragment analysis using capillary sequencer of the kelp, Saccharina. *J Appl Phycol* 2013; **25**: 337–347.
309. Kumar S, Stecher G, Tamura K. MEGA7: Molecular evolutionary genetics analysis version 7.0 for bigger datasets. *Mol Biol Evol* 2016; **33**: 1870–1874.
310. Ronquist F, Teslenko M, Van Der Mark P, Ayres DL, Darling A, Höhna S, et al. Mrbayes 3.2: efficient Bayesian phylogenetic inference and model choice across a large model space. *Syst Biol* 2012; **61**: 539–542.
311. Huson DH, Scornavacca C. Dendroscope 3: An interactive tool for rooted phylogenetic trees and networks. *Syst Biol* 2012; **61**: 1061–1067.
312. Carver T, Harris SR, Berriman M, Parkhill J, McQuillan JA. Artemis: an integrated platform for visualization and analysis of high-throughput sequence-based experimental data. *Bioinformatics* 2012; **28**: 464–469.
313. Larsen JB, Larsen A, Bratbak G, Sandaa RA. Phylogenetic analysis of members of the Phycodnaviridae virus family, using amplified fragments of the major capsid protein gene. *Appl Environ Microbiol* 2008; **74**: 3048–3057.
314. Starko S, Boo GH, Martone PT, Lindstrom SC. A molecular investigation of Saccharina sessilis from the Aleutian Islands reveals a species complex , necessitating the new combination Saccharina subsessilis. 2018; **33**: 157–166.
315. Wernberg T, Thomsen MS, Tuya F, Kendrick GA, Staehr PA, Toohey BD. Decreasing resilience of kelp beds along a latitudinal temperature gradient: potential implications for a warmer future. *IOP Conf Ser Earth Environ Sci* 2010; **13**: 685–694.
316. Mckeown DA, Schroeder JL, Stevens K, Peters AF, Claudio AS, Park J, et al. Phaeoviral infections are present in Macrocystis, Ecklonia and Undaria (Laminariales) and are influenced by wave exposure in Ectocarpales. *Viruses* 2018; **10**: 410.
317. Friess-Klebl AK, Knippers R, Müller DG. Isolation and characterization of a DNA virus infecting Feldmannia simplex (Phaeophyceae). *J Phycol* 1994; **30**: 653–658.
318. Triboush SO, Danilenko NG, Davydenko OG. A method for isolation of chloroplast DNA and mitochondrial DNA from sunflower. *Plant Mol Biol Report* 1998; **16**: 183–189.
319. Akita S, Koiwai K, Hanyuda T, Kato S, Nozaki R, Uchino T. Development of 11 Ecklonia radicosa (Phaeophyceae, Laminariales) SSRs markers using next-generation sequencing and intra-genus amplification analysis. *J Appl Phycol* 2018; **30**: 2111–2115.
320. Macaisne N, Liu F, Scornet D, Peters AF, Lipinska A, Perrineau M-M, et al. The Ectocarpus IMMEDIATE UPRIGHT gene encodes a member of a novel family of cysteine-rich proteins with an unusual distribution across the eukaryotes. *Development* 2017; **144**: 409–418.
321. Hu X, Reddy ASN. Cloning and expression of a PR5-like protein from Arabidopsis: Inhibition of fungal growth by bacterially expressed protein. *Plant Mol Biol* 1997; **34**: 949–959.
322. Plugge B, Gazzarrini S, Nelson M, Cerana R, Van Etten JL, Derst C, et al. A potassium channel protein encoded by Chlorella virus PBCV-1. *Science (80-)* 2000; **287**: 1641–1644.

323. Müller DG, Sengco M, Wolf S, Bräutigam M, Schmid CE, Kapp M, et al. Comparison of two DNA viruses infecting the marine brown algae Ectocarpus siliculosus and E. fasciculatus. *J Gen Virol* 1996; **77**: 2329–2333.
324. Klein M, Lanka STJ, Knippers R, Müller DG. Coat protein of the Ectocarpus siliculosus virus. *Virology* 1995; **206**: 520–526.
325. Henry EC, Meints RH. Recombinant viruses as transofrmation vectors of marine macroalgae. *J Appl Phycol* 1994; **6**: 247–253.
326. Roossinck MJ. Move over, bacteria! Viruses make their mark as mutualistic microbial symbionts. *J Virol* 2015; **89**: 6532–6535.
327. Xu P, Chen F, Mannas JP, Feldman T, Sumner LW, Roossinck MJ. Virus infection improves drought tolerance. *New Phytol* 2008; **180**: 911–921.
328. Nakatsukasa-Akune M, Yamashita K, Shimoda Y, Uchiumi T, Abe M, Aoki T, et al. Suppression of root nodule formation by artificial expression of the TrEnodDR1 (coat protein of White clover cryptic virus 1) gene in Lotus japonicus. *Mol Plant Microbe Interact* 2005; **18**: 1069–1080.
329. Shapiro LR, Salvaudon L, Mauck KE, Pulido H, De Moraes CM, Stephenson AG, et al. Disease interactions in a shared host plant: effects of pre-existing viral infection on cucurbit plant defense responses and resistance to bacterial wilt disease. *PLoS One* 2013; **8**: e77393.
330. Quispe CF, Sonderman O, Seng A, Rasmussen B, Weber G, Mueller C, et al. Three-year survey of abundance, prevalence and genetic diversity of chlorovirus populations in a small urban lake. *Arch Virol* 2016; **161**: 1839–1847.